October 2022

Principles of AAA+ Proteases

Samar Mahmoud
University of Massachusetts Amherst

Principles of AAA+ Proteases

A Dissertation Presented

by

Samar Ashraf Mahmoud

Submitted to the Graduate School of the
University of Massachusetts Amherst in partial fulfillment
of the requirements for the degree of

DOCTOR OF PHILOSOPHY

September 2022

Molecular and Cellular Biology

Principles of AAA+ Proteases

A Dissertation Presented

by

Samar Ashraf Mahmoud

Approved as to style and content by:

_____
Peter Chien, Chair

_____
Brian A. Kelch, Member

_____
Sloan M. Siegrist, Member

_____
Margaret M. Stratton, Member

_____
Thomas Maresca
Graduate Program Director
Molecular and Cellular Biology

DEDICATION

I dedicate this thesis to my parents, sisters, Mohamad, and my son, Zakareya for their unwavering support. Thank you for cheering me on these past years and encouraging me to pursue my dreams even if it meant being far away from you all. You believed in me when I did not believe in myself. You encouraged me when I felt like quitting. This thesis is as much yours as it is mine.

ACKNOWLEDGMENTS

I would like to thank my wonderful mentor Dr. Peter Chien. I am very thankful that you accepted me into your lab and gave me a better opportunity for personal and professional growth that I could have ever imagined. We met every week, and I always left your office feeling inspired to tackle new experiments and explore new biology. You motivated me to work very hard and you were the best example of this, exemplifying unwavering dedication and commitment. I will forever cherish my time in your lab, where I truly learned to think critically.

I would also like to thank my committee members, Dr. Meg Stratton, Dr. Sloan Siegrist, and Dr. Brian Kelch. Your collective feedback during my PhD was invaluable and has helped me address many gaps and unanswered questions in my research. Meg, in addition to being on my committee, your critiques and feedback during CS3R meetings helped shaped my projects. Sloan, I truly appreciated you taking the time to read my manuscript and providing helpful comments. Brian, I remember meeting you during the CBI retreat at UMass Amherst where you offered to help me look at the ClpX structure to figure out what the ClpX* mutation was doing. This was before I asked you to be on my committee and I have truly appreciated your structural insights into my work.

I would also like to thank Chien lab members, both the current ones and past members who have played a big role in shaping my PhD experience. Rilee, you basically taught me most of what I knew how to do in the Chien lab. You were also always willing to listen to new developments in my project and give helpful feedback. I have missed our midday coffee breaks after you graduated.

Nate, we started on this journey together and it was amazing to see how we both grew as people and as scientists. I would also like to thank Tommy, Justyne, and Berent for not only their friendship but also helpful discussion and feedback on my projects. You all made the Chien lab an amazing place to be, and I will truly miss working with all of you. I also want to thank my amazing undergraduate Patrick Cann. You were the best mentee I could have ever asked for and I'm so proud to see how far you've come.

I would like to thank my amazing family for all their support over the years. My wonderful parents immigrated to the US to seek a better life for me and my sisters and I could not be more grateful for your many sacrifices. You both inspired me to work hard and to follow my dreams. To my mom, you gave up your life in NJ to come to MA to help take care of Zakareya and I am forever indebted to you for your selflessness and love. To my sisters, Soha and Salma, you both are my rock! I could not have gotten through graduate school without your support. Your visits to MA brightened up my life and helped me get through many difficult times. To my amazing husband, Mohamad, I know these past years have not been easy, but your constant support and encouragement have motivated me more than you can know over the years. You also brought into my life my wonderful companions, Roo and Hermione (my cats) who have kept me company and staved off any feelings of loneliness for many years. To my son Zakareya, who has been my companion as I write this thesis, you have brightened up my life in so many ways and I'm so lucky to be your mom.

Principles of AAA+ Proteases

SEPTEMBER 2022

SAMAR ASHRAF MAHMOUD, B.A. DREW UNIVERSITY

M.S., MONTCLAIR STATE UNIVERSITY

Ph.D., UNIVERSITY OF MASSACHUSETTS AMHERST

Directed by: Professor Peter Chien

ATPases associated with diverse cellular activities (AAA+) proteases in bacteria help maintain protein homeostasis by degrading misfolded and regulatory proteins. While a handful of protein targets for these proteases have been identified in *Caulobacter crescentus* and other organisms, more research is needed to elucidate mechanisms that govern substrate specificity. In the second chapter of this thesis, I will elaborate on how AAA+ substrate specificity is less rigid than previous work has suggested and how limiting ATP or mutations can alter substrate preferences of the ClpXP protease. In the third chapter, I will highlight our efforts to use a quantitative proteomics approach and how this approach has provided us with insights on new phenotypes. The fourth chapter of this thesis is a compilation of our efforts to identify suppressors of *Δlon* defects. Lastly, the remainder of this thesis will present additional data that was generated in the pursuit of these three projects and other endeavors.

TABLE OF CONTENTS

Page

ACKNOWLEDGMENTS…….…... **v**

ABSTRACT…….……**vii**

LIST OF FIGURES…….……..…**xi**

Chapter

1. Introduction: Regulated Proteolysis in Bacteria……..……**1**

1.1 Abstract……**1**

1.2 Introduction……..…**2**

1.3 Operational Rules of Proteolysis ……**3**

1.4 Proteases as Quality Control Responders……**5**

1.5 Regulated Proteolysis During Balanced Growth……**12**

1.6 Perspective……..……**21**

1.7 References……**22**

2. Plasticity in AAA+ Proteases Reveals ATP-dependent Substrate Specificity Principles……..…**45**

2.1 Summary……...**45**

2.2 Highlights……..**46**

2.3 Introduction……..……**47**

2.4 Results……**49**

2.4.1 A suppressor screen identfiied a *clpX* mutant which rescues *Δlon*……..**49**

2.4.2 ClpX* restores degradation of Lon substrates *in vivo*…….……**51**

2.4.3 ClpX*P directly degrades Lon substrates *in vitro*……**53**

2.4.4 ClpX*P is deficient in degradation of native ClpXP substrates……..…**54**

2.4.5 Deficienes of ClpX* revealed when Lon is present……**55**

2.4.6 Limiting ATP alters wildtype ClpXP substrate specificity……...……**57**

2.5 Discussion……**61**

2.6 Limitations of the study……...…**64**

2.7 Materials and Methods……..……**65**

2.8 Acknowledgments……..……**76**

2.10 References……..……**76**

2.11 Additional data not included in manuscript……..**117**

2.12 ClpX* Purification……..……**122**

3. Quantitative Proteomics Screen Uncovers Novel Phenotypes…..……**128**

3.1 Abstract……...**129**

3.2 Introduction ……**129**

3.3 Results……**131**

3.4 Discussion……..……**138**

3.5 Methods……..……**139**

3.6 References……..……**143**

4. Suppression Analysis Reveals Lon-related Pathways……...**158**

4.1 Abstract……...……**158**

4.2 Introduction……..……**159**

4.3 Results……..……**160**

4.4 Discussion……..……**165**

4.5 Methods……..……**166**

4.6 References……..……**170**

5. Lessons I've learned and future perspectives……..…**178**

6. Appendix……..…**183**

A.1 Contributions to our understanding of *Vibrio Cholera* Lon……**186**

A.2 Purification of VclonA……**187**

A.3 Contributions to the Lon degradation project……**193**

A.4 Additional Data……..……**197**

A.5 AHA labeling and Click Chemistry Protocol……..……**211**

Bibliography....……**215**

List of Figures

Figure……..……..…….**Page**

Figure 1.1 Energy-dependent proteases are composed of an ATP-hydrolysis active unfoldase domain and a chambered peptidase domain……..…**37**

Figure 1.2 Proteases can survey protein quality in the cell……..……..**38**

Figure 1.3 Lon is subject to allosteric regulation……..……..……..…**39**

Figure 1.4 Adaptors assemble in a hierarchical manner to degrade various classes of substrates. ……..……..…….……..**41**

Figure 1.5 Substrate degradation by ClpXP is rate-limited by the commitment step……..……..……..……**42**

Figure 1.6 Regulated proteolysis is required during physiological transitions and changes in growth……..……**43**

Figure 2.1 Graphical Abstract……..……**88**

Figure 2.2 : *clpX** mutant suppresses *⊿lon* phenotypes……..…**89**

Figure 2.3: *clpX** mutant restores levels of Lon substrates through degradation……..……**91**

Figure 2.4: ClpX*P degrades some Lon substrates faster than ClpXP *in vitro*……..……..……..……**92**

Figure 2.5: ClpX* mutant is deficient in degradation of native ClpXP substrates……..……..……..……..……**94**

Figure 2.6: Limiting ATP alters wildtype ClpXP substrate specificity……..…**95**

Figure 2.7: ClpX adopts distinct ATP-dependent conformational states……..**98**

Figure 2.8: Validation of motility screen suppressor……..……**100**

Figure 2.9: RNA-seq gene set analysis…..……..……..**102**

Figure 2.10: *clpX** mutant is dominant……..……..….**104**

Figure 2.11: *In vitro* characterization of ClpX*……..……..……**105**

Figure 2.12: ClpX*P is deficient in native substrate degradation……..…….**106**

Figure 2.13: ClpX* is deficient in nucleotide binding…….**107**

Figure 2.14: Modulating ATP changes substrate preferences……..…**108**

Figure 2.15: ClpX* mutation and limiting ATP lead to increased dynamics of ClpX……**109**

Figure 2.16 Uncropped western blot for Figure 2.2B…….……**113**

Figure 2.17 Uncropped western blot for Figure 2.2C……**113**

Figure 2.18 Uncropped western blot for Figure 2.2D……**114**

Figure 2.19 Uncropped western blot for Figure 2.2E……..……..**114**

Figure 2.20 Uncropped gels for Figure 2.3A……...**115**

Figure 2.21 Uncropped western blot for Figure 2.4C……**116**

Figure 2.22 Uncropped gel for Figure 2.5D…….……**116**

Figure 2.23 Uncropped western blot for Figure 2.5E…….**117**

Figure 2.24 dsDNA modulates the degradation of DnaA by the Lon and ClpXP proteases……...…**117**

Figure 2.25 DnaAR357A is degraded robustly by ClpX*P and ClpXP…….. **118**

Figure 2.26 DnaA and SciP degradation by ClpXP is dependent on the N-terminal domain.……..……**119**

Figure 2.27 Substrate addition alters the ATPase rate of ClpX and ClpX*……**120**

Figure 2.28 Titration of ClpX/ClpX*……..…**121**

Figure 2.29 Yield and purity of ClpX*……..…**127**

Figure 3.1 Quantitative proteomics workflow……..……**146**

Figure 3.2 Overview of identified proteins……..…**148**

Figure 3.3 Identifying potential Lon substrates……...…..**149**

Figure 3.4 CcbF is preferentially degraded in *Δlon clpX**……**151**

Figure 3.5 *Δlon* suppressors of polymyxin sensitivity map to CcbF operon…..**153**

Figure 3.6 (Figure S1) Western blots of strains utilized in TMT experiments……...**154**

Figure 3.7 (Figure S2) Lon O/E TMT……**155**

Figure 3.8 (Figure S3) Half-lives of identified proteins……..…**156**

Figure 3.9 CcbF *in vitro* degradation assay……**157**

Figure 4.1 Using transposon mutagenesis to screen for motility suppressors……...**172**

Figure 4.2 Validation of motility suppressors ……..……**173**

Figure 4.3 Spontaneous motility suppressors. ……..……..…**174**

Figure 4.4 Minimal media suppresses *Δlon* defects……..…**175**

Figure 4.6 A. Antibiotic shutoff assays to monitor DnaA turnover in *wt, Δlon*, *Δlon, Δlon ΔssrA, Δlon ΔsmpB, and Δlon ΔpopA* strains……...……**176**

Figure 4.7 Characterization of *Δlon ΔPDH*……...……...……**177**

Figure A.1 *Δlon clpX** cells are less resistant to hydroxyurea than *Δlon* cells……..…**183**

Figure A.2 Growth curves in the presence of polymyxin B in M5G media…….**184**

Figure A.3. *Wildtype* cells are more resistant to L-canavanine under limiting phosphate conditions……..…..**185**

Figure A.4 C-di-GMP inhibits FITC-Casein degradation by LonA but does not affect ATP hydrolysis……...…**186**

Figure A.5 Cyclic di-GMP inhibits FITC-casein degradation by Caulobacter Lon but has no effect on 4E, a DNA-blind mutant……..**187**

Figure A.6 *In vitro* degradation assays with Lon and/or ClpAP…….……..**193**

Figure A.7 The C terminus of Lon is necessary for degradation……..…..**194**

Figure A.8. Induction of *lonM2* from the *xylX* promoter shifts cells toward G_1……..……..**195**

Figure A.9 Miller assays comparing DnaA'-lacZ expression in *wildtype* and *ΔclpA* cells……..……..…**196**

Figure A.10 Depleting DnaA levels in *Δlon* is not sufficient to restore motility or morphology……..……**197**

Figure A.11 CtrA is misregulated in a *Δlon*……..**199**

Figure A.12 MMC spot assays of *wildtype* and clpX* cells overexpressing CtrA and CtrAD51E……..……**200**

Figure A.13 ^{35}S-[Cys-Met] Pulse experiments…….…..**201**

Figure A.14 *Δlon* cells are sensitive to tetracycline……..…**202**

Figure A.15 *ClpX** restores pink coloration to *Δlon* cells on PYE agarose supplemented with xylose..……..……..…**203**

Figure A.16 DnaA steady state levels as a function of OD600……**204**

Figure A.17 Treating cells with uncoupling agent, carbonyl cyanide m-chlorophenylhydrazine (CCCP)……**205**

Figure A.18 Morphology in the presence of CCCP……...**207**

Figure A.19 Growth curves in the presence of amino acids as a sugar source……**208**

Figure A.20 Growth curves in the presence of alternative sugar sources. ……..…**209**

Figure A.21 MG132 inhibits *Caulobacter* Lon activity *in vitro*……..……**209**

Figure A.22 The *Caulobacter* Lon protease is sensitive to ADP inhibition……**210**

Chapter One

Introduction: Regulated Proteolysis in Bacteria

as written by Mahmoud SA and Chien P., published in Annual Reviews in Biochemistry in 2018 (https://doi.org/10.1146/annurev-biochem-062917-012848)

Contributions: I wrote this review with Peter during my first official year in the Chien lab. I did a deep literature search to write the text of the review, with edits and suggestions from Peter. I also made most of the figures, with edits and improvements made by Peter.

1.1 Abstract

Regulated proteolysis is a vital process that affects all living things. Bacteria use energy-dependent AAA+ proteases to power degradation of misfolded and native regulatory proteins. Given that proteolysis is an irreversible event, specificity and selectivity in degrading substrates is key. Specificity is often augmented through the use of adaptors that modify the inherent specificity of the proteolytic machinery. Regulated protein degradation is intricately linked to quality control, cell cycle progression, and physiological transitions. In this review, we highlight recent work that has shed light on our understanding of regulated proteolysis in bacteria. We discuss the role AAA+ proteases play during balanced growth as well as how proteases are mobilized during changes in growth. We present examples of how protease selectivity can be controlled in increasingly complex ways. We promote the concept that coupling a core recognition determinant to

one or more modifying agents is a general theme for regulated protein degradation.

1.2 Introduction

Regulated protein degradation is a vital process that affects all biological pathways. Because proteolysis is an irreversible event, the cell must take great care to avoid degrading proteins indiscriminately. As a consequence, energy-dependent proteases are finely tuned cellular machines that recognize substrates with exquisite sensitivity and selectivity.

In eukaryotes, proteins targeted for degradation are modified by the covalent linkage of ubiquitin, a small protein that is appended to a lysine residue on the target protein, for review see (1). Following additional extension by the ubiquitin ligase families, the target protein is recognized and degraded by the proteasome. In bacteria, regulated proteolysis is carried out by energy-dependent AAA+ (ATPases associated with cellular activities) proteases that use the power of ATP hydrolysis to recognize, unfold, translocate, and degrade substrates. Several energy-dependent proteases exist in bacteria: Lon, ClpXP, ClpAP, ClpCP, ClpEP, HslUV, and FtsH (2–4). The importance of these AAA+ proteases is highlighted by the defects in viability and virulence of bacteria deficient in one or more proteases (5, 6). For instance, bacteria lacking Lon are known to be filamentous and more sensitive to ultraviolet radiation than their wild-type counterparts (7). In the alpha-proteobacterium *Caulobacter crescentus*, ClpXP is essential as mutants lacking this protease are arrested during the cell

cycle (8). In the human pathogen *Vibrio cholerae*, Lon mutants were unable to compete with wild-type *V. cholerae* in colonizing the infant mouse intestine (9).

AAA+ proteases share a similar general architecture being composed of an ATPase and peptidase domain (10). In the case of Lon and FtsH, the two domains are encoded on a single polypeptide chain (11, 12). On the other hand, the Clp family of proteases encodes distinct hexameric ATPases, (either ClpA or ClpX in gram-negative bacteria and ClpC or ClpE in gram-positive bacteria) which associate with ClpP, a sequestered 14-subunit peptidase, to form ClpXP, ClpAP, ClpCP, or ClpEP (2, 13). ClpP alone has the ability to degrade small peptides, but in order to degrade larger, more stable substrates, ClpP must associate with an unfoldase that harvests the energy of ATP hydrolysis to power degradation (13, 14). This is separate from the properties of non-energy dependent proteases and peptidases that serve important recycling roles in the cell (15). The energy dependent AAA+ proteases will be the primary focus of this review.

1.3 Operational Rules of Proteolysis

Regardless of architecture or function, bacterial AAA+ proteases seem to follow similar operational rules. In the most general case, regulated proteolysis requires recognition of an initial degradation determinant (also known as degrons) followed by processive degradation of the polypeptide in an ATP dependent manner **(Figure 1.1)**. The unfolding power and processivity of an AAA+ protease depends on both substrate and protease. For example, poorly

folded substrates require less power to unfold (16). In addition, low complexity portions of a substrate protein can stall proteases, resulting in release of partially processed species (17, 18). By appending the same substrate with different degrons, the unfolding and processivity of the known bacterial AAA+ proteases classes were shown to vary over 2 orders of magnitude (19), with Lon being the "worse" unfoldase and ClpAP being the "best". Because unfolding parameters can vary wildly depending on the specific fold of the substrate, we are cautious in generalizing these results to all substrates, but single molecule experiments have recently shown similar correlations between some of these machines (20–22).

Due to the processive nature of these proteases, the most important governing feature *in vivo* is likely the pioneering round of substrate engagement, as once a substrate is committed for degradation it is unfolded and translocated relatively quickly (22). This initial commitment is a combination of the specificity of the protease for a given class of substrates and the ability of those substrates to be recruited to the protease. In order for any AAA+ protease to successfully degrade a substrate, there must be initial recognition of some determinant on the substrate for the protease to start pulling on. This intrinsic recognition can be modified through inhibition or activation by additional factors or the substrates themselves in complex ways dependent on the need of the cell. These needs can include quality control, as damaged or misfolded proteins must be cleared before they elicit toxic effects. On the other hand, energy-dependent proteases are also playing a major role in maintaining protein homeostasis during balanced growth and during physiological transitions, such as stationary phase or

sporulation. Although the mechanisms proteases employ for these distinct arms of degradation may differ, the general theme of linking a core recognition determinant to a modifier seems to be common.

1.4 Proteases as Quality Control Responders

Bacteria live in a dynamic, constantly fluctuating environment where they are subject to proteotoxic stressors, such as heat or oxidative stress. Because stress conditions require a swift response, regulated proteolysis allows bacteria an effective way to get rid of damaged proteins rapidly, without having to wait for protein removal by dilution through cell division (14, 23).

In addition, many stresses lead to the accumulation of misfolded proteins, a problem that needs to be addressed by the cell before lethal consequences ensue. The response to stress can be thought of as a competition between rescuing factors, such as chaperones or repair enzymes, which seek to restore proteins, and proteases, which seek to degrade them **(Figure 1.2a)**. A central challenge for the cell therefore lies in determining when a protein is terminally damaged or misfolded and when rescue attempts should be abandoned for proteolysis (24).

Recognizing failed quality products through specific tags: the ClpXP protease

Misfolded proteins are cleared by Lon in bacteria as well as in the mitochondrial matrix in eukaryotes (25, 26). In *Escherichia coli*, Lon is thought to be responsible for the degradation of approximately 50% of misfolded proteins

(27), which suggests that the protease recognizes general motifs in misfolded proteins with little sequence specificity. By contrast, the bacterial ClpXP protease is far more selective and requires a specific degron sequence, such as the ssrA tag, in order to recognize a substrate (28, 29). These two enzymes exemplify different mechanisms used to ensure degradation of poor quality proteins.

One of the best-studied examples in bacteria of regulated proteolysis is the recognition of the ssrA tag by ClpXP following *trans*-translation, a mechanism by which stalled ribosomes are rescued upon recruitment of tmRNA and nascent polypeptides are tagged with the ssrA peptide (30). Because these stalled ribosomes often arise from damaged messenger RNAs that lack a stop codon, the resulting polypeptide products cannot be complete. Therefore, the presence of the ssrA tag is itself the signal for a poor-quality protein. Recognition of the ssrA tag by ClpXP is highly specific, with even a single amino acid substitution abolishing substrate recognition (28). The amount of ssrA-tagged proteins is staggering, with some estimates that an ssrA tag is appended in approximately 1 in every 20 translation events (31). During starvation ribosome stalling and mRNA cleavage is enhanced, resulting in an even further taxing of the trans-translation system (32). Activation of certain endogenous toxins, such as MazF and RelE, can induce rampant mRNA cleavage as well that is counteracted by tmRNA (33). In these cases, the need for clearance of ssrA-tagged proteins becomes even more urgent to eliminate the surge in truncated polypeptides.

The ClpXP protease is fully capable of degrading ssrA-tagged proteins. However, the adaptor protein SspB enhances the ability of ClpXP to recognize and degrade ssrA-tagged substrates (34). SspB forms a homodimer, with each subunit containing a substrate binding domain that binds ssrA-tagged proteins, and a disordered C-terminal tail that interacts with ClpX. Efficient delivery of ssrA-tagged substrates requires both tails on each subunit of SspB to interact with ClpX, which tethers substrates to the protease to increase effective substrate concentration (35). Thus, the ssrA tag is the fundamental protease recognition determinant with the SspB adaptor acting as a modifier of this recognition by serving as a passive tether **(Figure 1.2b)**.

In addition to enhancing the ability of ClpXP to degrade ssrA-tagged substrates, SspB also promotes degradation of N-RseA, the N-terminal fragment of the stress response protein RseA (13, 36). During normal conditions, RseA binds σ^E, preventing it from activating transcription. However, during the envelope-stress response, RseA is cleaved by proteases, freeing the N-terminal segment of RseA in complex with σ^E. SspB then delivers N-RseA to the ClpXP protease, leaving σ^E free to upregulate the envelope-stress response. Remarkably, there is no clear sequence similarity between the region of N-RseA that interacts with SspB and the region of the SsrA tag that binds SspB, indeed, binding of N-RseA is in the opposite orientation as that of ssrA (36). Having a single adaptor bind multiple substrates would enable a coordinated response across several pathways and, perhaps not surprisingly, other examples of adaptors enabling degradation of several substrates are now emerging (37–39).

However, this multiplexing would eventually reach an upper limit as the need for selectivity begins to outweigh the advantages of coordinated degradation.

Recognition of poor quality proteins without specific tagging: the Lon protease

The cellular response to an acute stress must often occur at timescales faster than transcription and translation. Importantly, if the stress affects some of this central machinery, such as the fidelity of the ribosome, then the consequences of this stress must be repaired prior to restarting normal growth. It can be argued that the Lon protease is uniquely suited to serve as a quality control protease due to its ability to broadly recognize misfolded proteins and its ability to be allosterically activated.

Quality control through regulated proteolysis requires bacteria to discriminate between fatally misfolded or damaged proteins and proteins that simply share features associated with compromised proteins, such as folding intermediates or normal transient fluctuations in protein structures. Compared to other energy dependent proteases, the Lon protease has the weakest unfolding capacity (19), but a surprisingly promiscuous substrate repertoire. Indeed, Lon seems to recognize hydrophobic residues on misfolded substrates that are typically buried in the native structure as its primary recognition determinant rather than any unique sequence motif (40) **(Figure 2a)** for review, see (41).

To properly survey protein quality, Lon must be able to distinguish between fatally misfolded proteins and those that are in intermediate folding states. Given that terminally misfolded proteins are kinetically trapped, it seems

likely that the lifetime of the exposed hydrophobic regions may be a key determinant for this type of quality control surveillance. The shorter lifetime of exposed hydrophobic regions for a protein en route to the native state would set the lower boundary of timescales where Lon should recognize a 'poor quality' protein. By extension, this means that the Lon-substrate complex would need to have sufficiently transient kinetics to be compatible with this discrimination, otherwise, Lon would erroneously destroy proteins in the process of being folded or fluctuating with normal dynamics. Thus, by combining a low efficiency unfolding capacity with a broad recognition spectrum, the Lon protease gains selectivity in recognizing truly misfolded proteins. A similar model is thought to hold for eukaryotic quality control, where only persistent Hsp70 chaperone to a folding client recruits the CHIP ubiquitin ligase to target the client for ubiquitylation and degradation (42).

The ability of cells to use proteases and chaperones to ensure protein quality can also apply to the quaternary structure of complex assemblies. For example, individual subunits of protein complexes must be assembled in the correct stoichiometry to ensure function. Overflow of these subunits could be toxic, but AAA+ proteases are well-suited to destroy these unincorporated subunits. For example, degradation of the CcdA antitoxin by the Lon protease is inhibited when it is incorporated into the CcdAB complex (43) and degradation of subunits are often suppressed when complexes are fully assembled. In this respect, Lon is ensuring that active protein complexes maintain the proper stoichiometry.

Similarly, many protease substrates are DNA binding factors, including transcription factors, replication regulators, and components of polymerases (44–47). For some substrates, degradation is only evident when the substrate is not binding DNA, suggesting again that a surveillance of the proper active complex (in this case the degree of DNA-bound species) affords the cell the ability to ensure destruction of proteins when they are not performing their function. We caution that interpretation of this phenomenon is more complex as in some cases DNA can stimulate substrate recognition by the protease (46), and in the case of Lon, DNA can affect the protease directly (48, 49) and for review see (47).

The allosteric activation of Lon is an intriguing aspect to consider in light of its role in quality control in the cell and its fundamental broad specificity. Many enzymes exhibit substrate-activity relationships in line with the classic Michaelis-Menten equation. The ClpXP and ClpAP proteases fall into this class, where increasing substrate initially results in linear increases of degradation rates until the enzyme becomes saturated and maximum reaction velocity (vmax) is achieved **(Figure 1.3a).** In such cases, an underlying assumption is that the enzyme specific activity is unchanged as substrate is added.

By contrast, the Lon protease has long been known to respond to substrate concentration in a cooperative manner (50), with the working model that substrates allosterically activate the Lon protease and increase its proteolytic activity. Intriguingly it has been shown that substrates not only activate Lon for their own degradation, but can also serve to activate Lon for degradation of other substrates (51) . Thus, the behavior of Lon in the presence of two substrates

could lead to regulation conducive to quality control. For example, suppose substrate 1 has a higher affinity for Lon such that low concentrations of this substrate are needed to allosterically activate Lon, while substrate 2 can only activate Lon at a higher substrate concentration **(Figure 1.3b-1.3c)**. Titration of these substrates would show that at the same concentrations, substrate 2 is degraded more slowly than 1. However, addition of substrate 1, even at concentrations lower than substrate 2, would cause shifting of the Lon population to the more active species resulting in more rapid degradation of substrate 2 **(Figure 1.3d)**. Therefore, higher affinity substrates can effectively act as activators of lower affinity substrate degradation. In these cases, the basic recognition of the protease is modified by the presence of other substrates.

An intriguing extension of this biochemical framework is that it would result in the greatest activation of the Lon protease when demand is greatest *in vivo*. For example, during an acute proteotoxic stress, the rapid increase in misfolded proteins would result in allosteric activation of Lon to eliminate these misfolded proteins, but also to degrade fully active regulatory proteins as part of the stress response. Such a case was recently reported in *Caulobacter*, with the Lon dependent degradation of DnaA serving to halt cell cycle progression during proteotoxic stress (52). This type of regulation would also make sense for a protease such as Lon given its ability to recognize features found in all proteins (such as hydrophobic residues), as persistently high activation of Lon would inevitably result in the destruction of proteins not needed for quality control. Indeed overproduction of Lon in *E. coli* results in cell death, in part because of

rampant degradation of antitoxin proteins (53). Finally, because Lon can be allosterically regulated by non-protein molecules such as DNA, it is tempting to speculate that a surge in Lon activity upon allosteric activation could also be deployed under additional stress responses, such as during genotoxic stress where extended exposure of single-stranded DNA is a unique flag for DNA damage.

1.5 Regulated proteolysis during balanced growth

Coordinating proteolysis with cell division and replication

The cell cycle involves a highly regulated sequence of events in which DNA is faithfully replicated and divided into daughter cells. Progression through the cell-cycle requires regulated proteolysis to ensure the timely degradation of regulatory proteins necessary to drive this irreversible process. In eukaryotes, the concerted activity of APC/C and SCF ubiquitin ligases enforce the selective tagging and ultimate degradation of many regulatory factors (54).

In *Caulobacter crescentus*, asymmetric cell division yields a motile, flagellated swarmer cell and a sessile stalked cell (23, 55). The stalked cell is replication-competent and can immediately commence DNA replication and enter the cell cycle. However, the swarmer cell must first shed its flagellum and grow a stalk before it can initiate chromosome replication. Thus, the swarmer to stalked transition, also known G1 to S transition, is coupled to DNA replication and is intricately linked to regulated protein degradation (56). At the center of this transition is the essential master regulator, CtrA which is responsible for

regulating expression of approximately 100 genes (57–59). CtrA also binds to and inhibits the origin of replication in swarmer cells, preventing swarmer cells from initiating replication. Therefore, when it becomes time to resume DNA replication during the swarmer-to-stalked transition, CtrA must be eliminated. This occurs through dephosphorylation by the CckA pathway (60–62) and proteolysis by the ClpXP protease (8, 63).

Since the levels of ClpXP remain constant during the cell-cycle, additional mechanisms must exist to support the cyclic oscillations seen in CtrA levels during the cell cycle (8). Indeed, a tightly regulated series of events, involving the adaptor proteins CpdR, RcdA, PopA, and the second messenger cyclic di-GMP ensures the degradation of CtrA (and other substrates) and timely entrance into S phase (64).

Intriguingly, although CtrA degradation *in vivo* requires ClpXP as well as additional accessory factors, ClpXP can degrade CtrA without these adaptors *in vitro* (65, 66). This paradox was reconciled by data that showed that CpdR, RcdA, PopA can increase the rate of CtrA degradation *in vitro* as the addition of these factors lowered the K_m 10-fold, keeping V_{max} constant (66). Intriguingly, the assembly of the adaptors was shown to be essential during times when recognition of CtrA by ClpXP was less robust, such as when CtrA is bound to DNA and thereby inaccessible (67). This ensures that there is complete removal of CtrA to allow resumption of DNA synthesis as even a small amount of CtrA is enough to inhibit the origins of replication (66, 68).

Regulated protein degradation is linked to cell-cycle progression in other bacteria as well. In *E. coli*, FtsZ is an essential component of the cell division machinery. FtsZ polymerization is necessary to form the z-ring, the site where septation and cell division occurs. Studies in *Bacillus subtilis* determined that ClpX inhibits FtsZ polymerization in a Clp and ATP-independent manner (69). However, in *E. coli* ClpXP has been shown to degrade FtsZ directly, potentially functioning to promote the disassembly of FtsZ polymers (70, 71). Similarly, both ClpAP and ClpXP can degrade *Caulobacter* FtsZ *in vitro* as well as *in vivo* (72).

Diversifying proteolysis through hierarchies

Recently, CpdR, PopA, and RcdA have been shown to function as adaptors capable of degrading various classes of substrates in a hierarchical manner in *Caulobacter* (38) **(Figure 1.4).** The lowest level of the hierarchy consists of ClpXP alone, which can theoretically degrade many substrates limited only by the recognition determinants of those substrates. For example, trapping studies in *E. coli* and *Caulobacter* have identified hundreds of potential substrates, several of which are degraded by ClpXP alone *in vitro* (29, 73) and proteomic studies in *Staphylococcus aureus* illustrate the range of substrate degraded by the Clp family (74). The next tier consists of ClpXP and the adaptor CpdR. While traditional adaptors can bind their substrates directly, two-hybrid studies found that CpdR alone does not interact with its substrates strongly (37). Instead, CpdR primes ClpXP by binding to the N-terminal domain of the unfoldase domain, preparing ClpXP to engage its first class of substrates, which include McpA, a

chemoreceptor (62), and the cyclic di-GMP phosphodiesterase PdeA (37, 75). This priming event opens ClpXP to an array of adaptors and substrates that would have been inaccessible before such as RcdA, which binds a CpdR-primed ClpX directly to establish the third tier of the hierarchy. In this way, RcdA acts like a canonical adaptor in tethering cargo to ClpXP to enhance delivery of a second class of substrates, including the developmental regulator TacA and various proteins of unknown function (38).

The pinnacle of the hierarchy requires the addition of the adaptor PopA bound to cyclic di-GMP, which culminates in the degradation of CtrA (38, 66, 76) and likely other substrates such as GdhZ and KidO (77, 78). Strikingly, bacterial two-hybrid experiments demonstrated that PopA alleles which cannot engage cyclic di-GMP still bind RcdA (38, 76). This suggests that even in the absence of delivery, PopA can compete with the RcdA-dependent degradation of substrates like TacA, suggesting that members of the hierarchy can act as both adaptors and anti-adaptors (38, 56). Cross species comparisons find that CpdR and RcdA are highly conserved in all alpha proteobacteria, but the presence of PopA is more restricted (79), leading to the speculation that CpdR/RcdA represent a more ancient aspect of this adaptor hierarchy. Interestingly, RcdA is essential in *Agrobacterium tumefaciens* (80) , suggesting that this adaptor hierarchy might be more deeply woven into the essential physiology of other bacteria.

The costs and benefits of adaptors.

Balanced growth requires regular predictable changes in protein levels to drive replication and division. Although AAA+ proteases can have different ranges of selectivity, there is a clear need to augment their specificity through other regulators. Adaptor proteins in their most basic form can be thought of as simple tethers that locally increase the concentration of potential protease substrates. However, there is a conflict in that adaptors which bind cargo weakly may not efficiently deliver substrates to the protease while adaptors that grip cargo too tightly could also hinder the substrate degradation by the protease. Therefore, there must be an appropriate tuning of the lifetimes of the different subcomplexes involved in adaptor-dependent handoff to ensure robust degradation. Below, we illustrate how the well-characterized SspB/ssrA system demonstrates this principle.

As described previously, the SspB adaptor binds ssrA-tagged substrates and delivers them to the ClpXP protease. Bulk measurements find that GFP tagged with ssrA binds SspB with a k_{on} of ~ 5 $\mu M^{-1}s^{-1}$ at 30°C and a K_D of ~ 50 nM yielding a ~4 second lifetime for this complex (81) **(Figure 1.5).** Single-turnover experiments suggest that the limiting step for degradation by ClpXP is substrate commitment, rather than translocation or proteolysis, with an estimate of ~30 seconds for tagged GFP at saturating concentrations (82) . Therefore, cargo can be released from the adaptor's grip 7-8 times during the time that ClpXP is establishing commitment. However, if a cargo binds SspB 10-fold more tightly, with the same on rate, then this new 40 second lifetime exceeds the ClpXP commitment time and may result in paradoxically slower proteolysis.

Although such substrates have not yet been identified, this simple example illustrates the point that tighter binding of an adaptor to cargo may not result in more robust delivery to the protease and that an optimum balance likely exists between adaptor-cargo lifetimes and protease commitment timescales.

Adaptors can also serve as more than tethers. In addition to anchoring cargo to the protease, adaptor binding may also cause degrons in the cargo protein to be exposed, as described for YjbH/Spx (83) and RssB/RpoS (84, 85). Adaptors could also affect the protease itself. As described above, CpdR binds to ClpX and activates the ClpXP protease for degradation of the substrate PdeA, but CpdR on its own fails to bind PdeA (37). Binding of CpdR, or similar adaptors, may contribute to substrate engagement directly, e.g., providing additional low affinity contacts, or may affect ClpXP substrate engagement through allosteric changes of ClpX itself. Given our discussion above regarding the balance of protease commitment and adaptor-cargo lifetimes, it is tempting to consider that some adaptors may influence protease specificity through altering the commitment time of the protease rather than changing its ability to directly recognize a target.

Regulated proteolysis during changes in growth phase

Bacteria are constantly being challenged in their environments with changing conditions, such as nutrient deprivation, that necessitate a swift response. Regulated proteolysis is required for bacteria to undergo the necessary physiological transitions and adaptation needed for survival and persistence. An

example of this is the transition from logarithmic growth to stationary phase, when growth slows and cells alter their metabolism to accommodate this change in phase (86). This transition requires σ^S, also known as RpoS, an alternative sigma factor that can compete with σ^{70} during stationary phase to significantly alter gene expression profiles. During logarithmic growth, RpoS is rapidly degraded to undetectable levels by ClpXP with the required assistance of the adaptor RssB (85, 87) **(Figure 1.6a)**.

During entry to stationary phase, RpoS becomes stabilized and produces a surge in transcription of RpoS regulated genes (88, 89). Inhibition of RssB activity is accomplished by a group of anti-adaptors, each specific for a particular stress response. In *E. coli*, three anti-adaptors have been identified, IraP (Inhibitor of RssB activity during phosphate starvation), IraD (Inhibitor of RssB activity during DNA damage), and IraM (Inhibitor of RssB activity during magnesium starvation). Interestingly, each anti-adaptor binds to RssB in a different binding mode (2, 90, 91). IraP binds at the C-terminal domain of RssB while IraD interacts with the N-terminal domain, and IraM has been shown to make interactions with both domains. This example shows how a family of distinct anti-adaptors, each binding at a characteristic location, can each prevent the degradation of RpoS, allowing the cell to mount a rapid universal program in response to a variety of stresses.

In nutrient-poor conditions, *Bacillus subtilis* initiates a sporulation program resulting in mature spores that can withstand harsh environmental conditions. The structural protein SpoIVA is required for proper assembly of the spore

envelope. To ensure the fidelity of the sporulation program, *Bacillus* relies on regulated proteolysis as a quality control mechanism to remove spore envelopes that have been improperly assembled (92) **(Figure 1.6b)**. In sporulation defective cells, CmpA, an adaptor, delivers SpoIVA to ClpXP for degradation, ultimately leading to the lysis and removal of the defective cell from the population. However, in cells that properly constructed the spore envelope, CmpA is degraded, preventing the degradation of SpoIVA and allowing cells to continue the process of sporulation.

Bacteria growing in a liquid environment use flagella to swim in three-dimensional space. When shifted to solid media, bacteria transition their mode of motility from swimming to swarming. In *Bacillus subtilis*, this transition requires Lon-dependent degradation of SwrA, a master regulator of flagellar biosynthesis (93) **(Figure 1.6c)**. When *Bacillus* is in a liquid environment, Lon robustly degrades SwrA in the presence of SmiA, a Lon-specific adaptor protein. Lon was unable to degrade SwrA both *in vivo* as well as *in vitro* in the absence of SmiA. When *Bacillus* transitions to a solid surface, Lon-mediated degradation is inhibited via an unknown mechanism and SwrA levels increase, resulting in increased flagellar density which is necessary for swarming motility. Intriguingly, SmiA was the first Lon-specific adaptor to be discovered, but more recent work using a Lon trapping approach has led to the discovery of HspQ, a conserved, small heat shock protein, that can also enhance Lon-dependent degradation of known substrates in the gram-negative bacterium *Yersinia pestis* (39). Understanding how Lon activity can be controlled in so many different ways and

the consequences of this regulation is an outstanding question clearly worth exploring.

Proteolytic responses in response to starvation

Amino acids are the building blocks of proteins and all organisms must be able to accurately assess amino acid levels to avoid costly interruptions in protein synthesis (94). In times of amino acid starvation, protein degradation could replenish amino acid pools. In eukaryotes, inhibition of the ubiquitin-proteasome system results in a lethal depletion of amino acid pools which could be rescued by externally supplementing with additional amino acids or reducing translation (95). Earlier studies in *E. coli* found that starvation causes an increase in protein degradation which mirrored the rate of synthesis of new proteins (96). However, very little is currently known about how starvation mechanistically leads to amino acid recycling in bacteria.

In bacteria amino acid starvation leads to increased cellular levels of the alarmone (p)ppGpp , eliciting what is known as the stringent response (97). Increased levels of (p)ppGpp lead to many downstream effects, effectively allowing the cell to divert resources away from translation and towards amino acid biosynthesis (98). One of the effects of (p)ppGpp accumulation is the inhibition of the enzymes that break down polyphosphate, leading to increased polyphosphate levels (99). Work from Kornberg and colleagues have shown that polyphosphate can stimulate the proteolysis of ribosome subunits and other proteins by the Lon protease (100–102). This has led to the provocative

hypothesis that during amino acid stress, activation of the Lon protease via ppGpp/polyphosphate induction will reduce ribosome pools to slow down translation and replenish pools of amino acids. Although recent work suggests that polyphosphate activation of Lon proteolysis may not be a universal feature for all substrates (103) , the ability of regulated proteases such as Lon to contribute to nutrient stress responses to improve survival under starvation conditions is a very appealing notion. Indeed, prior work has shown that loss of energy dependent proteases in bacteria yields compromised responses to starvation (104, 105).

1.6 Perspective

Energy dependent proteases can differ dramatically in architecture and substrate preference. However, a recurring theme is that regulated proteolysis requires two elements for robust controlled substrate degradation. All substrates must contain some type of recognition determinant that can be engaged by the protease in order to begin unfolding and processing. This determinant can be highly sequence dependent, as in the case of ssrA and ClpXP, or it can be more general, as seen with recognition of hydrophobic residues by Lon. To truly maintain regulation, these determinants are further elaborated by modifying factors such as adaptors that deliver substrates directly or prime the protease for substrate recognition. These modifiers can also be a property of the protein itself, e.g., protein dynamics that cause transient or extended display of residues normally in the hydrophobic core. Finally, substrates themselves can act as

modifiers to alter the specific activity of a protease in an effort to mount an effective stress response.

From a therapeutic perspective, physiological consequences of protease loss are especially apparent during stressful situations, such as when pathogens invade their hosts. Therefore, these proteases would be opportune targets to explore for the development of future antibiotics. Indeed, recent studies have shown that small molecule inhibitors of both Clp and Lon family proteases can be highly efficacious for various bacteria (106–108). Perhaps most intriguingly is the fact that unconstrained activation of these proteases could be as toxic to the bacteria (or more so) than inhibition. As a recent illustration of this possibility, the ClpP activating acyldepsipeptide ADEP was able to eradicate *Staphylococcus aureus* even in conditions where the cells were tolerant of other antibiotics (109).

1.7 Acknowledgments

The authors wish to thank E. Strieter, all members of the Chien lab, and members that make up the Protein Homeostasis group in the Institute for Applied Life Sciences for invaluable feedback. Work in the Chien lab was provided in part by a grant from the National Institutes of Health (R01GM111706) to PC and from a Chemistry Biology Interface Program Training Grant (NIH T32GM08515) to SM.

1.8 Literature Cited

1. Strieter ER, Korasick DA. 2012. Unraveling the complexity of ubiquitin signaling. *ACS Chem. Biol.* 7(1):52–63

2. Gur E, Biran D, Ron EZ. 2011. Regulated proteolysis in Gram-negative bacteria — how and when? *Nat Rev Microbiol*. 9(12):839–48
3. Olivares AO, Baker TA, Sauer RT. 2016. Mechanistic insights into bacterial AAA+ proteases and protein-remodelling machines. *Nat. Rev. Microbiol.* 14(1):33–44
4. Gottesman S. 1996. Proteases and their targets in Escherichia coli. *Annu. Rev. Genet.* 30:465–506
5. Breidenstein EBM, Janot L, Strehmel J, Fernandez L, Taylor PK, et al. 2012. The Lon Protease Is Essential for Full Virulence in Pseudomonas aeruginosa. *PLoS One*. 7(11):e49123
6. Kanemori M, Nishihara K, Yanagi H, Yura T. 1997. Synergistic roles of Hs1VU and other ATP-dependent proteases in controlling in vivo turnover of ??32 and abnormal proteins in Escherichia coli. *J. Bacteriol.* 179(23):7219–25
7. Howard-Flanders P, Simson E, Theriot L. 1964. A locus that controls filament formation and sensitiviry to radiation in Escherichia coli K-12. *Genetics*. 49(February):237–46
8. Jenal U, Fuchs T. 1998. An essential protease involved in bacterial cell-cycle control. *EMBO J.* 17(19):5658–69
9. Rogers A, Townsley L, Gallego-hernandez AL, Beyhan S, Kwuan L, Yildiz FH. 2016. The LonA Protease Regulates Biofilm Formation, Motility, Virulence, and the Type VI Secretion System in Vibrio cholerae. *J. Bacteriol.* 198(6):973–85

10. Baker TA, Sauer RT. 2006. ATP-dependent proteases of bacteria: recognition logic and operating principles. *Trends Biochem. Sci.* 31(12):647–53
11. Lee I, Suzuki CK. 2008. Functional mechanics of the ATP-dependent Lon protease- lessons from endogenous protein and synthetic peptide substrates. *Biochim. Biophys. Acta - Proteins Proteomics*. 1784(5):727–35
12. Langklotz S, Baumann U, Narberhaus F. 2012. Structure and function of the bacterial AAA protease FtsH. *Biochim. Biophys. Acta - Mol. Cell Res.* 1823(1):40–48
13. Baker TA, Sauer RT. 2012. ClpXP, an ATP-powered unfolding and protein-degradation machine. *Biochim. Biophys. Acta - Mol. Cell Res.* 1823(1):15–28
14. Gottesman S. 2003. Proteolysis in bacterial regulatory circuits. *Annu. Rev. Cell Dev. Biol.* 19(1):565–87
15. Rawlings ND, Barrett AJ, Finn R. 2016. Twenty years of the MEROPS database of proteolytic enzymes, their substrates and inhibitors. *Nucleic Acids Res.* 44(D1):D343–50
16. Kenniston JA, Baker TA, Fernandez JM, Sauer RT. 2003. Linkage between ATP consumption and mechanical unfolding during the protein processing reactions of an AAA+ degradation machine. *Cell*. 114(4):511–20
17. Kraut DA. 2013. Slippery substrates impair ATP-dependent protease function by slowing unfolding. *J. Biol. Chem.* 288(48):34729–35
18. Vass RH, Chien P. 2013. Critical clamp loader processing by an essential

AAA+ protease in Caulobacter crescentus. *Proc. Natl. Acad. Sci. U. S. A.* 110(45):18138–43

19. Koodithangal P, Jaffe NE, Kraut DA, Fishbain S, Herman C, Matouschek A. 2009. ATP-dependent proteases differ substantially in their ability to unfold globular proteins. *J. Biol. Chem.* 284(28):18674–84
20. Olivares AO, Nager AR, Iosefson O, Sauer RT, Baker TA. 2014. Mechanochemical basis of protein degradation by a double-ring AAA+ machine. *Nat. Struct. Mol. Biol.* 21(10):871–75
21. Maillard RA, Chistol G, Sen M, Righini M, Tan J, et al. 2011. ClpX(P) generates mechanical force to unfold and translocate its protein substrates. *Cell*. 145(3):459–69
22. Aubin-Tam ME, Olivares AO, Sauer RT, Baker TA, Lang MJ. 2011. Single-molecule protein unfolding and translocation by an ATP-fueled proteolytic machine. *Cell*. 145(2):257–67
23. Konovalova A, Søgaard-Andersen L, Kroos L. 2014. Regulated proteolysis in bacterial development. *FEMS Microbiol. Rev.* 38(3):493–522
24. Mogk A, Huber D, Bukau B. 2011. Integrating protein homeostasis strategies in prokaryotes. *Cold Spring Harb. Perspect. Biol.* 3(4):1–19
25. Bezawork-Geleta A, Brodie EJ, Dougan DA, Truscott KN. 2015. LON is the master protease that protects against protein aggregation in human mitochondria through direct degradation of misfolded proteins. *Sci. Rep.* 5(October):17397
26. Van Melderen L, Aertsen A. 2009. Regulation and quality control by Lon-

dependent proteolysis. *Res. Microbiol.* 160(9):645–51

27. Chung CH, Goldberg AL. 1981. The product of the lon (capR) gene in Escherichia coli is the ATP-dependent protease, protease La. *Proc. Natl. Acad. Sci. U. S. A.* 78(8):4931–35
28. Flynn JM, Levchenko I, Seidel M, Wickner SH, Sauer RT, Baker TA. 2001. Overlapping recognition determinants within the ssrA degradation tag allow modulation of proteolysis. *Proc. Natl. Acad. Sci. U. S. A.* 98(19):10584–89
29. Flynn JM, Neher SB, Kim YI, Sauer RT, Baker TA. 2003. Proteomic discovery of cellular substrates of the ClpXP protease reveals five classes of ClpX-recognition signals. *Mol. Cell*. 11(3):671–83
30. Keiler KC, Waller PRH, Sauer RT. 1996. Role of a Peptide Tagging System in Degradation of Proteins Synthesized from Damaged Messenger RNA. *Science (80-.).* 271(5251):990–93
31. Lies M, Maurizi MR. 2008. Turnover of endogenous SsrA-tagged proteins mediated by ATP-dependent proteases in Escherichia coli. *J. Biol. Chem.* 283(34):22918–29
32. Li X, Yagi M, Morita T, Aiba H. 2008. Cleavage of mRNAs and role of tmRNA system under amino acid starvation in Escherichia coli. *Mol. Microbiol.* 68(2):462–73
33. Christensen SK, Pedersen K, Hansen FG, Gerdes K. 2003. Toxin-antitoxin loci as stress-response-elements: ChpAK/MazF and ChpBK cleave translated RNAs and are counteracted by tmRNA. *J. Mol. Biol.* 332(4):809–19

34. Levchenko I, Seidel M, Sauer RT, Baker TA. 2000. A Specificity-Enhancing Factor for the ClpXP Degradation Machine. *Science (80-.).* 289(5488):2354–56

35. Bolon DN, Wah DA, Hersch GL, Baker TA, Sauer RT. 2004. Bivalent Tethering of SspB to ClpXP Is Required for Efficient Substrate Delivery: A Protein-Design Study. *Mol. Cell*. 13(3):443–49

36. Levchenko I, Grant R a, Flynn JM, Sauer RT, Baker T a. 2005. Versatile modes of peptide recognition by the AAA+ adaptor protein SspB. *Nat. Struct. Mol. Biol.* 12(6):520–25

37. Lau J, Hernandez-Alicea L, Vass RH, Chien P. 2015. A Phosphosignaling Adaptor Primes the AAA+ Protease ClpXP to Drive Cell Cycle-Regulated Proteolysis. *Mol. Cell*. 59(1):104–16

38. Joshi KK, Bergé M, Radhakrishnan SK, Viollier PH, Chien P. 2015. An Adaptor Hierarchy Regulates Proteolysis during a Bacterial Cell Cycle. *Cell*. 163(2):419–31

39. Puri N, Karzai AW. 2017. HspQ Functions as a Unique Specificity-Enhancing Factor for the AAA+ Lon Protease. *Mol. Cell*. 66(5):672–683.e4

40. Gur E, Sauer RT. 2008. Recognition of misfolded proteins by Lon, a AAA+ protease. *Genes Dev.* 22(16):2267–77

41. Gur E. 2013. The Lon AAA+ Protease. In *Regulated Proteolysis in Microorganisms*. 66:35–51

42. Arndt V, Rogon C, Höhfeld J. 2007. To be, or not to be - Molecular chaperones in protein degradation. *Cell. Mol. Life Sci.* 64(19–20):2525–41

43. Melderen L Van, Hoa M, Thi D, Lecchi P, Gottesman S, et al. 1996. ATP-dependent Degradation of CcdA by Lon Protease. *J. Biol. Chem.* 271(44):27730–38

44. Kunová N, Ondrovičová G, Bauer JA, Bellová J, Ambro Ľ, et al. 2017. The role of Lon-mediated proteolysis in the dynamics of mitochondrial nucleic acid-protein complexes. *Sci. Rep.* 7(1):631

45. Lu B, Lee J, Nie X, Li M, Morozov YI, et al. 2013. Phosphorylation of Human TFAM in Mitochondria Impairs DNA Binding and Promotes Degradation by the AAA+ Lon Protease. *Mol. Cell*. 49(1):121–32

46. Kubik S, Wegrzyn K, Pierechod M, Konieczny I. 2012. Opposing effects of DNA on proteolysis of a replication initiator. *Nucleic Acids Res.* 40(3):1148–59

47. Ambro L, Pevala V, Bauer J, Kutejová E. 2012. The influence of ATP-dependent proteases on a variety of nucleoid-associated processes. *J. Struct. Biol.* 179(2):181–92

48. Karlowicz A, Wegrzyn K, Gross M, Kaczynska D, Ropelewska M, et al. 2017. Defining the crucial domain and amino acid residues in bacterial Lon protease for DNA binding and processing of DNA-interacting substrates. *J. Biol. Chem.* 292(18):7507–18

49. Chung CH, Goldberg a L. 1982. DNA stimulates ATP-dependent proteolysis and protein-dependent ATPase activity of protease La from Escherichia coli. *Proc. Natl. Acad. Sci. U. S. A.* 79(3):795–99

50. Waxman L, Goldberg AL. 1986. Selectivity of intracellular proteolysis:

protein substrates activate the ATP-dependent protease (La). *Science*. 232(4749):500–503

51. Gur E, Sauer RT. 2009. Degrons in protein substrates program the speed and operating efficiency of the AAA+ Lon proteolytic machine. *Proc. Natl. Acad. Sci. U. S. A.* 106(44):18503–8
52. Jonas K, Liu J, Chien P, Laub MT. 2013. Proteotoxic stress induces a cell-cycle arrest by stimulating Lon to degrade the replication initiator DnaA. *Cell*. 154(3):623–36
53. Christensen SK, Maenhaut-Michel G, Mine N, Gottesman S, Gerdes K, Van Melderen L. 2004. Overproduction of the Lon protease triggers inhibition of translation in Escherichia coli: Involvement of the yefM-yoeB toxin-antitoxin system. *Mol. Microbiol.* 51(6):1705–17
54. Vodermaier HC. 2004. APC/C and SCF: Controlling each other and the cell cycle. *Curr. Biol.* 14(18):787–96
55. Skerker JM, Laub MT. 2004. Cell-cycle progression and the generation of asymmetry in Caulobacter crescentus. *Nat. Rev. Microbiol.* 2(4):325–37
56. Joshi KK, Chien P. 2016. Regulated Proteolysis in Bacteria: Caulobacter. *Annu. Rev. Genet.* 50:423–45
57. Quon KC, Marczynski GT, Shapiro L. 1996. Cell cycle control by an essential bacterial two-component signal transduction protein. *Cell*. 84(1):83–93
58. Quon KC, Yang B, Domian IJ, Shapiro L, Marczynski GT. 1998. Negative control of bacterial DNA replication by a cell cycle regulatory protein that

binds at the chromosome origin. *Proc. Natl. Acad. Sci. U. S. A.* 95(1):120–25

59. Laub MT, Chen SL, Shapiro L, McAdams HH. 2002. Genes directly controlled by CtrA, a master regulator of the Caulobacter cell cycle. *Proc. Natl. Acad. Sci. U. S. A.* 99(7):4632–37

60. Lori C, Ozaki S, Steiner S, Böhm R, Abel S, et al. 2015. Cyclic di-GMP acts as a cell cycle oscillator to drive chromosome replication. *Nature*. 523(7559):236–39

61. Biondi EG, Reisinger SJ, Skerker JM, Arif M, Perchuk BS, et al. 2006. Regulation of the bacterial cell cycle by an integrated genetic circuit. *Nature*. 444(7121):899–904

62. Iniesta A a, McGrath PT, Reisenauer A, McAdams HH, Shapiro L. 2006. A phospho-signaling pathway controls the localization and activity of a protease complex critical for bacterial cell cycle progression. *Proc. Natl. Acad. Sci. U. S. A.* 103(29):10935–40

63. Domian IJ, Quon KC, Shapiro L. 1997. Cell-type specific phosphorylation and proteolysis of a transcriptional regulator controls the G1 to S transition in a bacterial cell cycle. *Cell*. 90:415–24

64. McGrath PT, Iniesta AA, Ryan KR, Shapiro L, McAdams HH. 2006. A dynamically localized protease complex and a polar specificity factor control a cell cycle master regulator. *Cell*. 124(3):535–47

65. Chien P, Perchuk BS, Laub MT, Sauer RT, Baker T a. 2007. Direct and adaptor-mediated substrate recognition by an essential AAA+ protease.

Proc. Natl. Acad. Sci. U. S. A. 104(16):6590–95

66. Smith SC, Joshi KK, Zik JJ, Trinh K, Kamajaya A, et al. 2014. Cell cycle-dependent adaptor complex for ClpXP-mediated proteolysis directly integrates phosphorylation and second messenger signals. *Proc. Natl. Acad. Sci.* 111(39):14229–34
67. Gora KG, Cantin A, Wohlever M, Joshi KK, Perchuk BS, et al. 2013. Regulated proteolysis of a transcription factor complex is critical to cell cycle progression in Caulobacter crescentus. *Mol. Microbiol.* 87(6):1277–89
68. Siam R, Marczynski GT. 2000. Cell cycle regulator phosphorylation stimulates two distinct modes of binding at a chromosome replication origin. *EMBO J.* 19(5):1138–47
69. Haeusser DP, Lee AH, Weart RB, Levin PA. 2009. ClpX Inhibits FtsZ Assembly in a manner that does not require its ATP hydrolysis-dependent chaperone activity. *J. Bacteriol.* 191(6):1986–91
70. Camberg JL, Hoskins JR, Wickner S. 2009. ClpXP protease degrades the cytoskeletal protein, FtsZ, and modulates FtsZ polymer dynamics. *Proc Natl Acad Sci U S A*. 106(26):10614–19
71. Camberg JL, Hoskins JR, Wickner S. 2011. The Interplay of ClpXP with the cell division machinery in Escherichia coli. *J. Bacteriol.* 193(8):1911–18
72. Williams B, Bhat N, Chien P, Shapiro L. 2014. ClpXP and ClpAP proteolytic activity on divisome substrates is differentially regulated following the Caulobacter asymmetric cell division. *Mol. Microbiol.* 93(5):853–66

73. Bhat NH, Vass RH, Stoddard PR, Shin DK, Chien P. 2013. Identification of ClpP substrates in Caulobacter crescentus reveals a role for regulated proteolysis in bacterial development. *Mol. Microbiol.* 88(6):1083–92

74. Michalik S, Bernhardt J, Otto a., Moche M, Becher D, et al. 2012. Life and Death of Proteins: A Case Study of Glucose-starved Staphylococcus aureus. *Mol. Cell. Proteomics*. 11(9):558–70

75. Abel S, Chien P, Wassmann P, Schirmer T, Kaever V, et al. 2011. Regulatory Cohesion of Cell Cycle and Cell Differentiation through Interlinked Phosphorylation and Second Messenger Networks. *Mol. Cell*. 43(4):550–60

76. Folcher M, Nicollier M, Schwede T, Amiot N, Duerig A. 2009. Second messenger-mediated spatiotemporal control of protein degradation regulates bacterial cell cycle progression. *Genes Dev.* 23:93–104

77. Beaufay F, Coppine J, Mayard A, Laloux G, Bolle X De, Hallez R. 2015. A NAD-dependent glutamate dehydrogenase coordinates metabolism with cell division in Caulobacter crescentus. *EMBO J.* 34(13):1–15

78. Radhakrishnan SK, Pritchard S, Viollier PH. 2010. Coupling Prokaryotic Cell Fate and Division Control with a Bifunctional and Oscillating Oxidoreductase Homolog. *Dev. Cell*. 18(1):90–101

79. Ozaki S, Schalch-Moser A, Zumthor L, Manfredi P, Ebbensgaard A, et al. 2014. Activation and polar sequestration of PopA, a c-di-GMP effector protein involved in Caulobacter crescentus cell cycle control. *Mol. Microbiol.* 94(3):580–94

80. Curtis PD, Brun Y V. 2014. Identification of essential alphaproteobacterial genes reveals operational variability in conserved developmental and cell cycle systems. *Mol. Microbiol.* 93(4):713–35

81. Hersch GL, Baker TA, Sauer RT. 2004. SspB delivery of substrates for ClpXP proteolysis probed by the design of improved degradation tags. *Proc. Natl. Acad. Sci.* 101(33):12136–41

82. Cordova JC, Olivares AO, Shin Y, Stinson BM, Calmat S, et al. 2014. Stochastic but highly coordinated protein unfolding and translocation by the ClpXP proteolytic machine. *Cell*. 158(3):647–58

83. Chan CM, Hahn E, Zuber P. 2014. Adaptor bypass mutations of Bacillus subtilisspx suggest a mechanism for YjbH-enhanced proteolysis of the regulator Spx by ClpXP. *Mol. Microbiol.* 93(3):426–38

84. Stüdemann A, Noirclerc-Savoye M, Klauck E, Becker G, Schneider D, Hengge R. 2003. Sequential recognition of two distinct sites in σS by the proteolytic targeting factor RssB and ClpX. *EMBO J.* 22(16):4111–20

85. Zhou Y, Gottesman S, Hoskins JR, Maurizi MR, Wickner S. 2001. The RssB response regulator directly targets σS for degradation by ClpXP. *Genes Dev.* 15(5):627–37

86. Hengge R. 2009. Proteolysis of σS (RpoS) and the general stress response in Escherichia coli. *Res. Microbiol.* 160(9):667–76

87. Jishage M, Ishihama A. 1995. Regulation of RNA polymerase sigma subunit synthesis in Escherichia coli: intracellular levels of sigma 70 and sigma 38. *J. Bacteriol.* 177(23):6832–35

88. Pratt LA, Silhavy TJ. 1996. The response regulator SprE controls the stability of RpoS. *Proc. Natl. Acad. Sci. U. S. A.* 93(6):2488–92

89. Muffler A, Fischer D, Altuvia S, Storz G, Hengge-Aronis R. 1996. The response regulator RssB controls stability of the sigma(S) subunit of RNA polymerase in Escherichia coli. *EMBO J.* 15(6):1333–39

90. Micevski D, Zammit JE, Truscott KN, Dougan DA. 2015. Anti-adaptors use distinct modes of binding to inhibit the RssB-dependent turnover of RpoS (σ(S)) by ClpXP. *Front. Mol. Biosci.* 2(April):15

91. Battesti A, Hoskins JR, Tong S, Milanesio P, Mann JM, et al. 2013. Anti-adaptors provide multiple modes for regulation of the RssB adaptor protein. *Genes Dev.* 27(24):2722–35

92. Tan IS, Weiss CA, Popham DL, Ramamurthi KS. 2015. A Quality-Control Mechanism Removes Unfit Cells from a Population of Sporulating Bacteria. *Dev. Cell*. 34(6):682–93

93. Mukherjee S, Bree AC, Liu J, Patrick JE, Chien P, Kearns DB. 2014. Adaptor-mediated Lon proteolysis restricts Bacillus subtilis hyperflagellation. *Proc. Natl. Acad. Sci. U. S. A.* 112(1):1–6

94. Efeyan A, Comb WC, Sabatini DM. 2015. Nutrient-sensing mechanisms and pathways. *Nature*. 517(7534):302–10

95. Suraweera A, Münch C, Hanssum A, Bertolotti A. 2012. Failure of amino acid homeostasis causes cell death following proteasome inhibition. *Mol. Cell*. 48(2):242–53

96. Mandelstam J. 1957. Turnover of protein in starved bacteria and its

relationship to the induced synthesis of enzyme. *Nature*. 179:1179–81

97. Hauryliuk V, Atkinson GC, Murakami KS, Tenson T, Gerdes K. 2015. Recent functional insights into the role of (p)ppGpp in bacterial physiology. *Nat. Rev. Microbiol.* 13(5):298–309

98. Srivatsan A, Wang JD. 2008. Control of bacterial transcription, translation and replication by (p)ppGpp. *Curr. Opin. Microbiol.* 11(2):100–105

99. Kuroda A, Murphy H, Cashel M, Kornberg A. 1997. Guanosine tetra- and pentaphosphate promote accumulation of inorganic polyphosphate in Escherichia coli. *J. Biol. Chem.* 272(34):21240–43

100. Kuroda A. 2001. Role of Inorganic Polyphosphate in Promoting Ribosomal Protein Degradation by the Lon Protease in E. coli. *Science (80-.).* 293(5530):705–8

101. Nomura K, Kato J, Takiguchi N, Ohtake H, Kuroda A. 2004. Effects of inorganic polyphosphate on the proteolytic and DNA-binding activities of Lon in Escherichia coli. *J. Biol. Chem.* 279(33):34406–10

102. Nomura K, Kato J, Takiguchi N, Ohtake H, Kuroda A. 2006. Inorganic polyphosphate stimulates lon-mediated proteolysis of nucleoid proteins in Escherichia coli. *Cell. Mol. Biol.* 52(4):23–29

103. Osbourne DO, Soo VW, Konieczny I, Wood TK. 2014. Polyphosphate, cyclic AMP, guanosine tetraphosphate, and c-di-GMP reduce in vitro Lon activity. *Bioengineered*. 5(4):264–68

104. Reeve CA, Bockman AT, Matin A. 1984. Role of Protein Degradation in the Survival of Carbon-Starved Escherichia coli and Salmonella typhimurium.

J. Bacteriol. 157(3):758–63

105. Damerau K, John ACS. 1993. Role of Clp protease subunits in degradation of carbon starvation proteins in Escherichia coli. *J. Bacteriol.* 175(1):53–63
106. Fetzer C, Korotkov VS, Thänert R, Lee KM, Neuenschwander M, et al. 2017. A Chemical Disruptor of the ClpX Chaperone Complex Attenuates Multiresistant Staphylococcus aureus Virulence. *Angew. Chemie*
107. Compton CL, Schmitz KR, Sauer RT, Sello JK. 2013. Antibacterial activity of and resistance to small molecule inhibitors of the clpp peptidase. *ACS Chem. Biol.* 8(12):2669–77
108. Famulla K, Sass P, Malik I, Akopian T, Kandror O, et al. 2016. Acyldepsipeptide antibiotics kill mycobacteria by preventing the physiological functions of the ClpP1P2 protease. *Mol. Microbiol.* 101(2):194–209
109. Conlon BP, Nakayasu ES, Fleck LE, LaFleur MD, Isabella VM, et al. 2013. Activated ClpP kills persisters and eradicates a chronic biofilm infection. *Nature*. 503(7476):365–70

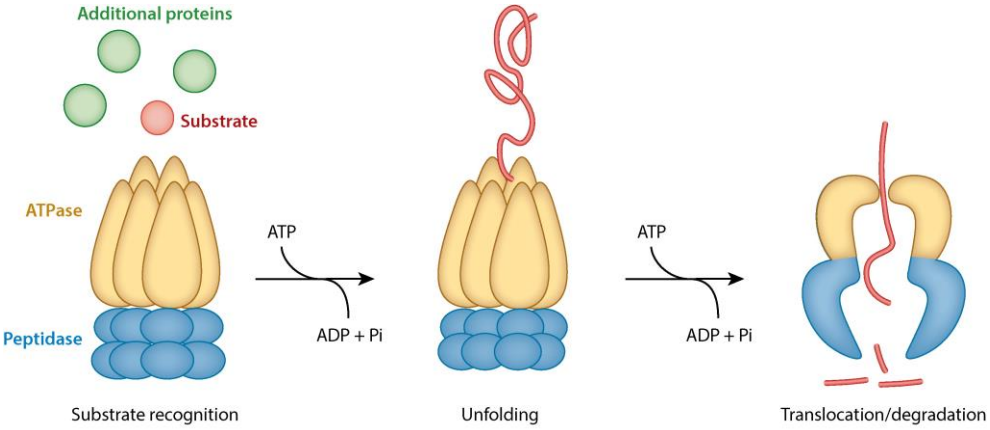

Figure 1.1 Energy-dependent proteases are composed of an ATP-hydrolysis active unfoldase domain and a chambered peptidase domain. Through successive rounds of ATP hydrolysis, a specific substrate protein is selected by the protease, unfolded by the ATPase domain, and translocated through a central pore to the peptidase chamber where it is degraded.

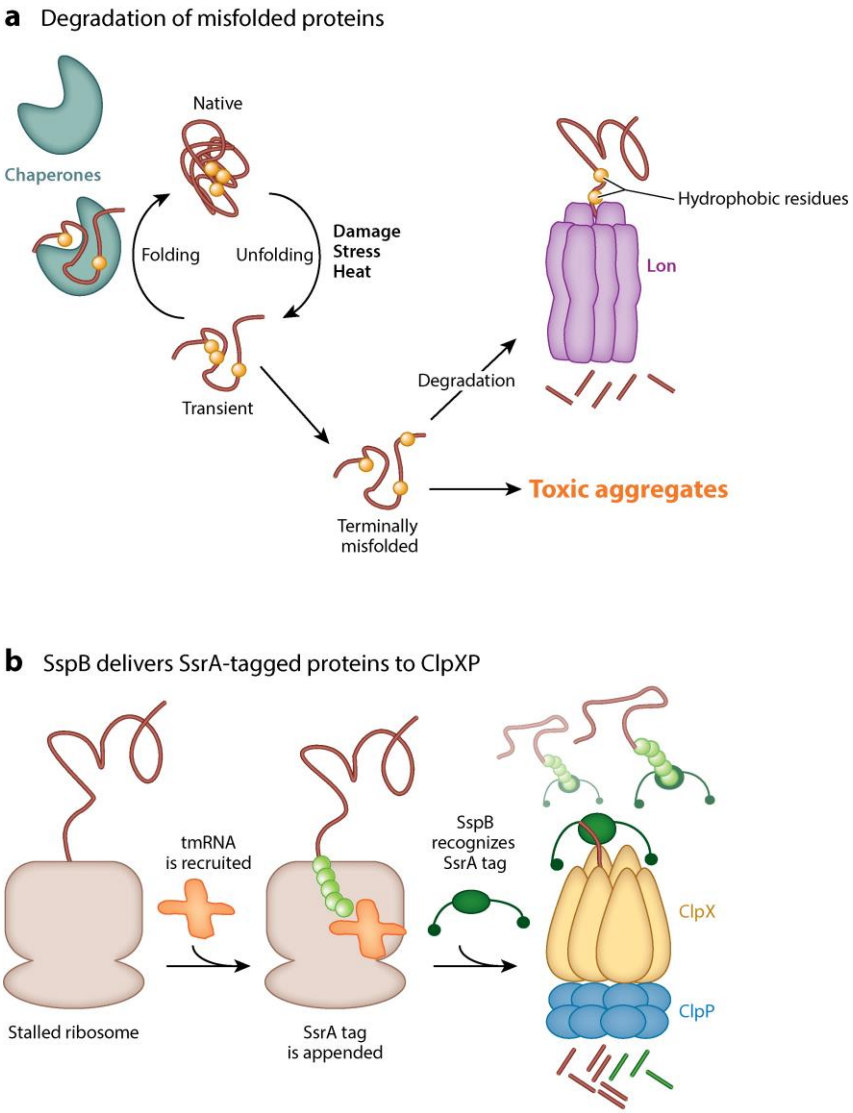

Figure 1.2 Proteases can survey protein quality in the cell. (*a*) Competition between chaperones and proteases dictates the fate of proteins. Proteases, such as Lon, must be able to distinguish between normal protein dynamics with transient excursions into non-native states and terminally misfolded proteins that must be degraded before forming toxic aggregates. Lon recognizes hydrophobic motifs (*yellow circles*) that are usually buried in the core of a native protein. These motifs are exposed more persistently for misfolded proteins than during the transient fluctuations of properly folded proteins, allowing Lon to recognize

and degrade the terminally misfolded proteins. Chaperones contribute to this flux by binding misfolded proteins in an effort to refold them. (*b*) Following the process of *trans*-translation, in which an ssrA tag is appended to incomplete polypeptides, the adaptor SspB binds tagged substrates and tethers them to ClpXP, enhancing the protease's ability to degrade these substrates.

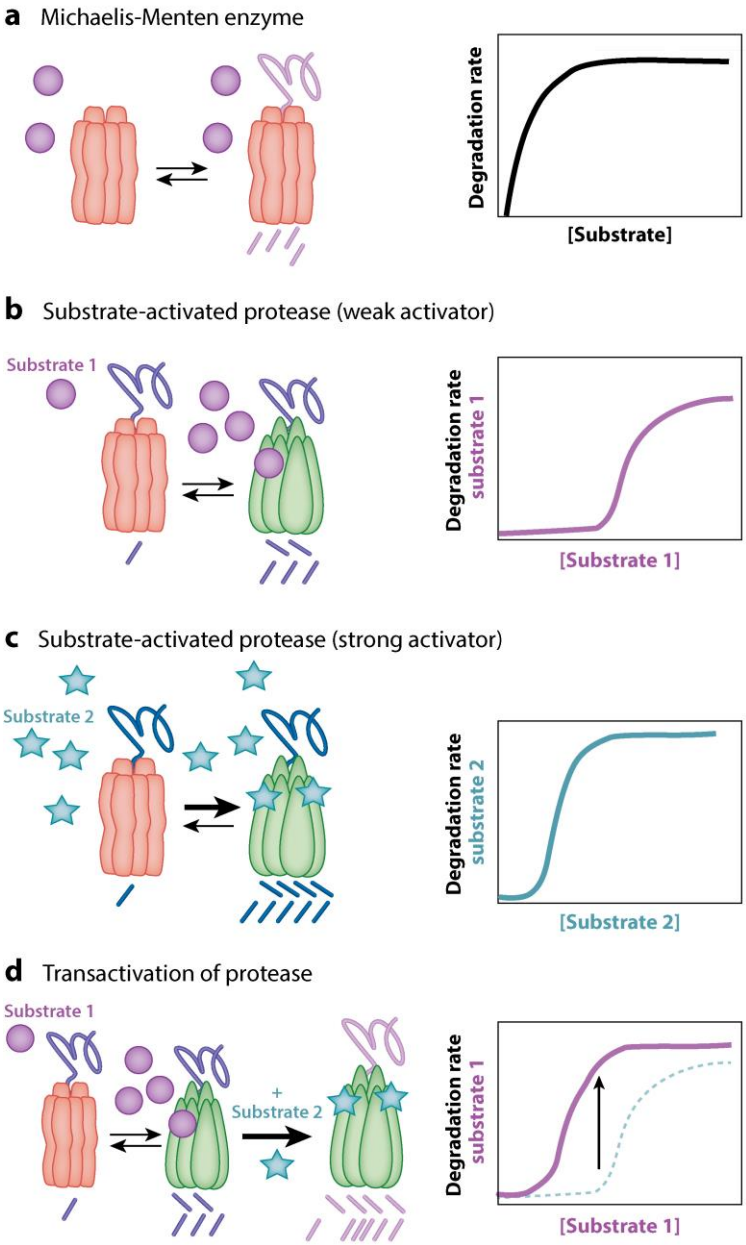

Figure 1.3 Lon is subject to allosteric regulation. (*a*) Many proteases, such as ClpXP and ClpAP, adhere to typical Michaelis-Menten kinetics, and adding increasing amounts of substrate will increase the rates of degradation until the protease becomes saturated and V_{max} is reached, resulting in the classic hyperbolic curve. This contrasts with Lon, which exhibits positive cooperativity upon increasing substrate concentration. The working model is that Lon exists in low (*red protease*) and high (*green protease*) activity states with substrate binding promoting the highly active state. (*b*) In the case of substrate 1, which binds Lon poorly, activation requires much higher concentrations of the substrate to shift Lon to the active state. (*c*) Substrate 2 has a strong affinity for Lon, and relatively low amounts of substrate are needed for activation. (*d*) If the concentration of substrate 1 is kept the same and the high-affinity substrate 2 is added, Lon will be shifted to the active form, leading to robust degradation of the normally poorly degraded substrate 1.

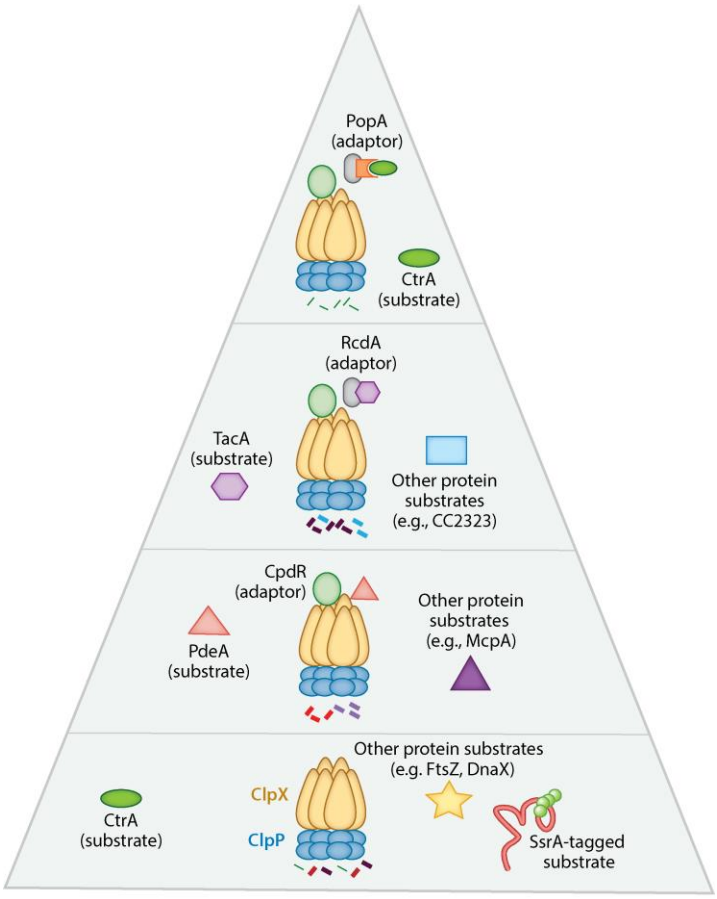

Figure 1.4 Adaptors assemble in a hierarchical manner to degrade various classes of substrates. ClpXP can degrade numerous substrates on its own, including ssrA-tagged proteins. During the G1-to-S transition in *Caulobacter crescentus*, the adaptor CpdR first primes ClpXP, allowing it to recruit the first class of substrates (PdeA, McpA, etc.) for degradation. The primed protease can now recruit another adaptor, RcdA, to degrade a second class of substrates, such as the transcription factor TacA and others. Finally, the adaptor PopA binds RcdA and in the presence of the second messenger cyclic di-GMP completes the hierarchy to deliver a third class of substrates, including the master regulator CtrA, to ClpXP. As the hierarchy is assembled and adaptors are added onto the protease, specificity increases. When ClpXP is limited, this increase in specificity

also comes at the cost of preventing degradation of other members of the substrate pool.

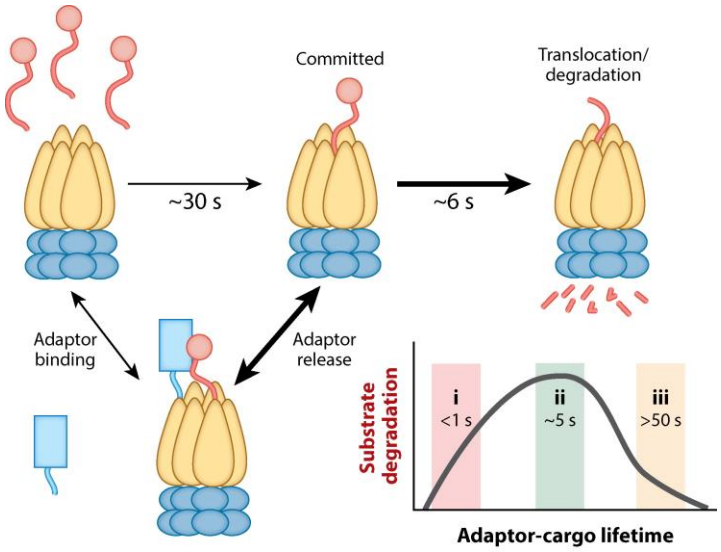

Figure 1.5 Substrate degradation by ClpXP is rate-limited by the commitment step, where the protease initially engages a target, rather than the unfolding or translocation steps, which are relatively fast. Commitment is estimated to be ~30 s for degradation of tagged GFP by ClpXP (82). Tethering adaptors (such as SspB and RcdA) enhance degradation of substrate, but the strength of the interaction between the adaptor and substrate must be tuned to the commitment time for the protease (*ii*). Poor adaptor-cargo binding results in failure to deliver (*i*), but binding too tightly (*iii*) hinders substrate release during the commitment step for protease engagement of the substrate.

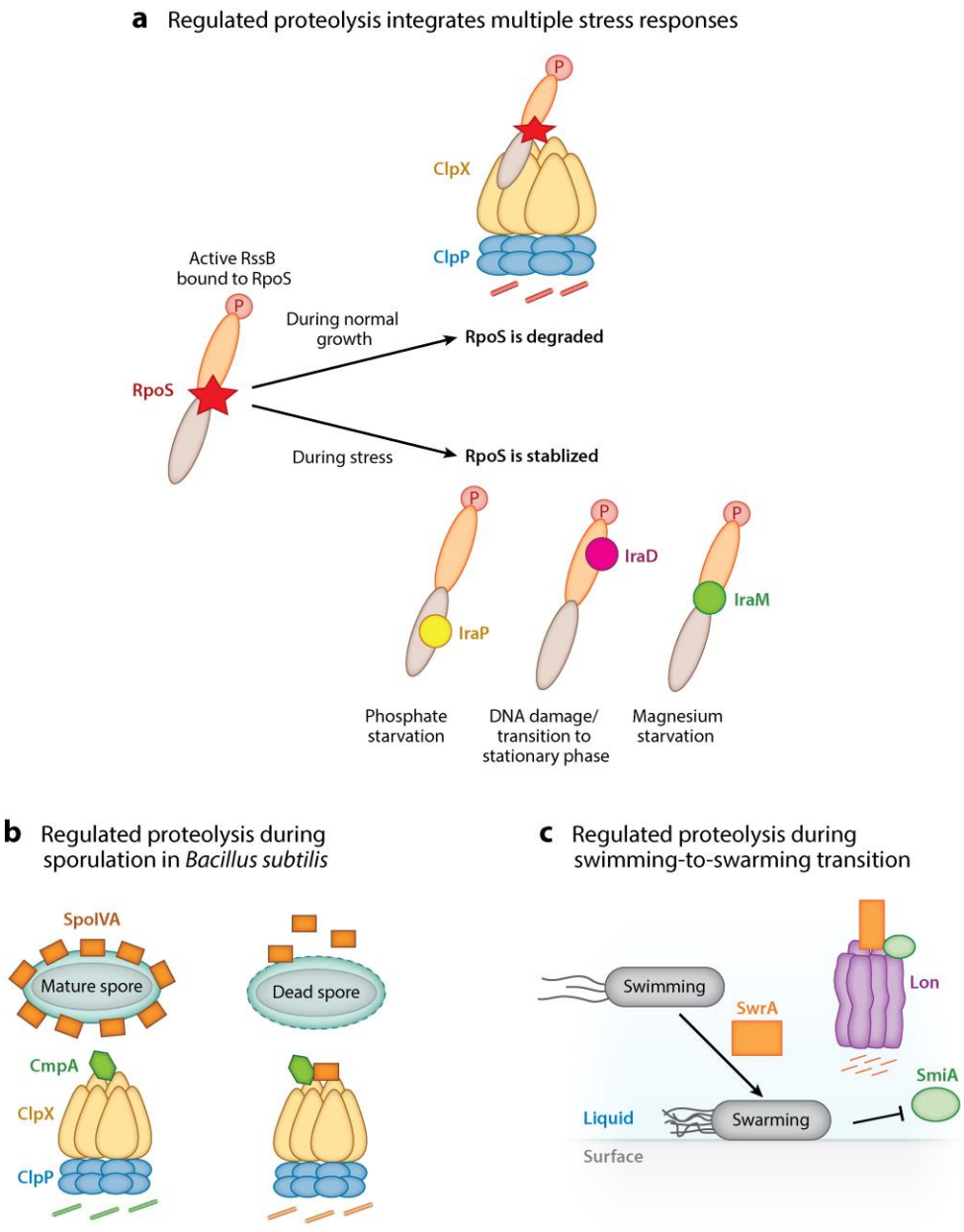

Figure 1.6 Regulated proteolysis is required during physiological transitions and changes in growth. (*a*) When bacteria are actively growing in logarithmic phase, ClpXP rapidly degrades the alternative sigma factor RpoS in an RssB-mediated manner. When RssB is phosphorylated, it has high affinity for RpoS and can deliver it to ClpXP for degradation. Anti-adaptors bind to RssB in different binding modes that depend on the kind of stress the bacteria encounters, preventing it

from delivering RpoS for degradation. (*b*) *Bacillus subtilis* requires proteolysis by ClpXP to ensure proper spore envelope assembly. In cells with improperly assembled envelopes, the adaptor CmpA delivers SpoIVA to ClpXP for degradation, leading to lysis of the defective cell. If the spore envelope is properly assembled, the adaptor is targeted for degradation by ClpXP instead. (*c*) Lon-mediated degradation is required for proper motility during the transition from liquid to solid media. In liquid media, Lon degrades SwrA with the help of SmiA, an adaptor protein. Upon shift to solid media, degradation of SwrA is inhibited, leading to an increase in SwrA levels necessary for swarming on solid media.

Chapter Two

Plasticity in AAA+ proteases reveals ATP-dependent substrate specificity principles

Samar A. Mahmoud[1,2], Berent Aldikacti[1,2], Peter Chien[1,2*]

Author Affiliations:

[1]Department of Biochemistry and Molecular Biology, [2]Molecular and Cellular Biology Program, University of Massachusetts Amherst, Amherst, MA 01003, USA

Most of the work presented in this chapter is currently preprinted on biorxiv and has been submitted (doi: https://doi.org/10.1101/2021.08.18.456811)

Contributions: I identified the *clpX** suppressor in my rotation in the Chien lab. I went on to complete all of the *in vivo* and later *in vitro* characterization of ClpX*. I also wrote the manuscript and made all the figures. Berent Aldikacti joined the lab with expertise in RNA sequencing and data analysis. We recruited him to the project to help us with the RNA sequencing analysis. His work on this projected helped us generate Supplementary Figure 2 (Figure 2.9).

2.1 Summary

In bacteria, AAA+ proteases such as Lon and ClpXP degrade substrates with exquisite specificity to promote normal growth and stress responses. Here, we show that a mutation in the ATP binding site of ClpX shifts protease specificity to promote degradation of normally Lon-restricted substrates, suppressing much of

the pleiotropic defects of a strain lacking Lon. However, this ClpX mutant is worse at degrading normal ClpXP targets, suggesting an optimal balance in substrate preference for a given protease that is surprisingly easy to alter. Reconstitution with purified proteins shows that these effects are due to changes in recognition and processing of substrates directly. We find that wildtype ClpXP specificity can be similarly altered when ATP is limited, which paradoxically increases degradation of some substrates. This activation corresponds to changes in ClpX conformation, leading to a model where ClpX cycles between 'open' and 'closed' states in an ATP-dependent manner. Limiting ATP or mutation can alter the conversion between states to yield better recognition of unorthodox substrates but worse recognition of native targets specifically bound by the closed state. Based on current structures of these unfoldases, we propose that other AAA+ unfoldases operate under similar ATP-dependent specificity principles.

2.2 Highlights

- A mutation in the Walker B region of ClpX induces recognition of new substrates.
- Proteases are optimized for specific functions but barrier to recognize new substrates is easily overcome.
- Expanding substrate recognition by a protease comes at the cost of reducing native substrate degradation.

- Decreasing ATP enhances ClpXP mediated degradation of certain classes of substrates.
- ClpX adopts distinct conformational states to favor better recognition of some substrates over others.

2.3 Introduction

Energy-dependent protein degradation regulates normal growth and stress responses in all cells. In bacteria, regulated proteolysis is carried out by several energy-dependent AAA+ (ATPases associated with cellular activities) proteases which include Lon, ClpXP, ClpAP, HslUV, FtsH (Gur et al., 2011; Mahmoud and Chien, 2018). These proteases share a similar general architecture containing an unfoldase domain and a non-specific peptidase (Sauer and Baker, 2011). The two domains can be encoded on a single polypeptide, such as in the case of Lon and FtsH, or they can be encoded by separate proteins, an ATPase, such as ClpX, and a peptidase, such as ClpP (Baker and Sauer, 2012; Langklotz et al., 2012; Lee and Suzuki, 2008). Using the power of ATP hydrolysis, the unfoldase recognizes, unfolds, and translocates substrates into the sequestered peptidase chamber to be degraded. Because they are critical for maintaining proteostasis, loss of these proteases results in defects in growth, cell-cycle progression, stress responses, and pathogenesis (Breidenstein et al., 2012; Howard-Flanders et al., 1964; Jenal and Fuchs, 1998; Rogers et al., 2016).

Despite the similarities in both architecture and mechanism, these proteases generally have distinct niches of substrate preference. For example, in

Caulobacter crescentus, Lon is the principal protease for degradation of the replication initiator DnaA (Jonas et al., 2013), the methyltransferase CcrM (Wright et al., 1996), and the transcriptional regulator SciP (Gora et al., 2013). By contrast, the ClpXP protease degrades cell-cycle factors like CtrA and TacA during cell-cycle progression through an adaptor hierarchy (Joshi et al., 2015). Lon is also responsible for misfolded protein degradation (Goldberg, 1972; Gur and Sauer, 2008; Jonas et al., 2013). However, while a handful of target substrates for these AAA+ have been identified, it remains unclear how proteases are able to discriminate among protein targets and recognize distinct substrates for irreversible degradation.

In this work, we find that a variant of ClpX (*clpX**) can compensate for the absence of the Lon protease. Expression of *clpX** suppresses defects in motility, growth, filamentation, and sensitivity to stress normally seen in a Δ*lon* strain. In addition to this phenotypic rescue, degradation of normal Lon substrates is restored *in vivo* and *in vitro* by ClpX*P. This increased ability to degrade noncanonical substrates comes at the cost of reduced degradation of ClpXP-specific substrates, resulting in fitness defects in otherwise wildtype strains expressing the *clpX** allele. Further mechanistic characterization shows that ClpX* has reduced catalytic efficiency for ATP hydrolysis, suggesting a connection between ATP utilization and substrate specificity. Consistent with this, limiting ATP for wildtype ClpXP shifts substrate preferences to that of ClpX*P. Limited proteolysis, differential scanning fluorimetry (DSF), and Hydrogen-deuterium exchange mass spectrometry (HDX-MS) show that the ClpX unfoldase

adopts distinct conformations under these ATP limiting or saturating conditions. Taken together, our work demonstrates that ATP-dependent dynamics between conformational states are important for substrate recognition by AAA+ unfoldases.

2.4 Results

2.4.1 A suppressor screen identifies a *clpX* mutant which rescues *Δlon*

We reasoned that a suppressor screen would allow us to identify novel Lon-related interactions and used a transposon library to identify mutations that restore motility to a *Δlon* strain. We isolated a high motility mutant with a transposon insertion in CCNA_00264; however, transduction experiments revealed that this transposon alone was not able to rescue motility (Figure S1A). Sequencing the genome of the suppressor strain showed a point mutation in *clpX*, which resulted in a single amino acid change from glycine 178 to alanine (*clpX**). This glycine is highly conserved among ClpX homologs and immediately adjacent to the Walker B motif (Figure S1C). By generating the *clpX** allele in a *Δlon* background, we found that *clpX** on its own partially restores motility (Figure 1A).

We were intrigued that a single mutation in *clpX* could restore motility to cells lacking Lon and chose to further characterize this strain. Cells lacking Lon show growth defects that exhibit as an extended lag phase and reduced cell mass accumulation in stationary phase (Figure 1A). The *clpX** allele rescues the mass accumulation defect, but not the extended lag (Figure 1A). *Δlon* strains also have significant morphological deficiencies including elongated cell length

and longer stalks, external polar organelles characteristic of *Caulobacter*. We found that the *clpX** mutant restored the cell length of Δ*lon* strains to near wildtype levels (Figure 1B, 1C). However, stalks remained elongated in the *Δlon clpX** strain (Figure 1B, 1C).

We next wondered if, in addition to suppression of *Δlon* morphological and growth defects, sensitivity to certain stressors would be suppressed by this *clpX** allele. One of the originally described phenotypes for *E. coli lon* mutants is DNA damage sensitivity (Mizusawa and Gottesman, 1983; Witkin, 1946) and *Caulobacter Δlon* strains are also highly sensitive to various DNA damaging agents (Zeinert et al., 2018), including mitomycin C (MMC) (Figure 1C). We found that Δ*lon clpX** was 100-fold more resistant to MMC than *Δlon* alone (Figure 1C).

As mentioned previously, Lon is the major protease responsible for the degradation of the replication initiator DnaA and *Δlon* strains accumulate excess chromosome content (Jonas et al., 2013; Wright et al., 1996). Like the morphological abnormalities, overreplication is suppressed in the Δ*lon clpX** strain which shows similar chromosome content as wildtype cells (Figure 1D, S1D). To determine if this rescue extended to a systems-level correction, we compared RNA-seq profiles of wildtype, Δ*lon* and Δ*lon clpX** strains. As expected, many genes (435) are differentially expressed upon loss of Lon (Figure 1E), while the Δ*lon clpX** strain shows fewer differences (119) with only 85 genes overlapping between these sets. Finally, we assayed the overall physiological consequence of ClpX* using competitive fitness in mixed cultures. We grew

cultures of Δ*lon* or the Δ*lon clpX** strain together with Δ*lon* strains constitutively expressing the Venus fluorescent protein (Persat et al., 2014). We found that Δ*lon clpX** cells were more fit than Δ*lon* cells (Figure S1E). Our interpretation is that expression of *clpX** in a Δ*lon* background largely shifts the phenotypes and transcriptional landscape to more wildtype profiles.

2.4.2 ClpX* restores degradation of Lon substrates *in vivo*

Because cells lacking Lon would accumulate normally degraded substrates, we hypothesized that the rescue we observed in the *Δlon clpX** strain was likely due to lower levels of Lon substrates, such as DnaA, CcrM, and SciP (Figure 2A) (Wright et al., 1996; Gora et al., 2013; Jonas et al., 2013). As expected, in unsynchronized cells, DnaA and CcrM levels are higher in the Δ*lon* strain than in wildtype (Figure 2B). Similarly, SciP levels are higher in Δ*lon* swarmer cells in comparison to wildtype (Figure 2D). Interestingly, levels of DnaA and SciP are restored to wildtype levels in the Δ*lon clpX** strain; however, CcrM remained at higher levels (Figure 2B). The reduced levels of DnaA likely explain the rescue of replication defects and enrichment analysis of the RNA-seq results shows that the SciP-controlled regulon and cell-cycle gene expression are largely restored in the Δ*lon clpX** strain (Figure S2). We reasoned that expression of *clpX** rescues normal growth and critical stress responses in a Δ*lon* strain through restoring wildtype levels of key proteins.

Next, we explored the mechanism by which a mutation in ClpX is able to restore steady state levels of DnaA and SciP. Because DnaA and SciP are

controlled by proteolysis, we suspected that protein turnover may be affected. As expected, DnaA is largely stabilized in Δ*lon* strains (Figure 2C; Jonas, et al. 2013); however, we found that DnaA degradation was restored in the Δ*lon clpX* strain*, with a half-life similar to that of wildtype (Figure 2D). SciP protein dynamics and cell-cycle phase specific levels were also restored in Δ*lon clpX** cells (Figure 2D). By contrast, CcrM degradation was still solely dependent on Lon, even when *clpX** was present, in both unsynchronized cells (Figure 2C) and during cell-cycle progression (Figure S3A).

We considered that changes in protein turnover could be either due to a gain-of-function in the *clpX** mutant or by indirect cellular effects associated with a loss-of-function in *clpX*. To test this, we created a merodiploid *Δlon* strain expressing a second copy of *clpX* or *clpX** under control of the native promoter along with a normal chromosomal copy of *clpX*. We reasoned that if the effect was direct, then expression of *clpX** would be sufficient to restore DnaA degradation. If the effect was indirect, then DnaA would remain stable. Consistent with a gain-of-function phenotype for the *clpX** allele, we found that DnaA turnover increased upon expression of *clpX** but not wildtype *clpX* (Figure 2E). Similarly, the phenotypic rescue we observed in the *Δlon clpX** strain was also due to a gain-of-function activity as the merodiploid strain expressing *clpX** suppressed *Δlon* defects, such as growth, motility, and genotoxic stress tolerance (Figure S3B-D). Because ClpXP is a AAA+ protease, we hypothesized

that ClpX*P (the protease complex of the variant ClpX* with wildtype ClpP) was now able to recognize and degrade substrates normally degraded by Lon.

2.4.3 ClpX*P directly degrades Lon substrates *in vitro*

As a direct test of our hypothesis, we purified the ClpX* variant and reconstituted degradation *in vitro*. Upon initial characterization of purified ClpX*, we found that it formed an active ATPase, but hydrolyzed ATP three times faster than wildtype (Figure S4A). Consistent with the fact that Lon is the principal protease for DnaA degradation (Jonas et al., 2013; Liu et al., 2016), we found that wildtype ClpXP poorly degraded DnaA *in vitro* (Figure 3A). However, purified ClpX*P could degrade DnaA four-fold faster than ClpXP (Figure 3A). Similarly, SciP was degraded three-fold faster by ClpX*P in comparison to ClpXP (Figure 3A). Finally, as predicted from our *in vivo* results, CcrM was not degraded by either ClpX*P or ClpXP (Figure 3A, Figure S4B), but was well degraded by Lon (Figure S4B). Thus, ClpX* appears to have an expanded substrate profile which includes some Lon substrates, but others, such as CcrM, remain exclusive to Lon.

Lon recognizes exposed hydrophobic amino acids (Gur and Sauer, 2008) and is best known as a quality control protease that eliminates mis/unfolded proteins (Goff et al., 1984). Given its altered specificity, we considered if ClpX* could now recognize these substrates. Casein is commonly used as an *in vitro* model substrate for mis/unfolded proteins. Lon robustly degrades fluorescently labeled casein, whereas wildtype ClpXP poorly degrades this substrate (Figure

3B). Intriguingly, ClpX*P degrades FITC-casein more than twice as fast as ClpXP (Figure 3B, Figure S4C). Similar to casein, ClpX*P degrades another unfolded Lon substrate, a chemically denatured domain of titin tagged with the hydrophobic sequence β20, better than wildtype ClpXP (Figure S4D).

Because cells lacking Lon are sensitive to proteotoxic stresses that create misfolded proteins and because ClpX*P is better at degrading mis/unfolded substrates than wildtype ClpXP, we wondered if the Δ*lon clpX** strain would be more resistant to stressors that induce cellular protein misfolding. Indeed, the presence of the *clpX** allele protected Δ*lon* cells from hypersensitivity to the proteotoxic amino acid L-canavanine (Figure 3B). We conclude that ClpX* has an altered substrate preference, that includes DnaA, SciP, and unfolded proteins, whose degradation are normally governed by the Lon protease.

2.4.4 ClpX*P is deficient in degradation of native ClpXP substrates

Mutations in ClpX that improve recognition of some substrates can have negative consequences on others (Farrell et al., 2007). GFP-ssrA is a well-characterized ClpXP substrate that is directly bound by the pore loops of ClpX (Fei et al., 2020; Gottesman et al., 1998). We purified GFP fused to the *Caulobacter* ssrA tag (Chien, et al. 2007), determined degradation rates by ClpX*P and ClpXP, and fit these rates to the Michaelis-Menten equation. We found that ClpX*P degrades GFP-ssrA more poorly than wildtype ClpXP, principally lowering the turnover rate (Figure 4A, Figure S5A), suggesting that either ClpX* fails to bind the ssrA tag as readily or is unable to translocate the reporter protein as well as ClpX. This effect was not due to the GFP as an ssrA-

tagged unfolded titin domain was also degraded more slowly by ClpX*P (Figure S5B). Given that the β20-tagged version of this same construct was degraded more rapidly (Figure S4D), we conclude that the altered specificity of ClpX* must rely on the recognition tag identity, rather than on changes in substrate translocation

CtrA is a master regulator in *Caulobacter* that inhibits replication initiation and regulates the transcription of many cell-cycle genes (Laub et al., 2002; Wortinger et al., 2000). *In vivo*, CtrA is degraded during the G1-S transition by ClpXP through the use of an adaptor hierarchy (Domian et al., 1999; Jenal and Fuchs, 1998; Joshi et al., 2015; Quon et al., 1996); however, *in vitro* CtrA can also be directly recognized by ClpXP as its C-terminus resembles the ssrA tag (Chien et al., 2007). Consistent with a reduced ability to recognize ClpXP substrates, ClpX*P degrades isolated CtrA more poorly than wildtype (Figure 4B) and also shows reduced degradation of a CtrA-derived GFP reporter (Smith et al., 2014) in the presence of the full adaptor hierarchy (Figure S5C). We conclude that ClpX*P overall has a diminished ability to recognize and degrade native substrates normally degraded by ClpXP.

2.4.5 Deficiencies of ClpX* revealed when Lon is present

The prior *in vitro* data suggests that rather than just expanding specificity, this mutation has allowed ClpX*P to degrade Lon-dependent substrates better but at the cost of degrading ClpXP-dependent ones. If this is true, while *clpX** is beneficial in a *ΔlonB* background, we reasoned that it may be detrimental to *lon*$^{+}$ cells.

To test this hypothesis, we generated a strain with *clpX** as its sole copy. We first examined ssrA tag turnover in this strain by using an ssrA derivative that relies on the SspB adaptor for degradation (eGFP-ssrA(DAS)) (Chowdhury et al., 2010) so that degradation would be sufficiently slowed to be visualized by western blotting. Consistent with our *in vitro* experiments, we observed stabilization and dramatically higher levels of eGFP-ssrA (DAS) in the *clpX** strain in comparison to wildtype (Figure 4C). We observed reduced CtrA degradation in the *clpX** strain, consistent with our *in vitro* observations (Figure 4C). Finally, DnaA degradation is accelerated in the *clpX** strains compared to wildtype – consistent with our findings that both Lon and ClpX*P are able to degrade DnaA (Figures 4C).

To assess the overall impact of ClpX* on wildtype cells, we performed competition assays as described previously using a wildtype strain constitutively expressing the Venus fluorescent protein (Persat et al., 2014). We found that while nonfluorescent wildtype cells could slightly outcompete the constitutive Venus expressing cells, the *clpX** strain showed a substantial competitive disadvantage (Figure 4D). We also tested for stress tolerances and found that *clpX** strains fail to survive genotoxic stress as robustly as wildtype (Figure 4E). Our conclusion is that reduced fitness of the wildtype *clpX** strain is likely due to reduced degradation of normal ClpXP substrates (such as CtrA) and prolific degradation of normal Lon substrates (such as DnaA) that together reduce overall fitness. Collectively, this supports our understanding that AAA+ proteases have been optimized for specific priorities in a cell – expansion of their

substrate profile, as seen with *clpX*,* can compensate for loss of other proteases, but at the cost of their ability to recognize their normal substrates.

2.4.5 Limiting ATP alters wildtype ClpXP substrate specificity

To understand how this mutation in ClpX leads to enhanced degradation of certain substrates, we further characterized the ATPase activity of ClpX*. While ClpX* hydrolyzes ATP three-fold faster than wildtype ClpX at saturating ATP concentrations (Figure S4A), Michaelis-Menten experiments showed that the K_M increases by 5-6 fold and the catalytic efficiency for ATP hydrolysis decreases by approximately 2 fold (Figure 5A). While K_M does depend on kcat, the magnitude of K_M increase given the change in kcat suggests that there is also deficiency in nucleotide binding of ClpX*. To test this, we used ATP to compete off mant-ADP, a fluorescent ADP analog and we observed at least a three-fold increase in the IC_{50} for ClpX*, suggesting that it binds ATP worse than wildtype ClpX (Figure S6A). However, to make sure that the observed difference in the IC_{50} between ClpX and ClpX* was due to changes in nucleotide binding and not because of the hydrolysis of ATP in the assay, we also competed off mant-ADP using ATPγS and assayed changes using fluorescence polarization. Consistent with the ATP titration described above, we calculated higher IC_{50}s for ATPγS in the presence of ClpX* (Figure S6B)

As seen previously, degradation of GFP-ssrA is precipitously lost below a minimum threshold of ATP (Martin et al., 2008), with the ClpX*P threshold being higher than that of wildtype, consistent with the higher K_M for ATP described above (Figure S7A). For ClpX*P, casein degradation reduced monotonically as

ATP concentration was lowered (Figure 5B). In striking contrast, we found that for wildtype ClpXP, casein degradation was increased at intermediate nucleotide concentrations compared to saturating ATP (Figure 5B). Kinetic analysis shows that at these lower ATP concentrations ClpXP degrades casein with a lower K_M and a similar V_{max} compared to saturating ATP conditions (Figure 5C). Since $K_M = K_D + k_{cat}/k_{on}$, the lower K_M rate suggests that, at a minimum, casein must bind better to ClpX at these concentrations.

These results suggest that ClpX specificity depends on ATP concentration in an unexpected fashion, with lower levels of ATP facilitating ClpX recognition of some substrates. We reasoned that this could explain the altered specificity of the ClpX* mutant, as its increased K_M for ATP may allow ClpX* to resemble a low ATP state even under saturating ATP conditions (Figure 5A). Remarkably, this enhanced degradation at low ATP extended to other ClpX* substrates, such as DnaA and SciP (Figure 5D and S7B). We conclude that ClpX preference depends on ATP state, with its specificity expanded under limiting ATP conditions.

This *in vitro* data suggests that ClpXP may be better at degrading some substrates such as DnaA *in vivo* under conditions in which ATP levels are limiting. To test this, we monitored degradation of DnaA during starvation using a Δ*lon* Δ*clpA* strain which should eliminate any non-ClpX dependent degradation (Liu et al., 2016). Glucose starvation has been shown to accelerate DnaA degradation (Gorbatyuk and Marczynski, 2005) which we found true for wildtype

cells as well (Figure 5E). Importantly, starving Δ*lon* Δ*clpA* also markedly increased DnaA degradation (Figure 5E) concurrent with a reduction in bulk ATP levels (Figure S7C).

We next considered how conformational changes in ClpX might explain the altered specificity at low ATP. Using limited proteolysis to probe conformational differences we found that ClpX at low ATP was more protease accessible than at high ATP (Figure 6A). Consistent with the shared altered specificity, protease accessibility of ClpX* at high ATP resembled the wildtype ClpX at low ATP (Figure 6A). This suggests that ClpX* adopts a state resembling the low ATP condition of ClpX, which we propose is more open of a structure than that found with ClpX under high ATP conditions. We next used differential scanning fluorimetry (DSF) to measure changes in stability, reasoning that if ClpX* was more likely to occupy the open state, as suggested by limited proteolysis, we would see a shift in thermal stability compared to wildtype ClpX even with saturating ATP. Consistent with the limited proteolysis, we found that ClpX* was destabilized in comparison to wildtype ClpX at high ATP (Figure 6B). As expected, limiting ATP for wildtype ClpX also resulted in less thermal stability as ATP binding is known to be needed for ClpX oligomerization (Hersch *et al.*, 2005).

Finally, we performed hydrogen-deuterium exchange coupled with mass spectrometry (HDX-MS) to determine specific regions of ClpX and ClpX* that differ in dynamics. As expected with ATP being needed for ClpX oligomerization,

we observed significantly more deuterium uptake spanning the entire sequence of ClpX under limiting ATP conditions (Figure S8A). We next compared ClpX and ClpX* at saturating ATP and found that ClpX* peptides generally showed faster exchange than the equivalent peptides from wildtype ClpX (Figure 6C; S8B-C). One of these peptides (residues 186-200) was the most deprotected in ClpX* compared to ClpX and is buried in the pore of the closed substrate-bound structure of ClpX (Protein Data Bank ID: 6PO1) (Figure 6C, Figure S8C). We created an open state model of ClpX by aligning six monomers with the AAA domains of substrate-free Lon from *Yersinia pestis* that is in an open state (Protein Data Bank ID: 6V11; Shin et al., 2020). The peptide corresponding to residues 186-200 was no longer buried in this modeled structure, consistent with our model that ClpX* can more readily adopt an open state (Figure S8C). We propose that in the closed state, the regions responsible for the ATP-dependent shift in substrate specificity are buried, leading to worse substrate degradation for substrates like FITC-Casein. Under limiting ATP or in the presence of ClpX*, these regions are more exposed, leading to enhanced recognition and degradation of certain substrates. We hypothesize that this low ATP-induced conformational difference may reflect the observed differences in AAA+ structures depending on substrate loading seen in recent cryo-EM studies and discuss their ramifications below.

2.5 Discussion

Because proteolysis is irreversible, degradation of substrates must be carefully monitored to avoid toxic consequences. In bacteria, different energy dependent proteases have distinct substrate preferences that allows them to collectively regulate proteome dynamics. However, how these energy-dependent proteases choose their target substrates from a pool of cellular proteins remains poorly understood. Certain determinants that dictate specificity include degrons, or degradation tags, such as the ssrA tag which marks proteins for degradation by ClpXP or ClpAP (Keiler, 2015; Keiler et al., 1996). Specificity can be augmented through adaptor proteins that help deliver substrates to proteases. For example, degradation of CtrA in *Caulobacter* is restricted to the ClpXP protease via a highly regulated series of adaptors (Joshi et al., 2015).

In this work, we identified a mutant allele of *clpX* (*clpX**) that compensates for the loss of Lon through expanding ClpXP substrate specificity. The variant ClpX*P protease complements the growth, motility, replication status, and morphology defects of a Δ*lon* strain (Figure 1A-1C) by restoring levels and degradation of the Lon substrates DnaA and SciP (Figure 2), which we confirm with biochemical experiments (Figure 3). Interestingly, ClpX*P has an improved ability to degrade unfolded protein substrates, a feature that likely explains the increased proteotoxic tolerance of Δ*lon clpX** strains (Figure 3). Finally, this *clpX* variant is deficient in proteolysis of normal ClpXP substrates, such as CtrA and ssrA-tagged proteins, suggesting a shift in substrate preference rather than just an expansion (Figure 4). Mechanistic enzymology revealed that ClpX* requires

~5-fold more ATP for saturation (Figure 5A), leading us to explore the role of ATP levels in controlling specificity. Surprisingly, our *in vitro* studies found that wildtype ClpXP is better at degrading unfolded proteins, DnaA, and SciP in ATP limiting conditions, but worse at degrading ssrA-tagged proteins, similar to that seen with ClpX*P in saturating ATP (Figure 5B, 5D, S7B). We recapitulate this effect *in vivo*, showing that in starvation conditions that deplete ATP, DnaA degradation by wildtype ClpXP is accelerated (Figure 5E). Our interpretation is that the ClpX oligomer adopts distinct conformations in the ATP-saturated and ATP-limited conditions, as suggested by limited proteolysis as well as DSF and HDX-MS experiments (Figure 6, S8A-S8C).

How does altered ATP loading alter substrate recognition? Our working model is that ClpX normally samples an 'open' state and a 'closed' state to capture substrates, and the closed state can engage ClpP to form a processive protease that uses cycles of ATP hydrolysis to power unfolding and degradation (Figure 6D). Substrates can be captured during the open-closed transition (as we propose for casein) or directly by the closed state (as proposed for the ssrA tag and ClpXP (Hersch *et al.*, 2005; Fei *et al.*, 2020). Recent cryo-EM structures reveal shared features of substrate-bound AAA+ complexes, namely a shallow right-handed ring with pore loops gripping the substrate and at least 4 ATP-bound protomers (Fei et al., 2020; Gates et al., 2017; Lopez et al., 2020; Ripstein et al., 2020; Shin et al., 2020), while substrate-free forms of these machines show more open, often left-handed, spiral structures (Shin et al., 2020; Yokom et al., 2016). Interestingly, the original crystals of ClpX shows a left-handed open

spiral packing (Kim and Kim, 2003), similar to substrate-free cryo-EM structures described for other AAA+ machines.

We propose that limiting ATP or mutations can shift the open/closed balance toward the open state, which allows ClpX to better capture certain substrates, such as unfolded proteins, which may not have as strict sequence requirements for recognition (Figure 6). However, degrons such as the ssrA tag which bind selectively to the closed conformation (Hersch et al., 2005) would be poorly recognized in these conditions. Interestingly, it was previously shown that mutation in the RKH loop of ClpX decreases degradation of ssrA tagged proteins but increases degradation of other substrates (Farrell et al., 2007). These mutants were also reported to have a 2-fold increase in the maximum ATP hydrolysis rate compared to wildtype, similar to the ClpX* variant characterized here; however, the K_M was not reported in that earlier work. Together with our current findings, it seems that specificity for ClpX is surprisingly plastic and dependent on features that alter ATP hydrolysis rates.

Prior work has shown that limiting nucleotide leads to loss of substrate degradation by ClpXP (Martin et al., 2008), as would make sense for an ATP-fueled unfoldase. We note that these studies exclusively used ssrA-tagged substrates, which requires an ATP-bound (and presumably closed) form of ClpX for recognition. Thus, the equivalent effects we are seeing here for casein, DnaA, and SciP would not have been previously observed. This dichotomy also highlights the importance of using a range of substrates in understanding activity. The open-capture / closed-processive model described here also has

precedence in the conformational states and activity of Hsp104 (Gates et al., 2017; Ye et al., 2020; Yokom et al., 2016), where doping in nonhydrolyzable ATP analogs results in enhanced unfolding activity (Doyle et al., 2007). In our current work, we suggest that different states of ClpX, favored by either limiting ATP or mutation, can result in meaningful biological consequences. Intriguingly, similar conclusions were drawn for the chaperonin GroEL, where mutants with a shifted specificity that improves folding of one class of clients at the expense of others also resulted in an altered ATPase cycle attributed to changes in conformational lifetimes (Wang et al., 2002). Overall, it seems that exclusive substrate profiles for AAA+ systems are not hard-wired but can be altered not only by mutations but also through modulation of ATP hydrolysis, demonstrating a plasticity in these machines that yield flexibility in maintaining cellular proteostasis.

2.6 Limitations of the study

While our final model that ATP affects the dynamics of open/closed oligomerization of ClpX satisfies our biochemical and cellular results, we recognize there are limitations in the experimental support of our model. Because ClpX* has a higher K_M for ATP and has properties similar to that of wildtype ClpX under limiting ATP conditions, the most parsimonious interpretation is that ClpX* at saturating ATP mimics ClpX under limiting ATP in terms of mechanisms changing substrate specificity. However, it is possible that ClpX* has shifted substrate preference for a reason completely different than why wildtype ClpX under limiting ATP conditions has a shifted specificity. Because we have not directly measured ATP loading, we cannot say whether ClpX or ClpX* differs in

nucleotide occupancy at saturating ATP concentrations. A final concern is that although open apo-state spirals and closed substrate-bound rings have been found for several AAA+ family members (as described above), these have yet to be seen for ClpX. The most concrete evidence for ATP-driven changes in open/closed ClpX states would be structural snapshots with different levels of ATP and with the ClpX* mutant that would demonstrate how these states were populated. This is beyond the scope of this current work; however, we are engaged in pursuing these studies.

2.7 Materials and Methods

Bacterial strains and growth conditions

Bacterial strains and plasmids used in this study are listed in supplementary file 2. *Caulobacter crescentus* strains were grown in PYE medium (2g/L peptone, 1g/L yeast extract, 1 mM $MgSO_4$, and 0.5 mM $CaCl_2$) at 30°C. To generate strains, antibiotics were added to plates at the following concentrations: kanamycin (25 µg/ml), spectinomycin (100 µg/ml), and oxytetracycline (2 µg/ml). After initial selection steps for strain construction (excluding plasmids), antibiotics were excluded for all assays. For *C. crescentus* motility assays, PYE with 0.3% agar was used and a single colony was stabbed into the agar using a sterile tip and left to incubate at 30°C for 2 to 3 days.

Escherichia coli strains were grown in LB (10g/L NaCl, 10g/L tryptone, 5g/L yeast extract) and supplemented with antibiotics at the following concentrations: ampicillin (100 ug/ml), oxytetracycline (15 µg/ml), spectinomycin (50 µg/ml), kanamycin (50 µg/ml), gentamycin (20 µg/ml). For solid medium,

1.5% agar was used regardless of bacterial species. For all strains, optical density was measured at 600 nm.

For induction purposes, the 477 plasmids were induced with xylose (0.2%) and repressed with glucose (0.2%). For protein expression, 0.4 M IPTG was used for induction.

Cloning and strain constructions

All Caulobacter strains were derived from CPC176, an isolate of NA1000. To generate the *Δlon clpX** strain, a two-step recombination protocol with a sucrose counter selection was utilized *(*Skerker et al., 2005*)*. The vector pNPTS138 was digested with HindIII and EcoRI. A PCR product of the clpX* sequence was amplified from the original motility suppressor and Gibson assembly was then used to generate pNPTS138_clpX*. Following transformation with pNPTS138_clpX* into NA1000 or *Δlon*, primary selection was on PYE supplemented with kanamycin. Primary colonies were grown overnight without selection and overnight cultures were played on PYE agar supplemented with 3% w/v sucrose. To validate allelic swap, strains were tested for sensitivity to kanamycin. *Δlon clpX** was also screened by motility and sequencing of the *clpX* locus validated candidate clones.

ClpX or *clpX** merodiploid strains were generated by Gibson assembly of PCR product and double digested plasmids of pMCS-2. The plasmids were then electroporated into *Δlon and selected onto kanamycin plates. Strains were validated by anti-ClpX westerns.*

eGFP-ssrA(DAS) induction strains were generated by electroporating eGFP-ssrA(DAS) 477 plasmid into *wildtype* and *wildtype clpX** and selecting on spectinomycin. Strains were validated by anti-M2 westerns.

Motility Suppressor screen

Transposon libraries were generated for *Δlon*. Two-liter PYE cultures were grown to mid exponential phase, pelleted, and washed with 10% glycerol. Competent cells were electroporated with Ez-Tn5 <Kan-2> transposome (Lucigen, Madison, WI). Cells recovered for 90 minutes at 30 °C and then played on PYE plates supplemented with kanamycin. Libraries were grown for 7 days. Colonies were then scraped from the surface, combined, and resuspended to form a homogenous solution of PYE + 20% glycerol.

The Tn library was thawed out and diluted into a flask containing two-liter 0.3% agar. The cell agar mixture was plated and grown at 30 °C for 3 to 5 days. Candidates that appeared motile were validated by innoculating single colonies into motility agar on the same plate as NA1000 as a positive control and *Δlon* as a negative control and incubating plates for 2-3 days at 30 °C.

Whole genome sequencing

Genomic DNA was extracted using the MasterPure Complete DNA and RNA purification kit (Epicenter Biotechnologies, Madison, WI). A Qubit Fluorometer (ThermoFisher Scientific, Waltham, MA) was utilized to assess DNA concentration. Illumina libraries were generated from the extracted genomic DNA

using the NexteraXT (Illumina, San Diego, CA) protocol. Libraries were multiplexed and sequenced at the University of Massachusetts Amherst Genomics Core Facility on the NextSeq 500 (Illumina). Single nucleotide polymorphisms (SNPs) were detected using breseq (Deatherage and Barrick, 2014).

RNA sequencing

RNA was extracted from stationary phase cells. Libraries were generated from the extracted RNA using the NEB Next RNA Library Prep kits (NEB, Ipswich, MA). Libraries were sequenced at the University of Massachusetts Genomics Core Facility on the NextSeq 500 with single end 75 base reads. Reads were mapped to the *Caulobacter* genome using BWA (Li and Durbin, 2009) and sorted with Samtools (Li et al., 2009).To obtain the number of reads per gene, *bedtools map* (Quinlan and Hall, 2010) was used. Rstudio and EdgeR was used to identify differentially expressed genes (R Core Team, 2019; Robinson et al., 2009).

Raw counts were normalized using the counts-per-million (CPM) method, and the *edgeR* package in R was used to perform differential gene expression analysis, KEGG pathway analysis, and FRY (Wu et al., 2010) gene set analysis. We filtered out any gene that had less than 30 normalized counts across 3 or more samples. To test for gene expression differences and identify differentially expressed genes across experimental groups, we used the quasi-likelihood F-test. The over-representation analysis for KEGG pathways done using the *kegga* function. FRY gene set analysis done using the *fry* function. The CcrM, DnaA,

and SciP regulons were obtained from (Gonzalez et al., 2014; Hottes et al., 2005; Tan et al., 2010).

Plating viability and drug sensitivity

All Caulobacter strains were grown overnight in liquid PYE media. After overnight growth, cells were back diluted to OD_{600} 0.1 and outgrown to mid-exponential phase before being normalized to OD_{600} 0.1 and 10-fold serially diluted on to media. For experiments using mitomycin C (Sigma, St. Louis, MO) and L-canavanine (Sigma), drugs were prepared at a stock concentration of 0.4 µg/ml mitomycin C, and 100 mg/ml L-canavanine and filter sterilized. PYE agar was cooled before the drugs were added and plates were left to air dry prior to serial dilution plating. All plates were incubated at 30℃ for 2-3 days and imaged with a gel doc.

***In vivo* assays**

The stability of proteins *in vivo* was determined by inhibiting protein synthesis upon addition of 30 µg/ml chloramphenicol to cells in exponential phase. At each time point, 1ml of culture was removed and centrifuged at 15,000 rpm for 2 minutes. The supernatant was removed and pellets were flash frozen in liquid nitrogen. Pellets were thawed, resuspended in 2x SDS dye, and normalized to the OD_{600} of the lowest sample. Samples were boiled for 10 minutes and centrifuged for 10 minutes at 15,000 rpm. Extracts were run on 10% Bis-Tris gels for 1 hour at room temperature at 150 V. Gels were then transferred to nitrocellulose membranes for 1 hour at room temperature at 20V. Membranes were blocked with 3% milk in Tris-based saline with 0.05% Tween-20 (TBST) for

1 hour. Membranes were probed with primary antibody in 3% milk in TBST at 4°C overnight with following dilution factors: 1:5000 dilution of DnaA, 1:5000 SciP, 1:5000 CcrM, 1:5000 ClpP, 1:2500 Lon, and 1:2000 M2. Membranes were washed with 1x TBST for 5 minutes three times and then probed with Licor secondary antibody with 1:10,000 dilution in 1x TBST at room temperature for 1 hour. The protein was visualized using Licor Odyssey CLx. Bands were quantified using imageJ and degradation rates were plotted using Prism.

To synchronize *Caulobacter* strains, cells were grown to an OD600 of 0.3-0.5 in PYE and swarmer cells were isolated using Percoll density centrifugation. Cells were released into PYE.

Flow cytometry was used to measure DNA content in rifampicin-treated cells as previously described (Chen et al., 2009). Cells were rifampicin treated for three hours prior to fixing in 70% ethanol.

Carbon Starvation

Cells were grown in M2G media (6.1 mM Na_2HPO_4, 3.9 mM KH_2PO_4, 9.3 mM NH_4Cl, 0.5 mM $MgSO_4$, 0.5 mM CaCl2, 10 µM $FeSO_4$ (EDTA chelate), 0.2% glucose). Cells were then washed twice in cold M2G media (+glucose samples) or in M2 media (-glucose samples) and resuspended in pre-warmed M2G or M2 media.

For bulk measurements of intracellular ATP, the Bactiter-Glo microbial cell viability assay kit (Promega) was used. Cells were mixed with an equal volume of BacTiter-Glo reagent in 384-well microtiter plates and incubated for five minutes before luminescence was measured.

Growth competition assay

Overnight cultures of CPC798 were mixed with either *NA1000* or *clpX** at a 1:1 ratio. For competition assays with *Δlon strains, overnight cultures of CPC807 were mixed with either Δlon or Δlon clpX* at a 1:1 ratio.* Mixed strains were diluted into fresh PYE and allowed to outgrow for 12 doublings overnight. The initial populations were verified by phase contrast and fluorescent microscopy. Final ratios were normalized to their starting ratios. Data was plotted using GraphPad Prism.

Microscopy

Phase contrast images of logarithmically growing cells were taken by Zeiss AXIO Scope A1. Cells were mounted on 1% PYE agar pads and imaged using a 100X objective. MicrobeJ (Ducret et al., 2016) for ImageJ (Schneider et al., 2012) was utilized to quantify cell lengths. Stalk lengths were quantified using ImageJ. Prism was utilized for representations of cell and stalk length measurements. Representative images of the same scale were cropped to display morphological defects.

Protein Purification and Modification

Untagged Lon, untagged ClpX and ClpX*, and his-tagged ClpP were purified as previously described (Chien et al., 2007b; Goldberg et al., 1994; Gur and Sauer, 2008b; Levchenko et al., 2000). Titin-I27-β20 and Titin-I27-ssrA were purified as previously described (Gur and Sauer, 2008b; Kenniston et al., 2003) and labeled with Fluorescein-5-maleimide (Thermo Scientific™) under guanidine hydrochloride denaturation. The modified protein was buffer exchanged into H-

buffer (20 mM Hepes pH 7.5, 100 mM KCl, 10 mM MgCl2, 10% glycerol) and stored at 4°C. The concentration of fluorescein-modified Titin-I27-β20 and Titin-I27-ssrA were determined using the Bradford assay (Thermo Scientific™). FITC-Casein (Type III, Sigma) was prepared in water and stored at -20°C. His_6SciP and his_6CtrA were purified as described in (Gora et al., 2013b). DnaA and CcrM were purified as his_6SUMO tagged proteins, followed by tag cleavage as described (Jonas et al., 2013; Liu et al., 2016; Wang et al., 2007). GFP-ssrA was purified as previously described (Yakhnin et al., 1998). CtrA-RD+15 was purified as described (Smith et al., 2014b). Detailed purification protocols are available upon request.

***In vitro* reconstitution assays**

Degradation assays were performed at 30°C and monitored using SDS-PAGE gels as described previously (Bhat et al., 2013). The final concentrations used can be found in the figure legends. Densitometry was performed with ImageJ and degradation rates were plotted using Prism.

Degradation of FITC-Casein, FT-Titin-B20, and FT-Titin-ssrA was monitored as an increase in fluorescence over time. GFP-CtrARD+15 degradation was observed as a loss of fluorescence over time as described previously (Smith et al., 2014b).

ATP hydrolysis for ClpXP and ClpX*P was measured using a coupled kinase assay as previously described (Burton et al., 2003)

Limited Proteolysis

To perform limited chymotrypsin digestion, 0.004 mg/mL chymotyrpsin was added to 0.01 mg/mL ClpX or ClpX* in the presence of ClpP and ATP regeneration system and incubated at 25°C in Hepes buffer (20 mM Hepes pH 7.5, 100 mM KCl, 10 mM MgCl2, 10% glycerol) for indicated time points. To quench the reactions, 5X SDS dye supplemented with 5 mM Protease inhibitor phenylmethylsulfonyl fluoride (PMSF) was added. The samples were run on a 10% Bis-Tris gel and transferred to nitrocellulose as described above. Membranes were probed with primary antibody in 3% milk in TBST at 4°C overnight with following dilution factors: 1:5000 dilution of ClpX. Membranes were washed with 1x TBST for 5 minutes three times and then probed with Licor secondary antibody with 1:10,000 dilution in 1x TBST at room temperature for 1 hour. The protein was visualized using Licor Odyssey CLx.

Binding of ADP to ClpX

625 nM mant-ADP was pre-incubated with 300 nM $ClpX_6$/$ClpX_6$* for 10 minutes. Subsequently, ATPγS was added to compete off the mant-ADP at various concentrations. Polarization measurements were read from 20 uL of these mixtures after an additional 15 minute incubation using opaque black 384-well plates and a SpectraMax M5 plate reader (Molecular Devices), with excitation and emission wavelengths set at 357 and 445 nm, respectively. IC50s were calculated by fitting the polarization data using GraphPad Prism to an inhibitor versus response – variable slope (four paramaters) function in GraphPad Prism:

Y=Bottom + (Top-Bottom)/(1+(IC50/X)^HillSlope) where IC50 is the ATPγS concentration halfway between bottom and top.

Differential Scanning Fluorimetry

Differential scanning fluorimetry was carried out in a Biorad realtime PCR thermocycler. 6 μM monomer of ClpX or ClpX* in the presence of 4 mM ATP or 12 μM ATP was mixed in a 1:1 ratio with 4X Sypro Orange in Hepes Buffer (20 mM Hepes pH 7.5, 100 mM KCl, 10 mM $MgCl_2$). The resulting mixtures were incubated at room temperature for 30 mins to allow the Sypro Orange to coat the proteins before subjecting triplicate samples to thermal unfolding from 25 °C to 95 °C. Melting temperatures were calculated by fitting of a 5-parameter sigmoid curve using the JTSA software (P. Bond, https://paulsbond.co.uk/jtsa).

Hydrogen-deuterium exchange mass spectrometry (HDX-MS)

Hydrogen-deuterium exchange experiments were carried out on a Synapt G2Si high-definition mass spectrometer (Waters) using an automated HDX robotics platform (Waters). Samples of 5.4 μM ClpX or ClpX* monomer were diluted 1:16 in D_2O buffer containing 20 mM Hepes, 10 mM $MgCl_2$, 100 mM KCl, and 5% glycerol. D_2O and H_2O buffers were supplemented with 4 mM ATP plus regeneration system (30 mM creatine kinase and 0.5 mg/mL creatine phosphate) for the high ATP condition and 12 μM ATP for the low ATP condition. Deuterium exchange was allowed to take place for 0, 10 seconds, 1 min, 10 minutes, and 60 min at 25 °C. The samples were subsequently quenched by addition of cold quench buffer (233 mM Sodium Phosphate pH 2.5) and run over an immobilized Waters ENZYMATE immobilized pepsin column (inner diameter: 2.1 × 30 mm) at

a flow rate of 0.15 mL/min at high pressure (~11,000 psi) for peptide digestion. Blank runs were run in between each analysis to avoid peptide carry over. Continuous lock-mass correction was performed using leu-enkephalin compound. Peptides were ionized and separated by electrospray ionization for analysis at a mass resolution of 50 to 2,000 *m*/*z* range. Peptides were identified with triplicate undeuterated samples from each condition. Identification of peptides and analysis of the uptake plots and charge states for each peptide were completed in Protein Lynx Global Server and DynamX (v. 3.0, Waters). The following processing paramaters were utilized: minimum peptide intensity of 1000, minimum peptide length of 5, maximum peptide length of 30, minimum MS/MS products of 2, minimum products per amino acid of 0.25, minimum score of 5, and maximum MH+ error threshold of 15 p.p.m. Woods plots were generated by Deuteros (Lau et al., 2021) using the peptide significance test (p-value <0.01). HDX data summary for each condition was exported from Deuteros and can be found in Supplementary File 3. No correction was made for back-exchange. Specific peptide regions were mapped onto the corresponding residues in the *E. coli* cryo-EM structure (PDB ID: 6PO1) using PYMOL (Version 2.5.0, Schrödinger). A model of ClpX in the potential open state was created by aligning each ClpX monomer to each ATPase monomer of the *Y. pestis* substrate-free cryo-EM structure (PDB ID: 6V11) by using the align function in PYMOL.

2.8 Acknowledgements

We thank the Chien, Strieter, Stratton, and Serio lab members for helpful comments and discussion on the manuscript. S.A.M. and B.A. were supported in part through the UMass NIH Chemistry Biology Interface Training Program (NIH T32GM008515) and S.A.M. in part by the HHMI Gilliam Fellowship program. Work in the Chien lab is funded by the NIH (R35GM130320). We thank the Genomics Resource Laboratory (Institute for Applied Life Sciences; University of Massachusetts Amherst) and the Mass Spectrometry Core Facilities for services and equipment support.

Author Contributions: Conceptualization: S.A.M. and P.C.; Investigation, S.A.M. and B.A.; Writing, S.A.M and P.C.; Funding Acquisition, P.C. Supervision, P.C.

2.9 Declaration of Interests: The authors declare no competing interests

2.10 References

Baker, T.A., and Sauer, R.T. (2012). ClpXP, an ATP-powered unfolding and protein-degradation machine. Biochimica et Biophysica Acta - Molecular Cell Research *1823*, 15–28.

Bhat, N.H., Vass, R.H., Stoddard, P.R., Shin, D.K., and Chien, P. (2013). Identification of ClpP substrates in Caulobacter crescentus reveals a role for regulated proteolysis in bacterial development. *88*, 1083–1092.

Breidenstein, E.B.M., Janot, L., Strehmel, J., Fernandez, L., Taylor, P.K., Kukavica-Ibrulj, I., Gellatly, S.L., Levesque, R.C., Overhage, J., and Hancock, R.E.W. (2012). The Lon Protease Is Essential for Full Virulence in Pseudomonas aeruginosa. PLoS ONE *7*.

Chen, Y.E., Tsokos, C.G., Biondi, E.G., Perchuk, B.S., and Laub, M.T. (2009). Dynamics of two phosphorelays controlling cell cycle progression in Caulobacter crescentus. Journal of Bacteriology *191*, 7417–7429.

Chien, P., Perchuk, B.S., Laub, M.T., Sauer, R.T., and Baker, T. a (2007). Direct and adaptor-mediated substrate recognition by an essential AAA+ protease. Proceedings of the National Academy of Sciences of the United States of America *104*, 6590–6595.

Chowdhury, T., Chien, P., Ebrahim, S., Sauer, R.T., and Baker, T.A. (2010). Versatile modes of peptide recognition by the ClpX N domain mediate alternative adaptor-binding specificities in different bacterial species. Protein Science *19*, 242–254.

Deatherage, D.E., and Barrick, J.E. (2014). Identification of mutations in laboratory evolved microbes from next-generation sequencing data using breseq. Methods Mol Biol. 165–188.

Domian, I.J., Reisenauer, a, and Shapiro, L. (1999). Feedback control of a master bacterial cell-cycle regulator. Proceedings of the National Academy of Sciences of the United States of America *96*, 6648–6653.

Doyle, S.M., Shorter, J., Zolkiewski, M., Hoskins, J.R., Lindquist, S., and Wickner, S. (2007). Asymmetric deceleration of ClpB or Hsp104 ATPase activity unleashes protein-remodeling activity. Nature Structural and Molecular Biology *14*, 114–122.

Ducret, A., Quardokus, E.M., and Brun, Y. V. (2016). MicrobeJ, a tool for high throughput bacterial cell detection and quantitative analysis. Nature Microbiology *1*, 1–7.

Farrell, C.M., Baker, T.A., and Sauer, R.T. (2007). Altered Specificity of a AAA+ Protease. Molecular Cell *25*, 161–166.

Fei, X., Bell, T.A., Barkow, S.R., Baker, T.A., and Sauer, R.T. (2020). Structural basis of clpxp recognition and unfolding of ssra-tagged substrates. ELife *9*, 1–39.

Gates, S.N., Yokom, A.L., Lin, J., Jackrel, M.E., Rizo, A.N., Kendsersky, N.M., Buell, C.E., Sweeny, E.A., Mack, K.L., Chuang, E., et al. (2017). Ratchet-like polypeptide translocation mechanism of the AAA+ disaggregase Hsp104. Science *357*, 273–279.

Goff, S.A., Casson, L.P., and Goldberg, A.L. (1984). Heat shock regulatory gene htpR influences rates of protein degradation and expression of the lon gene in Escherichia coli. Proceedings of the National Academy of Sciences of the United States of America *81*, 6647–6651.

Goldberg, A.L. (1972). Degradation of Abnormal Proteins in Escherichia coli. Proc Natl Acad Sci U S A *69*, 422–426.

Goldberg, A.L., Moerschell, R.P., Hachung, C., and Maurizi, M.R. (1994). ATP-dependent protease La (Lon) from Escherichia coli. Methods in Enzymology *244*, 350–375.

Gonzalez, D., Kozdon, J.B., McAdams, H.H., Shapiro, L., and Collier, J. (2014). The functions of DNA methylation by CcrM in Caulobacter crescentus: A global approach. Nucleic Acids Research *42*, 3720–3735.

Gora, K.G., Cantin, A., Wohlever, M., Joshi, K.K., Perchuk, B.S., Chien, P., and Laub, M.T. (2013). Regulated proteolysis of a transcription factor complex is critical to cell cycle progression in Caulobacter crescentus. Molecular Microbiology *87*, 1277–1289.

Gorbatyuk, B., and Marczynski, G.T. (2005). Regulated degradation of chromosome replication proteins DnaA and CtrA in Caulobacter crescentus. Molecular Microbiology *55*, 1233–1245.

Gottesman, S., Roche, E., Zhou, Y.N., and Sauer, R.T. (1998). The ClpXP and ClpAP proteases degrade proteins with carboxy-terminal peptide tails added by the SsrA-tagging system. Genes and Development *12*, 1338–1347.

Gur, E., and Sauer, R.T. (2008). Recognition of misfolded proteins by Lon, a AAA+ protease. Genes and Development *22*, 2267–2277.

Gur, E., Biran, D., and Ron, E.Z. (2011). Regulated proteolysis in Gram-negative bacteria — how and when? Nat Rev Microbiol *9*, 839–848.

Hersch, G.L., Burton, R.E., Bolon, D.N., Baker, T.A., and Sauer, R.T. (2005). Asymmetric interactions of ATP with the AAA+ ClpX6 unfoldase: Allosteric control of a protein machine. Cell *121*, 1017–1027.

Hottes, A.K., Shapiro, L., and McAdams, H.H. (2005). DnaA coordinates replication initiation and cell cycle transcription in Caulobacter crescentus. Molecular Microbiology *58*, 1340–1353.

Howard-Flanders, P., Simson, E., and Theriot, L. (1964). A locus that controls filament formation and sensitiviry to radiation in Escherichia coli K-12. Genetics *49*, 237–246.

Jenal, U., and Fuchs, T. (1998). An essential protease involved in bacterial cell-cycle control. EMBO Journal *17*, 5658–5669.

Jonas, K., Liu, J., Chien, P., and Laub, M.T. (2013). Proteotoxic stress induces a cell-cycle arrest by stimulating lon to degrade the replication initiator DnaA. Cell *154*, 623–636.

Joshi, K.K., Bergé, M., Radhakrishnan, S.K., Viollier, P.H., and Chien, P. (2015). An Adaptor Hierarchy Regulates Proteolysis during a Bacterial Cell Cycle. Cell *163*, 419–431.

Keiler, K.C. (2015). Mechanisms of ribosome rescue in bacteria. Nature Reviews Microbiology *13*, 285–297.

Keiler, K.C., Waller, P.R.H., and Sauer, R.T. (1996). Role of a Peptide Tagging System in Degradation of Proteins Synthesized from Damaged Messenger RNA. Science *271*, 990–993.

Kenniston, J.A., Baker, T.A., Fernandez, J.M., and Sauer, R.T. (2003). Linkage between ATP consumption and mechanical unfolding during the protein processing reactions of an AAA+ degradation machine. Cell *114*, 511–520.

Kim, D.Y., and Kim, K.K. (2003). Crystal Structure of ClpX Molecular Chaperone from Helicobacter pylori. Journal of Biological Chemistry *278*, 50664–50670.

Langklotz, S., Baumann, U., and Narberhaus, F. (2012). Structure and function of the bacterial AAA protease FtsH. Biochimica et Biophysica Acta - Molecular Cell Research *1823*, 40–48.

Lau, A.M., Claesen, J., Hansen, K., and Politis, A. (2021). Deuteros 2.0: Peptide-level significance testing of data from hydrogen deuterium exchange mass spectrometry. Bioinformatics *37*, 270–272.

Laub, M.T., Chen, S.L., Shapiro, L., and McAdams, H.H. (2002). Genes directly controlled by CtrA, a master regulator of the Caulobacter cell cycle. Proceedings of the National Academy of Sciences of the United States of America *99*, 4632–4637.

Lee, I., and Suzuki, C.K. (2008). Functional mechanics of the ATP-dependent Lon protease- lessons from endogenous protein and synthetic peptide

substrates. Biochimica et Biophysica Acta - Proteins and Proteomics *1784*, 727–735.

Levchenko, I., Seidel, M., Sauer, R.T., and Baker, T.A. (2000). A Specificity-Enhancing Factor for the ClpXP Degradation Machine. Science *289*, 2354–2356.

Li, H., and Durbin, R. (2009). Fast and accurate short read alignment with Burrows-Wheeler transform. Bioinformatics *25*, 1754–1760.

Li, H., Handsaker, B., Wysoker, A., Fennell, T., Ruan, J., Homer, N., Marth, G., Abecasis, G., and Durbin, R. (2009). The Sequence Alignment/Map format and SAMtools. Bioinformatics *25*, 2078–2079.

Liu, J., Francis, L.I., Jonas, K., Laub, M.T., and Chien, P. (2016). ClpAP is an auxiliary protease for DnaA degradation in Caulobacter crescentus. Molecular Microbiology *102*, 1075–1085.

Lopez, K.E., Rizo, A.N., Tse, E., Lin, J.B., Scull, N.W., Thwin, A.C., Lucius, A.L., Shorter, J., and Southworth, D.R. (2020). Conformational plasticity of the ClpAP AAA+ protease couples protein unfolding and proteolysis. Nature Structural and Molecular Biology *27*, 406–416.

Mahmoud, S.A., and Chien, P. (2018). Regulated Proteolysis in Bacteria. Annual Review of Biochemistry *87*, 677–696.

Martin, A., Baker, T.A., and Sauer, R.T. (2008). Protein unfolding by a AAA+ protease is dependent on ATP-hydrolysis rates and substrate energy landscapes. Nature Structural and Molecular Biology *15*, 139–145.

Mizusawa, S., and Gottesman, S. (1983). Protein degradation in Escherichia coli: the lon gene controls the stability of sulA protein. Proceedings of the National Academy of Sciences of the United States of America *80*, 358–362.

Persat, A., Stone, H.A., and Gitai, Z. (2014). The curved shape of caulobacter crescentus enhances surface colonization in flow. Nature Communications *5*, 1–9.

Quinlan, A.R., and Hall, I.M. (2010). BEDTools: a flexible suite of utilities for comparing genomic features. Bioinformatics *26*, 841–842.

Quon, K.C., Marczynski, G.T., and Shapiro, L. (1996). Cell cycle control by an essential bacterial two-component signal transduction protein. Cell *84*, 83–93.

R Core Team (2019). R: A language and Environment for Statistical Computing (R Foundation for Statistical Computing).

Ripstein, Z.A., Vahidi, S., Houry, W.A., Rubinstein, J.L., and Kay, L.E. (2020). A processive rotary mechanism couples substrate unfolding and proteolysis in the ClpXP degradation machinery. ELife *9*.

Robinson, M.D., McCarthy, D.J., and Smyth, G.K. (2009). edgeR: A Bioconductor package for differential expression analysis of digital gene expression data. Bioinformatics *26*, 139–140.

Rogers, A., Townsley, L., Gallego-hernandez, A.L., Beyhan, S., Kwuan, L., and Yildiz, F.H. (2016). and the Type VI Secretion System in Vibrio cholerae. *198*, 973–985.

Sauer, R.T., and Baker, T.A. (2011). AAA+ Proteases: ATP-Fueled Machines of Protein Destruction. Annu. Rev. Biochem *80*, 587–612.

Schneider, C.A., Rasband, W.S., and Eliceiri, K.W. (2012). NIH Image to ImageJ: 25 years of image analysis. Nature Methods *9*, 671–675.

Shin, M., Puchades, C., Asmita, A., Puri, N., Adjei, E., Luke Wiseman, R., Wali Karzai, A., and Lander, G.C. (2020). Structural basis for distinct operational modes and protease activation in AAA+ protease Lon.

Skerker, J.M., Prasol, M.S., Perchuk, B.S., Biondi, E.G., and Laub, M.T. (2005). Two-component signal transduction pathways regulating growth and cell cycle progression in a bacterium: A system-level analysis. PLoS Biology *3*.

Smith, S.C., Joshi, K.K., Zik, J.J., Trinh, K., Kamajaya, A., Chien, P., and Ryan, K.R. (2014). Cell cycle-dependent adaptor complex for ClpXP-mediated proteolysis directly integrates phosphorylation and second messenger signals. Proceedings of the National Academy of Sciences of the United States of America *111*, 14229–14234.

Tan, H.M., Kozdon, J.B., Shen, X., Shapiro, L., and McAdams, H.H. (2010). An essential transcription factor, SciP, enhances robustness of Caulobacter cell cycle regulation. Proceedings of the National Academy of Sciences of the United States of America *107*, 18985–18990.

Wang, J.D., Herman, C., Tipton, K.A., Gross, C.A., and Weissman, J.S. (2002). Directed evolution of substrate-optimized GroEL/S chaperonins. Cell *111*, 1027–1039.

Wang, K.H., Sauer, R.T., and Baker, T.A. (2007). ClpS modulates but is not essential for bacterial N-end rule degradation. Genes and Development *21*, 403–408.

Witkin, E.M. (1946). Inherited Differences in Sensitivity to Radiation in Escherichia Coli. Proceedings of the National Academy of Sciences of the United States of America *32*, 59–68.

Wortinger, M., Sackett, M.J., and Brun, Y. V. (2000). CtrA mediates a DNA replication checkpoint that prevents cell division in Caulobacter crescentus. The EMBO Journal *19*, 4503–4512.

Wright, R., Stephens, C., Zweiger, G., Shapiro, L., and Alley, M.R.K. (1996). Caulobacter Lon protease has a critical role in cell-cycle control of DNA methylation. Genes and Development *10*, 1532–1542.

Wu, D., Lim, E., Vaillant, F., Asselin-Labat, M.L., Visvader, J.E., and Smyth, G.K. (2010). ROAST: Rotation gene set tests for complex microarray experiments. Bioinformatics *26*, 2176–2182.

Yakhnin, A. V., Vinokurov, L.M., Surin, A.K., and Alakhov, Y.B. (1998). Green fluorescent protein purification by organic extraction. Protein Expression and Purification *14*, 382–386.

Ye, X., Lin, J., Mayne, L., Shorter, J., and Walter Englander, S. (2020). Structural and kinetic basis for the regulation and potentiation of Hsp104 function. Proceeding of the National Academy of Science.

Yokom, A.L., Gates, S.N., Jackrel, M.E., Mack, K.L., Su, M., Shorter, J., and Southworth, D.R. (2016). Spiral architecture of the Hsp104 disaggregase reveals the basis for polypeptide translocation. Nature Structural and Molecular Biology *23*, 830–837.

Zeinert, R.D., Liu, J., Yang, Q., Du, Y., Haynes, C.M., and Chien, P. (2018). A legacy role for DNA binding of Lon protects against genotoxic stress. BioRxiv.

Graphical Abstract

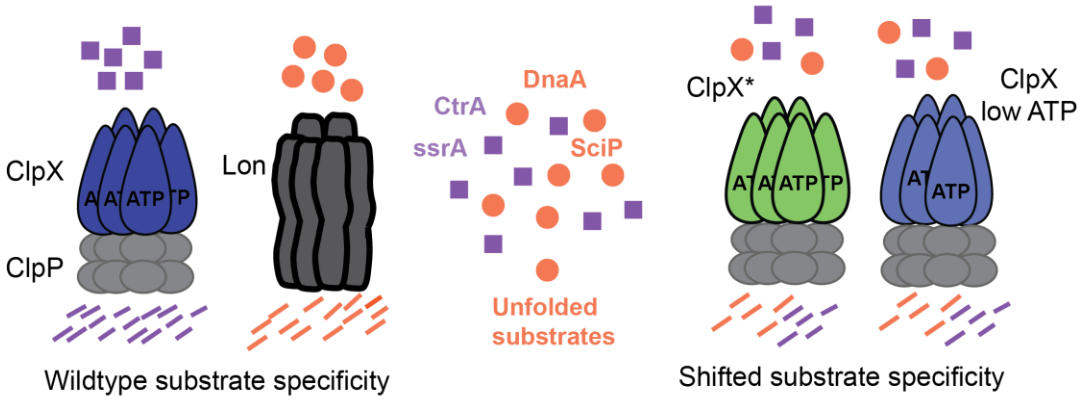

Figure 2.1 Graphical Abstract

AAA+ proteases, such as Lon and ClpXP, collectively regulate protein homeostasis by degrading distinct substrate. We identify a mutant allele of ClpX, ClpX*, that has altered substrate specificity, which allows cells to compensate for the loss of the Lon protease. We find that wildtype ClpX under limiting ATP

conditions undergoes a similar switch in substrate specificity. We propose that these changes in substrate preferences are due to alterations in ATP-dependent conformational dynamics.

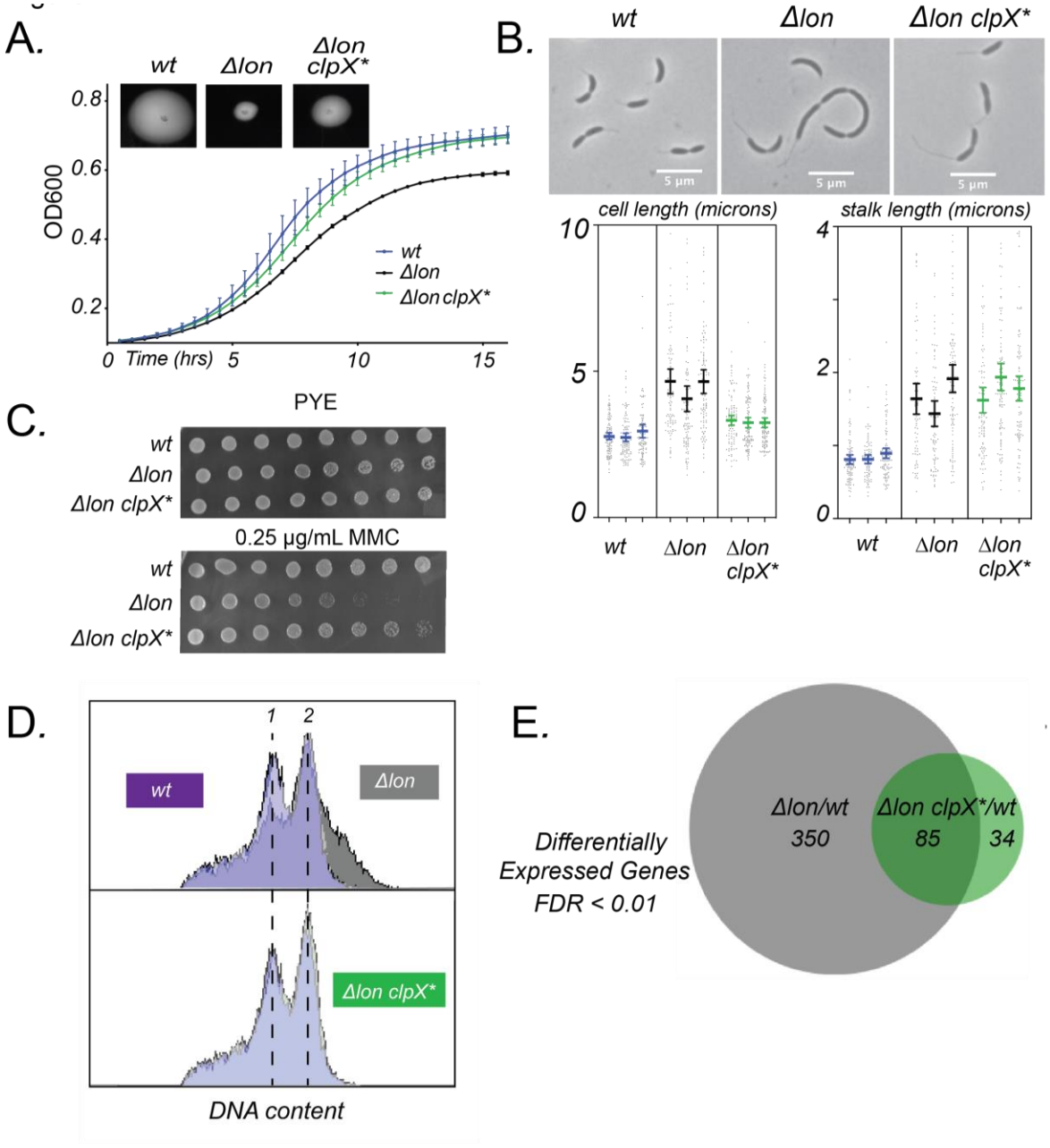

Figure 2.2 : *clpX mutant suppresses *Δlon* phenotypes**

A. Growth curves of *wild type* (*wt*), *⊿lon, and ⊿lon clpX** cells grown in PYE. Biological triplicate experiments are shown. Error bars represent 95% confidence interval. Inset shows motility assays as measured by growth in 0.3% PYE agar.

B. Representative phase-contrast microscopy images of *wt*, *⊿lon, and ⊿lon clpX** cells grown in PYE during exponential phase. Quantification of cell length and stalk length for three biological replicates of n=100 cells.

C. Serial dilution assays comparing colony formation of strains in PYE and PYE supplemented with mitomycin C. Spots are plated 10-fold dilutions of exponentially growing cells from left to right.

D. Flow cytometry profiles showing chromosome content of indicated strains after three-hour treatment with rifampicin. Cells were stained with SYTOX Green to measure DNA content. The fluorescent intensities corresponding to one chromosome (1) and two chromosomes (2) are indicated. Experiment was performed two times. Representative data from one of the biological replicates is shown here.

E. Venn diagram summarizing the number of differentially expressed genes with an FDR cutoff < 0.01 from RNA seq performed with stationary phase cells. Venn diagram created by BioVenn (Hulsen, de Vlieg and Alkema, 2008).

See also Figure S1.

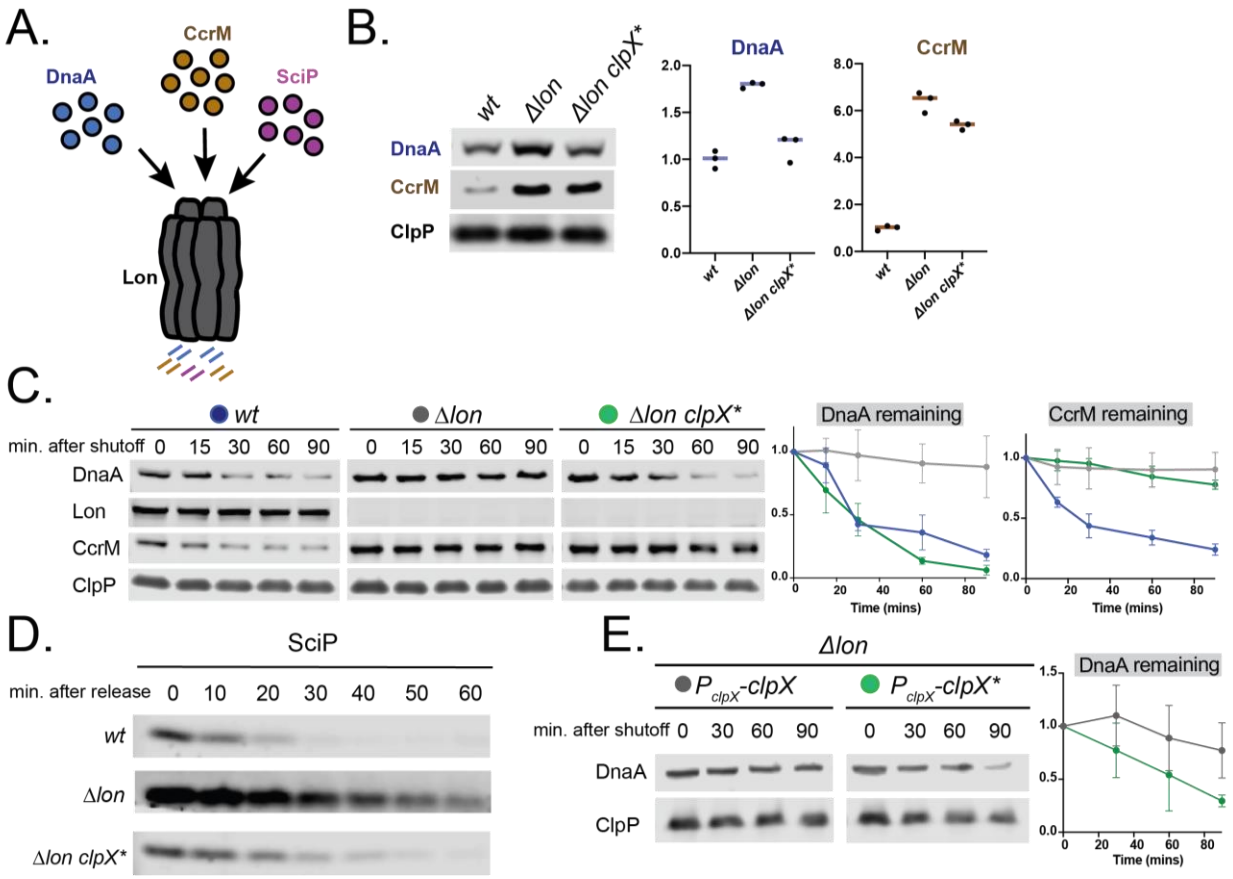

Figure 2.3: *clpX mutant restores levels of Lon substrates through degradation**

A. Lon degrades DnaA, SciP, and CcrM in *C. crescentus* (Wright *et al.*, 1996; Gora *et al.*, 2013; Jonas *et al.*, 2013).

B. Western blot showing DnaA and CcrM levels in *wt*, *Δlon, and Δlon clpX** cells. Lysates from an equal number of exponential phase cells were probed with anti-DnaA or anti-CcrM antibody. ClpP was used as a loading control. A representative image and quantifications of triplicate experiments are shown.

C. Antibiotic shutoff assays to monitor DnaA and CcrM stabilities in wt*, Δlon, and Δlon clpX** cells. Chloramphenicol was added to stop synthesis and lysates from samples at the indicated time points were used for western blot analysis.

Quantifications of triplicate experiments with substrate shown relative to ClpP control levels are shown to the right. Error bars represent SD.

D. Western blot showing SciP levels in synchronized populations of wt, *Δlon, and Δlon clpX** cells. Swarmer cells were isolated using a density gradient and an equal number of cells were released into fresh PYE medium. Samples were withdrawn at the indicated time points and probed with anti-SciP.

E. DnaA stability is measured in Δ*lon* strains expressing an extra copy of wildtype *clpX* or *clpX**. Experiment was performed four times. Representative data from one of the biological replicates is shown here. Quantifications of experiments shown to the right. Error bars represent SD.

See also Figure S2 and S3.

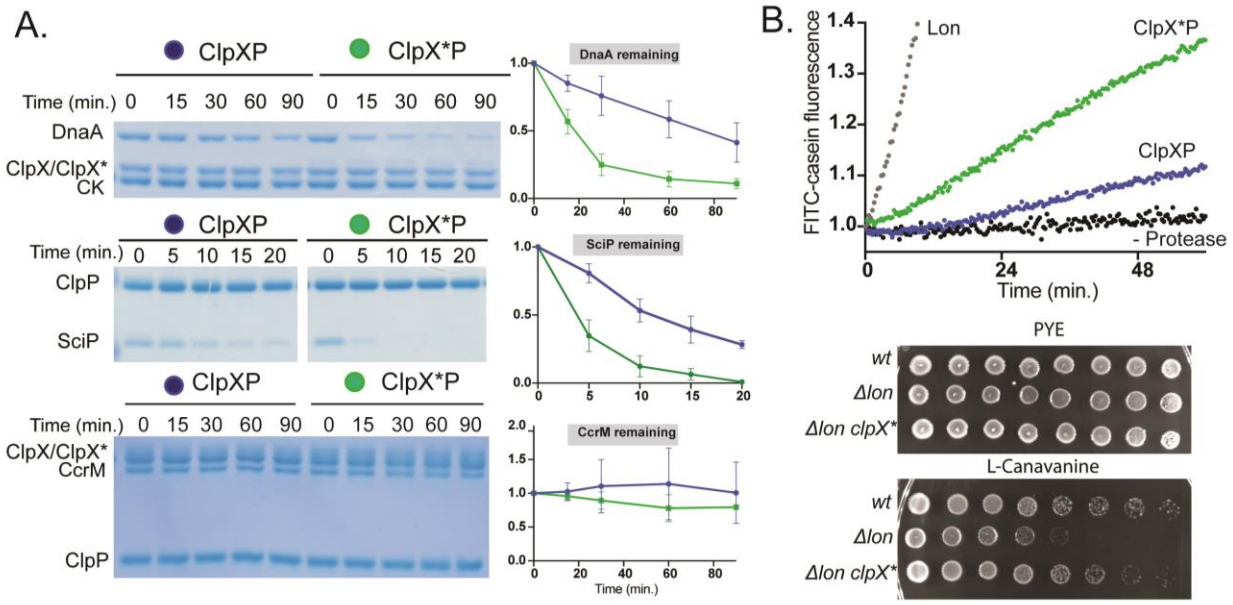

Figure 2.4: ClpX*P degrades some Lon substrates faster than ClpXP *in vitro*.

A. *In vitro* degradation of DnaA, SciP, or CcrM. Assays were performed with 0.1 μM $ClpX_6$ or $ClpX_6$*, and 0.2 μM $ClpP_{14}$. Substrate concentrations were 1 μM DnaA, 5 μM SciP, 0.5 μM CcrM. Quantification of triplicate experiments shown. Error bars represent SD.

B. *In vitro* fluorescence degradation assay of FITC-casein in the presence of ClpXP or ClpX*P or Lon. Degradation assays were performed with 10μg/mL FITC-Casein, 0.1 μM $ClpX_6$ or $ClpX_6$* and 0.2 μM $ClpP_{14}$ or 0.1 μM Lon_6. Serial dilution assays comparing colony formation of strains in PYE and PYE supplemented with L-canavanine. Spots are plated 10-fold dilutions of exponentially growing cells from left to right.

See also Figure S4.

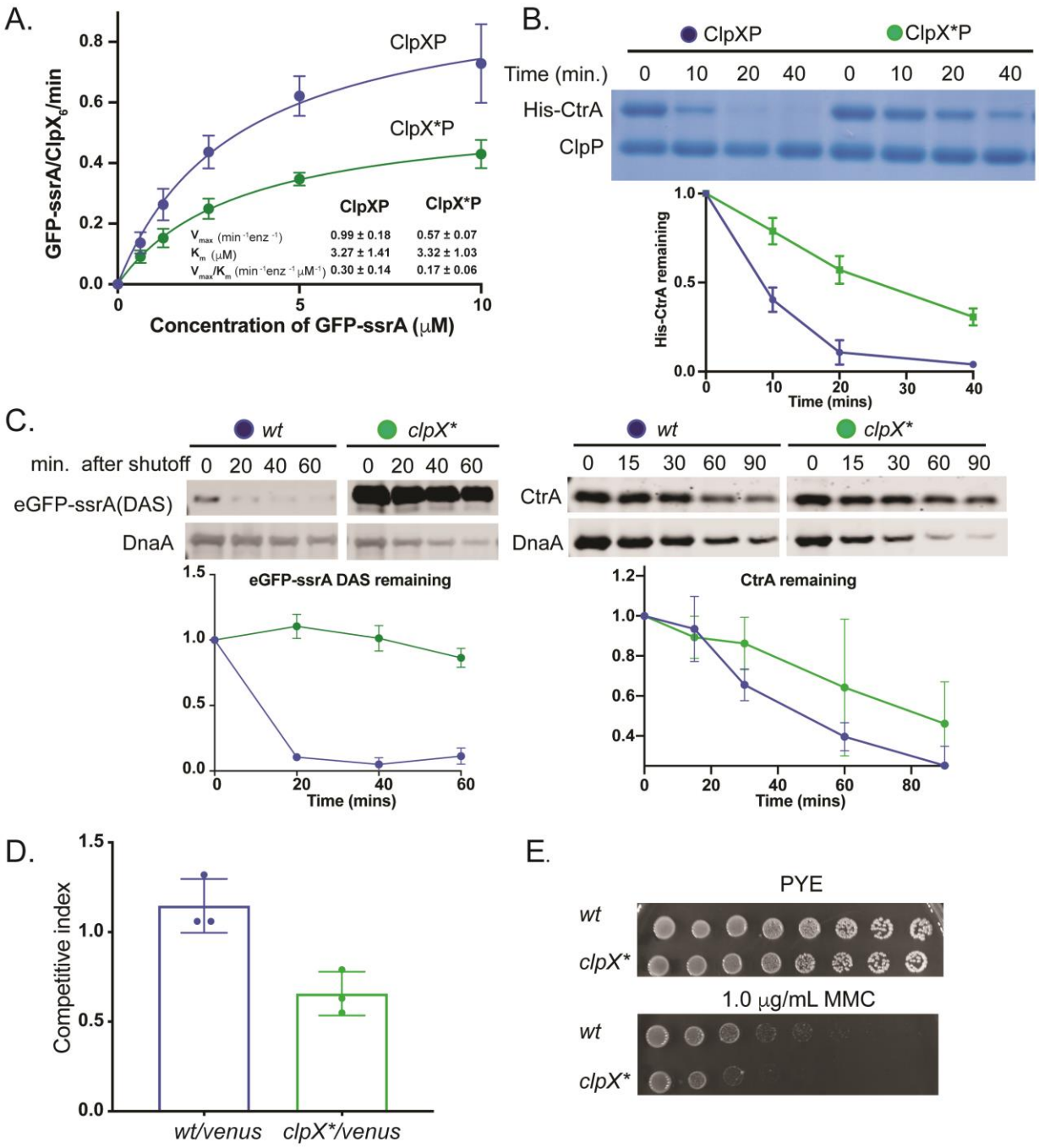

Figure 2.5: ClpX* mutant is deficient in degradation of native ClpXP substrates

A. Michaelis-Menten plot showing the rate of degradation as a function of GFP-ssrA concentration by ClpXP and ClpX*P. Inset displays kinetic parameters.

Assays were performed with 0.1 μM $ClpX_6$ or $ClpX^*_6$, 0.2 μM $ClpP_{14}$, ATP regeneration system, and the indicated concentrations of GFP-ssrA. Data was fitted to Michaelis-Menten equation. Triplicate experiments are shown.

B. *In vitro* degradation assay of His-CtrA in the presence of ClpXP or ClpX*P. Degradation assays were performed with 3 μM His-CtrA, 0.1 μM $ClpX_6$ or $ClpX^*_6$, 0.2 μM $ClpP_{14}$, and ATP regeneration system. Quantification of duplicate experiments is shown below. Error bars represent SD.

C. *In vivo* degradation assay showing eGFP-ssrA (DAS), DnaA, and CtrA stability in *wt* and *clpX** cells. The plasmid encoded M2FLAG-eGFP-ssrA (DAS) construct was induced with the addition of 0.2% xylose. Chloramphenicol was used to inhibit protein synthesis. Samples were withdrawn at the indicated time points and quenched in SDS lysis buffer. Lysate from an equal number of cells was used for western blot analysis and probed with anti-M2, or anti-CtrA, and anti-DnaA antibody. Quantification of triplicate experiments is shown below. Error bars represent SD.

D. Competition assay with wildtype cells harboring xylX::Plac-venus (constitutive venus expression) and nonfluorescent wt or *clpX** strains. exponential phase cells were mixed 1:1, diluted, and allowed to outgrow for 12 doublings. . Quantification of triplicate experiments is shown below. Error bars represent SD.

E. Serial dilution assays comparing colony formation of *wt* and *clpX** cells in PYE and PYE supplemented with MMC. Spots are plated 10-fold dilutions of exponentially growing cells from left to right.

See also Figure S5.

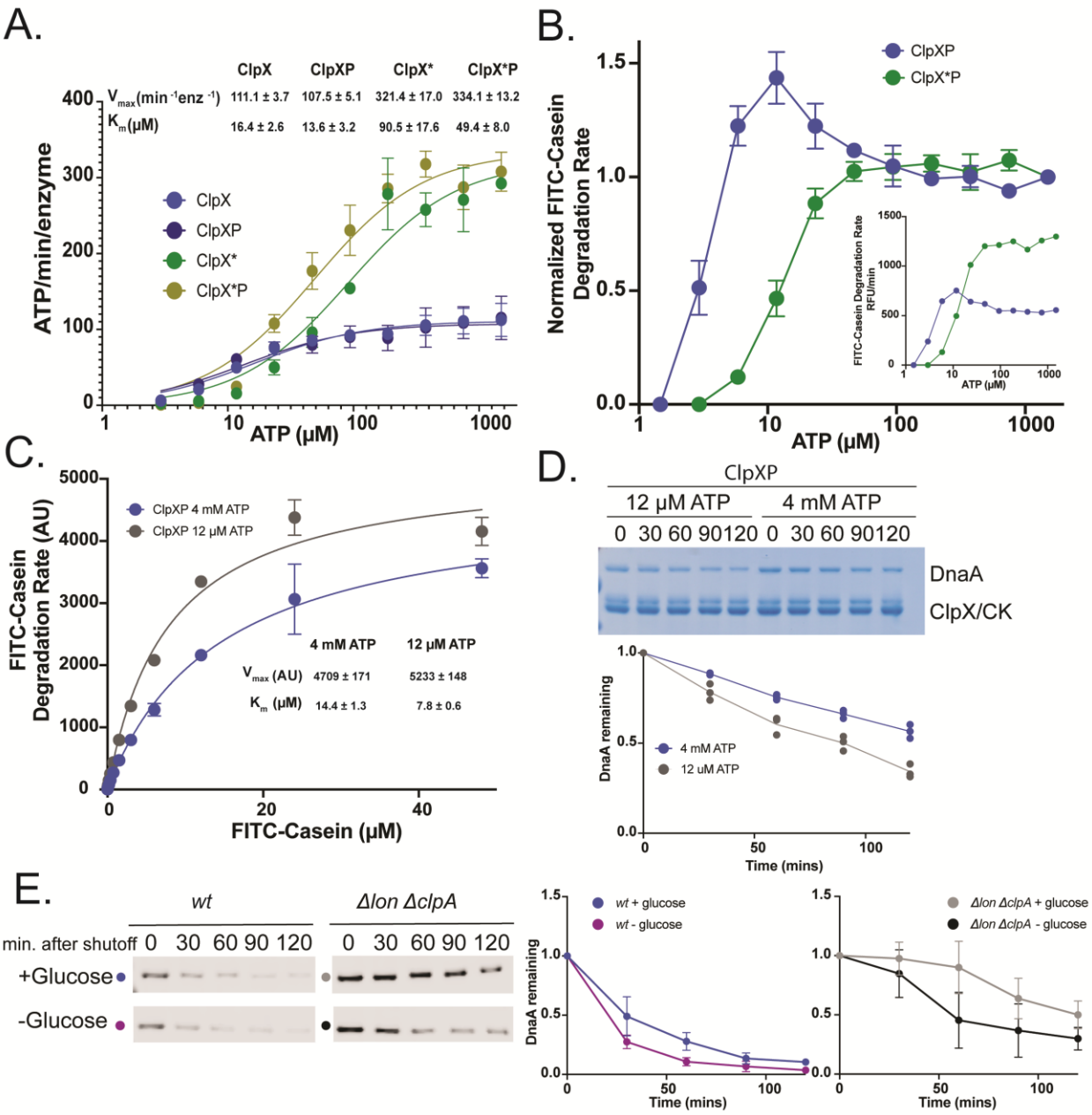

Figure 2.6: Limiting ATP alters wildtype ClpXP substrate specificity

A. Michaelis-Menten plot showing the rate of ClpX/ClpX* catalyzed ATP hydrolysis as a function of ATP concentration. Inset displays kinetic parameters. Assays were performed with 0.1 μM $ClpX_6$ or $ClpX^*_6$, in the presence and

absence of 0.2 μM $ClpP_{14}$. Data was fitted to Michaelis-Menten equation. Triplicate experiments are shown.

B. FITC-Casein degradation by ClpXP or ClpX*P as a function of ATP concentration. Assays were performed with 0.1 μM $ClpX_6$ or $ClpX^*_6$, 0.2 μM $ClpP_{14}$, ATP regeneration system, and 50 μg/mL FITC-Casein. Rates were normalized to highest concentration of ATP. Non-normalized rates shown in the inset.

C. Michaelis-Menten plot showing the rate of degradation as a function of FITC-Casein concentration by ClpXP under low and saturating ATP conditions. Inset displays kinetic parameters. Assays were performed with 0.1 μM $ClpX_6$, 0.2 μM $ClpP_{14}$, and ATP regeneration system. Data was fitted to Michaelis-Menten equation. Triplicate experiments are shown.

D. *In vitro* degradation of DnaA by ClpXP under low and saturating ATP conditions. Assays were performed with 0.1 μM $ClpX_6$, and 0.2 μM $ClpP_{14}$ and 0.5 μM DnaA. Quantification of triplicate experiments.

E. Antibiotic shutoff assays to monitor DnaA under ATP limiting conditions in *wt* and *Δlon ΔclpA* strains. Chloramphenicol was added to stop synthesis and lysates from samples at the indicated time points were used for western blot analysis. Quantifications of triplicate experiments shown to the right. Error bars represent SD.

See also Figure S6 and S7.

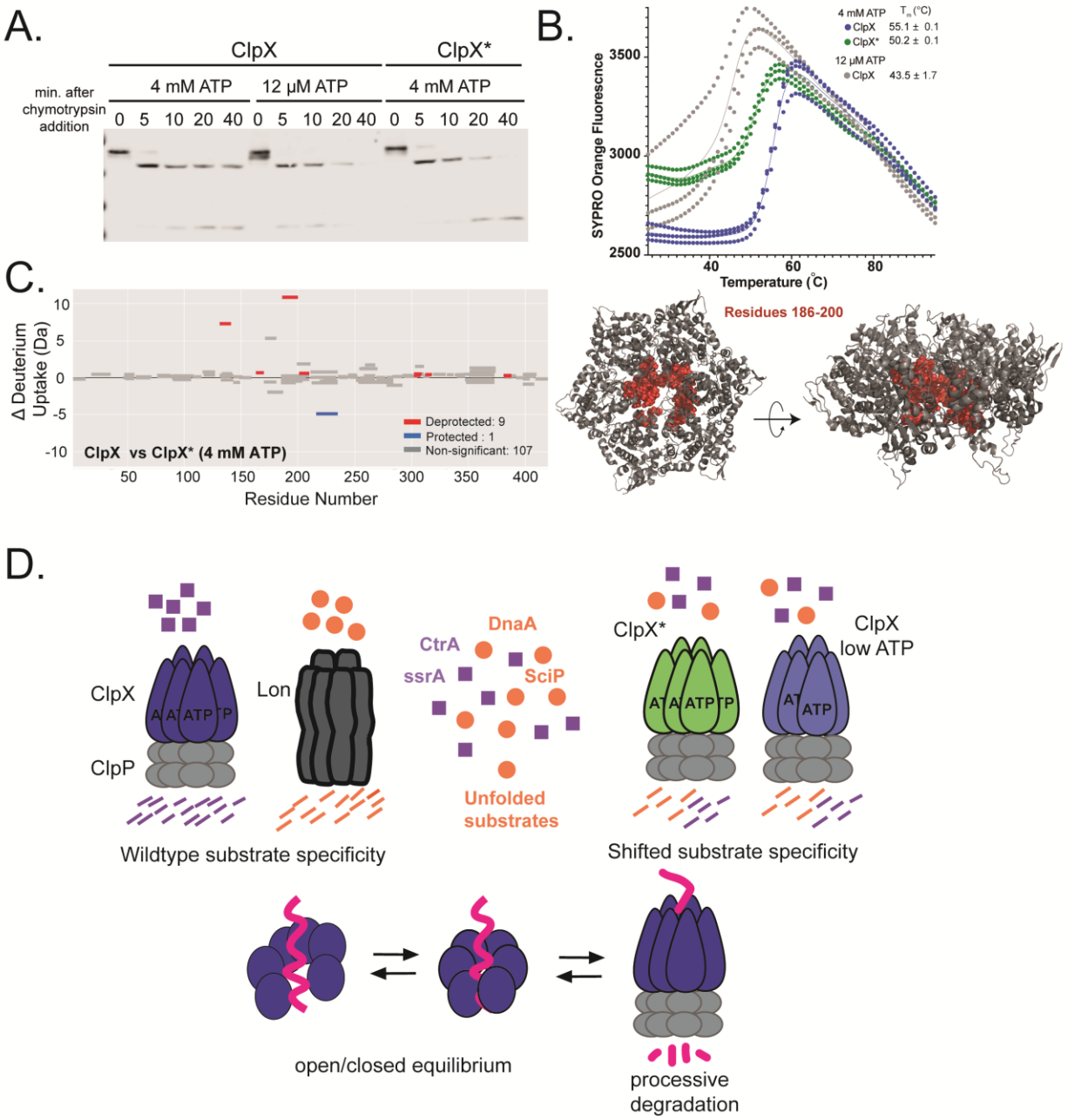

Figure 2.7: ClpX adopts distinct ATP-dependent conformational states

A. Limited proteolysis assay to probe conformational states. ClpX was incubated with Chymotrypsin with either 12 µM ATP or 4 mM ATP in the presence of ClpP and ATP regeneration system at 25 °C for the indicated time points. ClpX* was incubated with Chymotrypsin at 4 mM ATP in the presence of ClpP and ATP

regeneration system at 25 °C for the indicated time points. ClpX was detected using anti-ClpX antibodies.

B. Stability of ClpX* with 4 mM ATP, ClpX with 4 mM ATP, and ClpX with 12 µM ATP as measured by Differential scanning fluorimetry. Triplicate experiments shown.

C. Woods plot comparing deuterium uptake for wildtype ClpX vs ClpX* at 4 mM ATP after 60 minutes. Each bar on Woods plot represents a single peptide with peptide length corresponding to the bar length. Red bars indicate a deprotected (more deuterium uptake) region, blue represents a protected region, and gray bars are not significantly different. Woods plots were created with Deuteros (Lau et al. 2021) using the peptide significance test (p-value <0.01). Residues 186-200 are highlighted in red for the equivalent residues in the substrate-bound *E. coli* ClpX structure (Protein Data Bank ID: 6PO1) using PYMOL (Schrodinger).

D. In a wildtype cell, AAA+ proteases Lon and ClpXP promote normal growth by degrading distinct substrates. ClpX*P can compensate for the absence of the Lon protease by tuning ClpX substrate specificity to better degrade Lon-restricted substrates (such as DnaA, SciP, and misfolded proteins) but this comes at the cost of native ClpXP substrates (such as ssrA-tagged proteins and CtrA). We propose that ClpX exists in an equilibrium between a closed and open conformation and promoting one state over the other leads to alterations in substrate specificity. In the presence of ClpX* or in ATP-limited conditions, ClpX adopts a more open conformation, allowing capture and recognition of substrates such as casein. The balance shifts to the closed state under high ATP conditions,

allowing degradation of substrates such as GFP-ssrA, which preferentially bind the closed state.

See also Figure S8

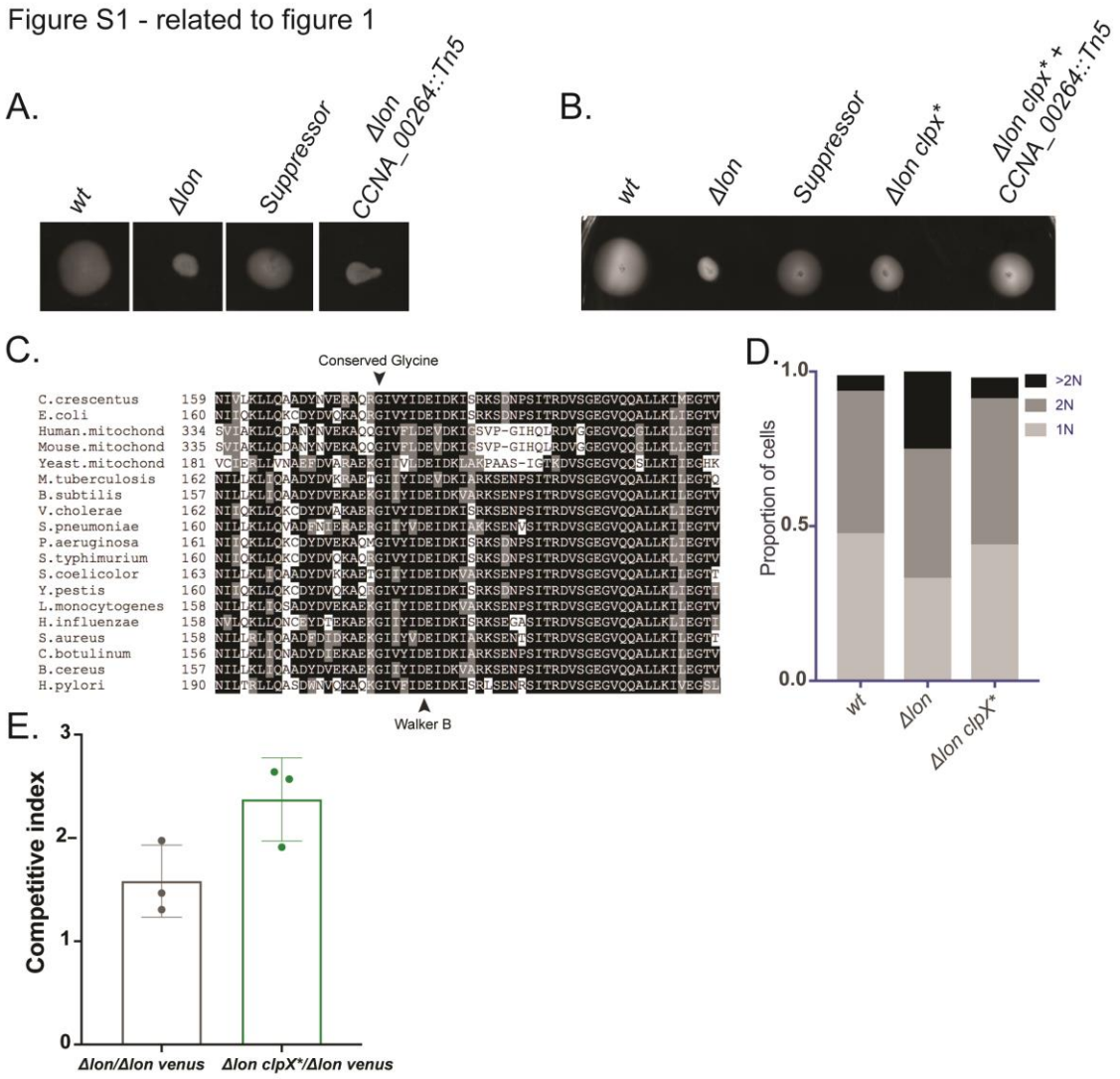

Figure 2.8: Validation of motility screen suppressor

(A-B) Motility assay on 0.3% PYE agar of indicated strains.

C. Sequence alignment of ClpX homologs. Conserved glycine residue and walker B motif are marked.

D. Quantification of the percent of cells with DNA content of 1N, 2N, and >2N in *wt*, *Δlon,* and *Δlon clpX** strains.

E. Competition assay with Δ*lon* cells harboring xylX::Plac-venus (constitutive venus expression) and nonfluorescent Δ*lon* or Δ*lon clpX** strains. Exponential phase cells were mixed 1:1, diluted, and allowed to outgrow for 12 doublings. Quantification of triplicate experiments is shown below. Error bars represent SD.

Figure S2- Related to Figure 2

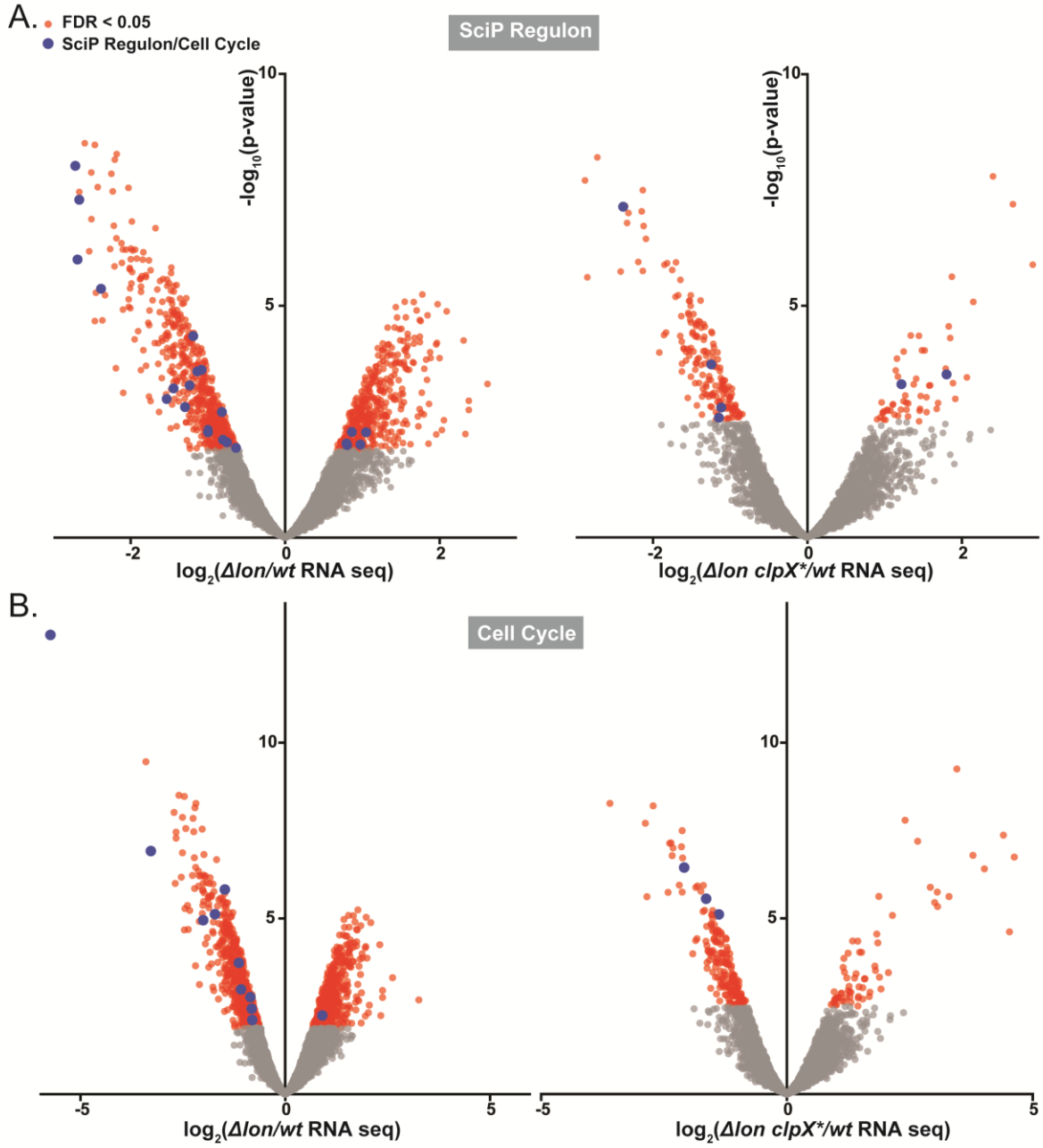

C.

FRY Gene Set Analysis

	Δlon vs *wt*				Δlon clpX* vs wt			
	Number of Genes	Direction	p-value	FDR	Number of Genes	Direction	p-value	FDR
SciP	61	Down	0.0029	0.0044	61	Down	0.3391	0.5042
CcrM	504	Up	0.0014	0.0014	504	Up	0.7391	0.7391
DnaA	32	Down	0.0989	0.0980	32	Down	0.0919	0.1275

KEGG Enrichment Analysis

	Cell Cycle		
	Number of Genes	Direction	p-value
Δlon vs wt	31	10, Down	0.0086
Δlon clpX vs wt*	31	3, Down	0.1725

Figure 2.9: RNA-seq gene set analysis

(A-B) Volcano plot showing the transcriptional differences of Δ*lon* compared to *wt* (left) and *Δlon clpX** compared to *wt* (right), as measured by RNA-seq. The negative $\log_{10}$ of the p value is plotted against $\log_2$ of the fold change mRNA counts. Genes that are marked in red have an FDR <0.05. Transcripts that are associated with either the SciP regulon (Tan *et al.*, 2010) or cell cycle (KEGG pathways) are highlighted in blue.

C. Kyoto Encyclopedia of Genes and Genomes (KEGG) pathway enrichment analysis and FRY gene set analysis. FRY gene set analysis performed using *fry* function from *edgeR* package in R (Robinson, McCarthy and Smyth, 2009; Wu *et al.*, 2010). The CcrM, DnaA, and SciP regulons were assigned according to (Hottes, Shapiro and McAdams, 2005; Tan *et al.*, 2010; Gonzalez *et al.*, 2014). Over-represented pathways in KEGG pathway database identified using the *kegga* function from *edgeR* package in R.

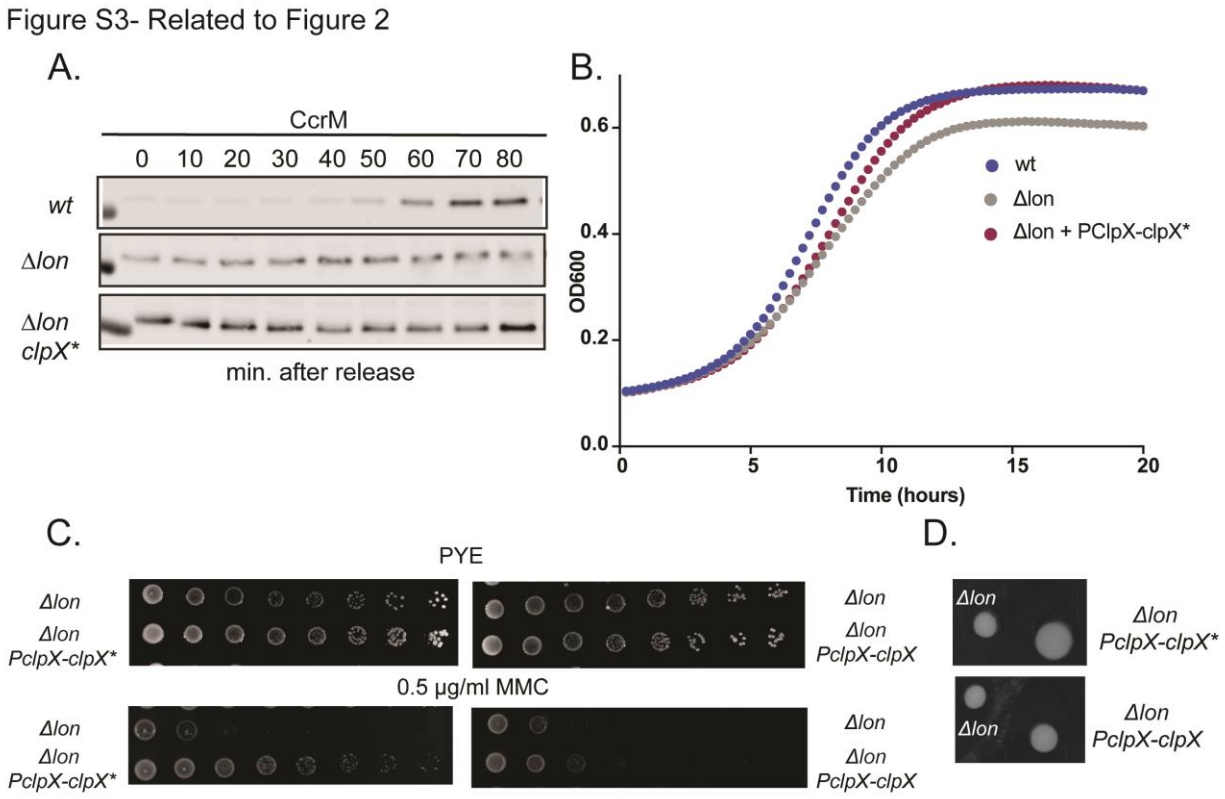

Figure 2.10: *clpX mutant is dominant**

A. Western blot showing CcrM levels in synchronized populations of wt, *Δlon, and Δlon clpX** cells. Swarmer cells were isolated using a density gradient and an equal number of cells were released into fresh PYE medium. Samples were withdrawn at the indicated time points and probed with anti-CcrM.

B**.** Growth curves of *wild type* (wt), *Δlon, and Δlon* merodiploid with second copy of *clpX** at native locus*.* Cells grown in PYE.

C. Spot assays comparing colony formation of strains in PYE and PYE supplemented with mitomycin C.

D. Motility assay on 0.3% PYE agar of indicated strains.

Figure S4- Related to Figure 3

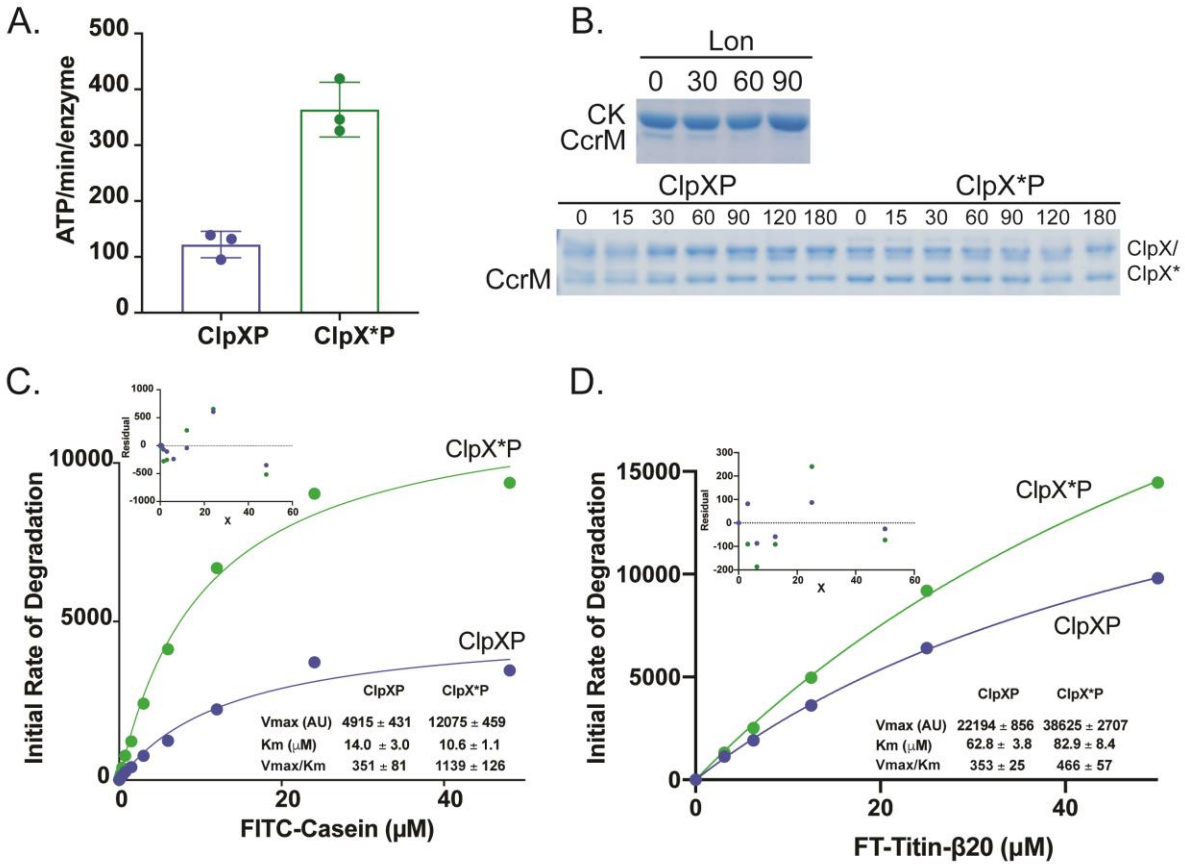

Figure 2.11: *In vitro* characterization of ClpX*

A. ATPase activity of 0.1 μM $ClpX_6$/$ClpX^*_6$ plus 0.2 μM $ClpP_{14}$ is displayed. Triplicate experiments are shown.

B. *In vitro* degradation of CcrM by 0.2 μM Lon_6 is shown as a control. The bottom gel shows CcrM degradation assay in the presence of ATP, with no regeneration mix.

C. FITC-Casein titration in the presence of either ClpXP or ClpX*P. Data was fit to the Michaelis-Menten equation. ClpX*P degrades FITC-Casein 2-3 fold better than ClpXP.

F. Fluorescin-*Titin*-I27-β20 titration in the presence of either ClpXP or ClpX*P. Data was fit to the Michaelis-Menten equation. V_{max}/K_M was 30% higher for ClpX*P in comparison to ClpXP. Inset shows residual plot for Michaelis-Menten fit.

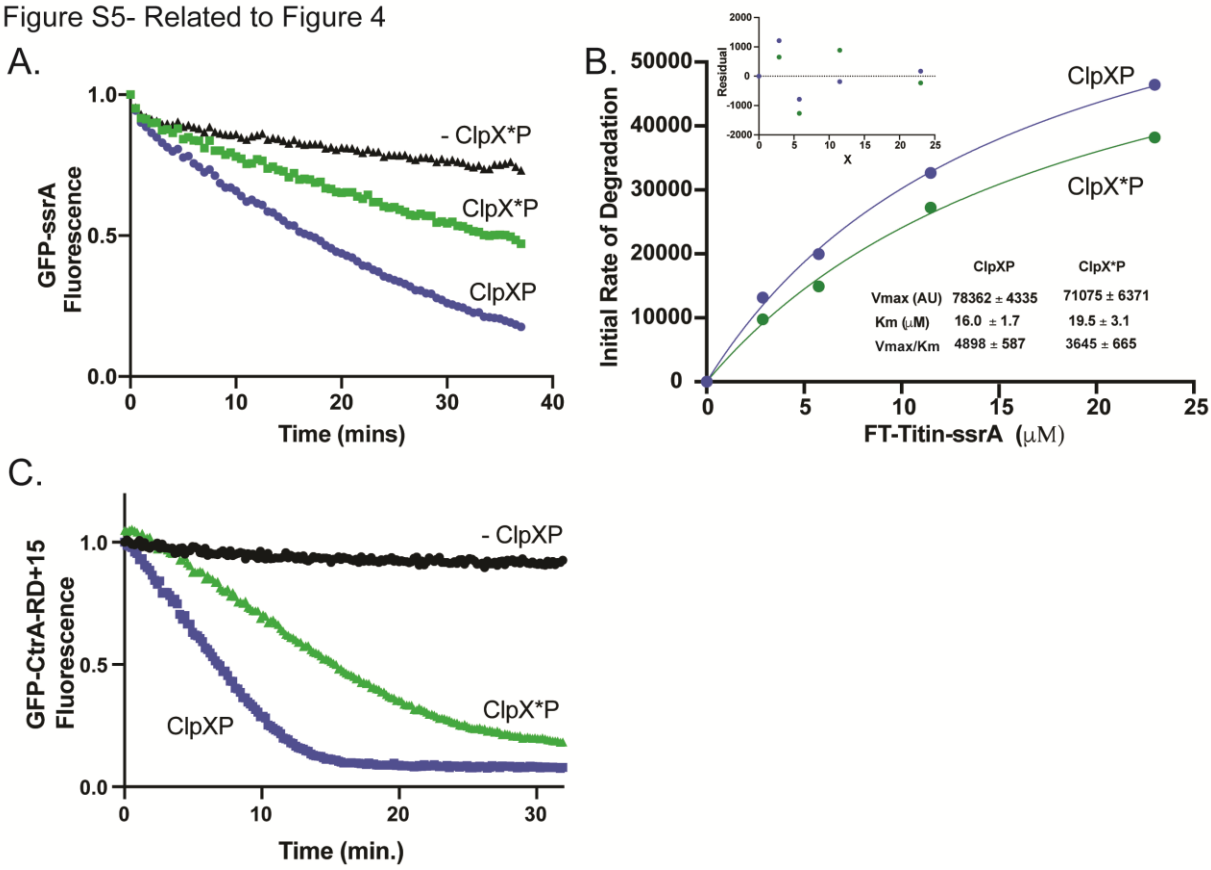

Figure 2.12: ClpX*P is deficient in native substrate degradation

A. *In vitro* degradation of GFP-ssrA.

B. Fluorescein-*Titin*-I27-ssrA titration in the presence of either ClpXP or ClpX*P. Data was fit to the Michaelis-Menten equation. V_{max}/K_M was 30% lower for ClpX*P in comparison to ClpXP. Inset shows residual plot for Michaelis-Menten fit.

C. *In vitro* fluorescence degradation assay of eGFP-CtrA-RD+15 in the presence of adaptors. Degradation assays were performed with 1 μM eGFP-CtrA-RD+15, 0.1 μM $ClpX_6$ or $ClpX^*_6$, 0.2 μM $ClpP_{14}$, 2 μM CpdR, 1 μM RcdA, 1 μM PopA, and 20 μM cyclic di-GMP, and ATP regeneration system.

Figure S6- Related to Figure 5

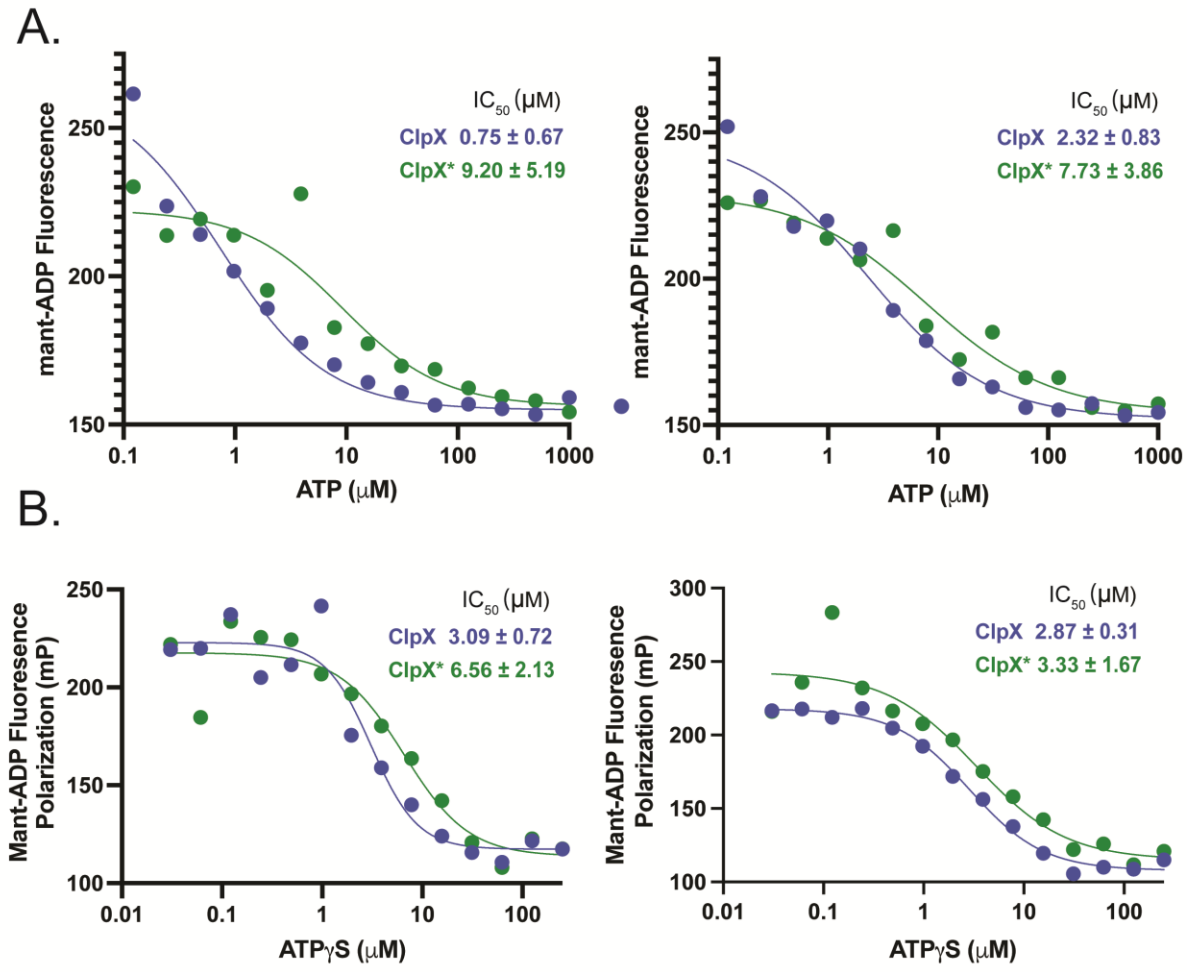

Figure 2.13: ClpX* is deficient in nucleotide binding

A. Titration of ATP against constant mant-ADP (1 μM) in the presence of either 300 nM $ClpX_6$ or $ClpX^*_6$ assayed by changes in fluorescence. Data was fit to an inhibitor versus response – variable slope (four paramaters) function in Graphad

Prism: Y=Bottom + (Top-Bottom)/(1+(IC50/X)^HillSlope) where IC50 is the ATP concentration halfway between bottom and top. Two independent replicates shown.

B. ATPγS competition assay in the presence of either 300 nM $ClpX_6$ or $ClpX^*_6$. Fluorescence polarization of 625 nM mant-ADP was measured as described in methods. Data was fit as described in A. Two independent replicates shown.

Figure S7- Related to Figure 5

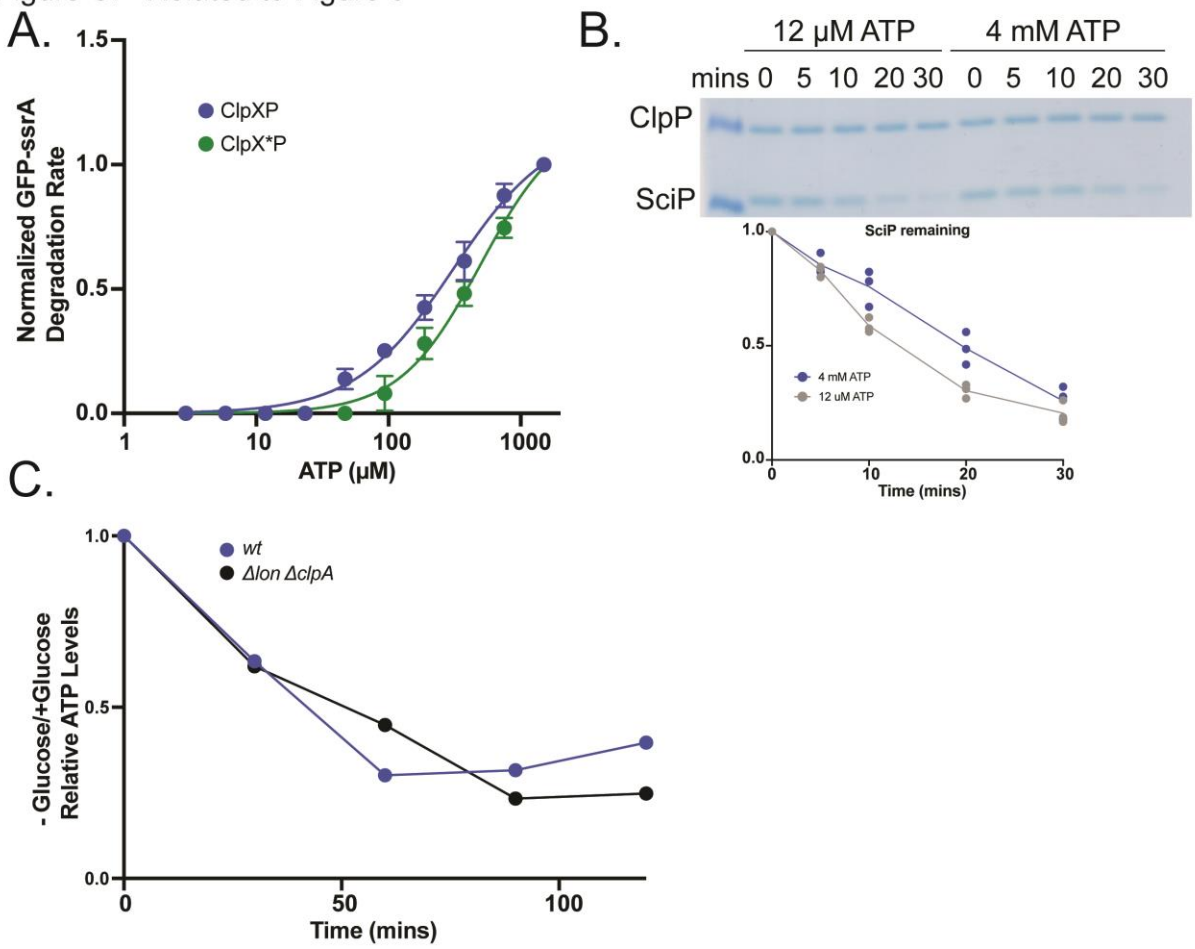

Figure 2.14: Modulating ATP changes substrate preferences

A. GFP-ssrA degradation by ClpXP or ClpX*P as a function of ATP concentration. Assays were performed with 0.1 μM $ClpX_6$ or $ClpX^*_6$, 0.2 μM $ClpP_{14}$, ATP regeneration system, and 10 μM GFP-ssrA.

B. *In vitro* degradation of SciP by ClpXP under low and saturating ATP conditions. Assays were performed with 0.1 μM $ClpX_6$, and 0.2 μM $ClpP_{14}$ and 5 μM SciP. Quantification of triplicate experiments shown.

C. Relative intracellular ATP concentrations measured using a luciferase-based assay during the course of antibiotic shutoff assay.

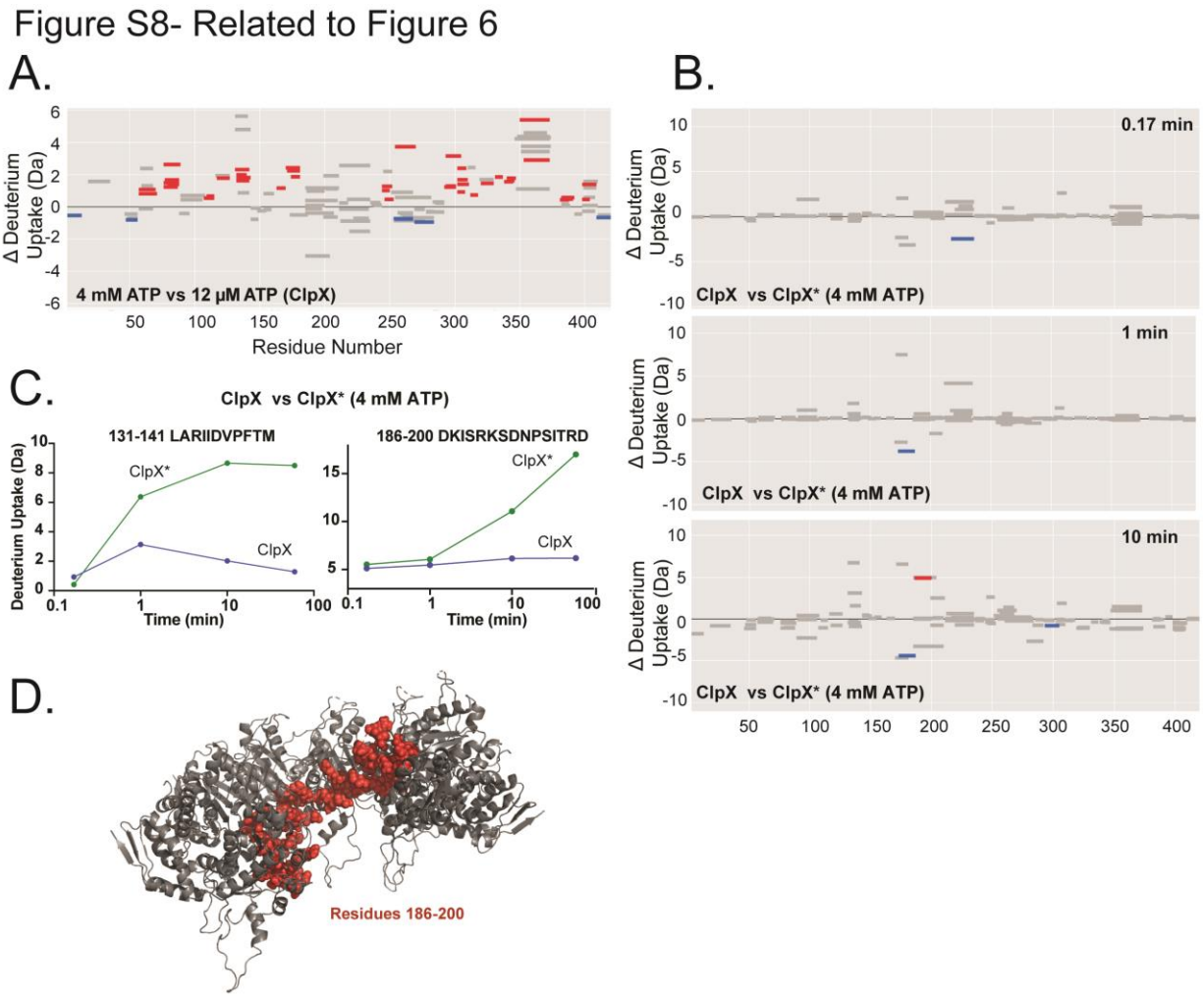

Figure 2.15: ClpX* mutation and limiting ATP lead to increased dynamics of ClpX

A. Woods plot comparing deuterium uptake for wildtype ClpX at 4 mM ATP vs 12 μM ATP at 60 mins. Each bar on Woods plot represents a single peptide with peptide length corresponding to the bar length. Red bars indicate a deprotected (more deuterium uptake) region, blue represents a protected region, and gray bars are not significantly different. Woods plots were created with Deuteros using the peptide significance test (p-value <0.01).

B. Woods plot comparing deuterium uptake for wildtype ClpX vs ClpX* at 4 mM ATP at 0.17, 1, and 10 minutes. Each bar on Woods plot represents a single peptide with peptide length corresponding to the bar length. Red bars indicate a deprotected (more deuterium uptake) region, blue represents a protected region, and gray bars are not significantly different. Woods plots were created with Deuteros (Lau et al. 2021) using the peptide significance test (p-value <0.01).

C. Comparison of deuterium uptake plots of selected peptides for wildtype ClpX vs ClpX*.

D. Each ClpX monomer (Protein Data Bank ID: 6PO1) was mapped onto the substrate-free Lon ATPase domain (Protein Data Bank: 6V11) using PYMOL. Residues 186-200 highlighted in red.

Supplemental File 2.1- Log file

State A: ClpX_CAUVN (clpx sat atp)
HDX time course (min): 0, 0.17, 1, 10, 60
HDX control samples: None
Back-exchange (mean / IQR): N/A
# of Peptides: 129
Sequence coverage: 93.10%
Average peptide length / redundancy: 13.07 / 4.31
Replicates (technical): 3

Repeatability: 0.1915 (average SD)

State B: CLPX_CAUVN (clpxg178a sat atp)
HDX time course (min): 0, 0.17, 1, 10, 60
HDX control samples: None
Back-exchange (mean / IQR): N/A
# of Peptides: 125
Sequence coverage: 92.62%
Average peptide length / redundancy: 13.35 / 4.29
Replicates (technical): 3
Repeatability: 0.2475 (average SD)

State B: CLPX_CAUVN (clpx 12um atp)
HDX time course (min): 0, 0.17, 1, 10, 60
HDX control samples: None
Back-exchange (mean / IQR): N/A
# of Peptides: 127
Sequence coverage: 93.10%
Average peptide length / redundancy: 13.23 / 4.30
Replicates (technical): 3
Repeatability: 0.3069 (average SD)

Table 2.1 Strain List

Organism	Name	Description	Source
C.crescentus	CPC176	Isolate of CB15N/NA1000	(Evinger and Agabian, 1977)
	CPC456	Δlon (SpecR)	LS2382 (Wright et al 1996)
	CPC667	Δlon	
	CPC753	Δlon (SpecR) clpXG178A	This study
	CPC798	xylX::PlacZVenus	This study
	CPC891	clpXG178A	This study
	CPC963	wt eGFP-ssrA(DAS)	This study
	CPC964	clpXG178A eGFP-ssrA(DAS)	This study
	CPC1006	Δlon PClpX-ClpX	This study
	CPC1007	Δlon PClpX-ClpXG178A	This study
	CPC413	ΔClpA Δlon	
	CPC807	Δlon xylX::PlacZVenus	This study
E. coli	TOP10	Cloning strain	Invitrogen

BL21(DE3) pLysS	recombinant protein expression	Invitrogen
EPC100	dh5alpha pQE70-his-ClpP	(Chien et al., 2007)
EPC112	BL21DE3 pLysS pET23 Ulp1his protease	
EPC162	BL21DE3 375 eGFP-His6-CtrARD+15	(Smith et al., 2014)
BPC238	BL21DE3 plysS pET23 ClpX	(Chien et al., 2007)
EPC196	BL21DE3 plysS pET23b His6Sumo-CpdR	(Lau et al., 2015)
EPC407	Top10 pBXMCS-2	
EPC 446	BL21DE3 plysS pET23b His6SUMO CcrM	
EPC677	BL21DE3 plysS 375 His6-TacA	(Joshi et al., 2015)
EPC970	BL21DE3 plysS pET23b His6Sumo-RcdA	(Joshi et al., 2015)
EPC1000	TOP10 pET23b His6Sumo-RcdA	(Joshi et al., 2015)
EPC1037	BL21DE3 plysS pET23b His6Sumo-PopA	(Joshi et al., 2015)
EPC1508	Delta ClpX W3110 pBAD GFPS65T ccssrA	
EPC1562	BL21DE3 plysS pBAD33 His6Sumo DnaA BL21DE3 plysS pET23 ClpXG178A	This study

Uncropped western blot for Figure 2B

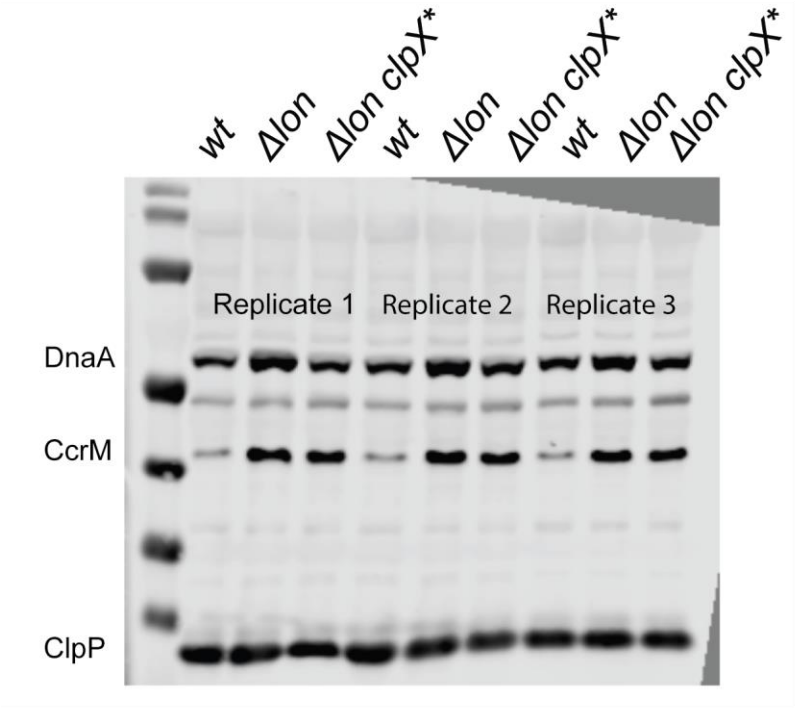

Figure 2.16 Uncropped western blot for Figure 2.2B

Uncropped western blot for Figure 2C

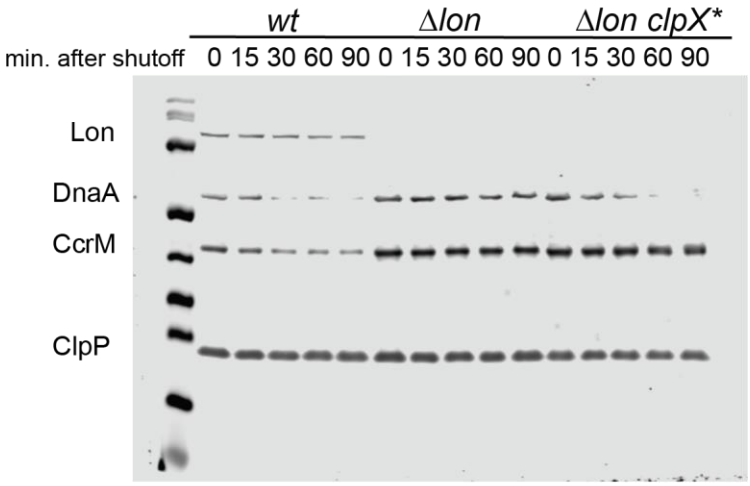

Figure 2.17 Uncropped western blot for Figure 2.2C

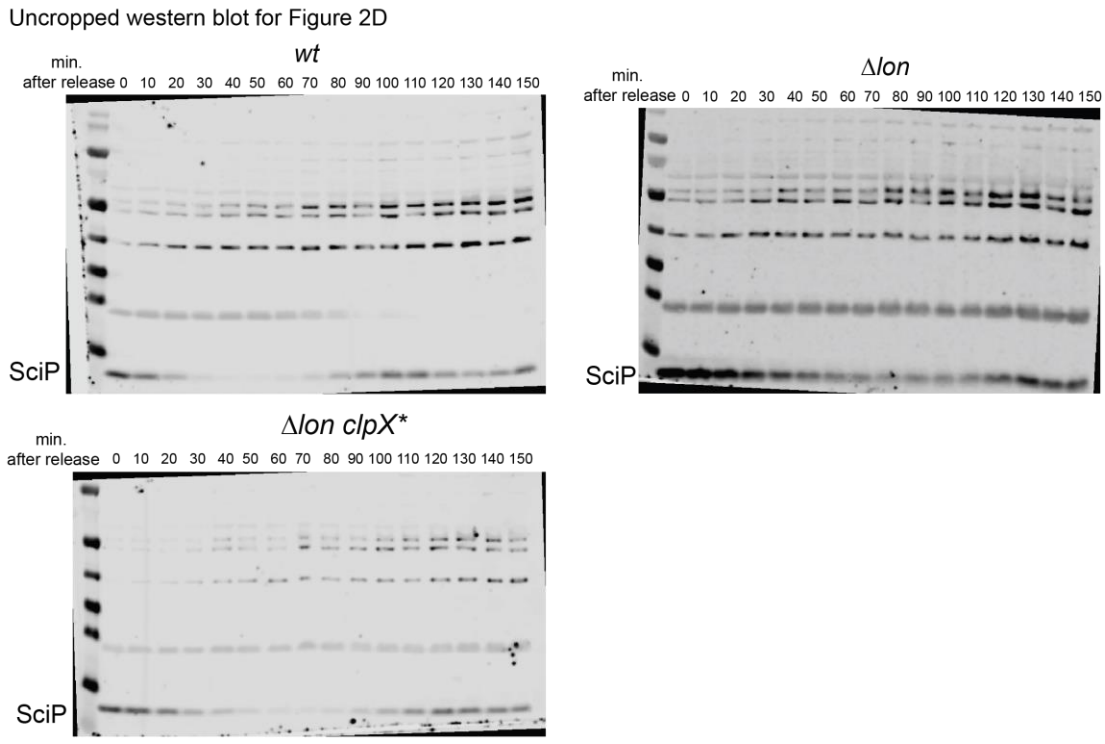

Figure 2.18 Uncropped western blot for Figure 2.2D

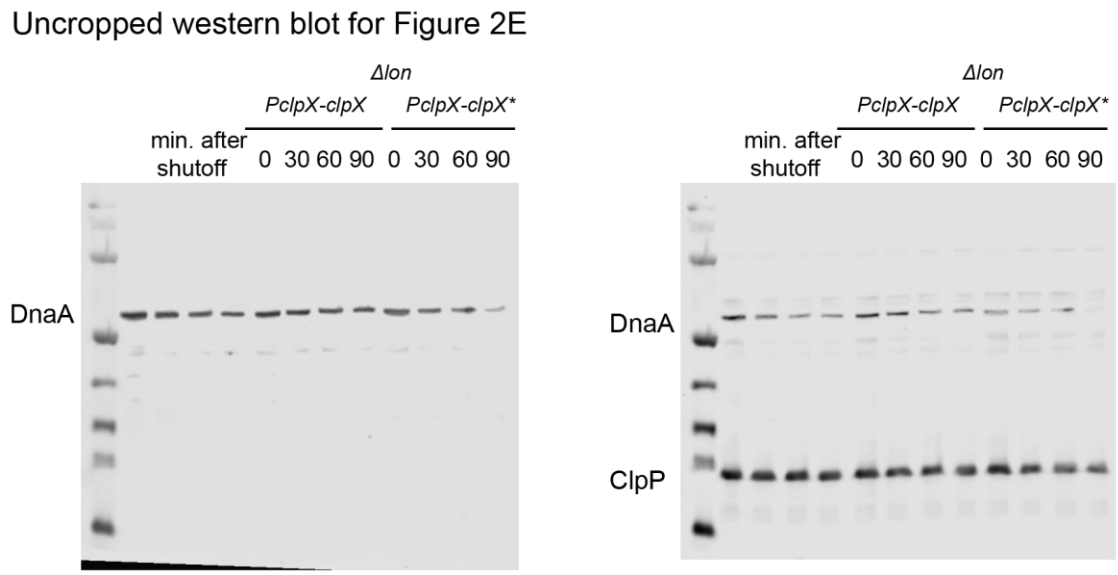

Figure 2.19 Uncropped western blot for Figure 2.2E

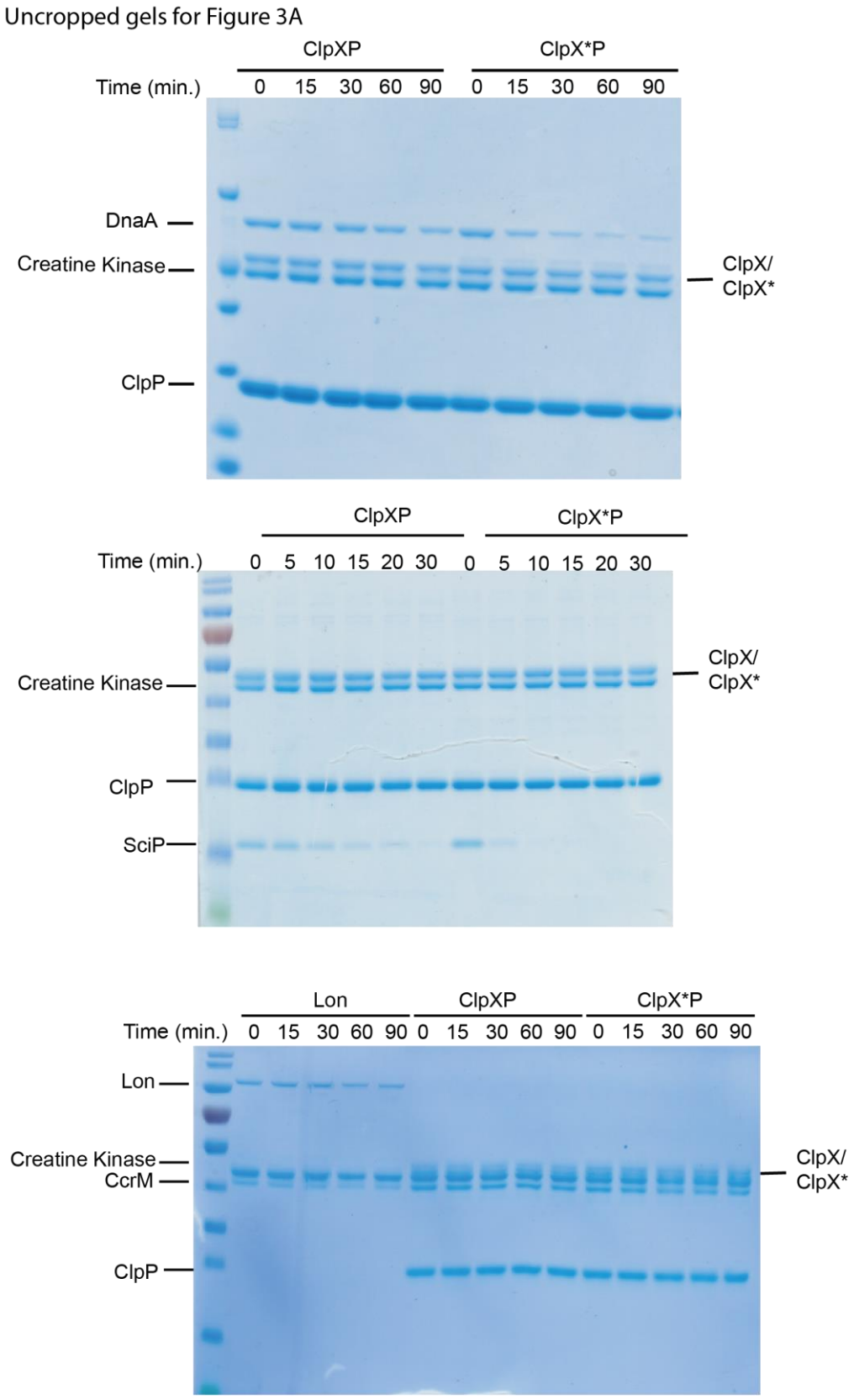

Figure 2.20 Uncropped gels for Figure 2.3A

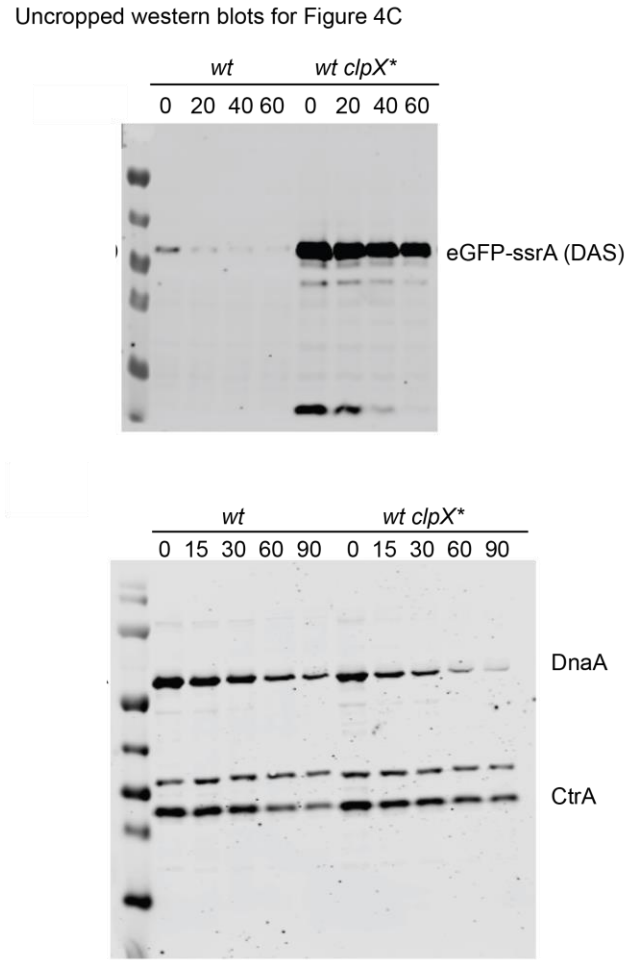

Figure 2.21 Uncropped western blot for Figure 2.4C

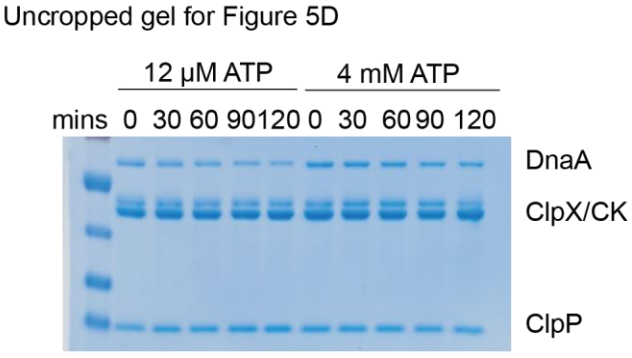

Figure 2.22 Uncropped gel for Figure 2.5D

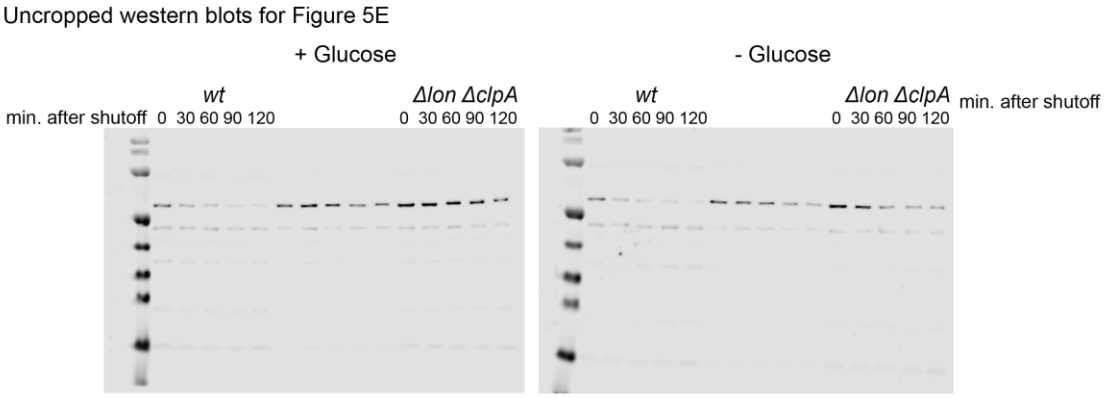

Figure 2.23 Uncropped western blot for Figure 2.5E

2.11 Additional data not included in manuscript

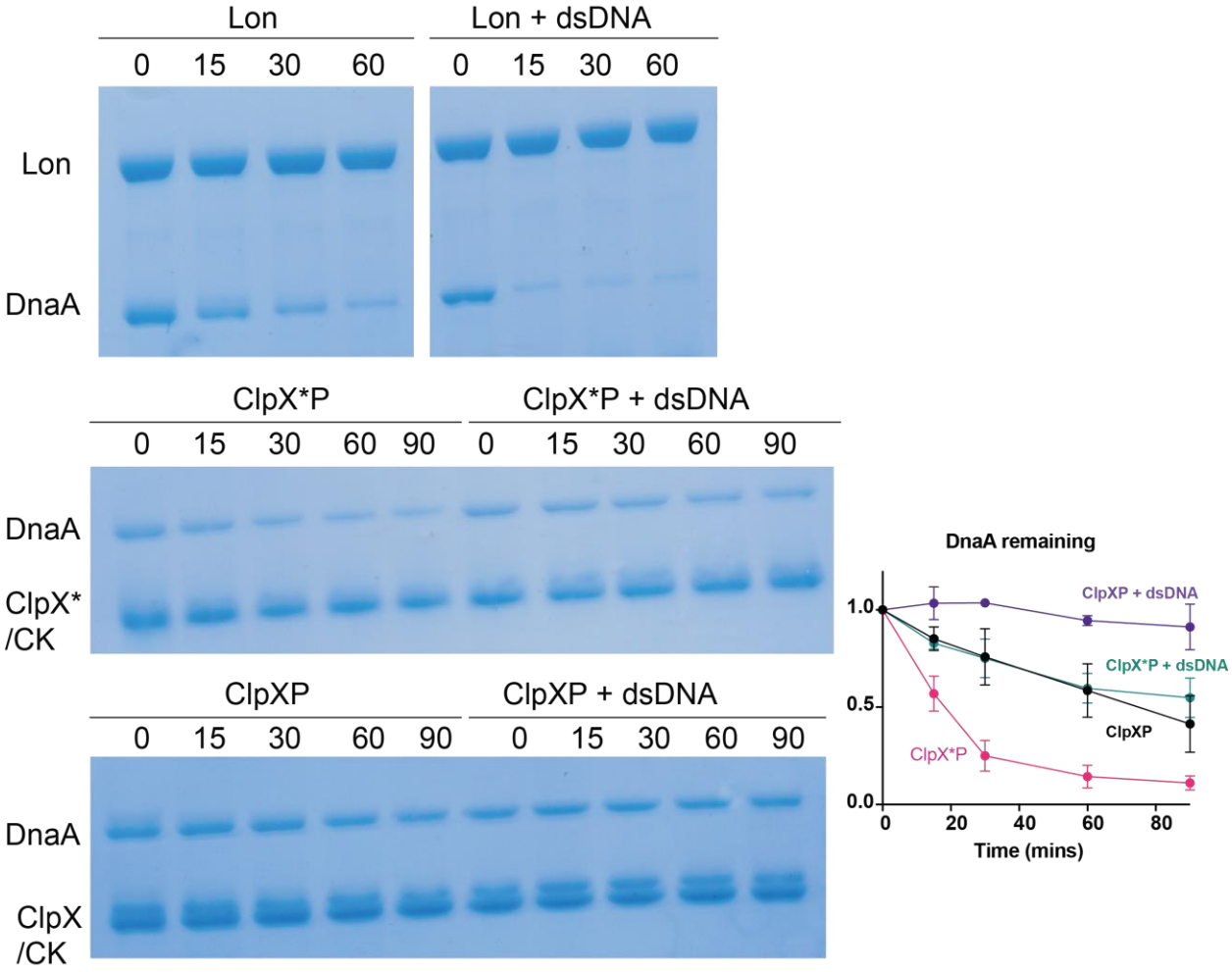

Figure 2.24 dsDNA modulates the degradation of DnaA by the Lon and ClpXP proteases

The addition of dsDNA stimulates Lon to degrade DnaA. However, addition of dsDNA to ClpX*P as well as ClpXP slows down DnaA degradation. Our working model for this is that Lon sluggishly degrades DnaA on its own. However, in the presence of this dsDNA, Lon can also bind it and cause faster degradation of DnaA. This contrasts with ClpXP and ClpX*P which cannot bind DNA so DnaA degradation is slowed down.

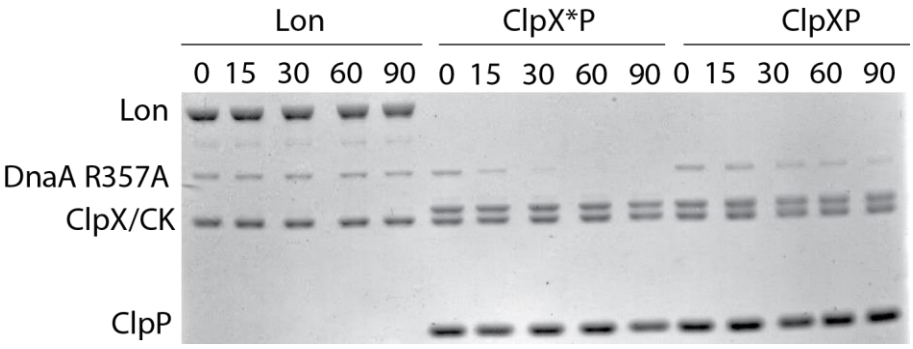

Figure 2.25 DnaAR357A is degraded robustly by ClpX*P and ClpXP.

Previous work has shown that Lon and ClpAP both can degrade DnaA although it was hypothesized that they might recognize different nucleotide bound versions of DnaA (Liu et. al 2016). DnaAR357A is a constitutively ATP-bound DnaA mutant that has been shown to be degraded poorly by Lon and degraded with a similar half-life to wildtype DnaA by ClpAP. We observed that the R mutant was degraded robustly by ClpX*P and by ClpXP although the rate of DnaA degradation by ClpX*P was still faster than ClpXP, similar to what we observed for wildtype DnaA.

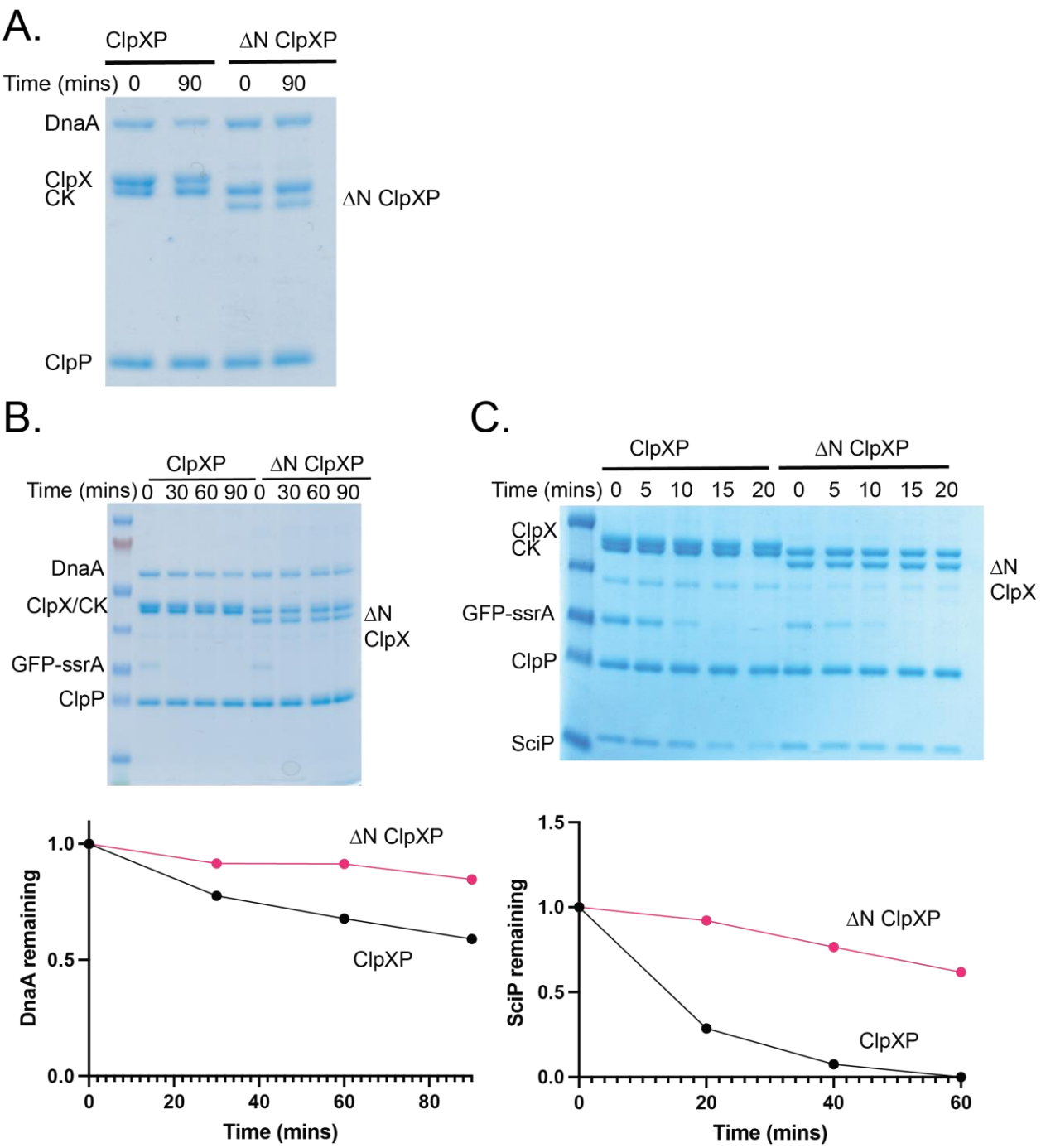

Figure 2.26 DnaA and SciP degradation by ClpXP is dependent on the N-terminal domain.

A-B. ΔN ClpXP fails to degrade DnaA (0.5 uM). GFP-ssrA degradation is shown as a control for ΔN ClpXP activity. Quantification shown below.

C. ΔN ClpXP fails to degrade SciP (5 uM). GFP-ssrA degradation is shown as a control for ΔN ClpXP activity. Quantification shown below.

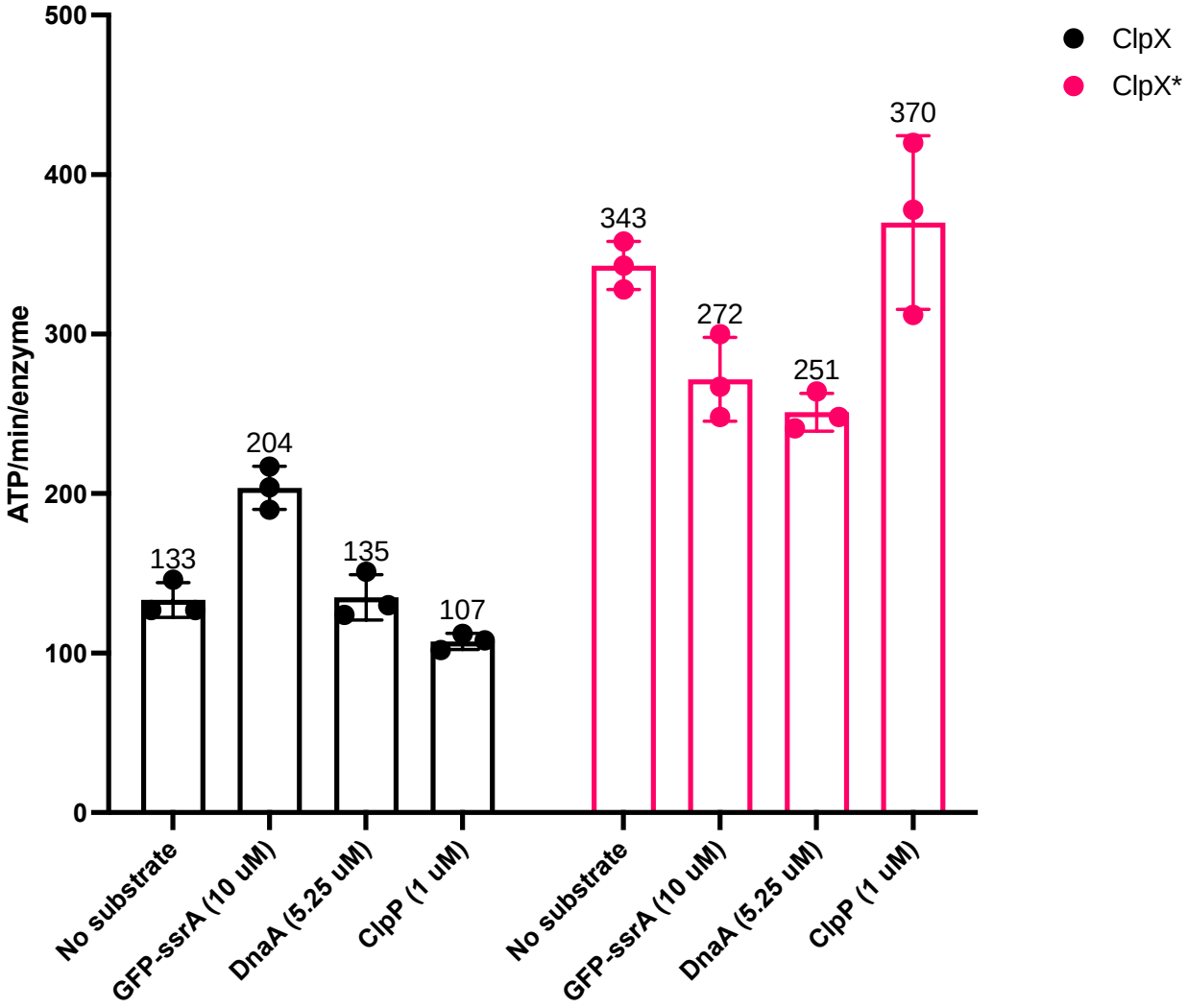

Figure 2.27 Substrate addition alters the ATPase rate of ClpX and ClpX*

Previous studies have shown that the ATPase rate of wildtype ClpX is decreased in the presence of ClpP and increased in the presence of GFP-ssrA (Kim et al. 2001, Burton et al. 2003). Given that we observed faster DnaA degradation and slower GFP-ssrA degradation by ClpX*P, we wondered if we would see similar effects on the ATPase rate of ClpX* in the presence of GFP-ssrA, DnaA, and

ClpP. Unlike the slight depression in ATPase rate observed for wildtype ClpX in the presence of ClpP, the addition of ClpP to ClpX* led to a stimulation of ATP hydrolysis. We also observed a drop in the ATPase rate of ClpX* in the presence of both DnaA and GFP-ssrA, suggesting that the effects on proteolysis were not mirrored by the ATPase rates. This data also suggests that wildtype ClpX and ClpX* recognize substrates differently since GFP-ssrA increases the ATPase rate of ClpX but decreases the ATPase rate of ClpX*.

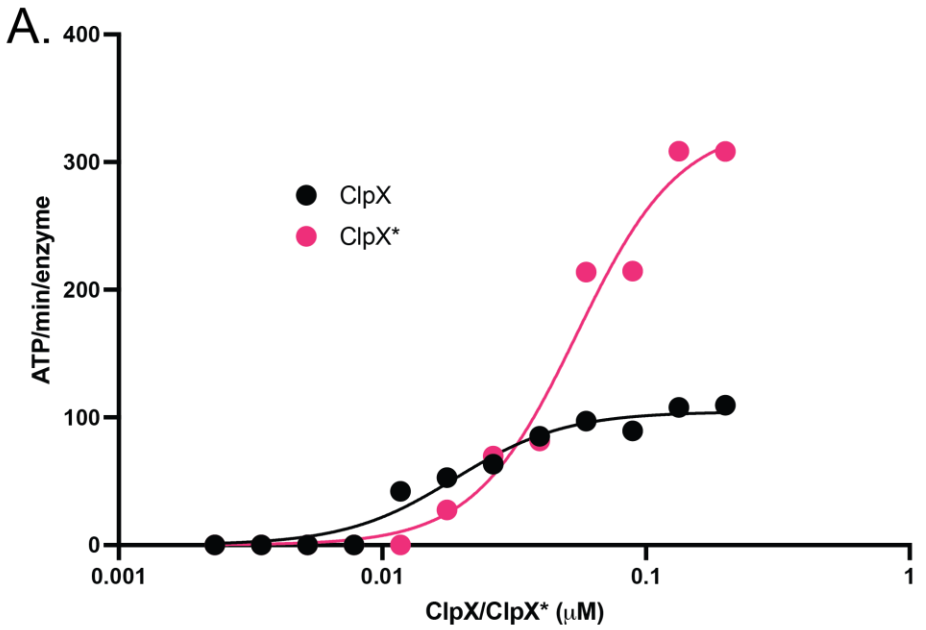

	ClpX	ClpX*
Allosteric sigmoidal		
Best-fit values		
Vmax	104.4	329.9
h	2.085	2.221
Khalf	0.01888	0.05453
Kprime	0.0002539	0.001562
95% CI (profile likelihood)		
Vmax	91.84 to 122.6	279.8 to 431.7
h	1.327 to 3.405	1.440 to 3.588
Khalf	0.01422 to 0.02719	0.04276 to 0.08353
Goodness of Fit		
Degrees of Freedom	9	9

Figure 2.28 Titration of ClpX/ClpX*. Here we titrated ClpX and ClpX* and monitored ATPase rates. We found that more ClpX* was needed to start hydrolyzing ATP (Khalf 54 nM vs 19 nM) than wildtype ClpX, suggesting that ClpX* requires ~ 3 fold more enzyme to assemble fully. This data seems to fit well with the data in our manuscript showing that ClpX* is more open (as demonstrated by HDX-MS) and less stable (as demonstrated by DSF).

2.12 ClpX* Purification

This protocol is modified from the Chien lab native CCX purification protocol with some adjustments

Buffers:

Lysis buffer/ Phenyl Sepharose buffer B/ Q-Sepharose buffer A

50 mM Tris, pH 8

100 mM KCl

5 mM MgCl2

10% glycerol

5mM DTT

Phenyl Sepharose buffer A

Same as PS-B, but with 0.5M AmSO4

Q-Sepharose buffer B

1X Lysis buffer

1M KCl

5mM DTT

1. Start an overnight from EPC1562 AMP plate
2. The next morning, back dilute the overnight culture 1:1000 (6L is sufficient as a grow-up)
3. Grow cells to a high density at 37°C (I normally induce at >0.8)
4. Shift cells to 30°C and induce with 0.4 mM IPTG and grow for another 4 hours at 30°C
5. Take gel sample and ensure ClpX* was induced.
6. After induction, spin cells at 7K rpm for 8 mins
7. Resuspend cells in lysis buffer and store at -80°C.
8. Thaw cells on ice when ready to begin purification
9. Add 1 mM final amount of PMSF (I make 100 mM stock in isopropyl alcohol fresh day of purification)
10. Disrupt cells at 18K psi, pass through microfluidizer 3 times
11. Take sample of lysate for gel
12. Spin lysate at 15K g for 30 mins
13. Transfer supernatant into graduated cylinder to find final volume of supernatant
14. Using the Encorbio AmS04 calclate, find the amount of AmSO4 needed to create a 50% sat'd solution starting from a 0% initial saturation https://www.encorbio.com/protocols/AM-SO4.htm
15. Take sample of supernatant for gel

AmSO4 cut

1. In the cold room, use the magnetic stir plate and gently agitate the supernatant in a beaker.
2. Over the course of an hour, add small amounts of the total AmSO4 calculated above
3. After the last bit is added, let the solution stir at 4°C for at least 1hr
4. Take sample for gel
5. Centrifuge the Supernatant /AmSO4 mix in the fixed angle rotor at 5K g for 30 mins
6. Carefully pour off supernatant and save
7. Take sample of AmSO4 supernatant for Gel
8. Gently resuspend pellet in minimal amount of Lysis buffer that has no PMSF (about the same volume as was when spun down) (This is where ClpX is supposed to be)
9. After allowing as much of the precipitate as possible to resolubilize, respin the resuspended pellet for 15mins at 5K g and take supernatant into new container.
10. Run a 10% TG gel of uninduced, induced, Lysate, 1st Sup, Pellet, AmSO4 sat'd, AmSO4 spun sup, and resuspended (clarified) AmSO4 pellet
11. If the gel shows that the protein is in the resuspended pellet, then you need to test the salinity of the resuspended solution and match it to the salinity of PS-A

Matching ClpX* conductivity to that of PS-A

1. Make a sat'd AMSO4 solution of Lysis buffer (10mls, 6.97g AmSO4)

2. Dilute PS-A (20 uL in 20 mL of water).
3. Measure the salinity of PS-A diluted with the Orion 013005MD conductivity probe
4. Measure the salinity of diluted resuspended pellet
5. Titrate in the sat'd AmSO4 Lysis buffer into resuspended pellet until the salinity matches that (can be a smidgeon higher that) of PS-A

Phenyl Sepharose column

1. Equilibrate PS-A column
2. Load the resuspended pellet into the superloop
3. Inject superloop onto the PS column at 5ml/min, make sure to add manufacturer recommended pressure alarms
4. Switch to load once all the sample is injected
5. Wash column until the A280 reaches that of the pre-equilibrated state
6. Wash with 50%B and do so until the A280 reaches baseline as before
7. Start elution, setting gradient to 100% in 60 mins with a flow rate of 2 mL per min. Collect 2 mL fractions.
8. Run gel to choose which fractions to pool. I don't normally run an activity assay at this point.

Matching ClpX* conductivity to that of PS-A

1. Check salinity of pooled fractions against QS-A, it should be **LOWER** than QS-A, if not, dilute in 50 mM Tris pH 8, 10% glycerol buffer (lysis buffer with no salts)

QFF column

1. Equilibrate QFF column
2. Load the pooled fractions into the superloop
3. Inject superloop onto the column at 5ml/min, make sure to add manufacturer recommended pressure alarms
4. Switch to load once all the sample is injected
5. Wash column with 100% A until the salinity reaches that of the pre-equilibrated state
6. Start gradient from 0%B to 100%B in 75 min
7. Run 10% TG gel of the fractions and run GFP-ssrA activity assay (This is critical because I have observed some ClpX* fractions that seem to have a lot of protein but have no activity)

MonoQ column

1. Equilibrate monoQ column
2. Load the pooled fractions into the superloop
3. Inject superloop onto the column at 1ml/min, make sure to add manufacturer recommended pressure alarms
4. Switch to load once all the sample is injected
5. Wash column with 100% A until the salinity reaches that of the pre-equilibrated state
6. Start gradient from 0%B to 40%B in 30 min
7. Run 10% TG gel of the fractions and run GFP-ssrA activity assay

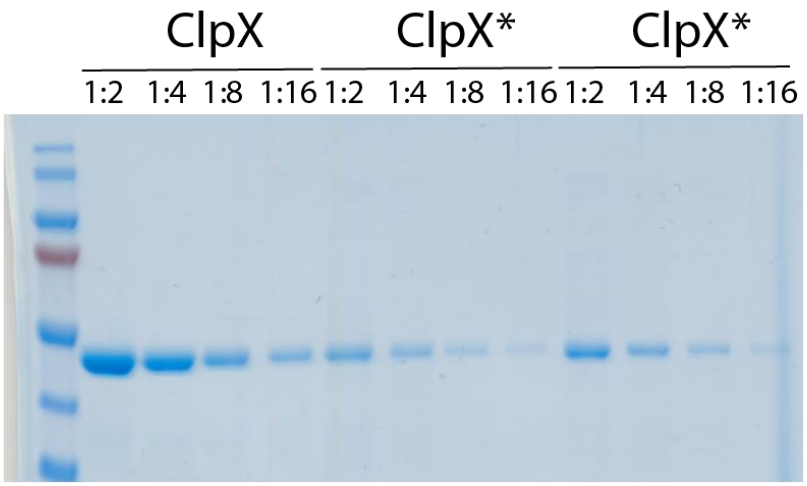

Figure 2.29 Yield and purity of ClpX*

While I have been able to achieve high purity for ClpX*, the yield (200, 10 ul aliquots at 0.5-0.75 uM hexamer) is often much lower than what we get for wildtype ClpX (200, 10 ul aliquots at more than 2 uM hexamer).

Chapter Three

Quantitative Proteomics Screen Uncovers Novel Phenotypes

Contributions: I performed all the sample preparation for the proteomics experiments described in this chapter. I also did all the analysis described here to identify potential Lon substrates and the follow-up experiments showing polymyxin B sensitivity in a *Δlon* strain and suppression in a *Δlon clpX** strain. Caiqin Wang, a rotation student in our lab, did the transposon suppressor screen identifying suppressors of *Δlon*'s polymyxin B sensitivity which mapped back to CcbF. Berent Aldikacti added the proteomics data to the Chienlab browser with the hopes of having this tool publicly available to anyone interested in looking at our proteomics data. Patrick Cann helped with the first phase of the TMT analysis, specifically comparing our dataset to the one published by Kristina Jonas' lab.

3.1 Abstract

Energy-dependent proteases maintain protein quality control by recognizing and degrading protein substrates that perform various cellular tasks. The biological significance of removing these cellular targets in a timely manner is highlighted by the defects in growth and stress responses that arise in the absence of one or more AAA+ proteases. However, to date, the degradome, consisting of the full repertoire of substrates for each protease, is not fully elucidated. Here, we present a quantitative proteomics approach which is amenable to multiple strains and various conditions. We utilize translational shutoffs to compare protein abundance and degradation rates in a *wildtype*, *Δlon*, and a strain overexpressing the Lon protease to identify putative Lon substrates. We performed similar experiments with a previously identified suppressor, *Δlon clpX** and identified preferential degradation of CcbF by ClpX*. We uncover that *Δlon*, cells are sensitive to polymyxin B, a novel phenotype, and screen for suppressors, which mapped back to CcbF, highlighting the utility of this approach in uncovering new phenotypes and related pathways.

3.2 Introduction

Maintenance of protein homeostasis is essential for survival. Bacteria utilize energy-dependent AAA+ proteases to degrade misfolded and regulatory proteins. There are several energy-dependent proteases that exist in bacteria, including Lon, ClpXP, ClpAP, HslUV, and FtsH (Mahmoud and Chien, 2018). These proteases are comprised of an AAA+ unfoldase and a compartmentalized

peptidase. The ATPase assembles into a hexameric ring with a central pore which undergoes ATP-dependent conformational changes that drive unfolding and translocation of protein substrates into the peptidase chamber, where irreversible destruction takes place (Sauer and Baker, 2011).

First discovered in *Escherichia coli*, Lon is a highly conserved member of the AAA+ family and is found in all domains of life (Gottesman, Halpern and Trisler, 1981). Posttranslational regulation by the Lon protease plays an important role in a range of cellular processes, including motility and pathogenesis (Breidenstein *et al.*, 2012; Rogers *et al.*, 2016). While Lon is principally known as a quality control protease, responsible for the degradation of approximately 50% of misfolded proteins in *E. coli*, Lon has also been shown to mediate the destruction of regulatory proteins (Chung and Goldberg, 1981). However, since its discovery, only a handful of Lon substrates have been identified. In *E. coli*, these substrates include the cell-division inhibitor, SulA, and the positive regulator of capsule synthesis, RcsA (Gottesman, Halpern and Trisler, 1981; Torres-Cabassa and Gottesman, 1987), and DNA-binding protein HU*β* (Liao *et al.*, 2010).

In the dimorphic alpha-proteobacterium *Caulobacter crescentus*, the number of validated Lon substrates remains small. Lon degrades the replication initiator DnaA, the methyltransferase CcrM, and the transcriptional repressor SciP (Wright *et al.*, 1996; Gora *et al.*, 2013; Jonas *et al.*, 2013). Recently, more Lon substrates have been uncovered in *Caulobacter*, including FixT and the HipB2 antitoxin (Stein, Fiebig and Crosson, 2020; Zhou, Eckart and Shapiro,

2021). The developmental regulator StaR and the flagellar regulator FliK were also recently validated as Lon substrates. StaR and FliK were shown to contribute to the defects in stalk biogenesis and motility observed in cells lacking Lon (Omnus *et al.*, 2021).

However, the presently identified substrates likely do not represent the full repertoire of proteins regulated by the Lon protease. Identifying and validating more Lon substrates is critical to uncovering novel Lon-related pathways. Here, we use a quantitative proteomics approach to elucidate the Lon-specific degradome in *Caulobacter*. We identify a list of putative Lon substrates by comparing protein abundance and degradation rates in a *wildtype*, *Δlon*, and Lon overexpression strain. We used the same proteomics workflow to profile the degradome of previously reported suppressor, *Δlon clpX** (Mahmoud, Aldikacti and Chien, 2021*).* We discovered that CcbF, an enzyme that catalyzes the first step in ceramide biosynthesis, is preferentially degraded in a *Δlon clpX** strain, leading to increased resistance to polymyxin B in a *Δlon clpX** in comparison to a *Δlon* strain (Stankeviciute *et al.*, 2019). We then used a *Δlon* transposon library to identify suppressors of polymyxin B sensitivity and found multiple hits in the CcbF operon, suggesting that *Δlon* cells are sensitive to polymyxin B due to misregulation of CcbF. Together, our work reveals that quantitative proteomics approaches can provide valuable insight on unexplored pathways and their link to novel phenotypes.

3.3 Results

Previous studies have identified the replication initiator, DnaA as a substrate of the Lon protease in *Caulobacter crescentus* (Jonas *et al.*, 2013). In *wildtype* cells, upon chloramphenicol addition to inhibit protein synthesis, DnaA is robustly degraded (Figure S1A). In the absence of the Lon protease, DnaA is stabilized, and steady state levels are increased in comparison to *wildtype* cells (Figure S1A). A strain with a C-terminal M2 tag, which protects the Lon protease from degradation (Barros *et al.*, 2020), and effectively functions as an overexpression strain, shows decreased DnaA levels upon Lon induction (Figure S1A).We reasoned that using these strains to perform a quantitative proteomics survey would allow us to identify new Lon substrates and uncover novel phenotypes.

Triplicate cells were treated with chloramphenicol and samples were withdrawn at 0, 30 minutes, and 90 minutes post antibiotic addition (Figure 3.1A). For Lon overexpression, triplicate samples were taken before xylose addition as well as 2 and 5 hours post addition. Samples were labeled with isobaric tags using the TMT10plex kit and pooled into three separate TMT experiments for each strain. The pooled samples were then fractionated using a high pH reversed-phase peptide fractionation kit (Pierce) into 8 fractions which were then pooled into 4 fractions and subject to downstream mass spectrometry (Figure 3.1A). To allow comparison between wildtype and *Δlon*, we reserved the last TMT label to serve as a normalization channel comprising of a mixture of the t=0 timepoints (Figure 3.1A). We used a synchronous precursor selection (SPS) MS^3 method for reporter ion quantitation (Figure 3.1A). As an example, DnaA showed

robust degradation in *wildtype* cells with a half-life of 24.6 minutes and stabilization in *Δlon* cells (Figure 3.1B).

In total, we identified 1347 and 1443 total proteins found in every sample of wildtype and *Δlon* datasets respectively, with 1193 proteins shared between the two strains (Figure 3.2A). We identified 1155 proteins in the Lon overexpression strain, with 971 proteins shared between the three strains (Figure S2A). We compared the proteins we identified in our TMT datasets with protein expression levels determined by RNA sequencing. We found, as expected, that the proteins identified in the proteomics survey were the most highly expressed in our RNA seq experiments, with a higher proportion of proteins identified in the highest quartiles of expression (Figure S2B). We were particularly interested in a subset of proteins highly expressed in *wildtype* cells but absent from the *wildtype* proteomics dataset and present in the *Δlon* dataset (Figure 3.2B). We identified 49 proteins that fit this criterion (Figure 3.2B, Table S1). We reasoned that these proteins could represent potential Lon substrates that are degraded rapidly in a *wildtype* and, therefore, are undetected in the *wildtype* proteomics dataset.

Next, we compared the t_0/t_{30} and t_0/t_{90} ratios in a *wildtype* to determine the distribution of degradation rates (Figure 3.2C). We reasoned that most proteins would be stable after 30 and 90 minutes. Indeed, we find that the average t_0/t_{30} and t_0/t_{90} ratios in a *wildtype* were close to 1 ($\log_2=0$). We fit the frequency distribution to a gaussian and observed an asymmetrical distribution with a tail to the right which was particularly evident in the t_0/t_{90} comparison (Figure 3.2C).

This suggested to us, that outside of expected noise in the data, there were proteins being truly degraded in a *wildtype*.

Next, we set out to identify potential Lon substrates by combining data from our 3 TMT experiments. We looked for substrates that would be more abundant in *Δlon* cells (comparing *Δlon* t=0 and *wt* t=0) and degraded in a wildtype (comparing *wt* t=0 and t=90) but stabilized in a *Δlon (*comparing *Δlon* t=0 and t=90). Lastly, we looked for proteins that were less abundant upon Lon overexpression (comparing Lon O/E t=0 and t=5-hour induction).

We detected known Lon substrates, DnaA, CcrM, and SciP in all samples. However, we were unable to identify recently reported Lon substrates FixT and HipB2 (Stein, Fiebig and Crosson, 2020; Zhou, Eckart and Shapiro, 2021). DnaA was two times as abundant in *Δlon* as *wildtype* and three times more stable (90-minute vs 0-minute) (Figure 3.2C). In addition, we found that DnaA levels were three times lower upon Lon overexpression (5-hour vs uninduced) (Figure S2C). CcrM was approximately four times more abundant but only 10% more stable in *Δlon* in comparison to wildtype (Figure 3.2C). SciP was approximately 20% more abundant and more than two times more stable in *Δlon* in comparison to wildtype (Figure 3.2C). CcrM and SciP were both approximately 40% less abundant upon Lon overexpression (5-hour vs uninduced) (Figure S2C).

We compared the proteome of *Δlon* t=0 *and wildtype* t=0. We set a 25% false discovery rate (FDR) cutoff, identifying 335 proteins that pass the cutoff (Figure 3.3A). We then calculated the average *Δlon* t_0/ *wt* t_0 ratio and determined the proteins that were found 1, 2, and 3 standard deviations away from the mean.

We reasoned proteins found 3 standard deviations away from the mean would likely represent authentic Lon substrates and we find CcrM in this group (Figure 3.3A, Supplementary File 1). DnaA was found in the group of proteins 2 standard deviations from the mean. We identified 4 proteins in sigma 3, 27 proteins in sigma 2, and 95 proteins in sigma 1 (Figure 3.3A , Supplementary File 1).

Next, we compared the proteome of *wt* t=0 *and wt* t=90 to identify proteins degraded in a *wildtype* (Figure 3.3B). We used a 25% FDR cutoff and identified proteins found 1, 2, and 3 standard deviations from the mean as described previously (Figure 3.3B). We identified 13 proteins in sigma 3, including DnaA and Scip, 28 proteins in sigma 2, and 112 proteins in sigma 1 (Supplementary File 1). To identify which of these proteins are potential Lon substrates, we compared the proteome of *Δlon* t=0 *and Δlon* t=90 and then determined which proteins were degraded in a *wildtype* but stabilized in a *Δlon,* identifying 96 total proteins fulfilling this criterion (Figure 3.3C). We identified 5 proteins in sigma 3, 14 proteins in sigma 2, and 77 proteins in sigma 3 (Supplementary File 1). As an example, we identify CtrA, a known ClpXP substrate (Joshi *et al.*, 2015) as being degraded in both a *wildtype* and *Δlon* but DnaA was only degraded in a *wildtype* (Figure 3.3C).

Lastly, we compared the proteome of the uninduced Lon overexpression strain and t=5-hour induction. We used a 25% FDR cutoff and identified proteins found 1, 2, and 3 standard deviations from the mean as described previously (Figure 3.3D). We identified 140 proteins that passed the 25% FDR cutoff. We then identified 7 proteins in sigma 3, including DnaA, 7 proteins in sigma 2, and

31 proteins in sigma 1 (Supplementary File 1). We also compared the proteome of wt t=0 and wt t=30 as well as the proteome of the uninduced Lon overexpression strain and after 2 hours of induction (Figure S3A-B). Using the 0, 30-minute, and 90-minute datapoints for a *wildtype*, we calculated half-lives for 219 proteins (Figure S3C, Supplementary File 1).

After we identified which proteins fulfilled each of our criteria separately, we gave each protein a score. Proteins found 3-SD away from the mean were given a score of 3, those found 2-SD away were given a score of 2, those found 1-SD away were given a score of 1. The scores were then added up for each criterion (Supplementary File 1). For example, DnaA tops the list with the highest score of 8, being more abundant in a *Δlon* at t=0 (score of 2), stabilized in a *Δlon* (score of 3*),* and less abundant upon Lon overexpression (score of 3) (Supplementary File 1). Overall, we identified 64 putative Lon substrates with a score of at least two (Supplementary File 1).

A recent proteomics screen identified two new Lon substrates StaR and FliK (Omnus *et al.*, 2021) using a similar approach to what we describe here. However, while we did not detect StaR and FliK in our dataset, out of the 64 proteins that we identified as potential Lon substrates, 14 were identified in the Omnus et al. study as fulfilling either 3 or 4 out of the study's 4 criteria, suggesting there is some overlap between the two studies and giving us more confidence in our dataset (Supplementary File 1).

Next, we performed an additional TMT experiment following translational inhibition with previously identified suppressor, *Δlon clpX** (Mahmoud, Aldikacti

and Chien, 2021). We utilized the normalization channel described above (mixture of t=0 time points for wildtype, *Δlon, and Δlon clpX**) to allow comparisons between the strains. Consistent with our previous work on *Δlon clpX*,* we observed faster degradation of SciP and DnaA in the *Δlon clpX** TMT dataset in comparison to the *Δlon* dataset (Figure 3.4A, 3.4B). Next, we compared degradation rates in *wildtype* and *Δlon* cells with rates in a *Δlon clpX** background. We observed that CCNA_01220, recently named CcbF, was degraded faster in *Δlon clpX** in comparison to both wildtype and *Δlon,* suggesting that ClpX* degrades CcbF faster than wildtype ClpX (Figure 3.4C, 3.4D). Recent work has implicated CcbF in ceramide synthesis in *Caulobacter* and deletion of CcbF was shown to increase resistance to polymyxin B, a lipopolysaccharide interacting antibiotic (Stankeviciute *et al.*, 2019). We reasoned that if CcbF were a substrate of ClpX*, then *Δlon clpX** should be more resistant to polymyxin B than *Δlon* alone. Indeed, we found that *Δlon* cells were highly sensitive to polymyxin B and this sensitivity was suppressed in the *Δlon clpX** background, suggesting that CcbF is being turned over by ClpX*, therefore decreasing its abundance in a *Δlon clpX** background (Figure 3.4E).

We were intrigued that we uncovered a novel phenotype for *Δlon* cells and decided to further explore the relationship between *Δlon* cells and polymyxin B. We used a transposon library generated in a *Δlon* background to find suppressors that increase resistance to polymyxin B. We identified 14 suppressors and used arbitrary PCR to identify the location of the transposon insertion. We found that 7/14 of the suppressors mapped to the same operon as

ccbF, suggesting that disrupting this operon is beneficial to restoring polymyxin B resistance to *⊿lon* cells.

3.4 Discussion

Bacterial AAA+ proteases, such as Lon and ClpXP, regulate protein homeostasis by balancing the degradation of misfolded proteins and regulatory proteins. To fully appreciate the scope of energy-dependent proteolysis inside the cell, it is imperative to expand our understanding of the specific substrates degraded by each protease. Here, we present a quantitative proteomics approach to identify potential Lon substrates (Supplementary File 1). We compared the proteomes of *wildtype*, *⊿lon,* and a Lon overexpression strain to identify substrates that are more abundant in the absence of Lon, are stabilized in *⊿lon* cells*,* and are less abundant upon Lon overexpression. We compare our dataset to a recently published quantitative proteomics dataset in *Caulobacter* (Omnus *et al.*, 2021) and found some overlap in putative Lon substrates (Supplementary File 1). We then compared the degradome of *⊿lon clpX** to the proteomes of *wildtype* and *⊿lon.* We found that CcbF, a protein responsible for the first step in ceramide biosynthesis (Stankeviciute *et al.*, 2019), was degraded faster in a *⊿lon clpX** background in comparison to a either a *wildtype* or *⊿lon* background (Figure 3.4C, Figure 3.4D). Previous work has shown that deletion of CcbF leads to increased resistance to polymyxin B. Consistent with faster degradation of CcbF by ClpX*, we observed increased resistance to the antibiotic polymyxin B in a *⊿lon clpX** compared to a *⊿lon*, suggesting that CcbF levels are decreased in a *⊿lon clpX** (Figure 3.4E).

While *Δlon* cells have been documented to be sensitive to various stressors, including agents that cause genotoxic and proteotoxic stress (Zeinert *et al.*, 2018), we found that *Δlon* cells were highly sensitive to polymyxin B in comparison to wildtype cells. In exploring this novel phenotype further, we performed a transposon-based suppressor screen to identify suppressors that restore polymyxin B sensitivity to a *Δlon.* We found that half of the transposons mapped to the CcbF operon, highlighting a link between CcbF misregulation in a *Δlon* and sensitivity to polymyxin B.

Our work highlights the power of using a quantitative proteomics approach to uncover novel protease-related pathways and to shed light on unexplored phenotypes. Similar approaches have been taken in mammalian cells where recent work combined a cycloheximide chase assay with a quantitative proteomics approach to identify short-lived proteins in human cell lines (Li *et al.*, 2021). We can envision using a similar approach to map the degradome under various stress conditions. Similarly, we can extend this approach to identify substrates degraded by other proteases, such as ClpAP, which only has a few identified substrates in the literature (Williams *et al.*, 2014; Liu *et al.*, 2016). Lastly, we can harness the power of quantitative proteomics to identify adaptor-dependent substrates by comparing the proteomes of *wildtype* cells and the proteome of various adaptor deletions, such as CpdR, RcdA, and popA (Joshi *et al.*, 2015).

3.5 Methods

Bacterial strains and growth conditions

Caulobacter crescentus strains were grown in PYE medium (2g/L peptone, 1g/L yeast extract, 1 mM $MgSO_4$, and 0.5 mM $CaCl_2$) at 30°C.

Western blots

The stability of proteins *in vivo* was determined by inhibiting protein synthesis with the addition of 30 µg/ml chloramphenicol to cells in exponential phase. At each time point, 1ml of culture was removed and centrifuged at 15,000 rpm for 2 minutes. The supernatant was removed, and pellets were flash frozen in liquid nitrogen. Pellets were thawed, resuspended in 2x SDS dye, and normalize. Samples were boiled for 10 minutes and centrifuged for 10 minutes at 15,000 rpm. Extracts were run on 10% Bis-Tris gels for 1 hour at room temperature at 150 V. Gels were then transferred to nitrocellulose membranes for 1 hour at room temperature at 20V. Membranes were blocked with 3% milk in Tris-based saline with 0.05% Tween-20 (TBST) for 1 hour. Membranes were probed with primary antibody in 3% milk in TBST at 4°C overnight with a 1:5000 dilution of DnaA. Membranes were washed with 1x TBST for 5 minutes three times and then probed with Licor secondary antibody with 1:10,000 dilution in 1x TBST at room temperature for 1 hour. The protein was visualized using Licor Odyssey CLx.

TMT proteomics and analysis

Strains were grown to mid exponential phase. A 5 ml sample from each strain was centrifuged in 15 ml centrifuge tubes at 6000g for 5 minutes. The supernatant was removed, and the pellet was resuspended in freshly made lysis buffer (8M urea, 50 mM Hepes pH 7.5). The cells were freeze/thawed 3 times in

liquid nitrogen to aid in cell lysis. The lysates were centrifuged at 16,000g for 10 minutes at 4°C and the supernatant was transferred to a new tube.

A Bradford measurement at OD_{595} was taken to normalize protein input to 50 ug of each sample. Each sample was reduced using TCEP for 1 hour at 55 °C. The samples were then alkylated with iodoacetamide for 30 mins in the dark at room temperature. Next, 6 volumes of prechilled acetone were added to each sample and samples were left overnight at -20°C.

Samples were spun down at 8000g for 10 mins at 4°C. The acetone was removed, and the acetone-precipitated pellet was resuspended in 100 ul of 50 mM TEAB. Trypsin (2.5 ug) was added to each peptide sample and allowed to digest overnight at room temperature.

Tandem mass tag labeling was performed using the TMT 10plex kit from ThermoFisher. Each sample was labeled with the TMT reagent according to the manufacturer's protocol. Each TMT label was resuspended in acetonitrile and then added to each peptide sample. The labeling reaction was allowed to proceed for 1 hour at room temperature. The reaction was quenched with 5% w/v hydroxylamine. We utilized the quantitative colorimetric peptide assay (Pierce) to ensure samples were combined at a 1:1 ratio. The samples were then dried by speed-vac and resuspended in freshly diluted 0.1% TFA. We then used the high pH reversed-phase peptide fractionation kit (Pierce) to fractionate each pooled sample into 8 fractions. We then combined fractions 1 and 5, 2 and 6, 3 and 7, and 4 and 8 for mass spectrometry analysis.

An aliquot of each sample was loaded onto a trap column (Acclaim PepMap 100 pre-column, 75 µm × 2 cm, C18, 3 µm, 100 Å, Thermo Scientific) connected to an analytical column (Acclaim PepMap RSLC column C18 2 µm, 100 Å, 50 cm × 75 µm ID, Thermo Scientific) using the autosampler of an Easy nLC 1000 (Thermo Scientific) with solvent A consisting of in 0.1% formic acid in water and solvent B consisting of 0.1% formic acid in acetonitrile. The peptide mixture was gradient eluted into an Orbitrap Fusion mass spectrometer (Thermo Scientific) using a 180 min gradient from 5%-40%B (A: 0.1% formic acid in water, B:0.1% formic acid in acetonitrile) followed by a 20 min column wash with 100% solvent B. The full scan MS was acquired over range 400-1400 m/z with a resolution of 120,000 (@ m/z 200), AGC target of 5e5 charges and a maximum ion time of 100 ms and 2 s cycle time. Data dependent MS/MS scans were acquired in the linear ion trap using CID with a normalized collision energy 35%. For quantitation scans, synchronous precursor selection was used to select 10 most abundant product ions for subsequent MS^3 using AGC target 5e4 and fragmentation using HCD with NCE 55% and resolution in the Orbitrap 60,000. Dynamic exclusion of each precursor ion for 30s was employed.

Mass spectrometry data was processed using Proteome Discoverer 2.2. For reporter ion quantification, the following parameters were used: a 1.2Da tolerance, a co-isolation threshold of 75 for MS^3, SPS Mass Matches > 65%. Proteins were searched against the *Caulobacter crescentus* database. Analysis was performed with Microsoft Excel and Prism.

3.6 References

Barros, B.B. *et al.* (2020) 'Degradation of Lon in Caulobacter crescentus', *Journal of Bacteriology*. Edited by Y.V. Brun, 203(1). doi:10.1128/JB.00344-20.

Breidenstein, E.B.M. *et al.* (2012) 'The Lon Protease Is Essential for Full Virulence in Pseudomonas aeruginosa', *PLoS ONE*. Edited by P. Cornelis, 7(11), p. e49123. doi:10.1371/journal.pone.0049123.

Chung, C.H. and Goldberg, A.L. (1981) 'The product of the ion (capR) gene in Escherichia coli is the ATP-dependent protease, protease La', p. 5.

Goff, S.A., Casson, L.P. and Goldberg, A.L. (1984) 'Heat shock regulatory gene htpR influences rates of protein degradation and expression of the ion gene in Escherichia coli', *Proc. NatL. Acad. Sci. USA*, p. 6.

Gonzalez, D. *et al.* (2014) 'The functions of DNA methylation by CcrM in Caulobacter crescentus: A global approach', *Nucleic Acids Research*, 42(6), pp. 3720–3735. doi:10.1093/nar/gkt1352.

Gora, K.G. *et al.* (2013) 'Regulated proteolysis of a transcription factor complex is critical to cell cycle progression in *Caulobacter crescentus*: Cell cycle regulated proteolysis in *Caulobacter*', *Molecular Microbiology*, 87(6), pp. 1277–1289. doi:10.1111/mmi.12166.

Gottesman, S., Halpern, E. and Trisler, P. (1981) 'Role of sulA and sulB in filamentation by lon mutants of Escherichia coli K-12', *Journal of Bacteriology*, 148(1), pp. 265–273. doi:10.1128/jb.148.1.265-273.1981.

Jonas, K. *et al.* (2013) 'Proteotoxic Stress Induces a Cell-Cycle Arrest by Stimulating Lon to Degrade the Replication Initiator DnaA', *Cell*, 154(3), pp. 623–636. doi:10.1016/j.cell.2013.06.034.

Joshi, K.K. *et al.* (2015) 'An Adaptor Hierarchy Regulates Proteolysis during a Bacterial Cell Cycle', *Cell*, 163(2), pp. 419–431. doi:10.1016/j.cell.2015.09.030.

Li, J. *et al.* (2021) 'Proteome-wide mapping of short-lived proteins in human cells', *Molecular Cell*, 81(22), pp. 4722-4735.e5. doi:10.1016/j.molcel.2021.09.015.

Liao, J.-H. *et al.* (2010) 'Binding and Cleavage of E. coli HUβ by the E. coli Lon Protease', *Biophysical Journal*, 98(1), pp. 129–137. doi:10.1016/j.bpj.2009.09.052.

Liu, J. *et al.* (2016) 'ClpAP is an auxiliary protease for DnaA degradation in *Caulobacter crescentus*: DnaA degradation in *Caulobacter crescentus*', *Molecular Microbiology*, 102(6), pp. 1075–1085. doi:10.1111/mmi.13537.

Mahmoud, S.A., Aldikacti, B. and Chien, P. (2021) *Plasticity in AAA+ proteases reveals ATP-dependent substrate specificity principles*. preprint. Molecular Biology. doi:10.1101/2021.08.18.456811.

Mahmoud, S.A. and Chien, P. (2018) 'Regulated Proteolysis in Bacteria', *Annual Review of Biochemistry*, 87(1), pp. 677–696. doi:10.1146/annurev-biochem-062917-012848.

Omnus, D.J. *et al.* (2021) 'The Lon protease temporally restricts polar cell differentiation events during the Caulobacter cell cycle', *eLife*, 10, p. e73875. doi:10.7554/eLife.73875.

Rogers, A. *et al.* (2016) 'The LonA Protease Regulates Biofilm Formation, Motility, Virulence, and the Type VI Secretion System in Vibrio cholerae', *Journal of Bacteriology*. Edited by V.J. DiRita, 198(6), pp. 973–985. doi:10.1128/JB.00741-15.

Sauer, R.T. and Baker, T.A. (2011) 'AAA+ Proteases: ATP-Fueled Machines of Protein Destruction', *Annual Review of Biochemistry*, 80(1), pp. 587–612. doi:10.1146/annurev-biochem-060408-172623.

Stankeviciute, G. *et al.* (2019) 'Caulobacter crescentus Adapts to Phosphate Starvation by Synthesizing Anionic Glycoglycerolipids and a Novel Glycosphingolipid', *mBio*. Edited by H.A. Shuman, 10(2). doi:10.1128/mBio.00107-19.

Stein, B.J., Fiebig, A. and Crosson, S. (2020) 'Feedback Control of a Two-Component Signaling System by an Fe-S-Binding Receiver Domain', *mBio*. Edited by P.J. Kiley and D.K. Newman, 11(2). doi:10.1128/mBio.03383-19.

Tan, H.M. *et al.* (2010) 'An essential transcription factor, SciP, enhances robustness of Caulobacter cell cycle regulation', *Proceedings of the National Academy of Sciences of the United States of America*, 107(44), pp. 18985–18990. doi:10.1073/pnas.1014395107.

Torres-Cabassa, A.S. and Gottesman, S. (1987) 'Capsule synthesis in Escherichia coli K-12 is regulated by proteolysis', *Journal of Bacteriology*, 169(3), pp. 981–989. doi:10.1128/jb.169.3.981-989.1987.

Williams, B. *et al.* (2014) 'CLPXP and CLPAP proteolytic activity on divisome substrates is differentially regulated following the *C aulobacter* asymmetric cell division', *Molecular Microbiology*, 93(5), pp. 853–866. doi:10.1111/mmi.12698.

Wright, R. *et al.* (1996) 'Caulobacter Lon protease has a critical role in cell-cycle control of DNA methylation.', *Genes & Development*, 10(12), pp. 1532–1542. doi:10.1101/gad.10.12.1532.

Zeinert, R.D. *et al.* (2018) *A legacy role for DNA binding of Lon protects against genotoxic stress*. preprint. Microbiology. doi:10.1101/317677.

Zeinert, R.D. *et al.* (2020) 'The Lon Protease Links Nucleotide Metabolism with Proteotoxic Stress', *Molecular Cell*, 79(5), pp. 758-767.e6. doi:10.1016/j.molcel.2020.07.011.

Zhou, X., Eckart, M.R. and Shapiro, L. (2021) 'A Bacterial Toxin Perturbs Intracellular Amino Acid Balance To Induce Persistence', *mBio*. Edited by M.J. Blaser, 12(1), pp. e03020-20. doi:10.1128/mBio.03020-20.

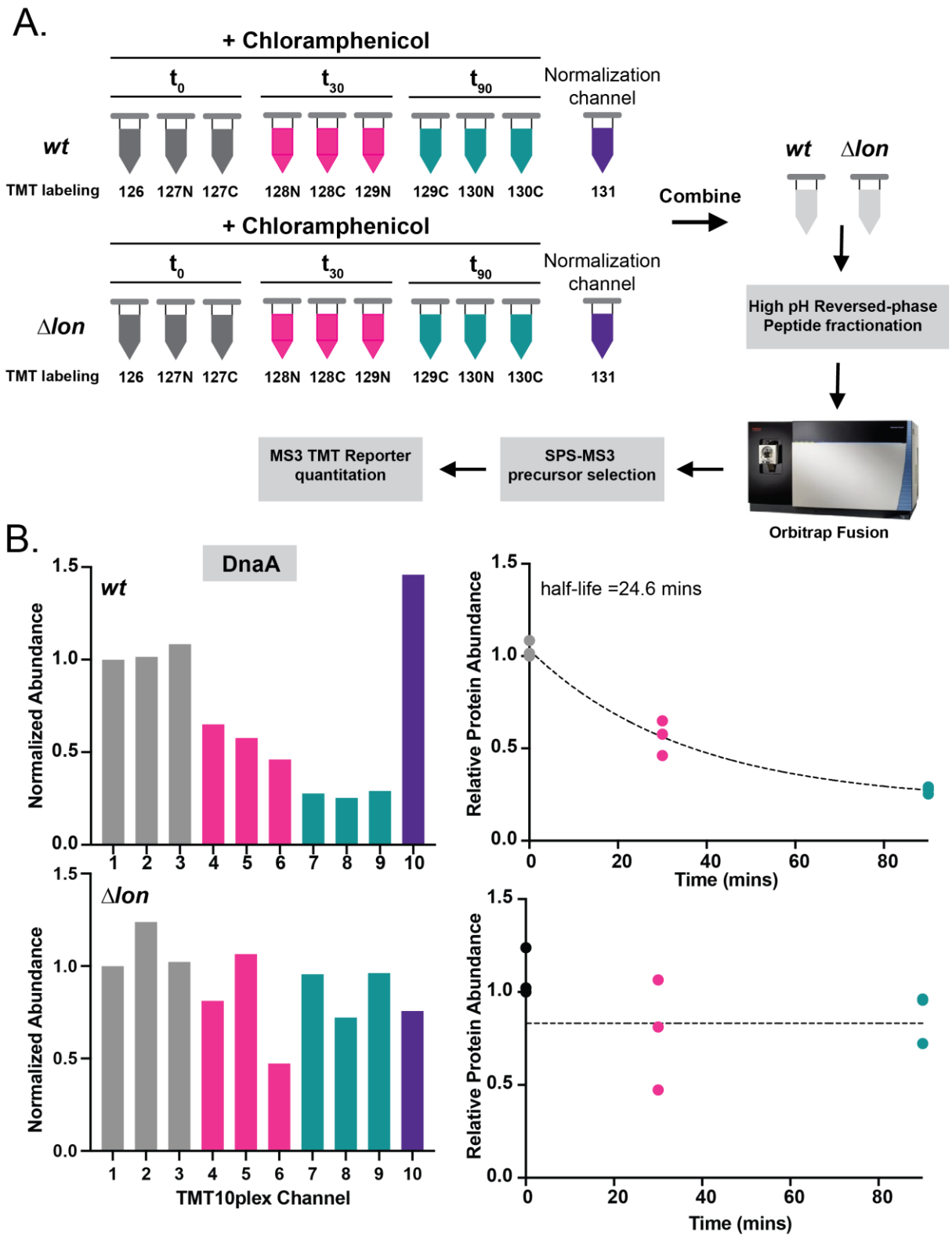
A.
+ Chloramphenicol
t0
t30
t90
Normalization channel
wt
TMT labeling
126 127N 127C 128N 128C 129N 129C 130N 130C 131
+ Chloramphenicol
Δlon
Combine
wt Δlon
High pH Reversed-phase Peptide fractionation
Orbitrap Fusion
SPS-MS3 precursor selection
MS3 TMT Reporter quantitation
B.
DnaA
wt
Normalized Abundance
half-life =24.6 mins
Relative Protein Abundance
Time (mins)
Δlon
TMT10plex Channel

Figure 3.1 Quantitative proteomics workflow. A. Triplicate *wildtype* and *⊿lon* cells were treated with chloramphenicol and samples were withdrawn at 0, 30 minutes, and 90 minutes post chloramphenicol addition. Samples were digested and labeled with TMT10plex reagents. Samples for each TMT experiment were pooled and fractionated and analyzed on an Orbitrap Fusion. The last TMT label was a mixture of t=0 samples and was reserved as a normalization channel to allow comparisons between *wildtype* and *⊿lon*. **B.** Protein abundance (not normalized to control channel) and half-life for DnaA in *wildtype* (top) and *⊿lon* (bottom). Half-life for DnaA was calculated by fitting the data to one-phase decay equation in Prism.

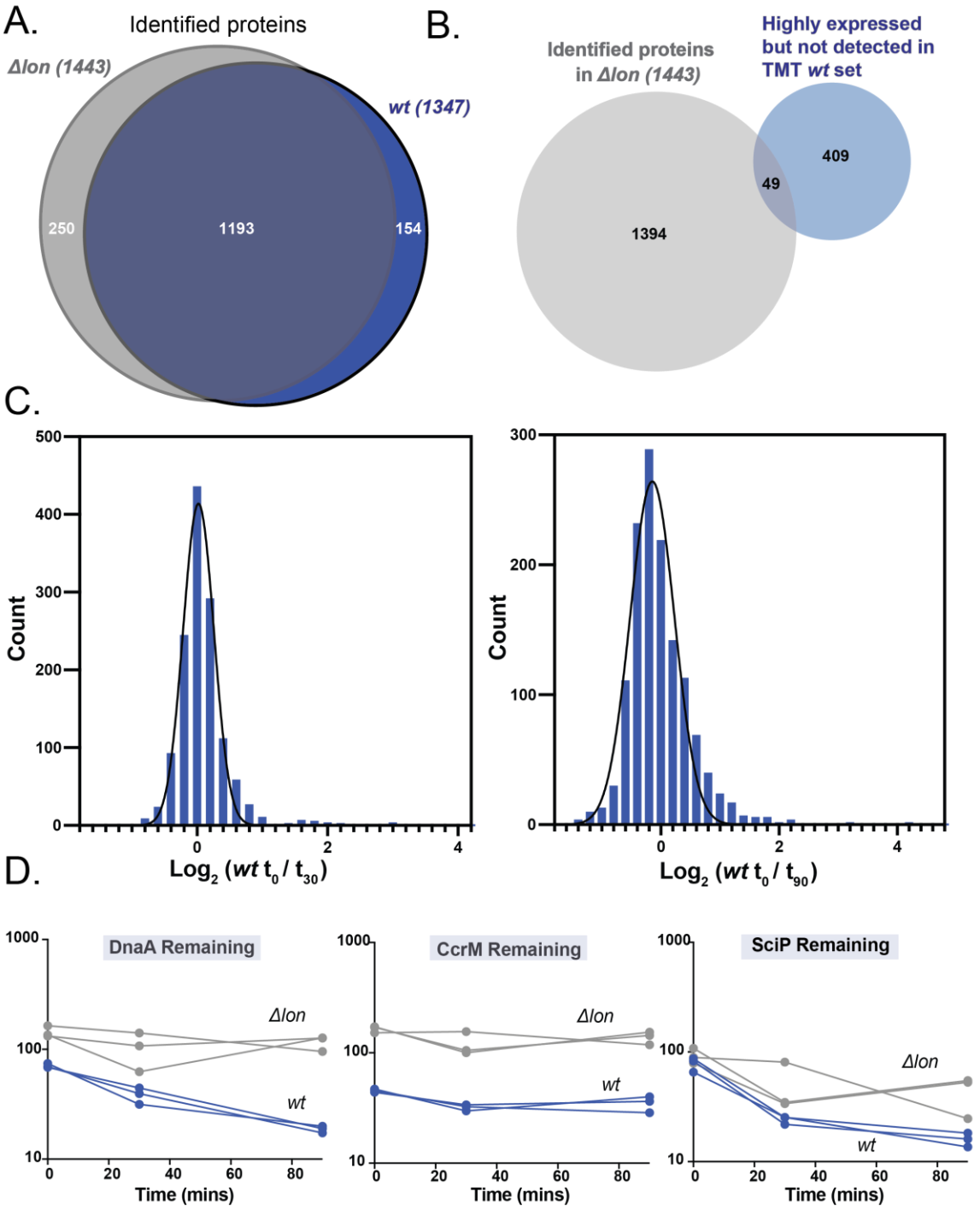

Figure 3.2 Overview of identified proteins. A. Venn diagram showing the overlap between the identified proteins in a *wildtype* and *Δlon.* **B.** Venn diagram showing the overlap between highly expressed genes in a *wildtype* (top 75%

percentile for expression from RNA seq data) not identified in the wildtype proteomics dataset and proteins identified in the *Δlon* proteomics dataset. **C.** Frequency distribution of *wildtype* degradation rates (t=0/t=30, left) and (t=0/t=90, right). Data was fit to a gaussian distribution in Prism. D. Plot showing protein abundance triplicates for t=0, t=30, and t=90 for *wildtype* and *Δlon* for known Lon substrates, DnaA, CcrM, and SciP. Data was normalized to control channel to allow comparison between *wildtype* and *Δlon.*

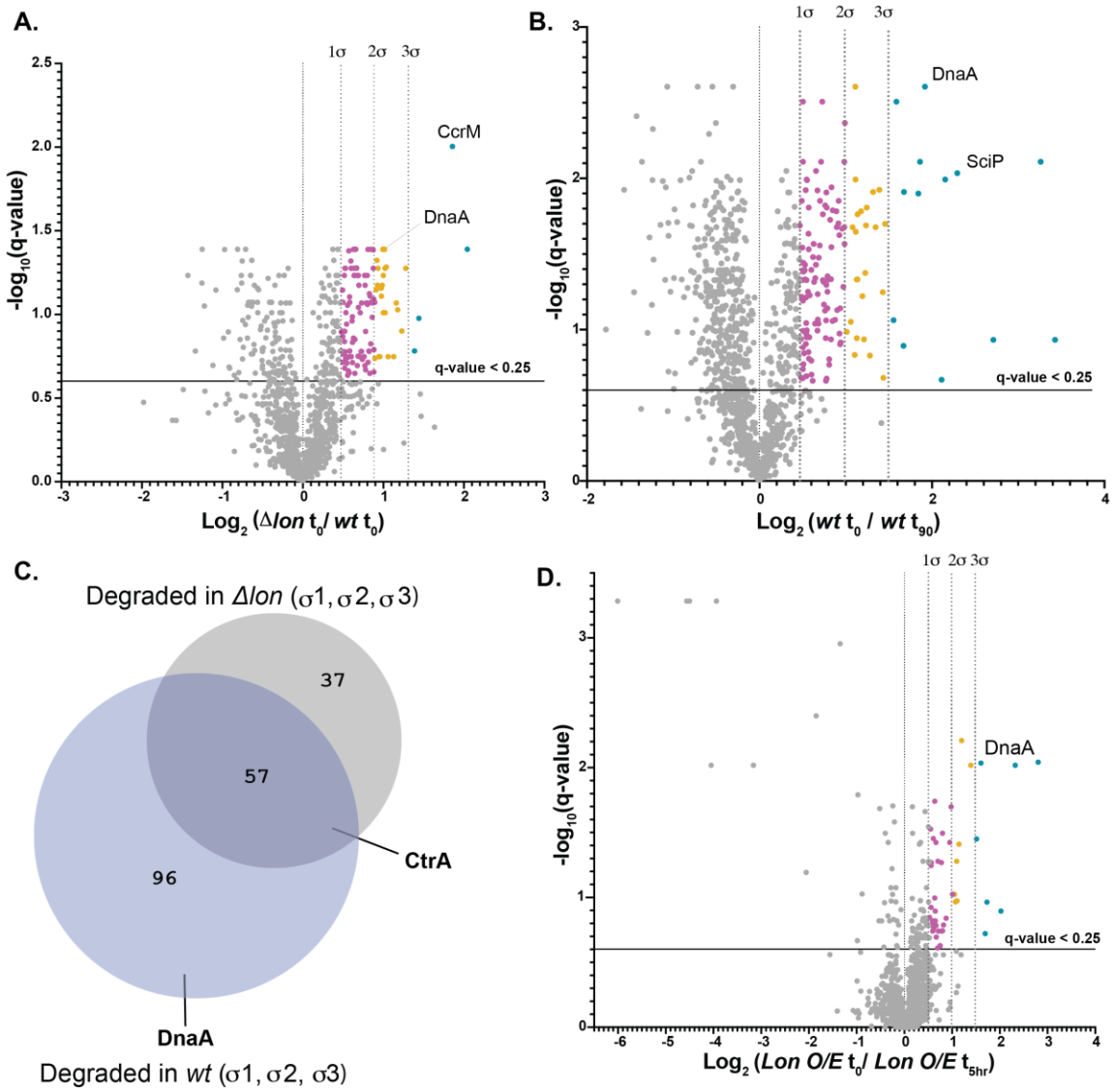

Figure 3.3 Identifying potential Lon substrates. A. Volcano plot comparing the proteomes of *Δlon* t=0 and wildtype t=0 with an FDR cutoff of 25%. **B.** Volcano plot comparing the proteomics of *wildtype* t=0 and *wildtype* t=90 with an FDR cutoff of 25%. **C**. Venn diagram showing overlap of proteins degraded in a *wildtype* and proteins degraded in a *Δlon.* CtrA was degraded in both strains while DnaA was degraded in a *wildtype*. **D**. Volcano plot comparing the proteomes of *Lon O/E strain* t=0 (uninduced) and t=5 hours post induction with an FDR cutoff of 25%. For all volcano plots, proteins found 1 standard deviation from the mean (1 sigma) are shown in purple. Proteins found 2 standard deviations from the mean (2 sigma) are shown in yellow. Proteins found 3 standard deviations from the mean (3 sigma) are shown in teal.

Fi

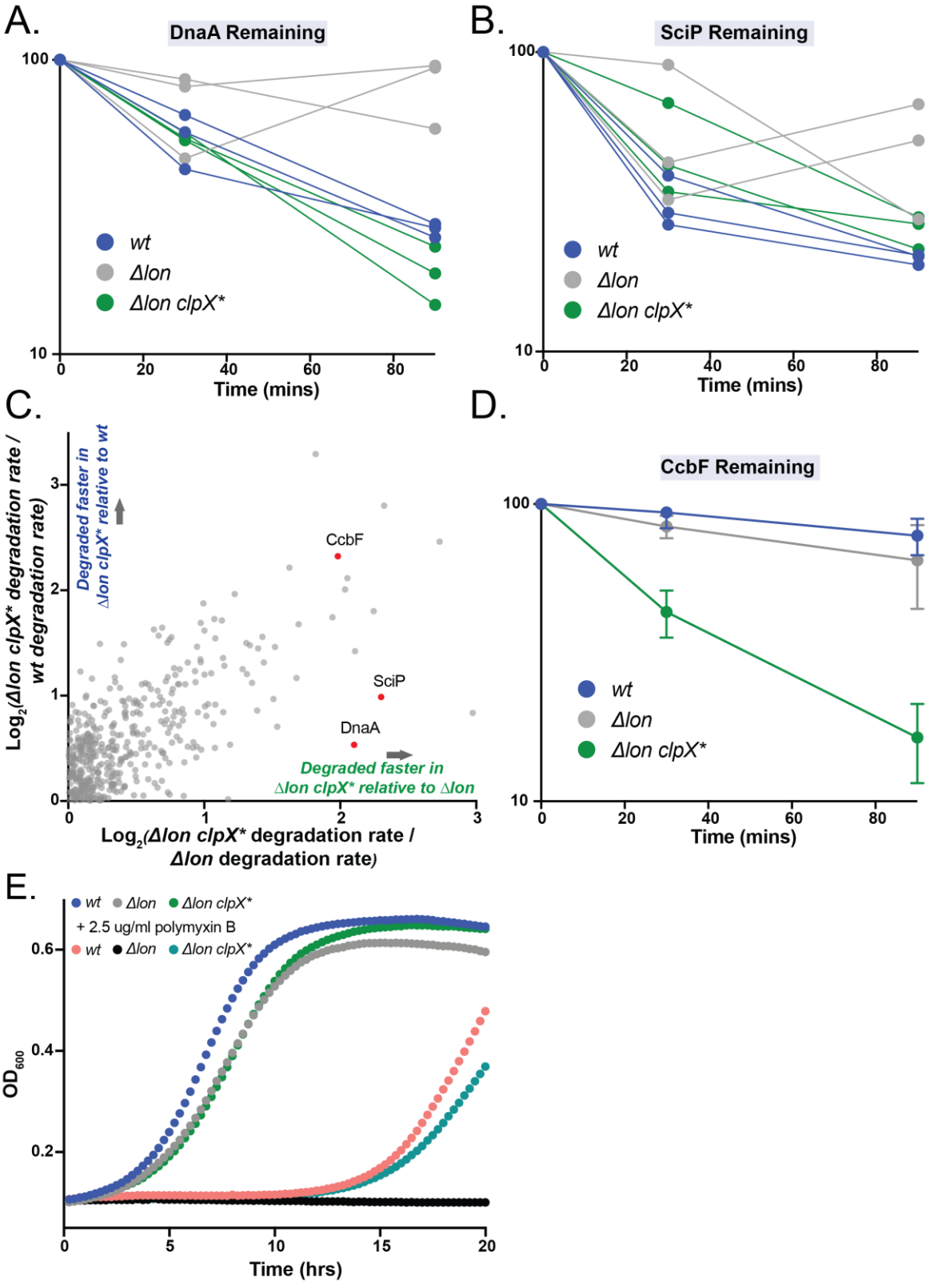
A.
DnaA Remaining
100
10
0
20
40
60
80
Time (mins)
wt
Δlon
Δlon clpX*
B.
SciP Remaining
100
10
0
20
40
60
80
Time (mins)
wt
Δlon
Δlon clpX*
C.
Log2(Δlon clpX* degradation rate / wt degradation rate)
Degraded faster in Δlon clpX* relative to wt
CcbF
SciP
DnaA
Degraded faster in Δlon clpX* relative to Δlon
0
1
2
3
Log2(Δlon clpX* degradation rate / Δlon degradation rate)
D.
CcbF Remaining
100
10
0
20
40
60
80
Time (mins)
wt
Δlon
Δlon clpX*
E.
wt
Δlon
Δlon clpX*
+ 2.5 ug/ml polymyxin B
wt
Δlon
Δlon clpX*
OD600
0.2
0.4
0.6
0
5
10
15
20
Time (hrs)

Figure 3.4 CcbF is preferentially degraded in *Δlon clpX*.* A-B. Plot showing protein abundance triplicates for t=0, t=30, and t=90 for *wildtype, Δlon*, and *Δlon clpX** for DnaA (left) and SciP (right). Data was normalized to control channel to allow comparison between *wildtype*, *Δlon, and Δlon clpX** and normalized to t=0 timepoint. **C**. Plot showing Log_2 (*Δlon clpX** degradation rate/ *Δlon* degradation rate) on the x-axis and Log_2 (*Δlon clpX** degradation rate/ *wt* degradation rate*)* on the y-axis. Degradation rate was defined as t=0/t=90 for each strain. CcbF, DnaA, and SciP are highlighted in red. **D.** Plot showing protein abundance triplicates for t=0, t=30, and t=90 for *wildtype, Δlon*, and *Δlon clpX** for CcbF. Data was normalized to control channel to allow comparison between *wildtype*, *Δlon, and Δlon clpX** and normalized to t=0 timepoint. **E**. Growth curves in the presence of polymyxin B for *wildtype, Δlon*, and *Δlon clpX*.* Each strain was grown in PYE only as a control.

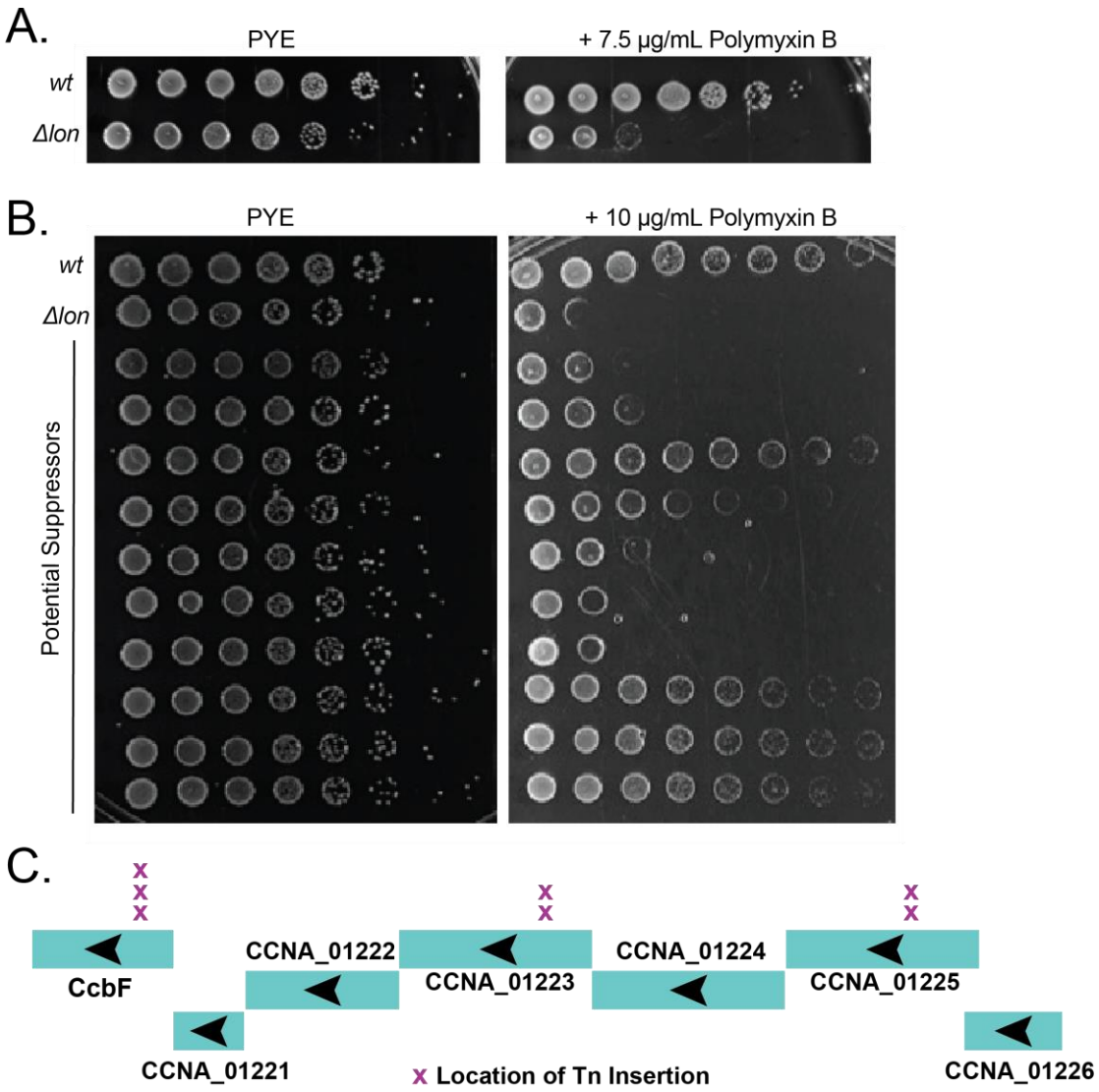

Figure 3.5 *Δlon* suppressors of polymyxin sensitivity map to CcbF operon. **A.** Logarithmically growing *wildtype* and *Δlon* were normalized by OD600 and 10-fold serial dilutions were plated on PYE and PYE polymyxin B plates. **B.** 10-fold serial dilutions of wildtype, *Δlon,* and potential *Δlon* suppressors plated on PYE and PYE polymyxin B plates. **C.** Location of transposon (Tn) insertions in 7 validated *Δlon* polymyxin B suppressors.

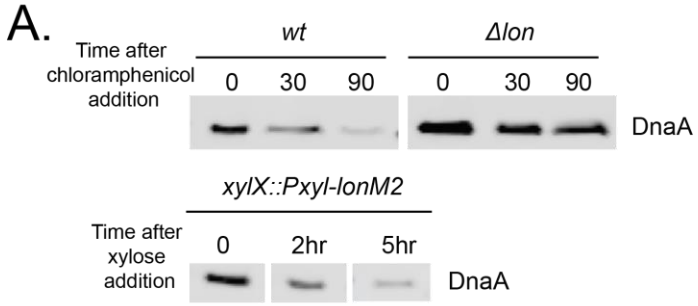

Figure 3.6 (Figure S1) Western blots of strains utilized in TMT experiments. Representative of triplicates of *wildtype*, *Δlon*, and Lon O/E strains. For *wildtype* and *Δlon*, samples were withdrawn post chloramphenicol addition at the indicated time points. For the Lon O/E strain, samples were withdrawn post xylose addition. Lysates were used for western blot analysis and probed with anti-DnaA.

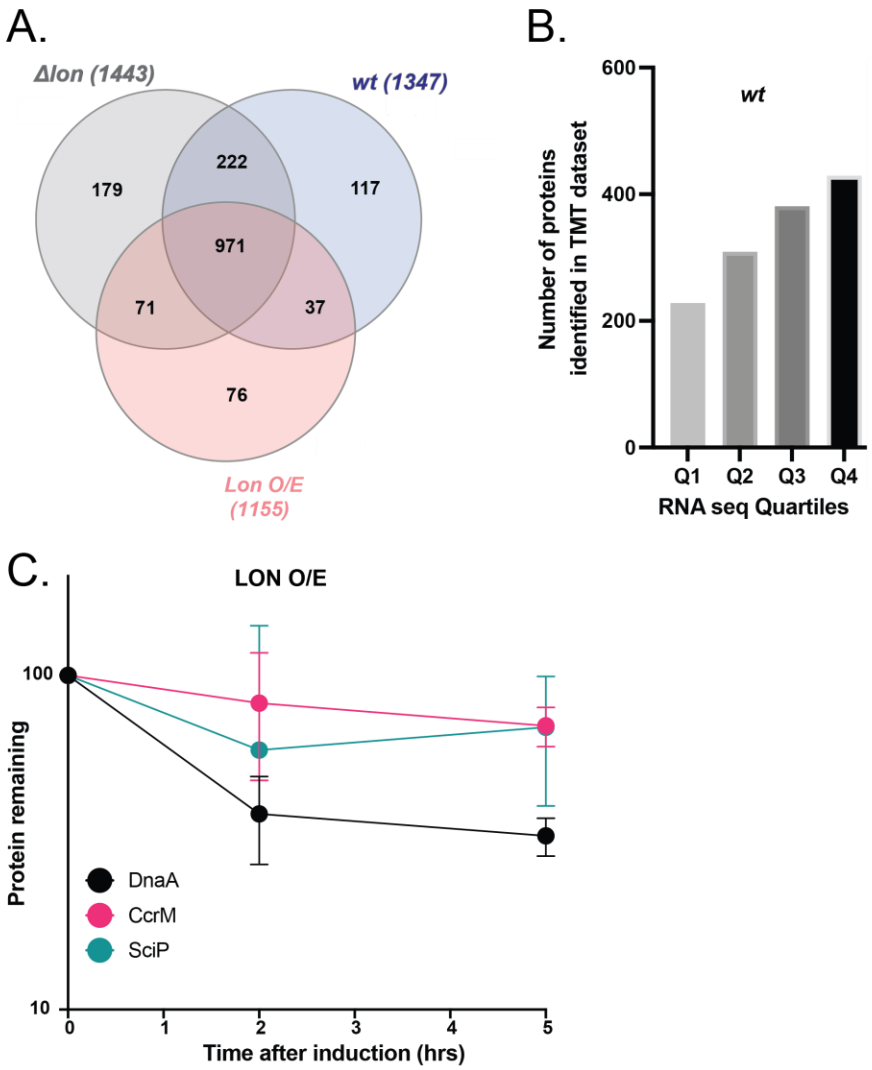

Figure 3.7 (Figure S2) Lon O/E TMT

A. Venn diagram showing the overlap between the identified proteins in a *wildtype*, *⊿lon*, and Lon O/E strain. **B. C.** Plot showing t=0, t=2 hour, and t=5 hour protein abundances in the Lon O/E dataset for DnaA, CcrM, and SciP. Data was normalized to t=0 timepoint.

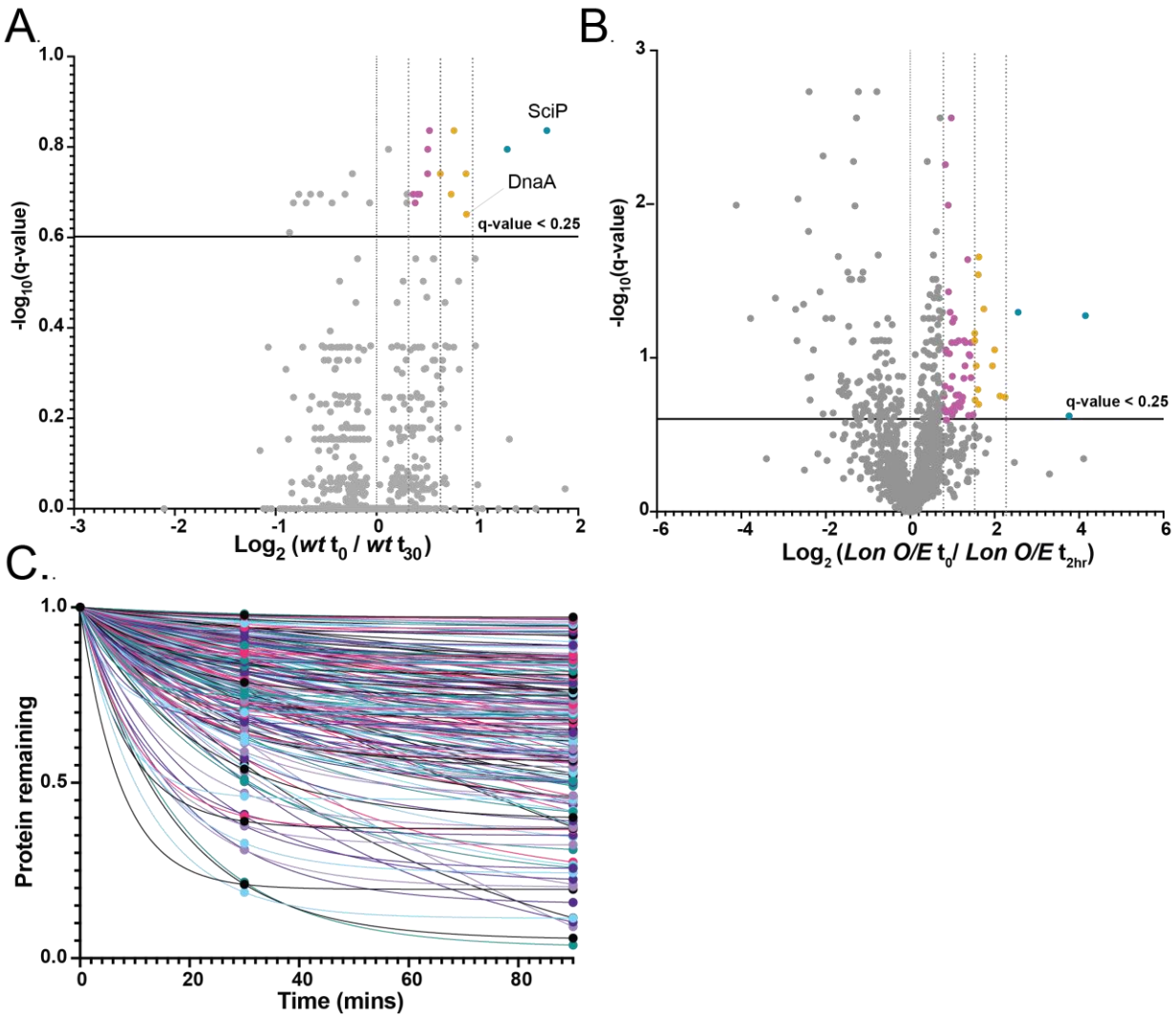

Figure 3.8 (Figure S3) Half-lives of identified proteins

A. Volcano plot comparing the proteomics of *wildtype* t=0 and *wildtype* t=30 with an FDR cutoff of 25%. **B**. Volcano plot comparing the proteomes of *Lon O/E strain* t=0 (uninduced) and t=2 hours post induction with an FDR cutoff of 25%. For all volcano plots, proteins found 1 standard deviation from the mean (1 sigma) are shown in purple. Proteins found 2 standard deviations from the mean (2 sigma) are shown in yellow. Proteins found 3 standard deviations from the mean (3 sigma) are shown in teal. **C**. Plot showing normalized protein abundances at t=0, t=30, and t=90 in a *wildtype* strain for all proteins where a

half-life calculation was possible. Half-lives were calculated using the one-phase decay equation in Prism.

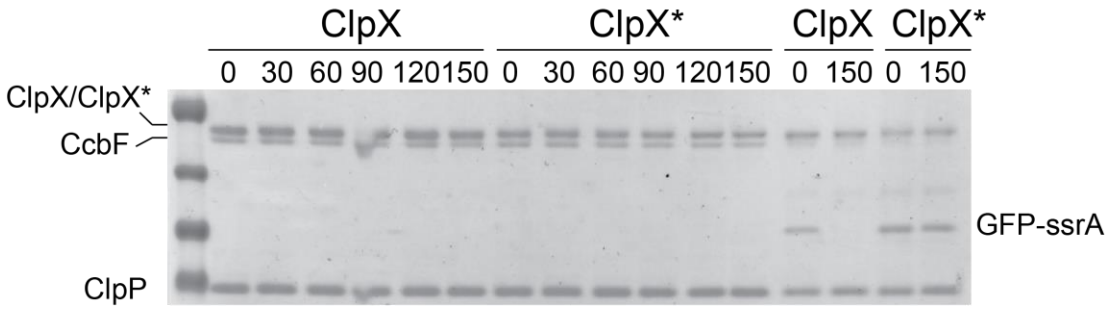

Figure 3.9 CcbF *in vitro* degradation assay in the presence of 0.1 uM ClpX and ClpX*. GFP-ssrA degradation assay shown as a positive control to ensure ClpX is active.

Chapter 4

Suppression Analysis Reveals Lon-related Pathways

Contributions: I performed the transposon-based and spontaneous suppressor screens to pull up the hits discussed in this chapter. I detailed our understanding of suppressor 18 (*Δlon clpX**) in chapter 2 of this thesis. Additional characterizations beyond this chapter have been completed by Patrick Cann, especially for suppressor 25. He has also done some wonderful work on using translational inhibitors to suppress *Δlon* defects.

4.1 Abstract

Caulobacter crescentus cells lacking the AAA+ protease Lon are non-motile and sensitive to various stressors. Here, we screen for *Δlon* motility suppressors using both a transposon-mutagenesis approach and a spontaneous suppressor approach. We identify motility suppressors that also suppressed other *Δlon* defects including filamentation and response to Mitomycin C. We identified a spontaneous motility suppressor that has a deletion of the 16s ribosomal RNA, suggesting a link between Lon and translation. We explore this link further by showing that decreasing translation through either slowing down growth or low levels of translational inhibition is beneficial for *Δlon* cells. Lastly, we show that there are other ways to suppress *Δlon* defects including deletions of *ssrA* and *smpB* and pyruvate dehydrogenase.

4.2 Introduction

Energy-dependent proteases are found in all domains of life. They are critical for driving normal growth and response to stresses (Mahmoud and Chien, 2018). Lon is a highly conserved member of the AAA+ (ATPases associated with diverse cellular activities) family and is primarily known for degrading misfolded proteins (Goff, Casson and Goldberg, 1984). In addition to its role in removing damaged and unfolded proteins, Lon plays a role in degrading regulatory proteins as well, including the replication initiator DnaA, the methyltransferase CcrM, and the transcriptional repressor SciP in *Caulobacter crescentus* (Wright *et al.*, 1996; Gora *et al.*, 2013; Jonas *et al.*, 2013).

Although cells lacking Lon are still viable, they exhibit multiple defects, including filamentation and decreased motility on soft agar (Wright *et al.*, 1996; Leslie *et al.*, 2015). However, it is not always clear why *Δlon* cells exhibit these defects and if these defects arise from stabilization of certain Lon substrates in cells lacking Lon. In some cases, there is a direct link between a *Δlon* defect and stabilization of a direct Lon target. For example, recent work has established a link between elongated stalks in *Δlon* cells and stabilization of the developmental regulator and newly discovered Lon substrate, StaR (Omnus *et al.*, 2021). However, for some *Δlon* phenotypes, the effect is indirect. For example, *Δlon* cells are more resistant to hydroxyurea (HU), a known inhibitor of ribonucleotide reductase (RNR). Recent work has suggested that stabilization of the Lon substrate, CcrM, transcriptionally upregulates RNR, explaining why *Δlon* cells are resistant to HU (Zeinert *et al.*, 2020).

Here, we use a suppressor screen approach to identify suppressors of *Δlon's* motility defect. We identify motility suppressors that also restore stress responses to *Δlon* cells. We pull up a suppressor with a deletion of the 16s ribosomal RNA, hinting at a potential link between the Lon protease and translation. We find that slowing down growth or using low levels of translational inhibition is beneficial in *Δlon* cells. Finally, we uncover other ways to suppress *Δlon* defects.

4.3 Results

Cells lacking the Lon protease are non-motile when grown on soft agar (Figure 4.1A). We generated a transposon-library in a *Δlon* background to identify suppressors that restore motility to *Δlon* cells. We inoculated 0.3% PYE agar with the *Δlon* transposon library and looked for colonies that showed enhanced motility. We then validated these targets and found three suppressors that increased motility in a *Δlon* background (Figure 4.1B). We named these suppressors #18, #22, and #25 (Figure 4.1B).

We further characterized these three suppressors and found that in addition to restoring motility to *Δlon* cells, these suppressors also suppressed filamentation (Figure 4.1C) and sensitivity to Mitomycin C (Figure 4.1D).

To identify the site of the transposon insertion in suppressors 18,22, and 25, we performed sequential PCR amplifications using arbitrary primers and a Tn-5 specific primer. We found that suppressor 18 had a transposon insertion in CCNA_00264, annotated as a C4-dicarboxylate transport protein. Suppressor 22 had a transposon insertion in phosphate regulon response regulator *phoB* and

suppressor 25 had a transposon insertion in CCNA_01509, annotated as 3-oxoacyl synthase III.

Next, we asked whether the transposon insertion was responsible for the phenotypic rescue described above. To answer this, we used a *Caulobacter*-specific phage, Cr30, to move the transposon and surrounding regions to a new *Δlon* background, which would be free of any background mutations that could have been present in the original *Δlon* strain. We then checked the motility of the resulting phage transductions. We reasoned that if the transposon insertion was the reason for the motility rescue, these strains should remain as motile as the original isolated suppressors. However, we found that for all three suppressors, moving the transposon insertion into a fresh *Δlon* background did not restore motility to *Δlon* cells (Figure 4.2A). This suggested to us that the mutation responsible for the motility rescue observed in the original suppressors was a spontaneous mutation. To identify these spontaneous suppressor mutations, we performed whole genome sequencing on suppressors 18, 22, and 25.

Whole genome sequencing revealed that suppressor 18 had a single point mutation in the ClpX protease. We have recently explored the mechanism behind how this *clpX* point mutant is able to rescue *Δlon* defects (Mahmoud, Aldikacti and Chien, 2021). Suppressor 22 has a frameshift mutation in the developmental regulator and ClpXP substrate, TacA (Biondi *et al.*, 2006). We next asked if this mutation led to non-functional TacA protein. Indeed, we performed western blots on suppressors 18, 22, and 25 in addition to wildtype and *ΔtacA* as controls and found that TacA was not expressed in suppressor 22, like a *ΔtacA* strain (Figure

4.2B). However, we found that a *⊿lon ⊿tacA* strain was not as motile as the original 22 suppressor, suggesting that the phenotypic rescue was not due to deletion of *tacA* in a *⊿lon* (Figure 4.2B).

Suppressor 25 had a point mutation upstream of the coding region of the master regulator and ClpXP substrate, CtrA. This mutation occurs upstream of the P1 promoter in the GANTC methylation motif for CtrA (Reisenauer, 2002). Intriguingly, this methylation site is acted on by CcrM, a Lon substrate, where methylation acts to inhibit CtrA transcription. We reasoned that altering this methylation site might alter CtrA's methylation status which would be mis regulated in the absence of Lon and the resulting buildup of CcrM.

In addition to the CtrA methylation mutation, whole genome sequencing of suppressor 25 revealed a single point mutation (N87K) in the S1P protein. We reasoned that since the transposon insertion could not explain the phenotypic rescue observed with suppressor 25, the rescue could be explained by either the CtrA methylation mutation or the S1P mutation or a combination of the two mutations. We created a *⊿lon* strain with the mutation in the CtrA methylation site and tested motility. We did not find that this strain was as motile as the original suppressor 25 and reasoned that mutating the CtrA methylation site on its own is not sufficient to suppress motility (Figure 4.2C).

Given that our previous suppressor screen using a transposon library did not lead to any hits due to the transposon insertions, we reasoned that we might be able to find spontaneous motility suppressors in *⊿lon* background directly. To do this, we inoculated *⊿lon* cells into 0.3% PYE agar and looked for flares,

indicative of increased motility. We identified three promising suppressors, which we named 5, 7, and 9 (Figure 4.3A). However, upon validation we observed that 5,7, and 9 only marginally increased motility in *Δlon* (Figure 4.3A). Instead, we found that these strains suppressed Mitomycin C sensitivity, especially suppressor # 5 which was as resistant to Mitomycin C as *wildtype* (Figure 4.3B). In addition, suppressor 5 was less filamentous than *Δlon* cells (Figure 4.3C). We did whole genome sequencing and found that suppressor 5 had a deletion of CCNA_R0069, which is the 16S ribosomal RNA, and two neighboring genes, CCNA_02708 and CCNA_02709. This suggested that it was beneficial to delete 16S ribosomal RNA in a *Δlon.* We next wondered if this mutation was slowing down translation and somehow that was beneficial in cells lacking Lon.

Next, we explored other ways to slow down translation and their impact on *Δlon* cells. We grew *Δlon* cells and *Δlon ΔclpA cells* in PYE, a nutrient-rich media, and M2G, a defined media which slows down growth rate (Hottes *et al.*, 2004). We found that in PYE, *Δlon* and *Δlon ΔclpA* cells were highly filamentous (Figure 4.4A). This filamentation was suppressed in M2 media with 0.2% glucose and in M2G with 0.04% glucose (Figure 4.4A). Similarly, we monitored growth of wildtype, *Δlon,* and *Δlon ΔclpA* cells in PYE, M2 with 0.2% glucose, and M2 with 0.04% glucose. We observed that *Δlon* was not able to grow as well as wildtype cells, exhibiting a lag and growing to a lower stationary phase OD, as previously reported (Figure 4.4B) (Mahmoud, Aldikacti and Chien, 2021). *Δlon ΔclpA* cells exhibited a much longer lag in comparison to both wildtype and *Δlon,* eventually reaching the same final OD as *Δlon* (Figure 4.4B). In M2 with 0.2% glucose, the

lag for *Δlon ΔclpA* was much less pronounced and *wildtype* and *Δlon* grew similarly (Figure 4.4B). In M2 with 0.04% glucose, the three strains were comparable in growth, although they only doubled two times before reaching saturation (Figure 4.4B). We also grew wildtype and *Δlon* cells in M5G media and observed a similar trend in phosphate-replete conditions (Figure 4.4C). This data suggested to us that slowing down translation by slowing down growth is beneficial in cells lacking Lon and in those lacking Lon and ClpA.

Next, we tested directly if slowing down translation was beneficial in cells lacking Lon. We exposed wildtype and *Δlon* cells to PYE plates supplemented with Mitomycin C and to plates supplemented with Mitomycin C and low amounts of chloramphenicol, a translational inhibitor. We found that *Δlon* cells were more sensitive to Mitomycin C than wildtype cells (Figure 4.5A). However, addition of chloramphenicol made *Δlon* cells more resistant to Mitomycin C, suggesting that slowing down translation allows *Δlon* cells to better respond to DNA damage (Figure 4.5A).

Next, we explored other ways to suppress *Δlon* defects. In bacteria, proteins whose synthesis has stalled are cleared and marked for degradation in a process called *trans*-translation (Karzai, Roche and Sauer, 2000). This system is mediated by a ribosome-bound ssrA RNA and a protein factor, SmpB. We found that deleting either ssrA or SmpB restored some DnaA degradation in a *Δlon* strain, where DnaA is stabilized (Figure 4.6A). We explored whether motility was suppressed in a *Δlon ΔsmpB* or a *Δlon ΔssrA* strain and did not observe any increase in motility. We also observed some restoration of DnaA degradation in a

Δlon ΔpopA strain, which was intriguing because it is another ClpXP substrate (Joshi *et al.*, 2015), suggesting there an interplay between the two protease pathways.

Lastly, we found that *Δlon*'s filamentation defect was suppressed in a *Δlon* strain with a deletion of pyruvate dehydrogenase (Figure 4.7A). While we saw that DnaA degradation was somewhat enhanced in a *Δlon Δpyruvate dehydrogenase* strain, this effect was not consistent. We also did not see any suppression of Mitomycin C sensitivity or L-canavanine sensitivity in a *Δlon Δpyruvate dehydrogenase* strain.

4.4 Discussion

The importance of AAA+ proteases is highlighted by the defects in growth and response to stress that arises in their absence (Breidenstein *et al.*, 2012; Rogers *et al.*, 2016). In *Caulobacter crescentus*, cells lacking Lon are non-motile, have elongated cell and stalk length, and are sensitive to various stressors (Mahmoud, Aldikacti and Chien, 2021; Omnus *et al.*, 2021). In this study, we sought to identify novel Lon-related pathways by looking for suppressors of *Δlon*'s motility defect. We pull up three suppressors in the ClpXP pathway, a point mutation in ClpX, a frameshift mutation in TacA, a ClpXP substrate, and a mutation in the promoter region of CtrA, another ClpXP substrate (Figure 4.1, 4.2). We also found that deleting popA, a ClpXP adaptor, in a *Δlon* restored some DnaA degradation (Figure 4.6). These suppressors suggest that the Lon and ClpXP protease pathways are not independent but that changes that affect one pathway can be corrected by alterations to the other pathway.

We also identified a spontaneous motility suppressor, 5, that had a deletion in the 16S ribosomal RNA (Figure 4.3). This suggests that somehow slowing down translation in a *Δlon* is beneficial. We further explore this link by finding that other ways that slow down translation, such as growth in minimal media or the addition of translational inhibitors to *Δlon* cells, are beneficial to *Δlon* cells. It is intriguing to think about a connection between the Lon protease and the process of translation. Afterall, proteases break down proteins into their component amino acids, which then go on to serve as fuel for making more proteins. For instance, inhibition of the eukaryotic proteasome is lethal due to the resulting shortage of amino acid pools (Suraweera *et al.*, 2012). In the absence of degradation, perhaps there is a shortage of amino acid pools which can be replenished by slowing down translation. However, working is ongoing to elucidate the mechanism governing the benefit of translational inhibition in a *Δlon.*

4.5 Methods

Bacterial strains and growth conditions

Strains were grown in PYE medium (2g/L peptone, 1g/L yeast extract, 1 mM $MgSO_4$, and 0.5 mM $CaCl_2$) or M2G (6.1 mM Na_2HPO_4, 3.9 mM KH_2PO_4, 9.3 mM NH_4Cl, 0.5 mM $MgSO_4$, 10 μM $FeSO_4$[EDTA chelate], 0.5 mM $CaCl_2$, and 0.2% glucose as the sole carbon source) or M5G (10 mM PIPES, pH 7, 1 mM NaCl, 1 mM KCl, 0.05% NH_4Cl, 0.01 mM Fe/EDTA, 0.2% glucose, 0.5 mM $MgSO_4$, 0.5 mM $CaCl_2$ and 10 mM phosphate) at 30°C.

For *C. crescentus* motility assays, PYE with 0.3% agar was used and a single colony was stabbed into the agar using a sterile tip and left to incubate at 30°C for 2 to 3 days.

For solid medium, 1.5% agar was used. For all strains, optical density was measured at 600 nm.

Motility Suppressor screen

Transposon libraries were generated for *Δlon* cells. Two-liter PYE cultures were grown to mid log phase, pelleted, and washed with 10% glycerol. Competent cells were electroporated with Ez-Tn5 <Kan-2> transposome (Lucigen, Madison, WI). Cells recovered for 1.5 hours at 30 °C and then plated on PYE + kanamycin plates. Libraries were grown for 7 days. Colonies were then scraped from the surface, combined, and resuspended to form a homogenous solution of PYE + 20% glycerol.

The Tn library was thawed out and diluted into a flask containing two-liter 0.3% agar. The cell agar mixture was plated and grown at 30 °C for 3 to 5 days. Candidates that appeared motile were validated by innoculating single colonies into motility agar on the same plate as NA1000 as a positive control and *Δlon* as a negative control and incubating plates for 2-3 days at 30 °C.

The motility screen with spontaneous suppressors was performed by inoculating a 2L flask of 0.3% PYE agar with diluted *Δlon* cells. The cell agar mixture was plated and grown at 30 °C for 3 days. Candidates that appeared motile were validated by innoculating single colonies into motility agar on the same plate as

NA1000 as a positive control and *Δlon* as a negative control and incubating plates for 2-3 days at 30 °C.

Whole genome sequencing

Genomic DNA was extracted using the MasterPure Complete DNA and RNA purification kit (Epicenter Biotechnologies, Madison, WI). A Qubit Fluorometer (ThermoFisher Scientific, Waltham, MA) was utilized to assess DNA concentration. Illumina libraries were generated from the extracted genomic DNA using the NexteraXT (Illumina, San Diego, CA) protocol. Libraries were multiplexed and sequenced at the University of Massachusetts Amherst Genomics Core Facility on the NextSeq 500 (Illumina). Single nucleotide polymorphisms (SNPs) were detected using breseq (Deatherage and Barrick, 2014).

Plating viability and drug sensitivity

All C*aulobacter* strains were grown overnight in liquid media. After overnight growth, cells were back diluted to OD_{600} 0.1 and outgrown to mid-exponential phase before being normalized to OD_{600} 0.1 and 10-fold serially diluted on to media. For experiments using mitomycin C (Sigma, St. Louis, MO) and L-canavanine (Sigma), drugs were prepared at a stock concentration of 0.4 µg/ml mitomycin C. PYE agar was cooled before the drugs were added and plates were left to air dry prior to serial dilution plating. All plates were incubated at 30℃ for 2-3 days and imaged with a gel doc.

***In vivo* assays**

The stability of proteins *in vivo* was determined by inhibiting protein synthesis upon addition of 30 μg/ml chloramphenicol to cells in exponential phase. At each time point, 1ml of culture was removed and centrifuged at 15,000 rpm for 2 minutes. The supernatant was removed and pellets were flash frozen in liquid nitrogen. Pellets were thawed, resuspended in 2x SDS dye, and normalized to the OD_{600} of the lowest sample. Samples were boiled for 10 minutes and centrifuged for 10 minutes at 15,000 rpm. Extracts were run on 10% Bis-Tris gels for 1 hour at room temperature at 150 V. Gels were then transferred to nitrocellulose membranes for 1 hour at room temperature at 20V. Membranes were blocked with 3% milk in Tris-based saline with 0.05% Tween-20 (TBST) for 1 hour. Membranes were probed with primary antibody in 3% milk in TBST at 4°C overnight with a 1:5000 dilution of DnaA. Membranes were washed with 1x TBST for 5 minutes three times and then probed with Licor secondary antibody with 1:10,000 dilution in 1x TBST at room temperature for 1 hour. The protein was visualized using Licor Odyssey CLx. Bands were quantified using imageJ and degradation rates were plotted using Prism.

Microscopy

Phase contrast images of logarithmically growing cells were taken by Zeiss AXIO Scope A1. Cells were mounted on 1% PYE agar pads and imaged using a 100X objective. MicrobeJ (Ducret et al., 2016) for ImageJ (Schneider et al., 2012) was utilized to quantify cell lengths. Representative images of the same scale were cropped to display morphological defects.

4.6 References

Biondi, E.G. *et al.* (2006) 'A phosphorelay system controls stalk biogenesis during cell cycle progression in *Caulobacter crescentus*: Regulation of stalk biogenesis in *C. crescentus*', *Molecular Microbiology*, 59(2), pp. 386–401. doi:10.1111/j.1365-2958.2005.04970.x.

Goff, S.A., Casson, L.P. and Goldberg, A.L. (1984) 'Heat shock regulatory gene htpR influences rates of protein degradation and expression of the ion gene in Escherichia coli', *Proc. NatL. Acad. Sci. USA*, p. 6.

Gora, K.G. *et al.* (2013) 'Regulated proteolysis of a transcription factor complex is critical to cell cycle progression in *Caulobacter crescentus*: Cell cycle regulated proteolysis in *Caulobacter*', *Molecular Microbiology*, 87(6), pp. 1277–1289. doi:10.1111/mmi.12166.

Hottes, A.K. *et al.* (2004) 'Transcriptional Profiling of *Caulobacter crescentus* during Growth on Complex and Minimal Media', *Journal of Bacteriology*, 186(5), pp. 1448–1461. doi:10.1128/JB.186.5.1448-1461.2004.

Hottes, A.K., Shapiro, L. and McAdams, H.H. (2005) 'DnaA coordinates replication initiation and cell cycle transcription in Caulobacter crescentus', *Molecular Microbiology*, 58(5), pp. 1340–1353. doi:10.1111/j.1365-2958.2005.04912.x.

Jonas, K. *et al.* (2013) 'Proteotoxic Stress Induces a Cell-Cycle Arrest by Stimulating Lon to Degrade the Replication Initiator DnaA', *Cell*, 154(3), pp. 623–636. doi:10.1016/j.cell.2013.06.034.

Joshi, K.K. *et al.* (2015) 'An Adaptor Hierarchy Regulates Proteolysis during a Bacterial Cell Cycle', *Cell*, 163(2), pp. 419–431. doi:10.1016/j.cell.2015.09.030.

Karzai, A.W., Roche, E.D. and Sauer, R.T. (2000) 'The SsrA–SmpB system for protein tagging, directed degradation and ribosome rescue', *Nature Structural Biology*, 7(6), pp. 449–455. doi:10.1038/75843.

Leslie, D.J. *et al.* (2015) 'Nutritional Control of DNA Replication Initiation through the Proteolysis and Regulated Translation of DnaA', *PLOS Genetics*. Edited by W.F. Burkholder, 11(7), p. e1005342. doi:10.1371/journal.pgen.1005342.

Mahmoud, S.A., Aldikacti, B. and Chien, P. (2021) *Plasticity in AAA+ proteases reveals ATP-dependent substrate specificity principles*. preprint. Molecular Biology. doi:10.1101/2021.08.18.456811.

Reisenauer, A. (2002) 'DNA methylation affects the cell cycle transcription of the CtrA global regulator in Caulobacter', *The EMBO Journal*, 21(18), pp. 4969–4977. doi:10.1093/emboj/cdf490.

Rogers, A. *et al.* (2016) 'The LonA Protease Regulates Biofilm Formation, Motility, Virulence, and the Type VI Secretion System in Vibrio cholerae', *Journal of Bacteriology*. Edited by V.J. DiRita, 198(6), pp. 973–985. doi:10.1128/JB.00741-15.

Suraweera, A. *et al.* (2012) 'Failure of Amino Acid Homeostasis Causes Cell Death following Proteasome Inhibition', *Molecular Cell*, 48(2), pp. 242–253. doi:10.1016/j.molcel.2012.08.003.

Wright, R. *et al.* (1996) 'Caulobacter Lon protease has a critical role in cell-cycle control of DNA methylation.', *Genes & Development*, 10(12), pp. 1532–1542. doi:10.1101/gad.10.12.1532.

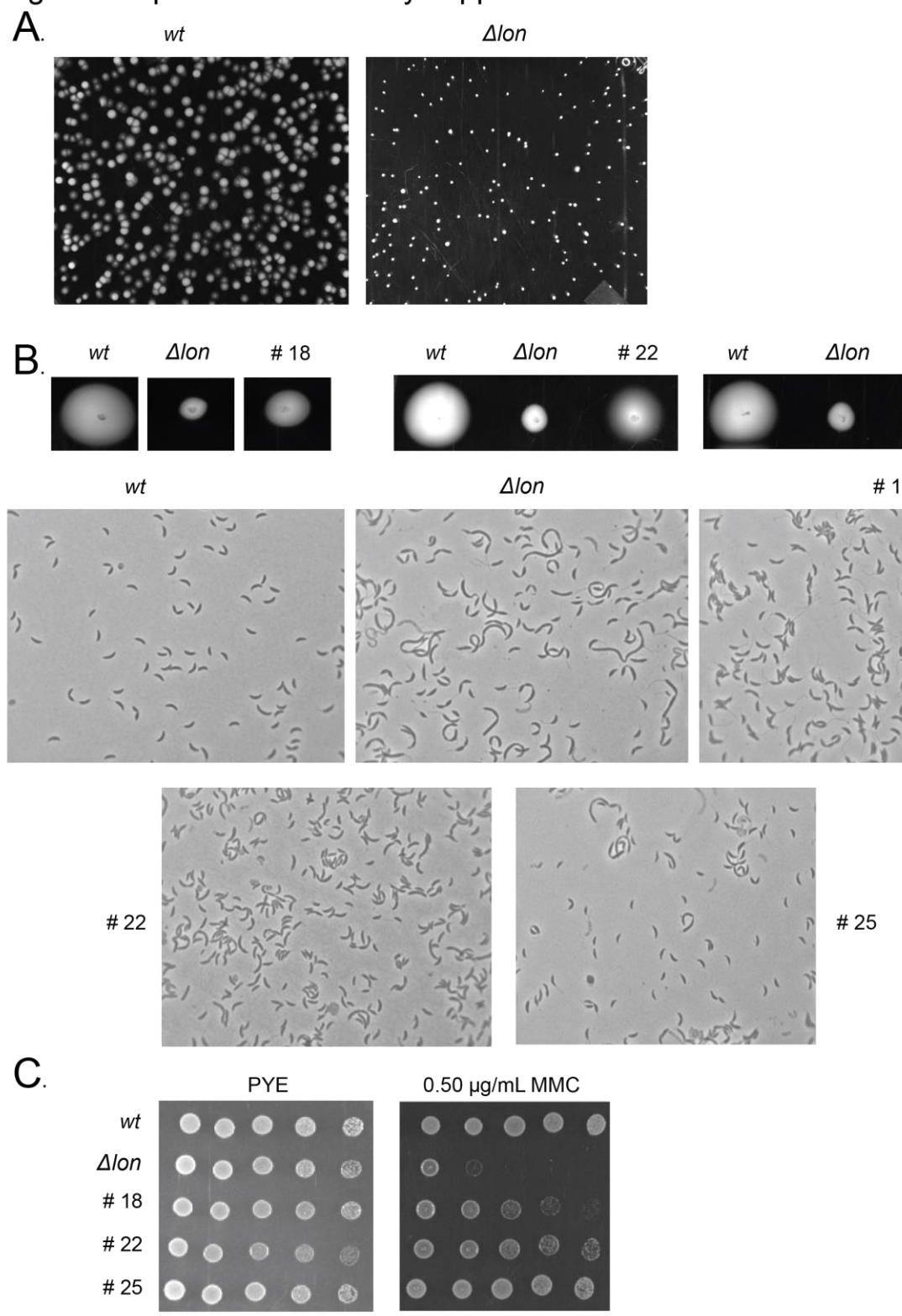

Figure 4.1 Using transposon mutagenesis to screen for motility suppressors. A. Set-up of motility screen. Wildtype cells are more motile than

Δlon cells. **B**. Validation of hits from motility screen compared to wildtype and *Δlon* on 0.3% PYE agar and morphology of wildtype, *Δlon,* Suppressors 18, 22, and 25. **C.** MMC spot assays. These are 10-fold serial dilutions of the indicated strains on PYE and PYE + MMC plates.

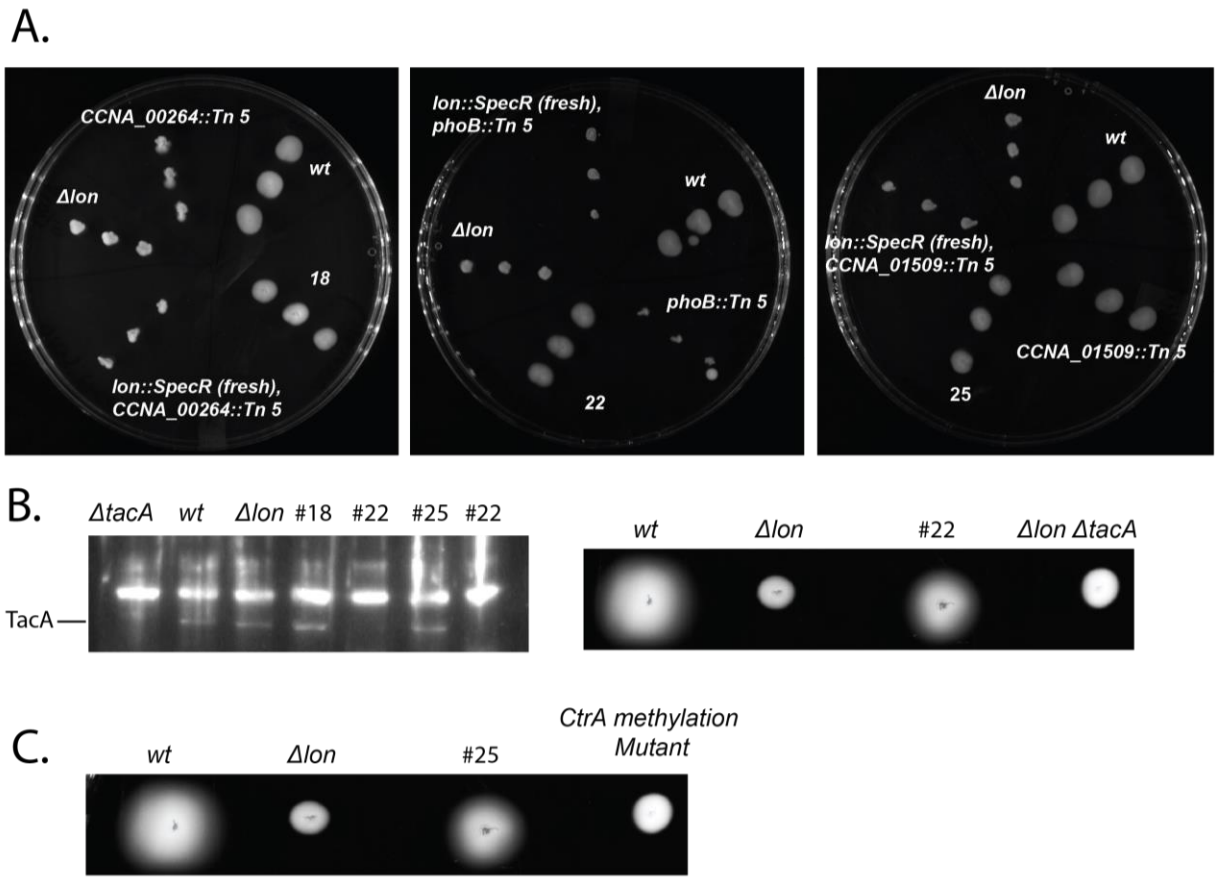

Figure 4.2 Validation of motility suppressors. A. Motility assays after phage transduction was used to move the transposon insertions into fresh *Δlon* strains. The resulting strains were no longer motile. **B.** Western blot showing suppressor 22 is not expressing TacA protein. Controls include Δ*tacA* and *wildtype* cells. Motility on 0.3% PYE agar showing *Δlon ΔtacA* is non-motile. **C.** Motility on 0.3% PYE agar showing *Δlon* cells with the CtrA promoter mutation are non-motile.

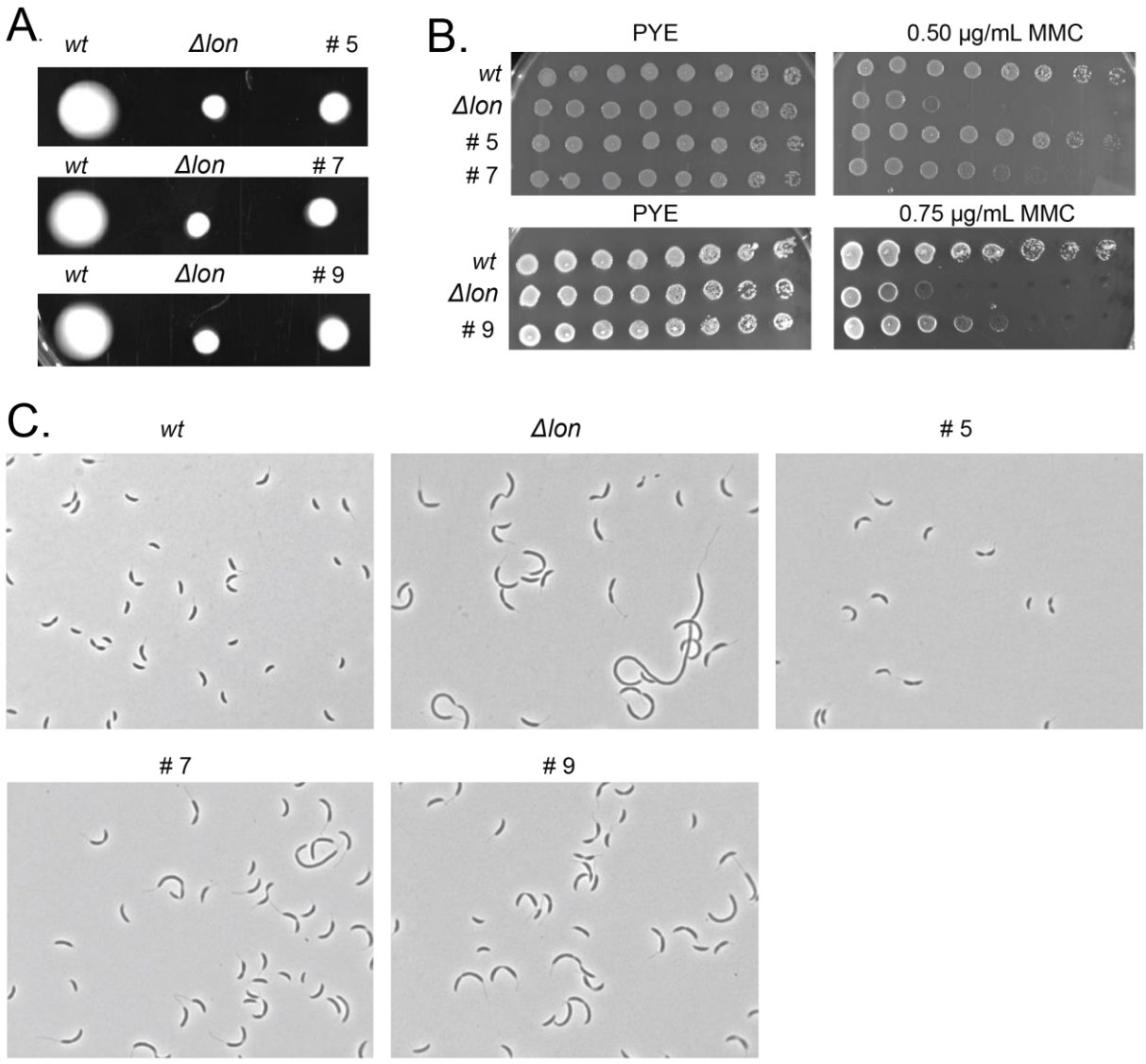

Figure 4.3 Spontaneous motility suppressors. A. Validation of spontaneous motility suppressors 5, 7, and 9 on 0.3% PYE agar. **B**. MMC spot assays of indicated strains. These are 10-fold serial dilutions of exponentially growing cells on PYE and PYE supplemented with the indicated concentrations of MMC. Suppressors 5, 7, and 9 suppress *Δlon's* sensitivity to MMC. **C.** Microscopy of indicated strains in PYE.

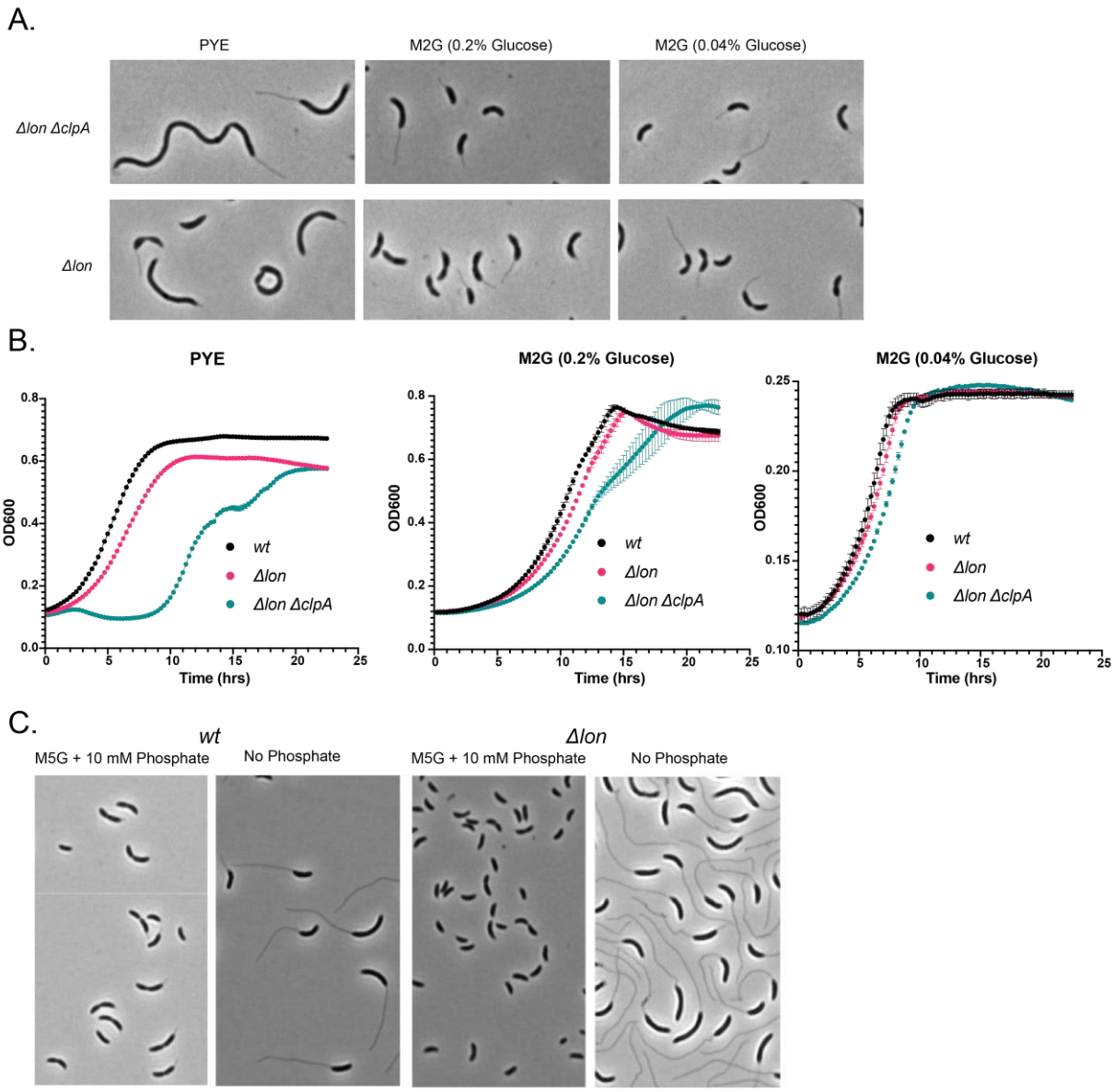

Figure 4.4 Minimal media suppresses *Δlon* defects. A. Microscopy of *Δlon* and *Δlon ΔclpA* cells grown in PYE, M2G (0.2% glucose), and M2G (0.04% glucose). **B**. Growth curves of *wildtype*, *Δlon* and *Δlon ΔclpA* cells in PYE, M2G (0.2% glucose), and M2G (0.04% glucose). **C.** Microscopy of *Δlon* and *wildtype* cells grown in M5G plus 10 mM phosphate and M5G no phosphate.

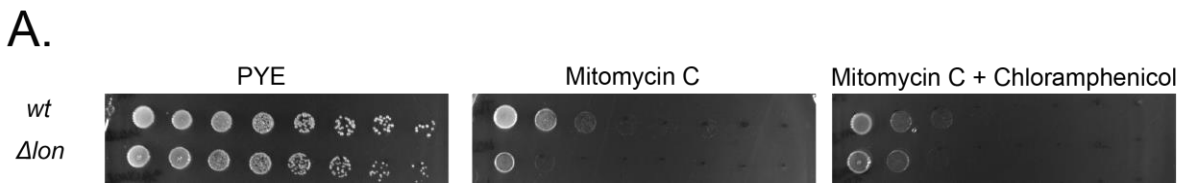

Figure 4.5 Spot assays of *Δlon and wildtype* cells on PYE, PYE + MMC, PYE + MMC + chloramphenicol.

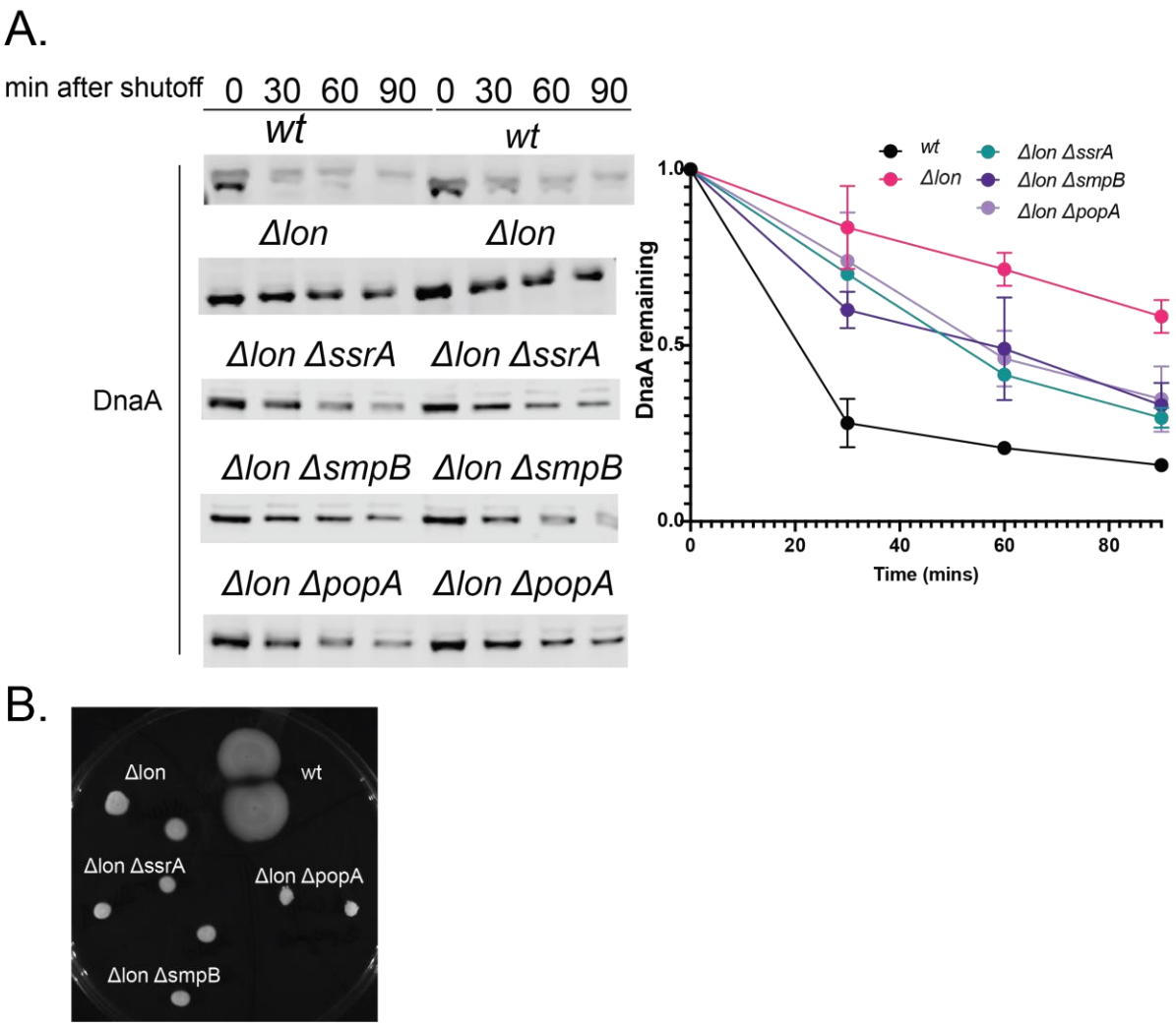

Figure 4.6 A. Antibiotic shutoff assays to monitor DnaA turnover in *wt, Δlon, Δlon, Δlon ΔssrA, Δlon ΔsmpB, and Δlon ΔpopA* strains. Chloramphenicol was added to stop synthesis and lysates from samples at the indicated time points

were used for western blot analysis. Quantifications of duplicate experiments shown to the right. Error bars represent SD. **B.** Motility on 0.3% PYE agar of indicated strains.

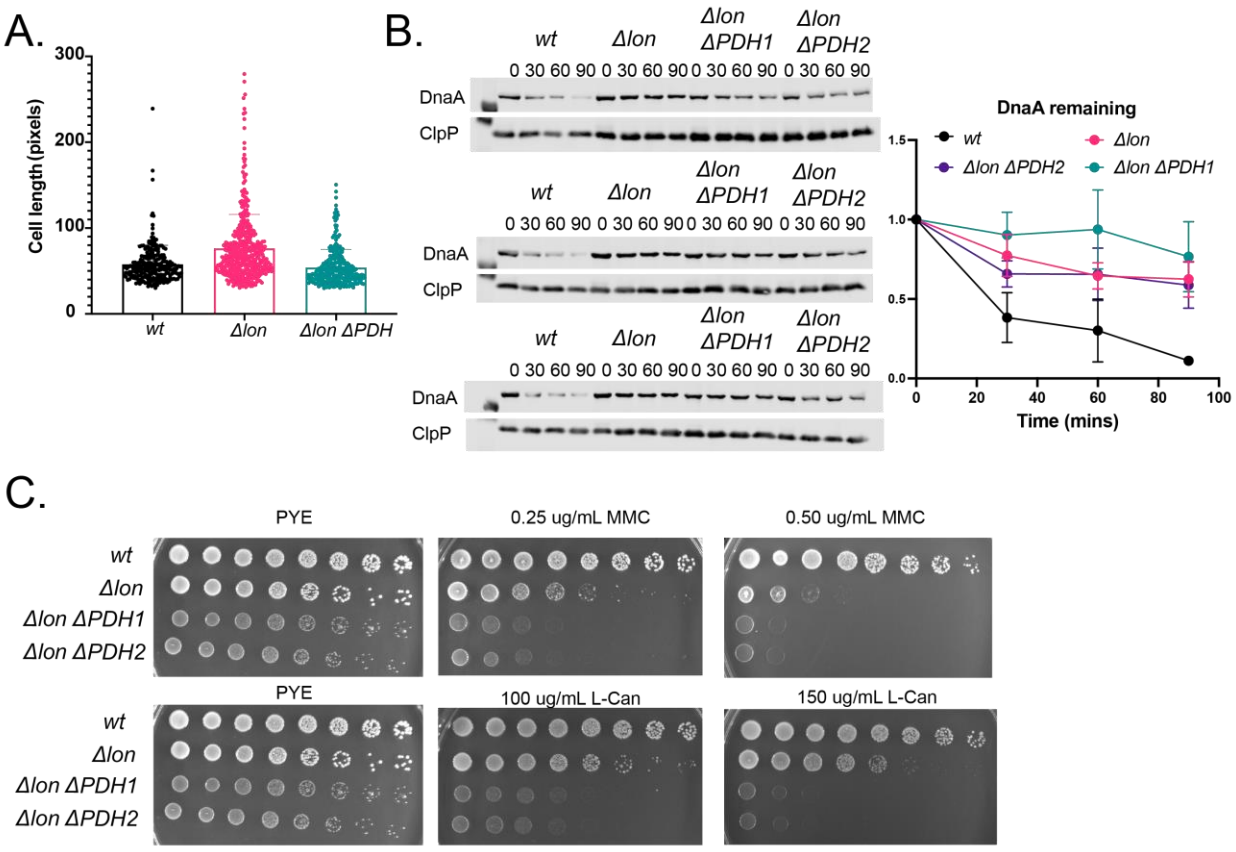

Figure 4.7 Characterization of *Δlon ΔPDH*. A. Quantification of cell length in *wt, Δlon*, *Δlon ΔPDH* cells. B. Antibiotic shutoff assays to monitor DnaA turnover in *wt, Δlon*, *Δlon ΔPDH* cells. Chloramphenicol was added to stop synthesis and lysates from samples at the indicated time points were used for western blot analysis. Quantifications of triplicate experiments shown to the right. Error bars represent SD. **C.** Spot assays of *Δlon, wildtype,* and *Δlon ΔPDH* cells on PYE, PYE + MMC, PYE + L-canavanine.

Chapter 5: Lessons I've learned and future perspectives

5.1 Overview

In this chapter I will reflect on the lessons I've learned from each chapter in this thesis as well as explore any remaining future directions.

5.2 ClpX*: Elucidating the mechanisms that govern substrate specificity

In the second chapter of this thesis, I present a mutant of ClpX, ClpX*, which has gained the ability to degrade Lon substrates *in vivo* and *in vitro.* We find this allows ClpX* to compensate for the absence of Lon, suppressing many *Δlon* defects. We go on to show that this comes at the cost of native ClpXP substrates, suggesting a cost-benefit to altering substrate specificity. While the mechanism of how ClpX* could shift substrate specificity eluded us for a long time, we finally were able to show that ClpX* adopts a more open conformation than wildtype ClpX and in the process we made a very interesting discovery. We found that wildtype ClpX could undergo a similar shift in specificity when ATP is limiting, with similar changes in conformation in these conditions as ClpX*.

This work surprisingly shows us that ATP not only functions as fuel for AAA+ protease to drive unfolding and translocation but ATP levels can also dictate substrate specificity. I think our work also shows biochemical consequences of recently published structures showing open and closed conformations of these AAA+ proteases (Shin et al. 2021). Although an open state of ClpX has not been published, our work hints at its existence and

suggests that the equilibrium between these states has real effects on substrate choice.

I foresee three major unanswered questions that can be addressed with future experiments. The first is, while we propose a model where ClpX* shifts the equilibrium towards the open state of ClpX, how this glycine to alanine mutation *actually does* this remains unanswered. Structural studies on the mutant ClpX* in addition to wildtype ClpX under high and low ATP conditions could provide insight into the mechanism by which the mutation alters specificity. Additionally, I wonder if molecular dynamics could be useful in answering this question. Secondly, how conserved is this idea that altering the dynamic between conformational states can alter substrate specificity across various AAA+ proteases? While we did not really explore this idea, I think it would be very interesting to see if limiting ATP for Lon or ClpA has a similar effect to what we observed for wildtype ClpX. Lastly, we show that DnaA gets degraded faster under starvation conditions in *vivo* accompanied by a drop in ATP levels. However, can we see further evidence of this phenomenon *in vivo* under other conditions that deplete ATP.

5.3 Profiling the degradome using a quantitative proteomics approach

In chapter three of this thesis, we present a quantitative proteomics approach we use to identify potential Lon targets. We go on to profile the degradome of *Δlon clpX** to identify novel substrates of ClpX*. The point of this work is to present an approach that can be applicable to various strains and conditions as well as to

provide the protein degradation community with a resource. We validate that CcbF is degraded faster by ClpX*, which is evidenced by the increased resistance to the antibiotic polymyxin B we observed in *Δlon clpX** cells.

Several unanswered questions about this work remain. Firstly, we do not follow up on the list of potential Lon targets in the paper. Experiments to validate these candidates as Lon substrates would include deleting these substrates in a *Δlon* and characterizing the mutant. This is important because we're interested in Lon substrates that can explain *Δlon* defects. Next, follow-up experiments can include purifying these proteins and testing degradation *in vitro*. Lastly, validation efforts should include overexpressing these substrates in a *wildtype* and determining if any defects arise.

Additionally, we have had many discussions on the way to go about defining potential Lon substrates. One of our first iterations involved used the known Lon substrates, DnaA, CcrM, and SciP to set the lower limits for each criterion: increased abundance upon Lon deletion, stabilization in a *Δlon,* and decreased abundance upon Lon deletion. However, the issue with this approach is that only DnaA really shows up as expected for a Lon substrate. While CcrM levels are more abundant in a *Δlon,* we did not observe much faster degradation in a *wildtype* compared to a *Δlon.* For SciP, we did not see a big difference between steady state levels in a wildtype and *Δlon,* which is consistent with my work showing that in mixed populations, *Δlon* cells do not have elevated SciP levels. The approach we took in chapter 3 seems more robust than using Lon substrates to set limits, however, it is not without flaws. For instance, I was

surprised that there was little overlap between the three criteria we set when determining Lon substrates. I would expect that there would be good overlap between the substrates that were more abundant in a *Δlon* and substrates that were stabilized in a *Δlon* background.

Lastly, in terms of the discovery of CcbF as a potential ClpX* substrate, we validate this indirectly using growth curves in the presence of polymyxin B. However, CcbF was not degraded faster *in vitro* by ClpX*, suggesting that perhaps an adaptor is necessary for degradation.

5.4 Suppressor analysis

Chapter 4 is a combination of all the different ways I've found over the years that have suppressed *Δlon* defects. Suppressor 25 showed a lot of promise at first because it suppressed many *Δlon* phenotypes, such as morphology and response to stress. However, many open questions remain, including determining which mutation is responsible for the phenotypic rescue and elucidating the mechanism.

An intriguing outcome of this chapter is the link between Lon and translation which Patrick Cann, an undergraduate in the lab, is actively following up on. It seems natural that there would be a connection between the pathway that synthesize proteins and the pathways that degrade proteins. We also have observed sensitivity of cells lacking Lon to translational inhibitors, such as tetracycline, and decreased translational efficiency as evidenced by pulse chase experiments. However, it is not clear how this fits in with data showing the

translational inhibition is beneficial in a *Δlon.* In addition to degrading misfolded and regulatory proteins, proteases play an important role in recycling amino acids, with previous work showing that the lethality of proteasome deletion is due to an amino acid shortage. If this is also the case for Lon remains to be explored.

Chapter 6: Appendix

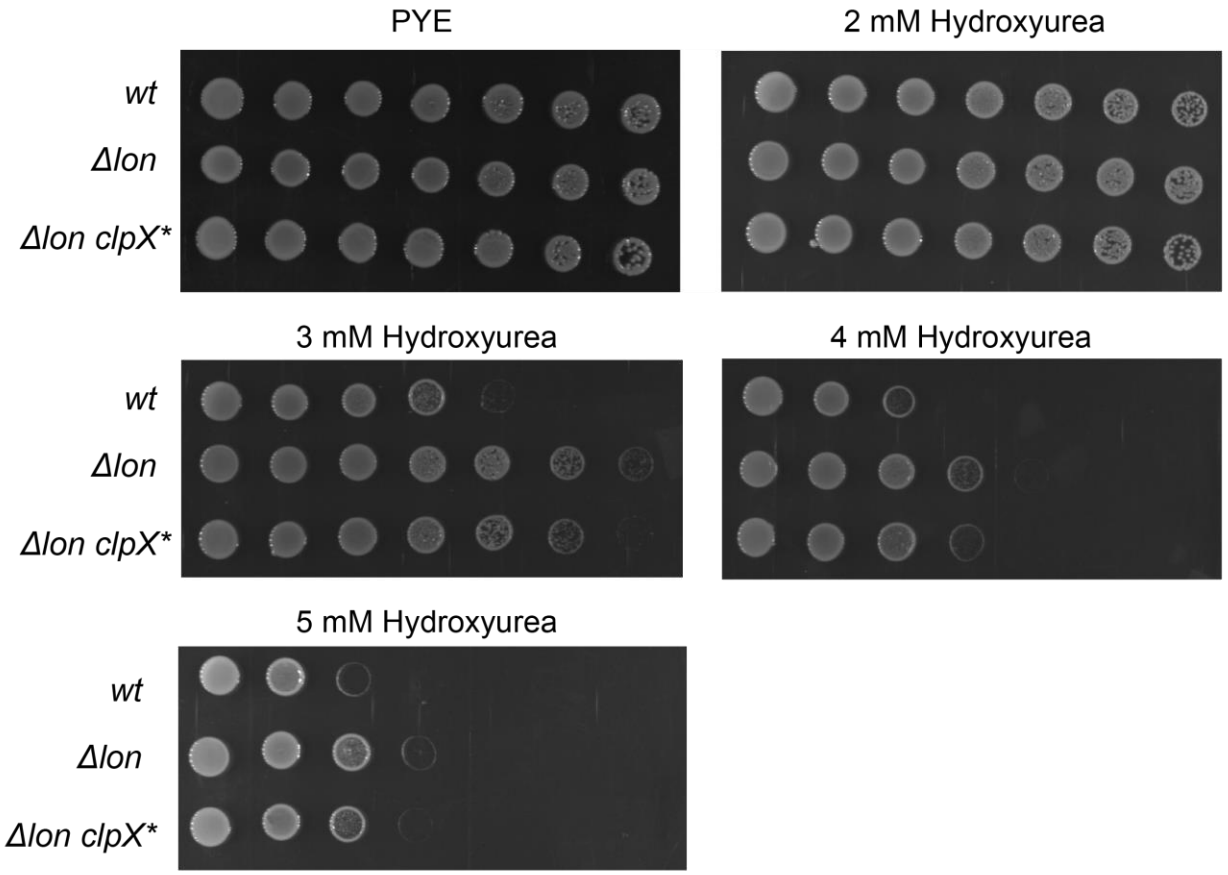

Figure A.1 *⊿lon clpX** cells are less resistant to hydroxyurea than *⊿lon* cells. These are 10-fold serial dilutions on plates supplemented with the indicated concentrations of hydroxyurea. This is interesting because we know that *⊿lon*'s increased resistance to HU is driven by elevated CcrM levels. However, CcrM levels remain elevated in *⊿lon clpX** cells so I'm not sure why we are seeing a difference between *⊿lon* and *⊿lon clpX*.*

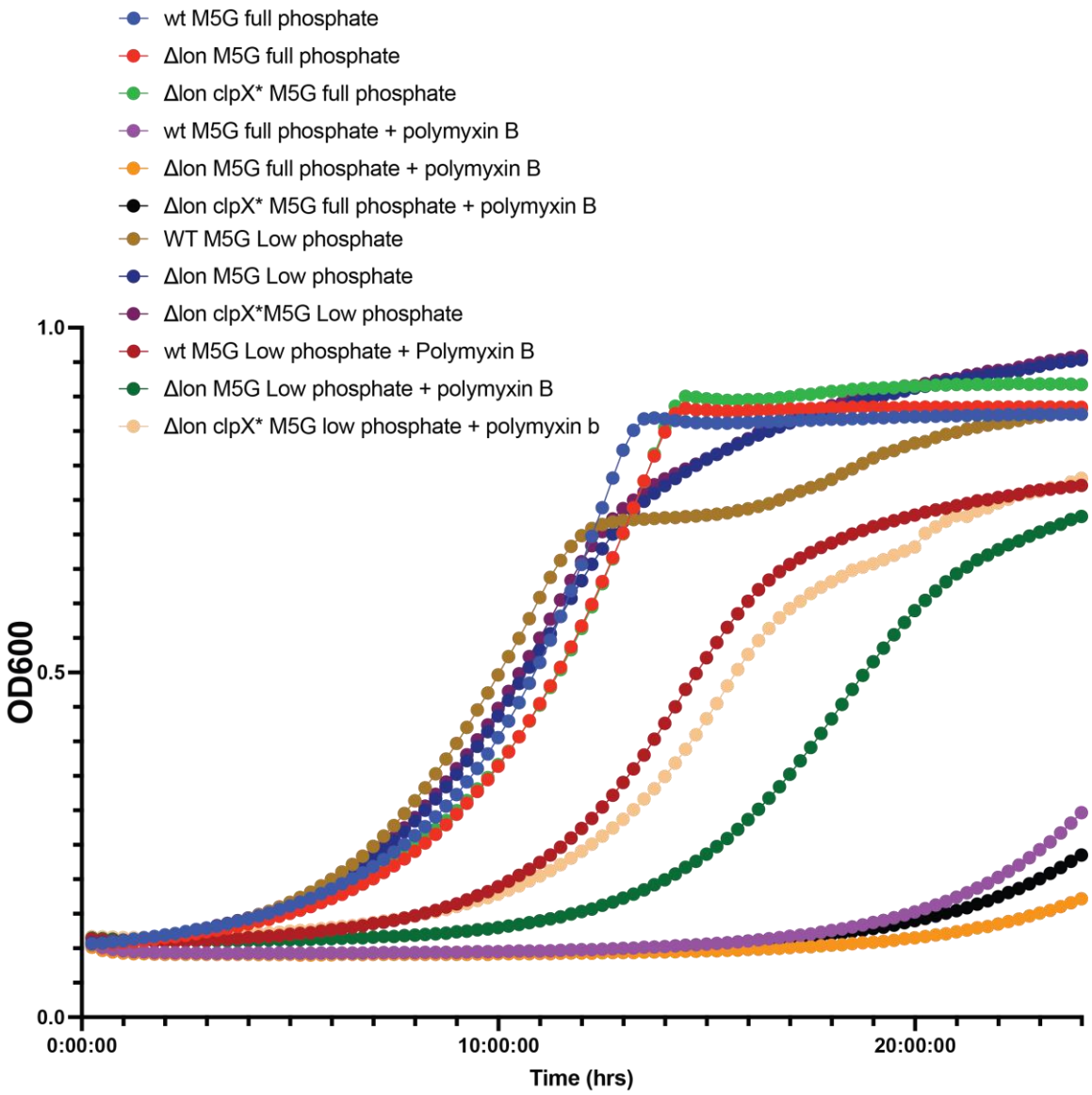

Figure A.2 Growth curves in the presence of polymyxin B in M5G media. I backdiluted cells to an OD600 of 0.1 in M5G media, either in full phosphate (10 mM) or low phosphate. All 3 strains are sensitive to polymyxin B under high phosphate conditions with *Δlon* cells being more sensitive than wt and *Δlon clpX*.* We see that growing these cells in low phosphate makes them more resistant to polymyxin. An interesting hypothesis is that under limiting phosphate conditions which should deplete ATP levels, wildtype ClpX can now degrade

CcbF, resulting in increased resistance in *Δlon* and wildtype cells. However, we are also seeing increased resistance to polymyxin in low phosphate conditions in a *Δlon clpX** background which I would not expect since ClpX* should not degrade CcbF faster when ATP is limited.

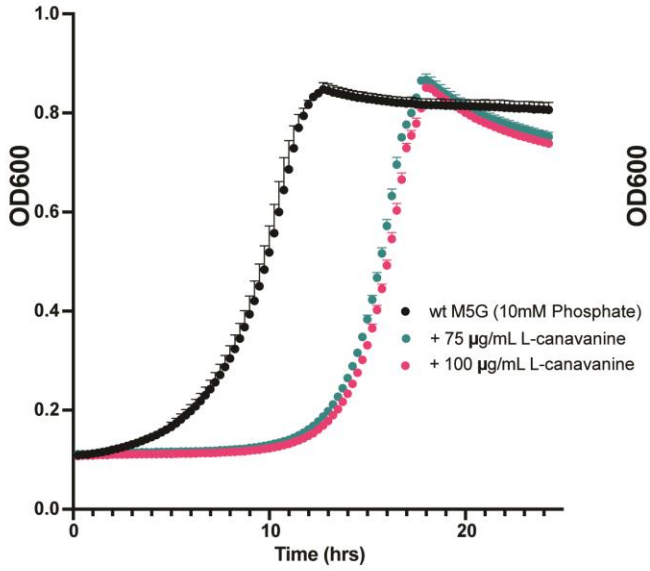

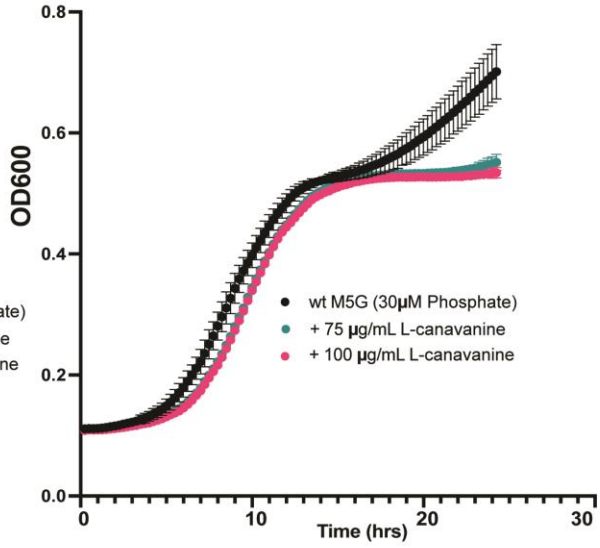

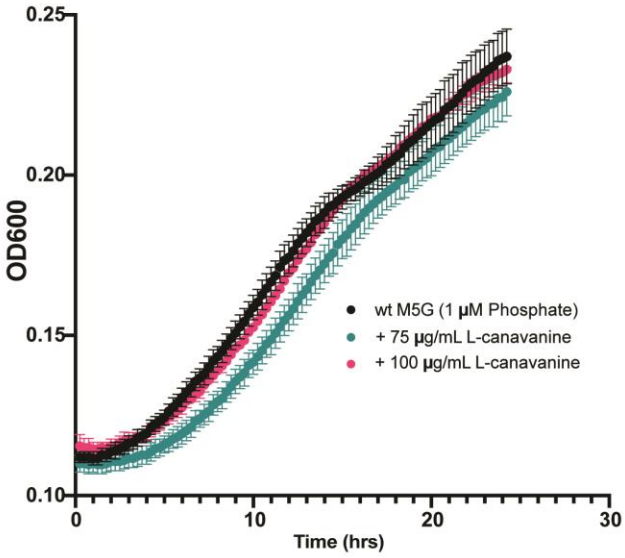

Figure A.3. Wildtype cells are more resistant to L-canavanine under limiting phosphate conditions. I backdiluted wildtype to an OD600 of 0.1 in M5G media, either in 10 mM or 30 uM or 1 uM phosphate.

A.1 Contributions to our understanding of *Vibrio Cholera* Lon

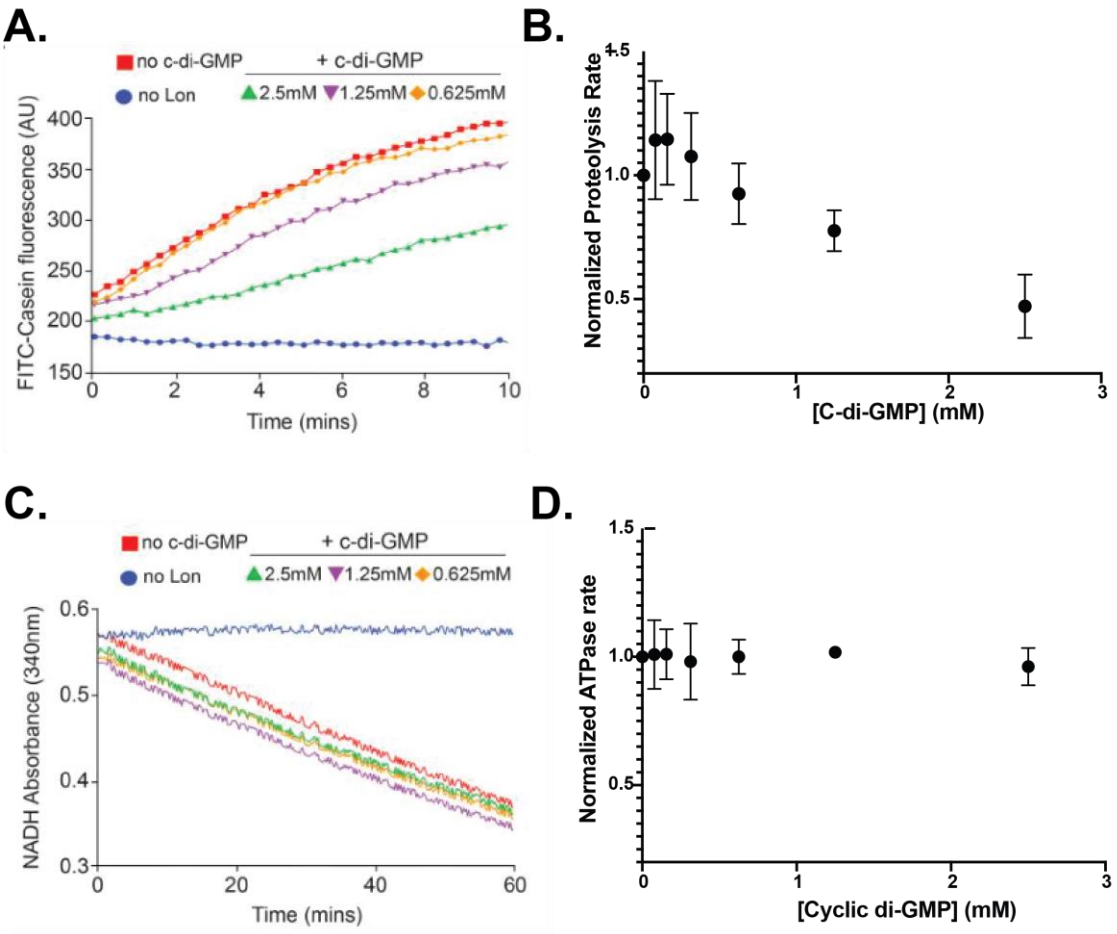

Figure A.4 C-di-GMP inhibits FITC-Casein degradation by LonA but does not affect ATP hydrolysis. This is adapted from Figure 6 from (Joshi *et al.*, 2020). A. FITC-casein degradation assay by purified LonA. B. Initial rate of substrate degradation as a function of c-di-GMP concentration. C. ATP

hydrolysis for LonA alone and in the presence of c-di-GMP. D. Rate of ATP hydrolysis as a function of c-di-GMP concentration.

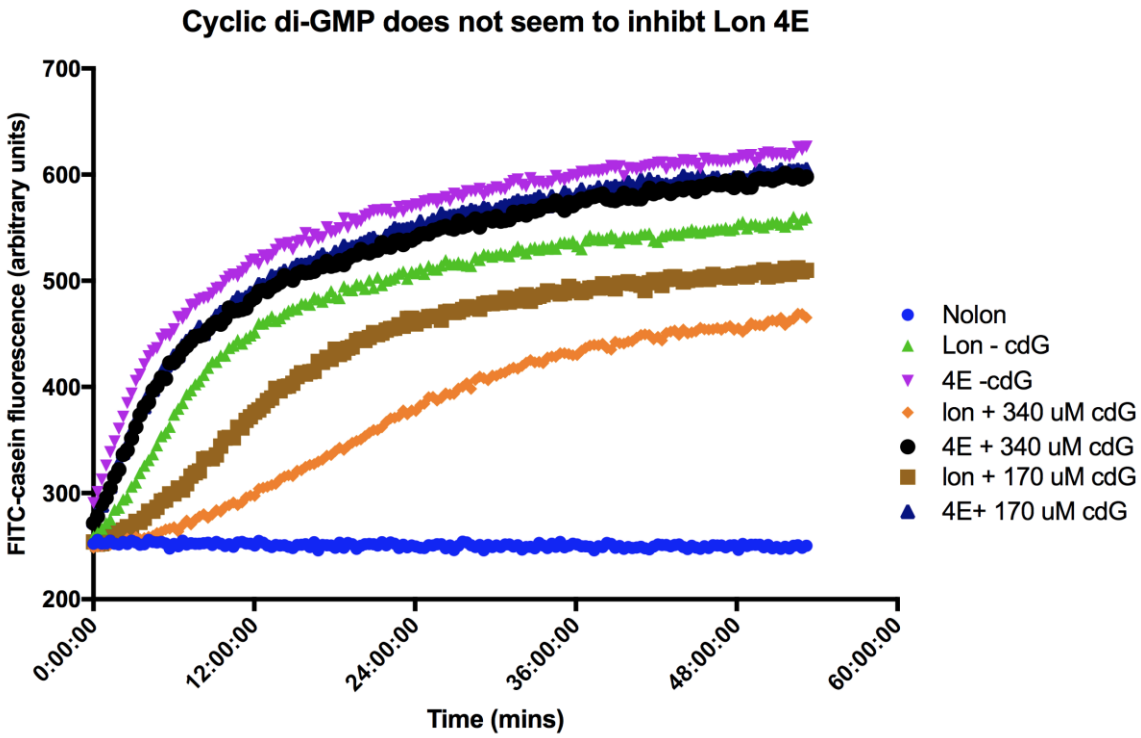

Figure A.5 Cyclic di-GMP inhibits FITC-casein degradation by Caulobacter Lon but has no effect on 4E, a DNA-blind mutant. FITC-Casein degradation assay with Lon and 4E in the absence of cyclic di-GMP and in the presence of 340 uM and 170 uM cyclic di-GMP.

A.2 Purification of VclonA

Grow-up and Induction

- I grew 6 L of cells
- Strain: EPC 1201
- Induction conditions: Grew in LB + AMP until OD was approximately 1.0, took pre-induction sample

- Induced with 0.2% arabinose for 3 hours, took post-induction sample
- Spun cells down at 7000 rpm for 8 minutes (I usually do 5000 rpm for 15 minutes)
- Resuspended pellet in lysis buffer (100 mM potassium phosphate at pH 6.5, 1 mM DTT, 1 mM EDTA, 10% glycerol

Hydroxyapatite Batch Binding

- I measured out approximately 5 mls of HA resin into two 50 ml conicals
- Washed once (filling 50 ml conical) with water, spinning at 2000g for 2 mins
- Washed twice with buffer A (100 mM potassium phosphate at pH 6.5, 1 mM DTT, 1 mM EDTA, 10% glycerol), spinning at 2000g for 2 mins
- After lysing cells with microfluidizer, I spun the cells down at 15,000g for 30 minutes.
- I poured off the supernatant and applied it to the prewashed HA resin
- Let batch bind for 30 minutes to 1 hour

*Resin is very pasty, I just take a serological pipette and manually mix it. I sometimes worry that this is too harsh, but it seems to work out fine.

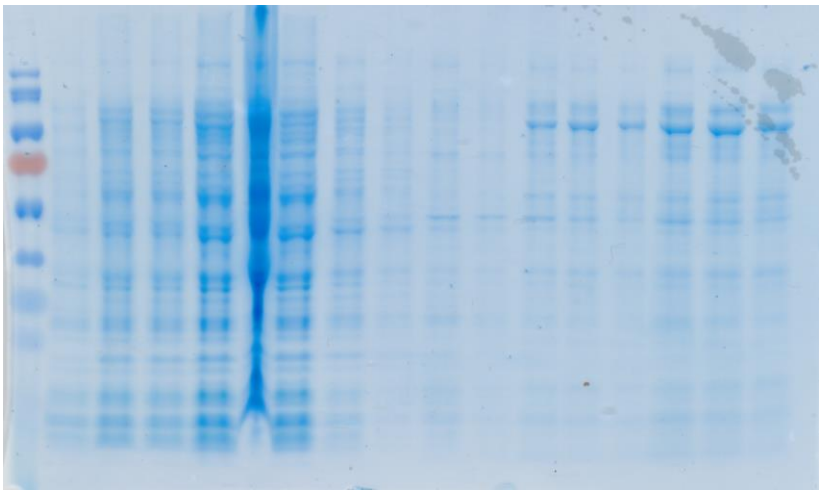

Gel after hydroxyapatite batch binding. Loading: Uninduced, induced 1, induced 2, supernatant, pellet, flowthrough, wash 1 (100 mM, wash 2 (100 mM), wash 3 (200 mM), wash 4 (200 mM), E1-E3 (400 mM), and then last three lanes are larger volume loading.

Washing and Elution

- After batch binding, I spin at 2000g for 10 minutes and collect FT
- Wash with 3CV (15 mls) of buffer A (100 mM potassium phosphate at pH 6.5, 1 mM DTT, 1 mM EDTA, 10% glycerol)
- Again, mix and spin at 2000g for 10 minutes, collect wash
    - I did two washes with buffer A (15 mls each) for each 50 ml conical
- Wash with 3CV (15 mls) of buffer B (200 mM potassium phosphate at pH 6.5, 1 mM DTT, 1 mM EDTA, 10% glycerol)
    - I did two washes with buffer B (15 mls each) for each 50 ml conical
- Elute with 3X, 1 CV (5 mls) of elution buffer (400 mM potassium phosphate at pH 6.5, 1 mM DTT, 1 mM EDTA, 10% glycerol)

- Since I had two 50 ml conicals, I ended up pooling approximately 30 mls of elution
- I filtered the elution using a 0.22 µm and concentrated down to 5 mls using 10 kDA cutoff to run over sephacryl-S200 gel filtration column

S200

- The S200 was equilibrated with 50 mM Tris (pH 8), 1 mM DTT, 1 mM EDTA, and 20% glycerol.
- Activity assays monitoring FITC-Casein degradation
  - 10 ug/ml FITC
  - ATP Regeneration Mix
  - S200 Fractions with Caulobacter Lon as positive control

S200 gel

MonoQ

- MonoQ buffer A: 25 mM Tris pH 8, 50 mM KCl, 10% glycerol, 1 mM DTT
- MonoQ buffer B: 25 mM Tris pH 8, 1M KCl, 20% glycerol, 1 mM DTT
- Activity assays monitoring FITC-Casein degradation

- 10 ug/ml FITC
- ATP Regeneration Mix
- S200 Fractions with Caulobacter Lon as positive control

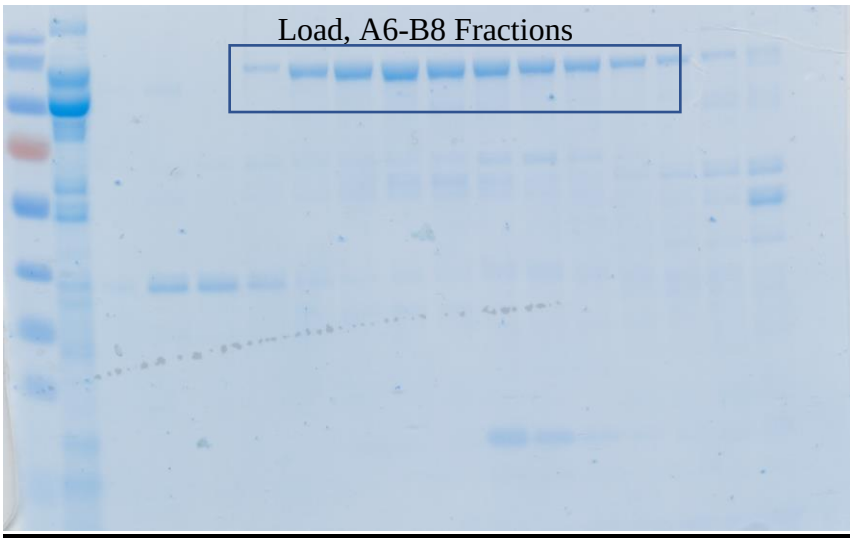

MonoQ gel 1. Note: This is not Lon!!

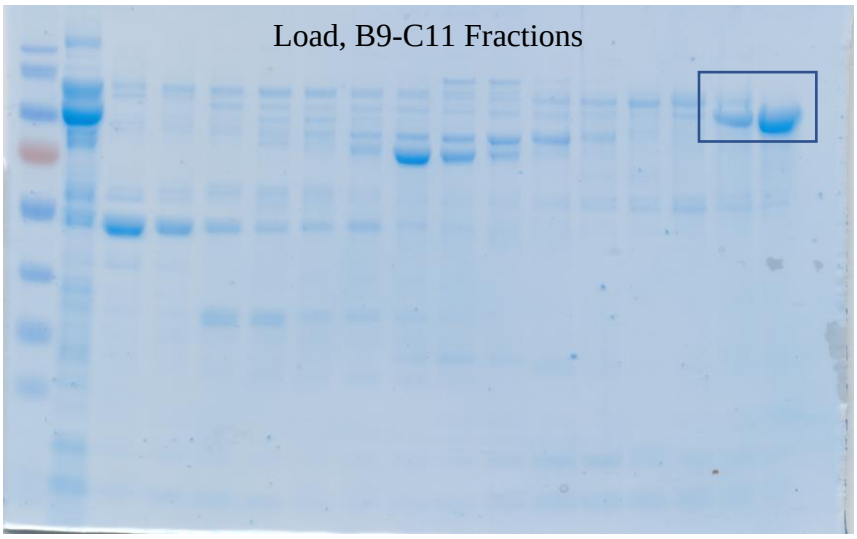

MonoQ gel 2. Note: this is Lon, so I ran other fractions close to C10 and C11

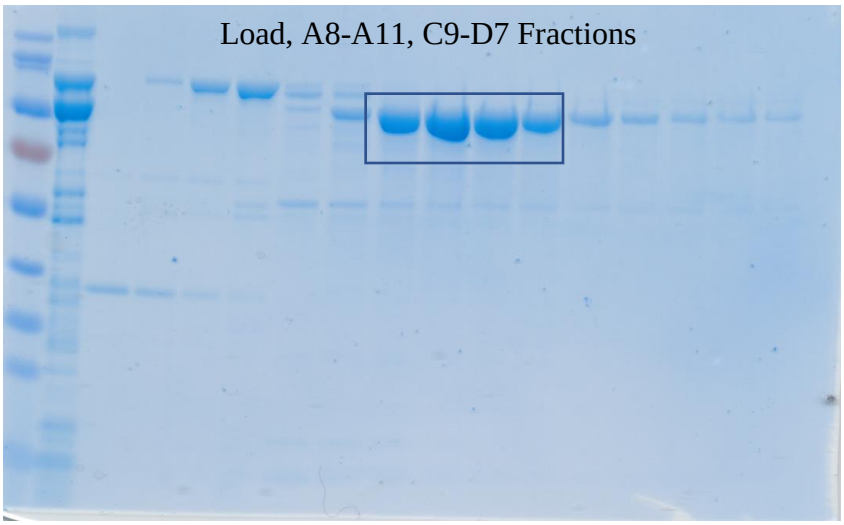

MonoQ gel # 3

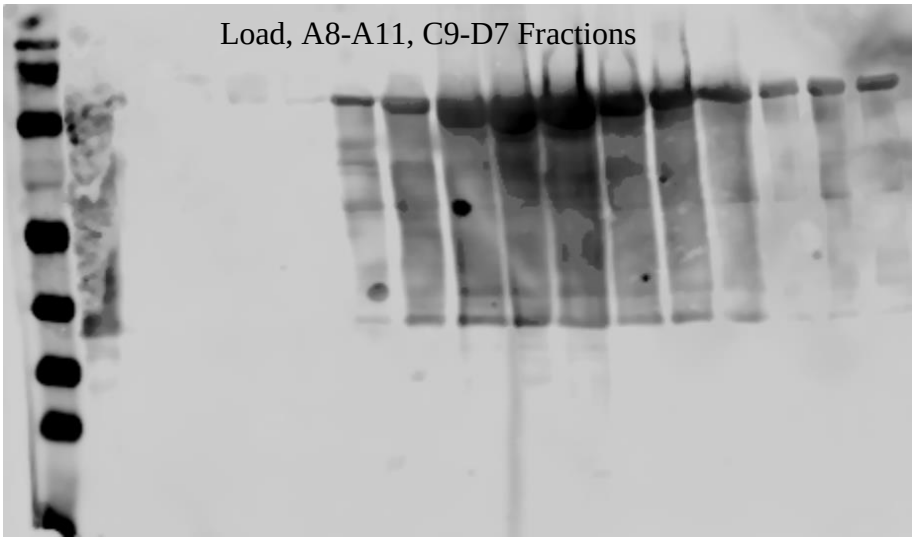

Anti-vclon western blot of the same fraction gel above showing that earlier fractions are not vcLon.

I pooled fractions C11, C12, D1, and D2 (also had FITC-Casein degradation activity)

A.3 Contributions to the Lon degradation project

These figures are adapted from (Barros *et al.*, 2020)

A

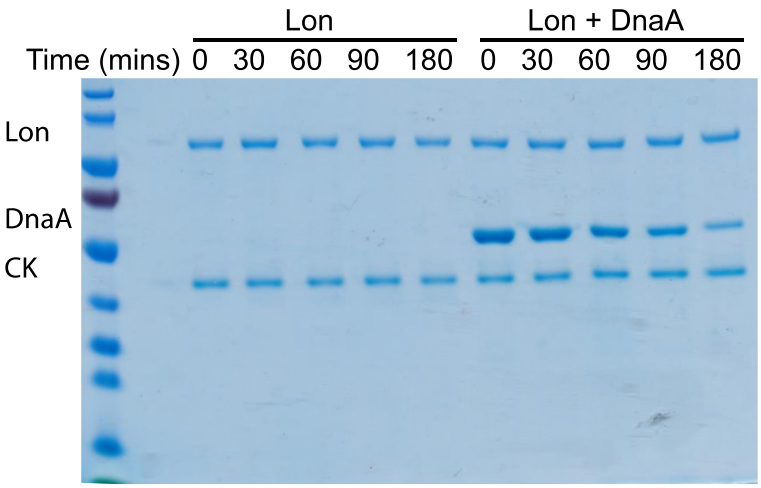

B

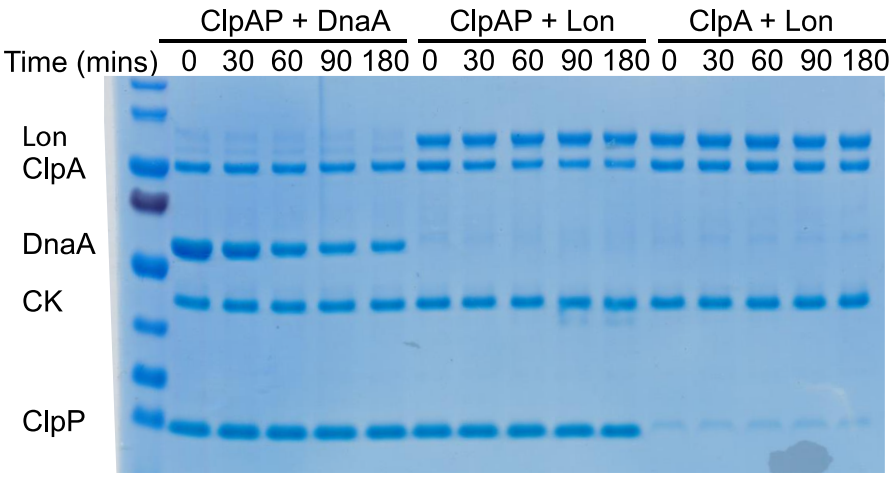

Figure A.6 *In vitro* degradation assays with Lon and/or ClpAP. (A)(B) Degradation assays were performed using the native Lon substrate DnaA to test protease activity, Lon alone, ClpAP with Lon. Reactions consisted of (when listed) 2.5 µM DnaA, 0.1 µM Lon hexamer, 0.2 µM ClpA, 0.4 µM ClpP. All reactions contained 4 mM ATP and a regeneration system.

Figure 2

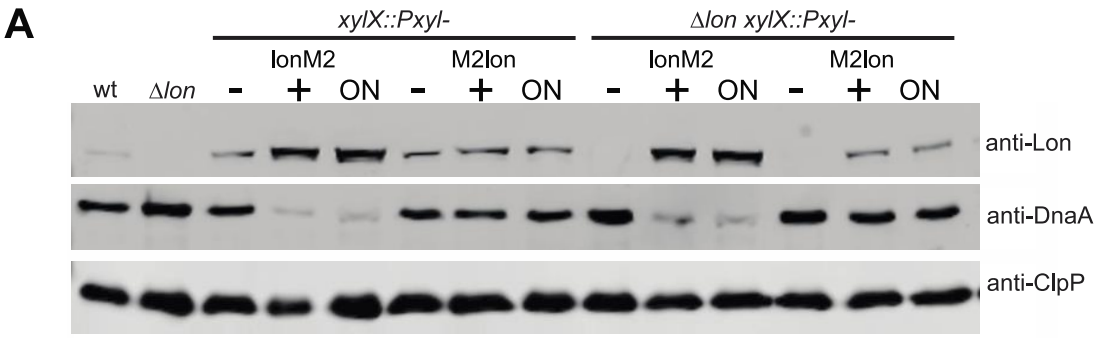

Figure A.7 The C terminus of Lon is necessary for degradation. (A) Steady-state protein levels of Lon, DnaA, and ClpP in wt or *Δlon* strains alone or with Lon, amino terminus M2-FLAG epitope Lon (M2lon), or carboxy terminus M2-FLAG epitope Lon (lonM2). Three conditions were tested; − and + were samples grown overnight under noninducing conditions and then back diluted for outgrowth in either noninducing (−) or inducing (+) medium. ON samples were grown under inducing conditions overnight and back diluted under inducing conditions for outgrowth. In all cases, the outgrowth was done for 6 h. Samples were normalized to starting OD_{600} in lysis buffer prior to Western blot analysis. Cropped images are of Western blots probing for Lon, DnaA, and ClpP.

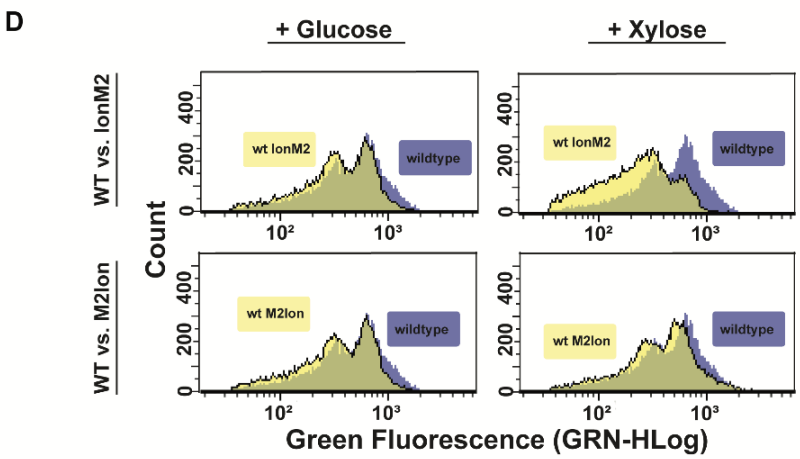

Figure A.8. Induction of *lonM2* from the *xylX* promoter shifts cells toward G_1 **(Adapted from Figure 3D**). Strains grown were overnight in the presence of 0.2% xylose or 0.2% glucose and then treated with rifampin for 3 hours. Cells were fixed and stained with Sytox green before measuring their DNA content by flow cytometry. Because of the rifampin treatment, cells which have initiated replication will complete replication, resulting in two distinct peaks of fluorescence and representing either 1 or 2 chromosomes per cell. The wt cells are represented by purple, and wt strains containing *M2lon* or *lonM2*are in yellow.

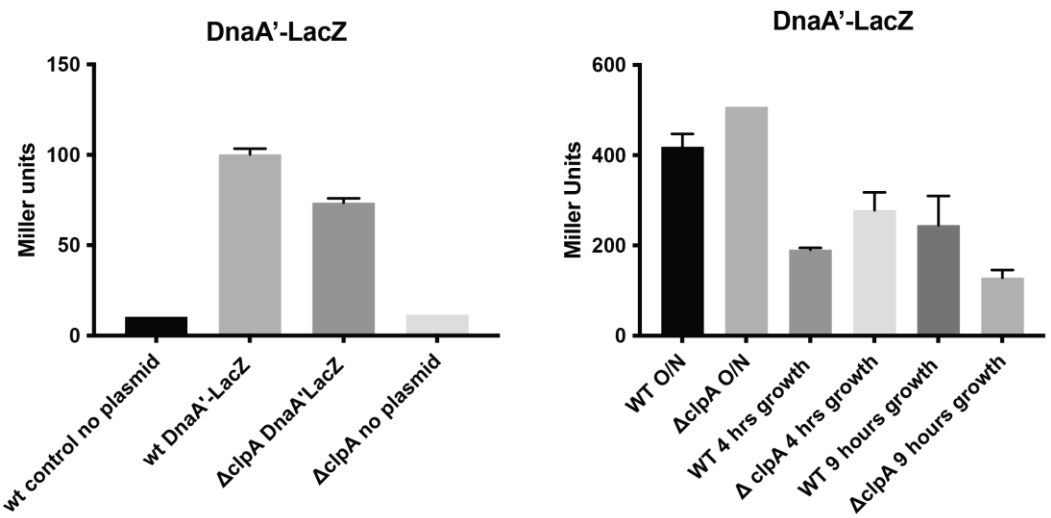

Figure A.9 Miller assays comparing DnaA'-lacZ expression in *wildtype* and *ΔclpA* cells. A. We found that DnaA'-lacZ was less expressed in *ΔclpA* cells in comparison to wildtype cells. B. We noticed a growth-phase specific pattern of expression where DnaA'-lacZ was more highly expressed in *ΔclpA* cells in stationary phase and after 4 hours of outgrowth but expression decreased in *ΔclpA* cells after 9 hours of outgrowth, suggesting DnaA'-lacZ expression drops in *ΔclpA*.

A.4 Additional Data

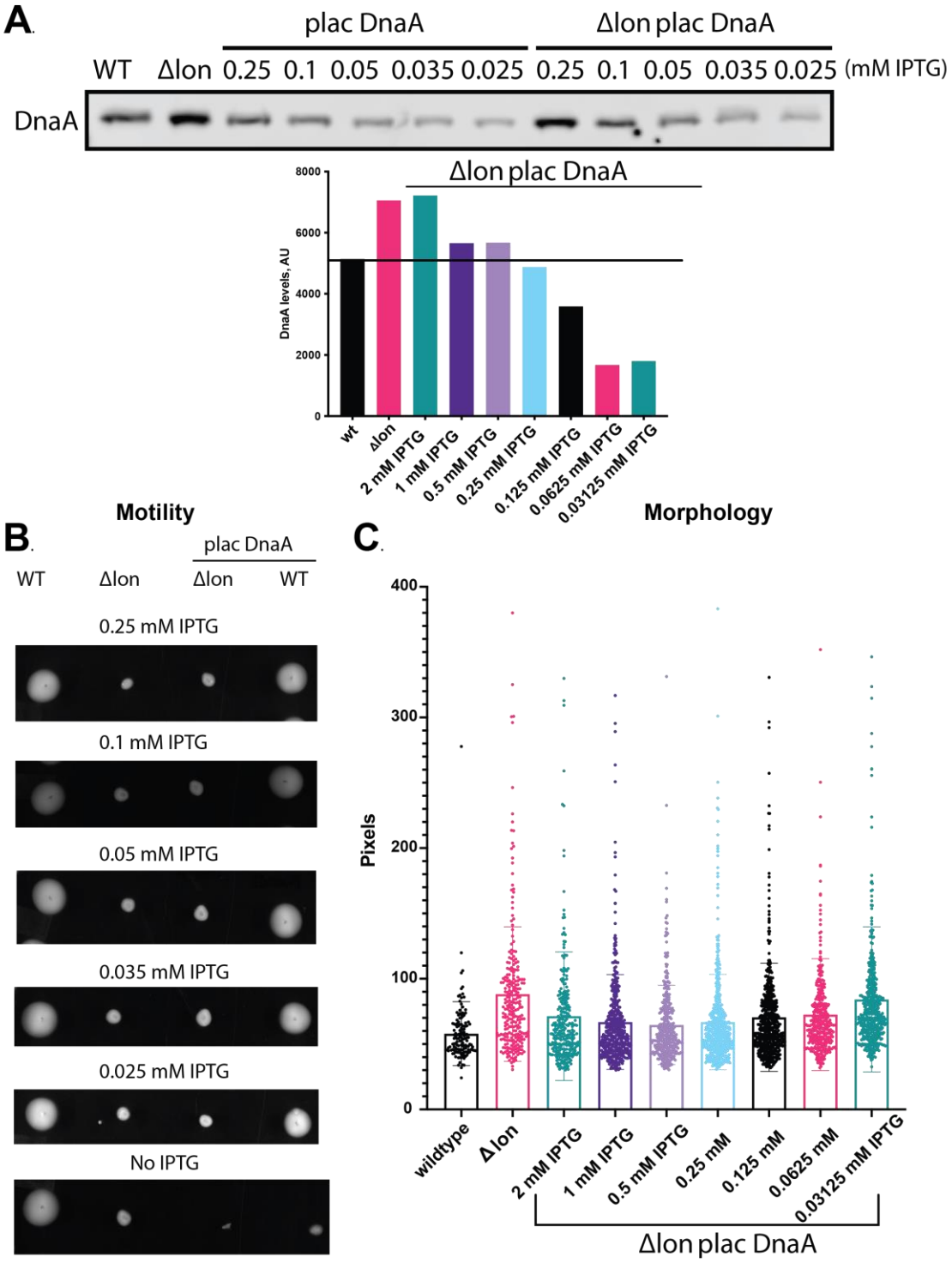

Figure A.10 Depleting DnaA levels in *Δlon* is not sufficient to restore motility or morphology. A. western blot showing DnaA levels in a DnaA

depletable strain in a *Δlon* background. DnaA levels seem to be matched at 0.25 mM IPTG. B. Motility in 0.3% agar. Motility is not restored at any IPTG concentration suggesting that elevated DnaA levels are not responsible for the loss of motility in a *Δlon* strain. C. Morphology of *wildtype* and *Δlon* and *Δlon plac DnaA* strain at various IPTG concentrations. At high IPTG concentrations which would lead to high DnaA levels (like a Δlon), *Δlon plac DnaA* are less filamentous than Δlon cells. However, this suggests that elevated DnaA levels are not the sole drivers of filamentation in a *Δlon* because then the highest concentrations of IPTG in *Δlon plac DnaA* would be as filamentous as *Δlon*.

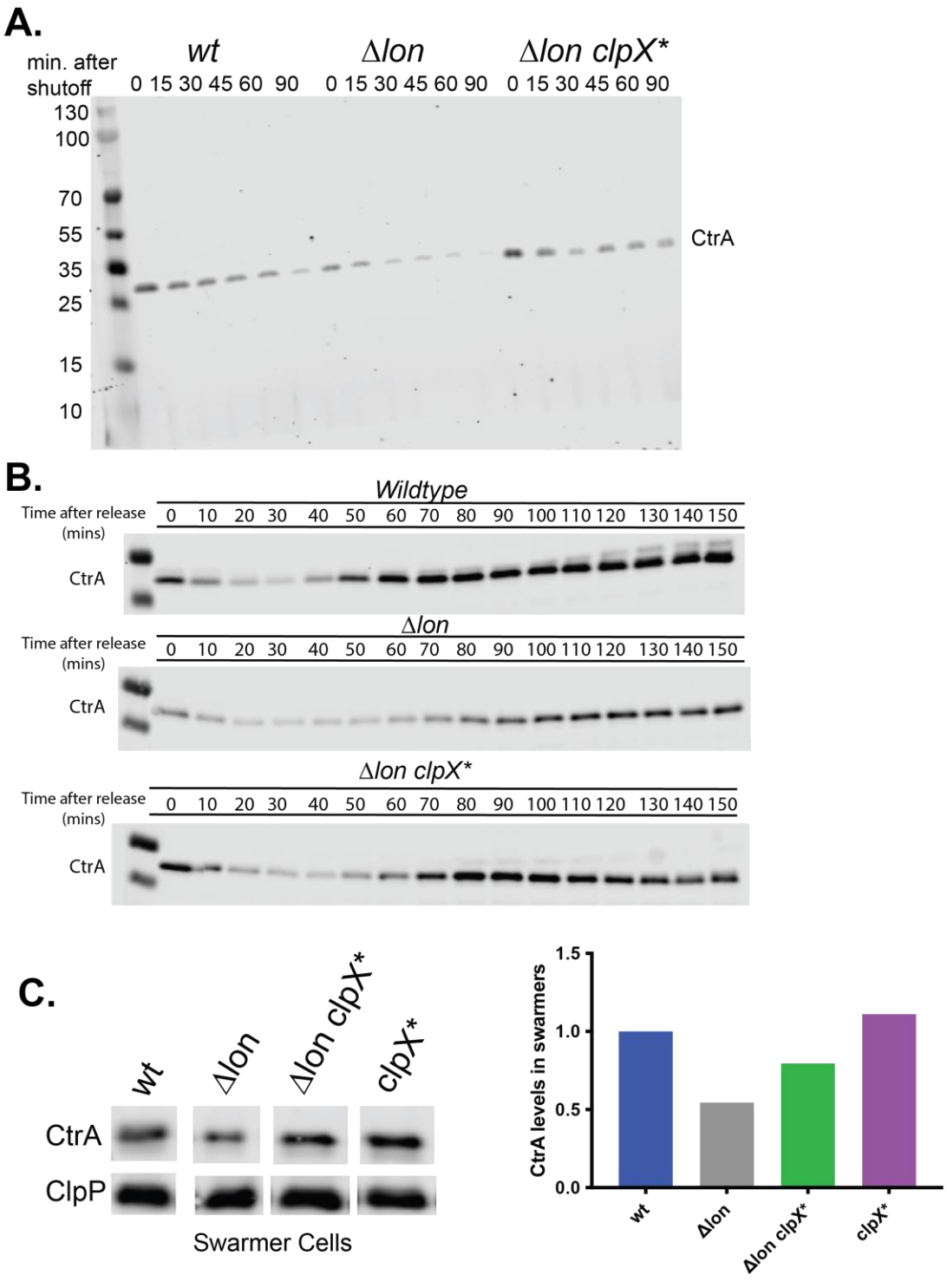

Figure A.11 CtrA is misregulated in a *Δlon*. A. Chloramphenicol shutoff showing DnaA is degraded faster in a *Δlon* strain compared to wildtype and *Δlon clpX**. B. Synchrony in *wt*, *Δlon*, and *Δlon clpX**. *Δlon* swarmer (t=0) cells seem to

have reduced CtrA levels in comparison to *wildtype* and *Δlon clpX** cells. In addition, *Δlon* cells seem to have delayed CtrA accumulation in comparison to *wildtype* cells. C. Steady state levels in swarmer cells. *Δlon* cells have reduced CtrA levels.

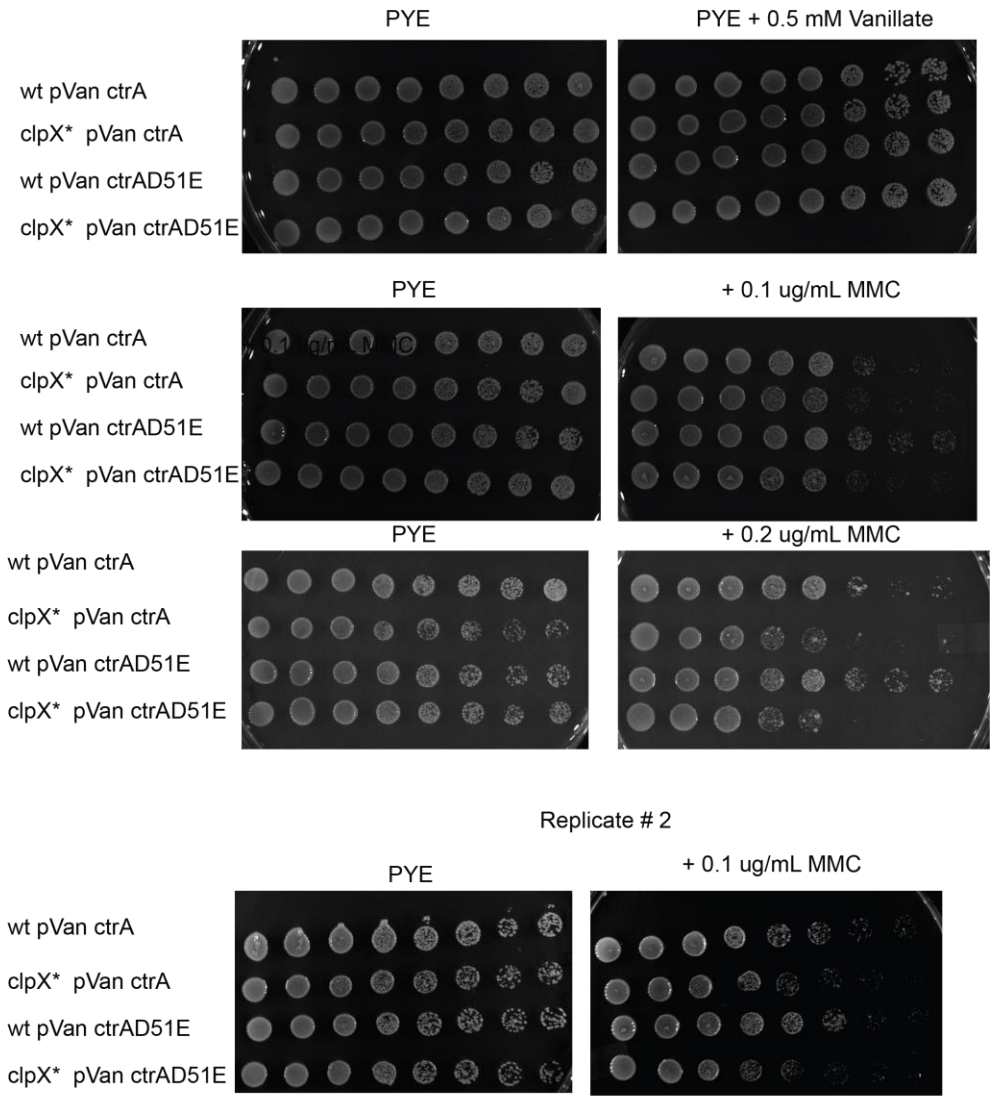

Figure A.12 MMC spot assays of *wildtype* and clpX* cells overexpressing CtrA and CtrAD51E. These are 10-fold serial dilutions of wildtype and clpX*

cells with pVan ctrA and pVan ctrAD51E (phosphomimetic) grown on PYE as a control and in the presence of MMC.

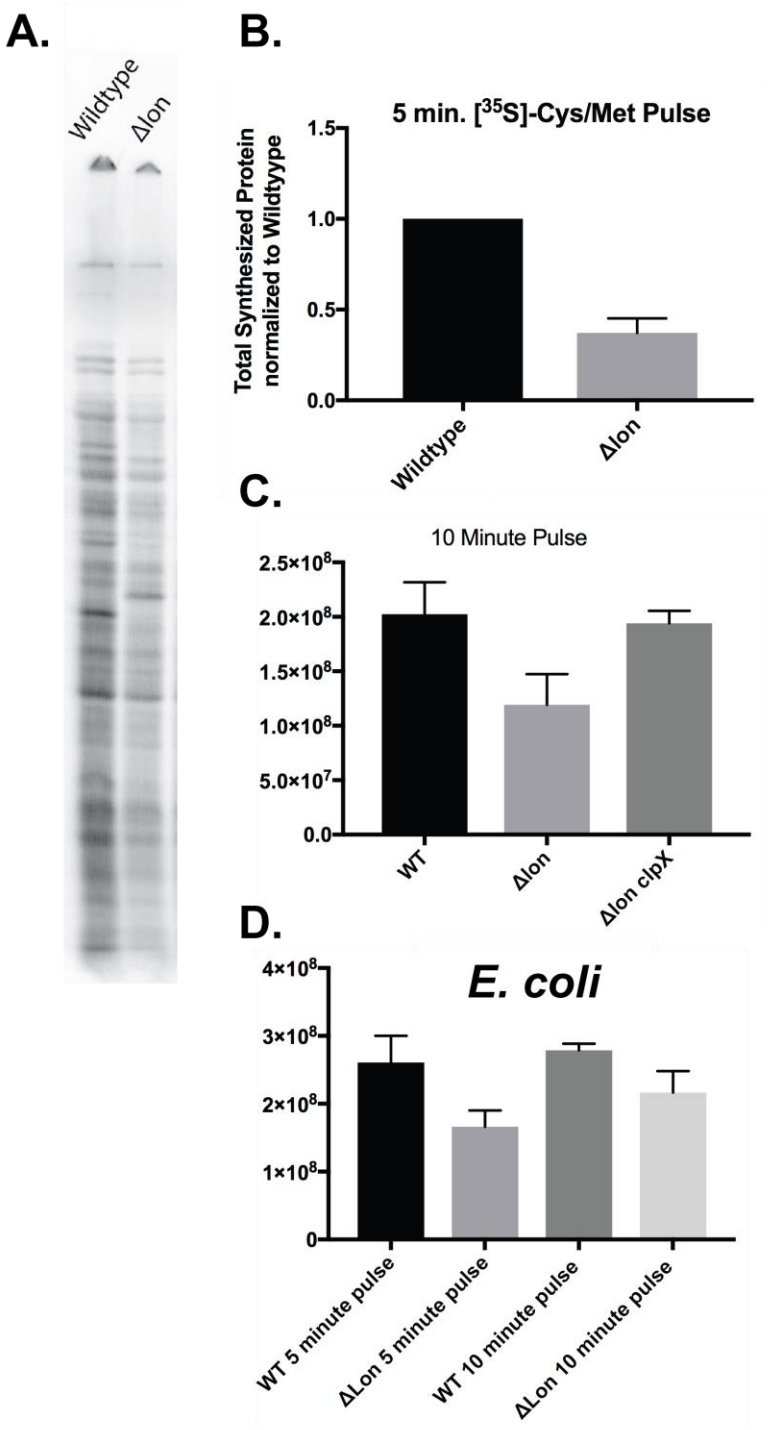

Figure A.13 ^{35}S-[Cys-Met] Pulse experiments. A. Logarithmically growing *wildtype* and *⊿lon* cells were pulsed for 5 and 10 minutes with [35S]-Cys/Met. The cells were lysed and samples were run on an SDS-page gel and imaged by phosphorimager. Total protein was quantified in each sample. B. The average of three biological triplicates is shown for the 5-minute pulse, error bars represent standard deviation. *Wildtype* (black) has higher translational efficiency than *⊿lon* (grey). C. The average of three biological triplicates is shown for the 10-minute pulse, error bars represent standard deviation. *Wildtype* (black) has higher translational efficiency than *⊿lon* (light grey) and translational efficiency is restored in *⊿lon clpX** (dark grey). D. *E. coli ⊿lon* cells have lower translational efficiency than wildtype *E. coli* cells suggesting that the link between Lon and translation is conserved. **These experiments were graciously completed by Ben Adams from the Hebert lab.**

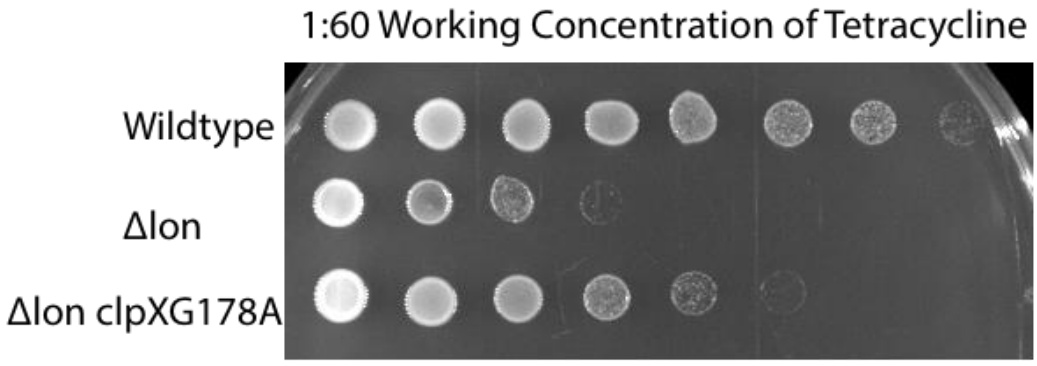

Figure A.14 *⊿lon* cells are sensitive to tetracycline. Logarithmically growing *wildtype*, *⊿lon*, and *⊿lon clpX** (clpXG178A) were normalized by OD600 and 10-fold serial dilutions were plated on PYE and PYE tetracycline plates. *Wildtype*

and *⊿lon* are equally viable when grown on PYE. However, ΔLon is more susceptible to tetracycline in comparison to *wildtype* and this sensitivity is suppressed in a *⊿lon clpX** strain.

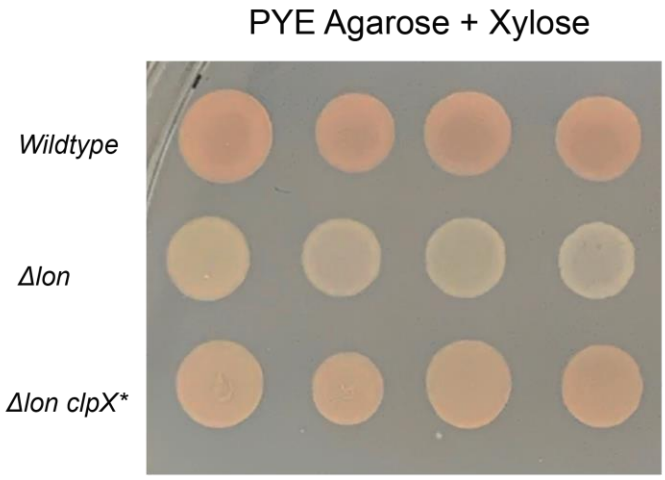

Figure A.15 *ClpX** **restores pink coloration to *⊿lon* cells on PYE agarose supplemented with xylose**. A previous study has determined that FixT is a Lon substrate in *Caulobacter* (Stein, Fiebig and Crosson, 2020). In our lab, Kethney Massenat previously showed that deleting FixT in a ΔLon background restores the pink phenotype. This suggests that ClpX* might degrade FixT faster than wildtype ClpX which would lower FixT levels in a *⊿lon clpX** strain and restore the pink phenotype.

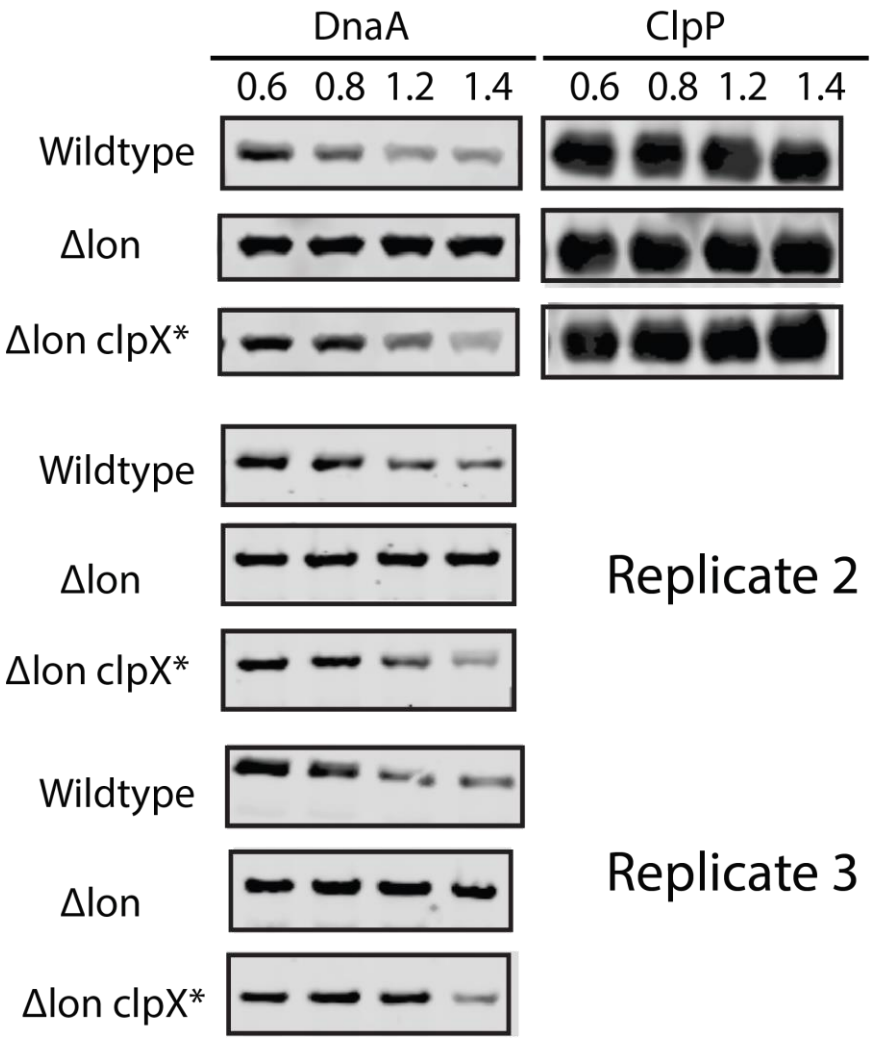

Figure A.16 DnaA steady state levels as a function of OD600. The indicated strains were backdluted to an OD600 of 0.1 in triplicate. Samples were withdrawn at the indicated OD600s. The samples were lysed and resuspended in 2X SDS dye. Westerns were probed by anti-DnaA and anti-ClpP antibodies. As expected, wildtype cells decreased DnaA levels as the OD600 increased which is consistent with DnaA levels dropping as cells enter stationary phase. We did not observe this trend for *Δlon* cells. However, *Δlon clpX** cells showed a similar pattern to *wildtype* cells.

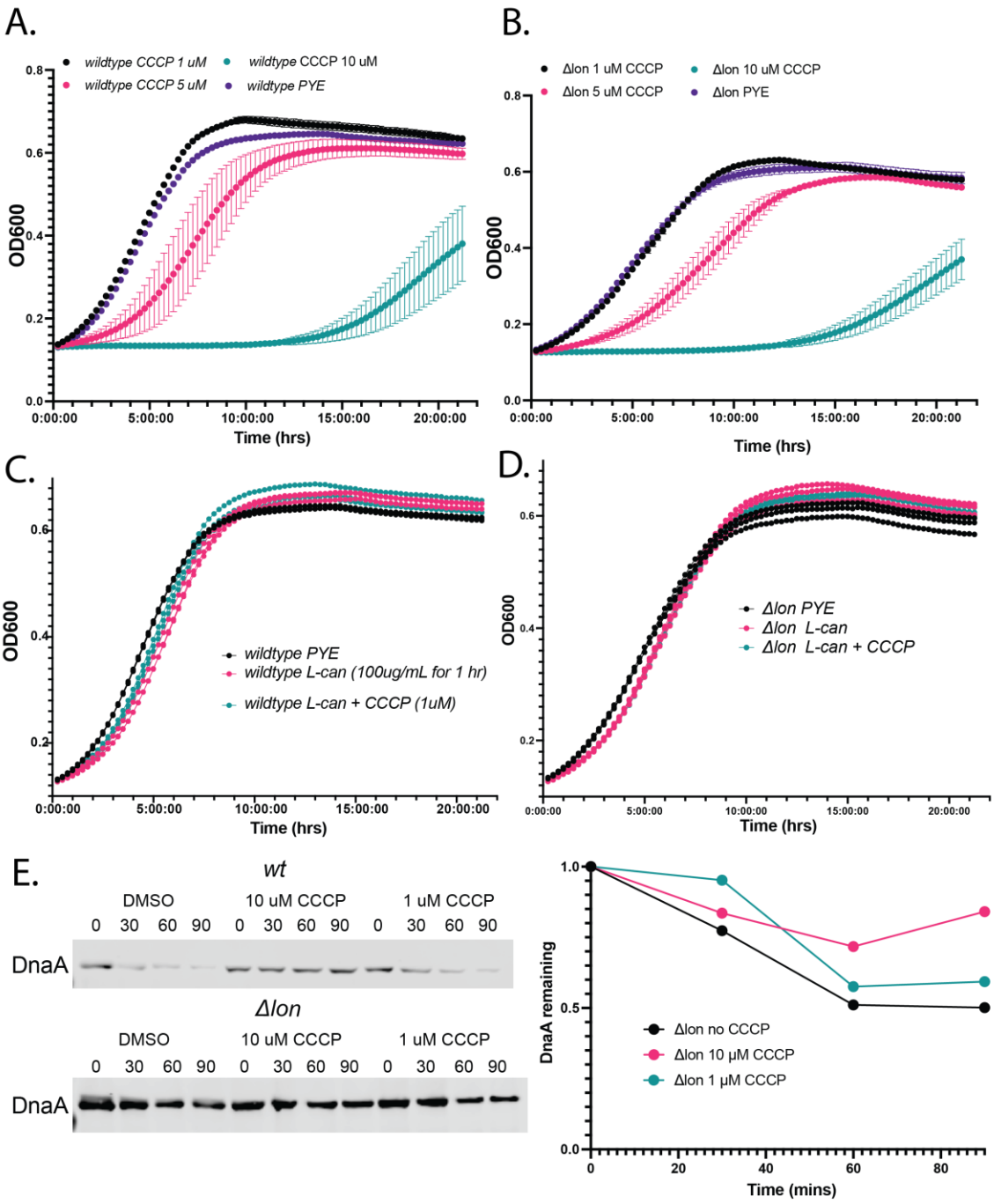

Figure A.17 Treating cells with uncoupling agent, carbonyl cyanide m-chlorophenylhydrazine (CCCP). A-B Wildtype and *Δlon* cells were grown in PYE and backdiluted to an OD600 of 0.1 in PYE or PYE supplemented with either 1 uM CCCP, 5 uM CCCP, or 10 uM CCCP. We observed that 1 uM CCCP

did not have an effect on the growth of wildtype or *Δlon* cells but we started to see an impact on growth when using 5 uM CCCP and 10 uM CCCP. **C-D.** Wildtype and *Δlon* cells were grown in PYE and backdiluted to an OD600 of 0.1 in PYE or PYE supplemented with 1 uM CCCP. Cells treated with 100ug/mL L-can were treated in liquid culture for an hour before either being backdiluted into PYE alone or PYE plus 1 uM CCCP. The goal of this experiment is to hit cells with L-canavanine to create a burst of misfolded proteins and the idea is to deplete ATP levels with CCCP which should activate ClpX to start degrading these misfolded proteins so we should observe that cells grown in CCCP + L-can do better than cells treated with L-can alone. However, we did not see that the L-can on its own had an effect so this would be worth repeating with various concentrations of L-canavanine. Although we do see that the CCCP + L-canavanine cells might be slightly outperforming the L-canavanine alone cells, this could be also do to the slightly better growth we see with 1 uM CCCP in A and B. **E**. Monitoring DnaA degradation *in vivo* in the presence of CCCP. The goal of this experiment was to validate our in vitro findings that DnaA is degraded faster by wildtype ClpX under limiting ATP. However, we observed that 10 uM CCCP stabilized DnaA in a wt and we still observed some stabilization in the 1 uM CCCP condition. In a *Δlon,* when we quantify DnaA degradation, we see that the 1 uM CCCP also leads to a slight stabilization of DnaA.

A.

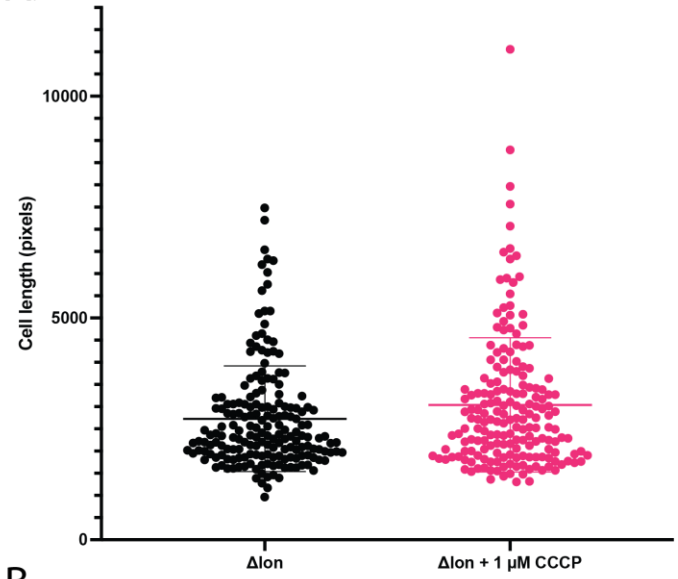

B.

Before CCCP Addition		After 30 min CCCP addition		After end of shutoff (2 hr time pts)	
ATP standards (uM)	Luminescence	ATP standards (uM)	Luminescence	ATP standards (uM)	Luminescence
10	317	10	344	10	313
1	68.8	1	54	1	58.8
0.1	8.49	0.1	10.6	0.1	7.05
0.01	1.16	0.01	1.44	0.01	0.76
0.001	0.13	0.001	0.26	0.001	0.08
0.0001	0.13	0.0001	0.09	0.0001	0.08
0.00001	0.05	Buffer (M2G)	0.1	Buffer (M2G)	0.39
0.000001	0.02				
0.0000001	0.01				
0.00000001	0.06				
WT - cccp	26	WT - cccp	36.2	WT - cccp	72.7
WT + cccp	24.9	WT + cccp	13.6	WT + cccp	2.46
dlon - cccp	15.3	dlon - cccp	21.8	dlon - cccp	35
dlon + cccp	15.1	dlon + cccp	4.84	dlon + cccp	1.57
dlon dclpA - cccp	18.7	dlon dclpA - cccp	29	dlon dclpA - cccp	41.7
dlon dclpA + cccp	21.2	dlon dclpA + cccp	14.1	dlon dclpA + cccp	1.78
raw data in 1000s					
	Ratio -cccp/+cccp		Ratio -cccp/+cccp		Ratio -cccp/+cccp
wt	1.044176707		2.661764706		29.55284553
dlon	1.013245033		4.504132231		22.29299363
dlon dclpA	0.882075472		2.056737589		23.42696629

Figure A.18 Morphology in the presence of CCCP. A. *Δlon* cells were backdiluted into PYE and in PYE plus 1 uM CCCP. Cells were imaged in stationary phase to allow them the opportunity to undergo many doublings. The purpose of this experiment was to see if addition of CCCP could suppress filamentation in a *Δlon*. However, *Δlon* cells grown in the presence of CCCP were

more filamentous than *Δlon* cells in PYE. **B**. CCCP depletes ATP levels as measured by the Bactiter Glo assay.

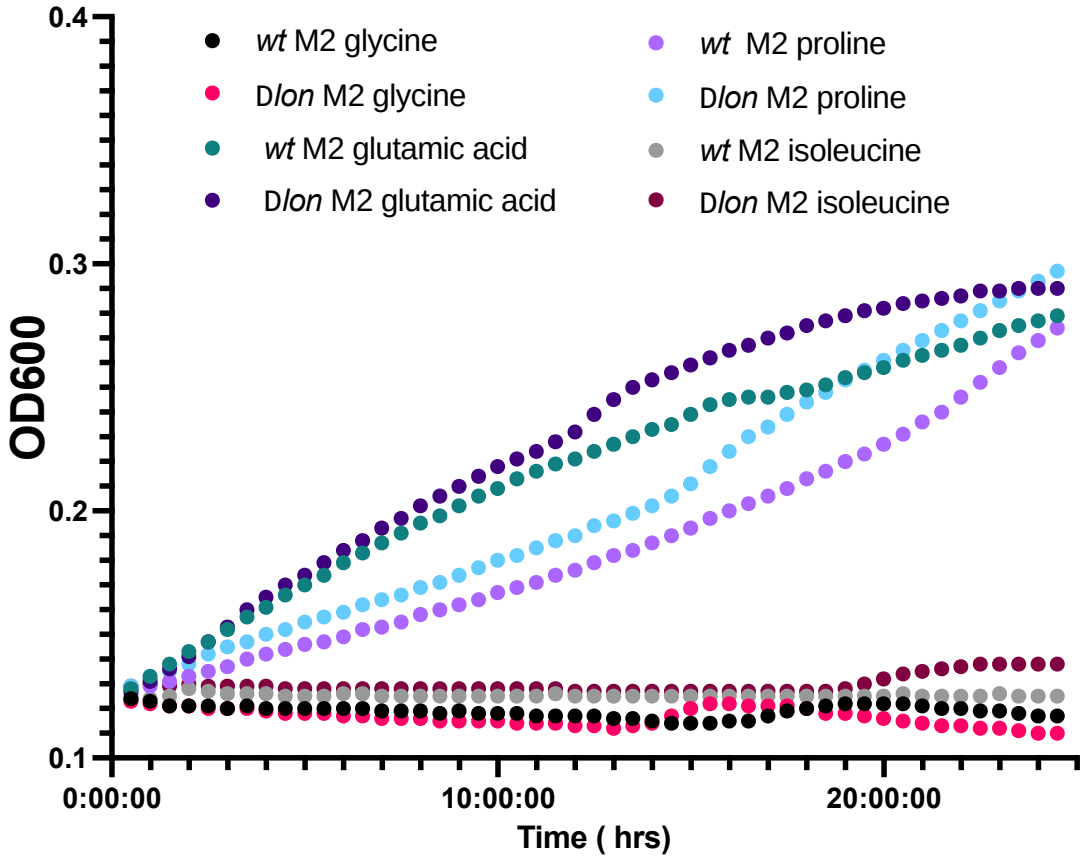

Figure A.19 Growth curves in the presence of amino acids as a sugar source. I have previously observed that *Δlon* cells grow better in minimal media supplemented with glucose (see chapter 4). Here instead of using 0.2% glucose, I supplemented M2 media with different amino acids. In this experiment, we see *Δlon* cells growing better than wildtype in the presence of M2 glutamic acid and M2 proline.

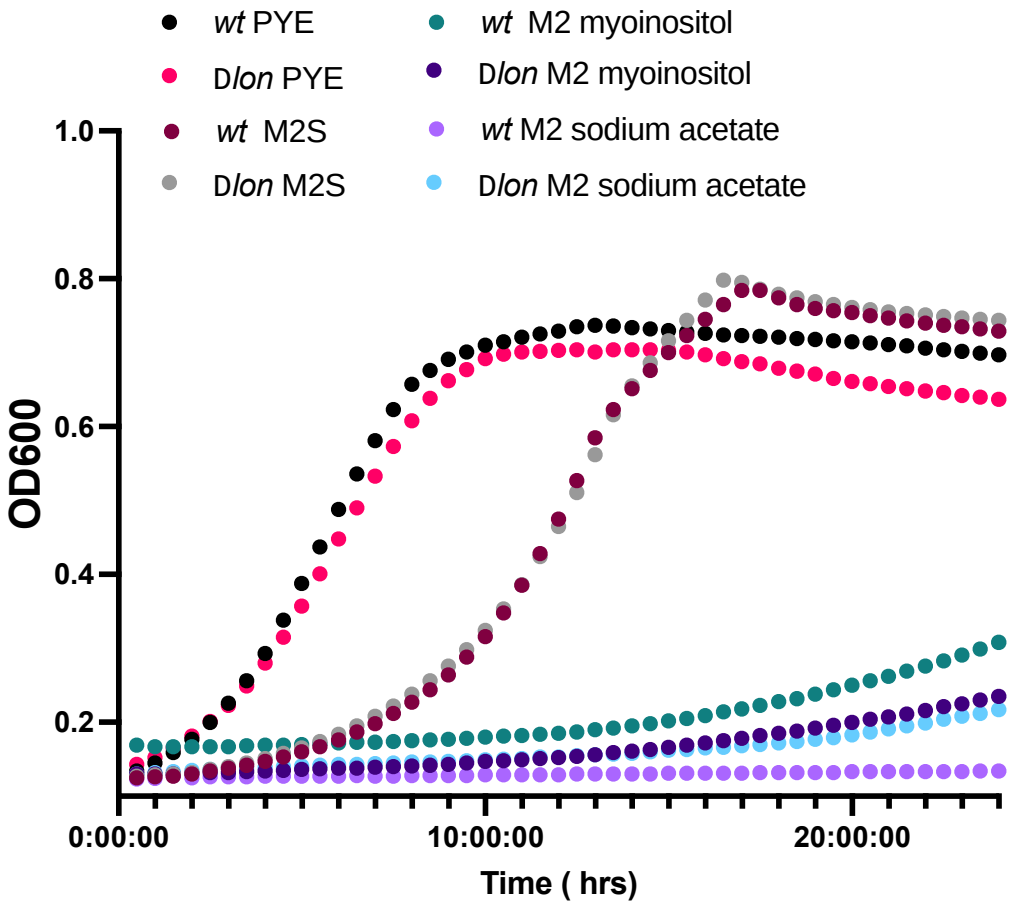

Figure A.20 Growth curves in the presence of alternative sugar sources.

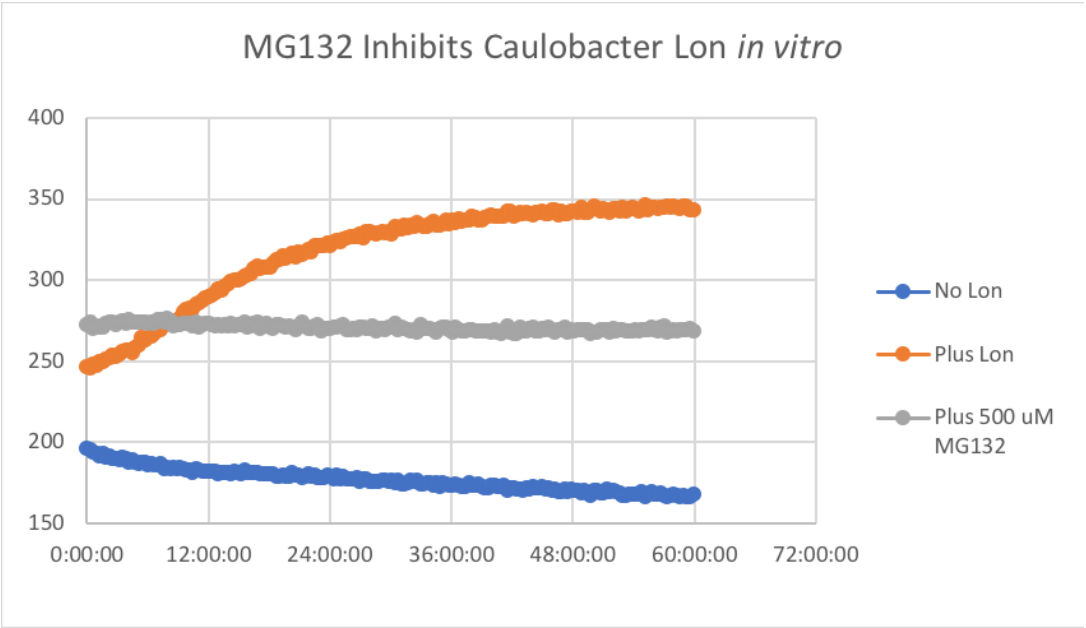

Figure A.21 MG132 inhibits *Caulobacter* Lon activity *in vitro*. FITC-Casein degradation assay in the absence of Lon, presence of Lon, and presence of Lon and 500 uM MG132.

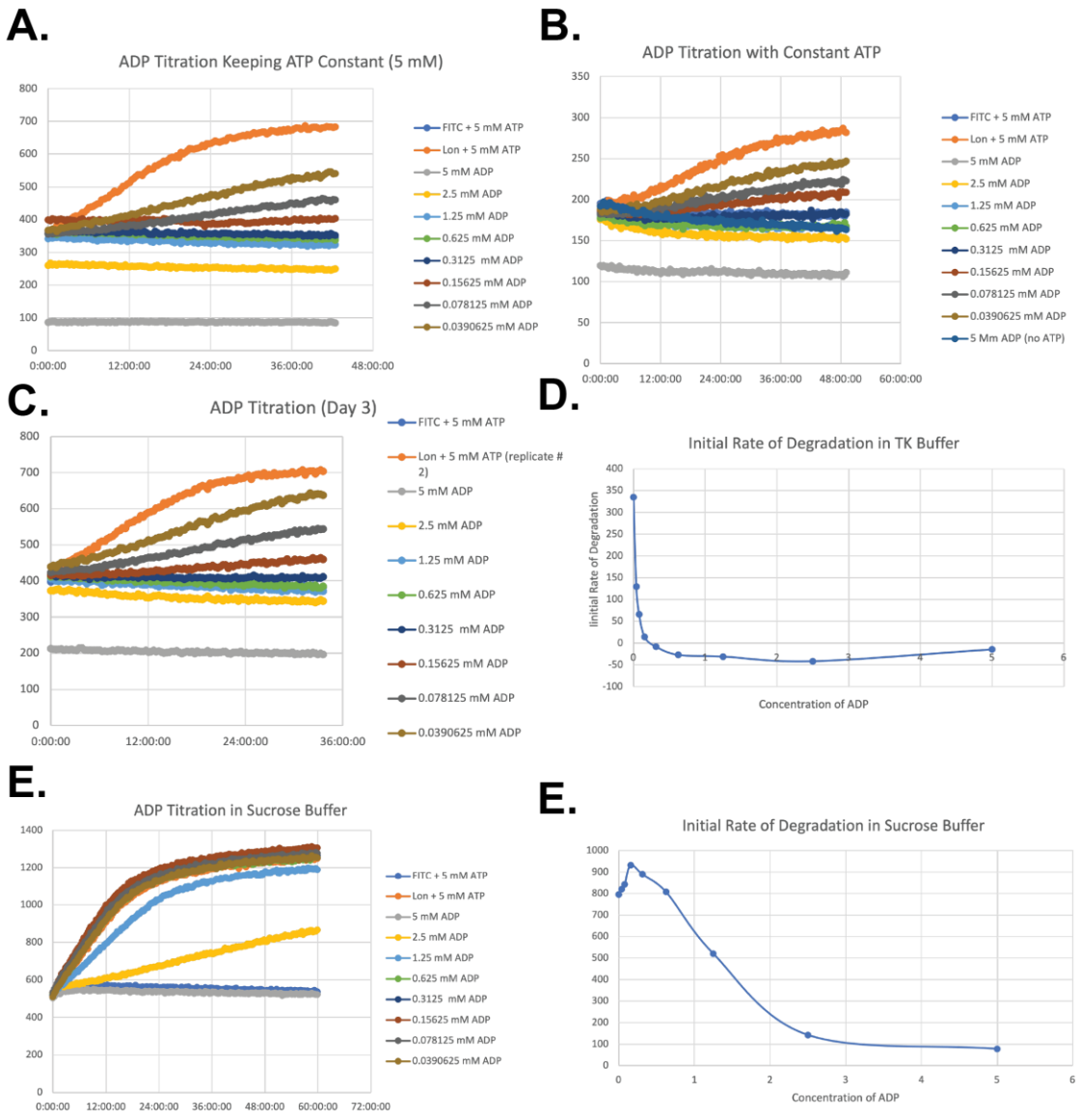

Figure A.22 The *Caulobacter* Lon protease is sensitive to ADP inhibition. A-C Titrating ADP while keeping ATP constant in TK buffer**.** Monitoring FITC-

Casein degradation. **D.** Plot of initial rate of FITC-Casein degradation as a function of concentration of ADP (mM). **E.** Titrating ADP while keeping ATP constant in Sucrose buffer**. E.** Plot of initial rate of FITC-Casein degradation as a function of concentration of ADP (mM) in sucrose buffer. Lon is less susceptible to ADP inhibition in sucrose buffer.

A.5 AHA labeling and Click Chemistry Protocol

Pulsing cells with AHA

1) Resuspend AHA probe in DMSO

- 100 mg in 1 mL DMSO so stock is 100 mg/mL or 554 mM
- Store aliquots at -20 degree Celsius

2) Grow cells to mid exponential phase in M2G

3) Dilute AHA probe 1:1000 into cells so 0.55mM final so added 20ul to 20 mL cultures and let it incubate for 60 minutes

4) Spun down AHA-treated cells at 6000g for 5 minutes then washed three times in cold Phosphate BS.

5) Freeze pellets at -80 °C until ready for next steps

6) Thaw AHA-labeled cells and resuspend in lysis buffer (50 mM Tris-HCl pH 8.0, 5% glycerol, 0.5% SDS, 1 mM PMSF).

7) Sonicate

- 40 Amplitude
- 10 second pulses for 1 minute
- After every 10 second pulse, put back on ice briefly

8) Spin to clear lysate at max speed at 4 °C for 20 minutes

9) Transfer supernatant to new tube

Copper Catalyzed Rxn

Reagents

CuSO4: Made 50 mM stock in water (make fresh)

Sodium ascorbate: 12mg/mL stock in water (60.6 uM) (make fresh)

AF 488 Alkyne: 1 mg/mL in water (1.3mM) (stored aliquots at -20 °C)

TBTA (borrowed from Hebert lab, they make it at 25mg/mL in DMSO and store at -20°C)

1) Had 500 ul lysate from each strain

2) Added the following in this order:

10 ul CuSO4 (1mM final)

10 ul Sodium Ascorbate (final 1.2 mM)

20 ul fluorphore (Final 50 uM)

1.36 ul TBTA (Final 128 uM)

3) Incubate covered in foil for 30 minutes

Methanol chloroform extraction

1)) Add 1800 ul methanol and vortex briefly

2) Add 450 ul chloroform and vortex briefly

3) Add 1200 ul water, becomes cloudy

4) Centrifuge at 14,000 g for 5 mins

5) Remove upper aqueous layer (was bright green)

6) Add 1350 ul methanol

7) Spin again at 14,000 g for 5 mins

8) Remove liquid and add 1350 ul of methanol again

9) Spin at 14,000 g for 5 mins

10) Remove supernatant and let pellet dry with cap off for 15 mins

11) Store pellet at -20 °C

Running SDS-PAGE gel

1) Resuspend pellet in 2X SDS dye

I first resuspend in water and took a Bradford measurement to normalize protein input? Then added 5X SDS dye to dilute to 2X

2) Heat at 65 °C for 10 mins (covered in foil)

3) Spin at max speed for 10 mins

4) Load samples on gel and run gel in the dark (can cover with Styrofoam container)

5) Put gel in water and cover with aluminum foil

6) Image with Typhoon

- Use software on Typhoon computer for analysis
- Image quant, 1D gel analysis
- Automatic, rolling ball
- Set radius to 100
- Click once and drag to quantify total lane

7) Can stain with Coomassie after to make sure protein loading is the same

Controls to include:

- AHA, - click

- AHA, + click

+ AHA, - click

BIBLIOGRAPHY

Baker, T.A., and Sauer, R.T. (2012). ClpXP, an ATP-powered unfolding and protein-degradation machine. Biochimica et Biophysica Acta - Molecular Cell Research *1823*, 15–28.

Barros, B.B. *et al.* (2020) 'Degradation of Lon in Caulobacter crescentus', *Journal of Bacteriology*. Edited by Y.V. Brun, 203(1). doi:10.1128/JB.00344-20.

Bhat, N.H., Vass, R.H., Stoddard, P.R., Shin, D.K., and Chien, P. (2013). Identification of ClpP substrates in Caulobacter crescentus reveals a role for regulated proteolysis in bacterial development. *88*, 1083–1092.

Biondi, E.G. *et al.* (2006) 'A phosphorelay system controls stalk biogenesis during cell cycle progression in *Caulobacter crescentus*: Regulation of stalk biogenesis in *C. crescentus*', *Molecular Microbiology*, 59(2), pp. 386–401. doi:10.1111/j.1365-2958.2005.04970.x.

Breidenstein, E.B.M., Janot, L., Strehmel, J., Fernandez, L., Taylor, P.K., Kukavica-Ibrulj, I., Gellatly, S.L., Levesque, R.C., Overhage, J., and Hancock, R.E.W. (2012). The Lon Protease Is Essential for Full Virulence in Pseudomonas aeruginosa. PLoS ONE *7*.

Chen, Y.E., Tsokos, C.G., Biondi, E.G., Perchuk, B.S., and Laub, M.T. (2009). Dynamics of two phosphorelays controlling cell cycle progression in Caulobacter crescentus. Journal of Bacteriology *191*, 7417–7429.

Chien, P., Perchuk, B.S., Laub, M.T., Sauer, R.T., and Baker, T. a (2007). Direct and adaptor-mediated substrate recognition by an essential AAA+ protease. Proceedings of the National Academy of Sciences of the United States of America *104*, 6590–6595.

Chung, C.H. and Goldberg, A.L. (1981) 'The product of the ion (capR) gene in Escherichia coli is the ATP-dependent protease, protease La', p. 5.

Chowdhury, T., Chien, P., Ebrahim, S., Sauer, R.T., and Baker, T.A. (2010). Versatile modes of peptide recognition by the ClpX N domain mediate alternative adaptor-binding specificities in different bacterial species. Protein Science *19*, 242–254.

Deatherage, D.E., and Barrick, J.E. (2014). Identification of mutations in laboratory evolved microbes from next-generation sequencing data using breseq. Methods Mol Biol. 165–188.

Domian, I.J., Reisenauer, a, and Shapiro, L. (1999). Feedback control of a master bacterial cell-cycle regulator. Proceedings of the National Academy of Sciences of the United States of America *96*, 6648–6653.

Doyle, S.M., Shorter, J., Zolkiewski, M., Hoskins, J.R., Lindquist, S., and Wickner, S. (2007). Asymmetric deceleration of ClpB or Hsp104 ATPase activity unleashes protein-remodeling activity. Nature Structural and Molecular Biology *14*, 114–122.

Ducret, A., Quardokus, E.M., and Brun, Y. V. (2016). MicrobeJ, a tool for high throughput bacterial cell detection and quantitative analysis. Nature Microbiology *1*, 1–7.

Farrell, C.M., Baker, T.A., and Sauer, R.T. (2007). Altered Specificity of a AAA+ Protease. Molecular Cell *25*, 161–166.

Fei, X., Bell, T.A., Barkow, S.R., Baker, T.A., and Sauer, R.T. (2020). Structural basis of clpxp recognition and unfolding of ssra-tagged substrates. ELife *9*, 1–39.

Gates, S.N., Yokom, A.L., Lin, J., Jackrel, M.E., Rizo, A.N., Kendsersky, N.M., Buell, C.E., Sweeny, E.A., Mack, K.L., Chuang, E., et al. (2017). Ratchet-like polypeptide translocation mechanism of the AAA+ disaggregase Hsp104. Science *357*, 273–279.

Goff, S.A., Casson, L.P., and Goldberg, A.L. (1984). Heat shock regulatory gene htpR influences rates of protein degradation and expression of the lon gene in Escherichia coli. Proceedings of the National Academy of Sciences of the United States of America *81*, 6647–6651.

Goldberg, A.L. (1972). Degradation of Abnormal Proteins in Escherichia coli. Proc Natl Acad Sci U S A *69*, 422–426.

Goldberg, A.L., Moerschell, R.P., Hachung, C., and Maurizi, M.R. (1994). ATP-dependent protease La (Lon) from Escherichia coli. Methods in Enzymology *244*, 350–375.

Gonzalez, D., Kozdon, J.B., McAdams, H.H., Shapiro, L., and Collier, J. (2014). The functions of DNA methylation by CcrM in Caulobacter crescentus: A global approach. Nucleic Acids Research *42*, 3720–3735.

Gora, K.G., Cantin, A., Wohlever, M., Joshi, K.K., Perchuk, B.S., Chien, P., and Laub, M.T. (2013). Regulated proteolysis of a transcription factor complex is critical to cell cycle progression in Caulobacter crescentus. Molecular Microbiology *87*, 1277–1289.

Gorbatyuk, B., and Marczynski, G.T. (2005). Regulated degradation of chromosome replication proteins DnaA and CtrA in Caulobacter crescentus. Molecular Microbiology *55*, 1233–1245.

Gottesman, S., Halpern, E. and Trisler, P. (1981) 'Role of sulA and sulB in filamentation by lon mutants of Escherichia coli K-12', *Journal of Bacteriology*, 148(1), pp. 265–273. doi:10.1128/jb.148.1.265-273.1981.

Gottesman, S., Roche, E., Zhou, Y.N., and Sauer, R.T. (1998). The ClpXP and ClpAP proteases degrade proteins with carboxy-terminal peptide tails added by the SsrA-tagging system. Genes and Development *12*, 1338–1347.

Gur, E., and Sauer, R.T. (2008). Recognition of misfolded proteins by Lon, a AAA+ protease. Genes and Development *22*, 2267–2277.

Gur, E., Biran, D., and Ron, E.Z. (2011). Regulated proteolysis in Gram-negative bacteria — how and when? Nat Rev Microbiol *9*, 839–848.

Hersch, G.L., Burton, R.E., Bolon, D.N., Baker, T.A., and Sauer, R.T. (2005). Asymmetric interactions of ATP with the AAA+ ClpX6 unfoldase: Allosteric control of a protein machine. Cell *121*, 1017–1027.

Hottes, A.K., Shapiro, L., and McAdams, H.H. (2005). DnaA coordinates replication initiation and cell cycle transcription in Caulobacter crescentus. Molecular Microbiology *58*, 1340–1353.

Hottes, A.K. *et al.* (2004) 'Transcriptional Profiling of *Caulobacter crescentus* during Growth on Complex and Minimal Media', *Journal of Bacteriology*, 186(5), pp. 1448–1461. doi:10.1128/JB.186.5.1448-1461.2004.

Howard-Flanders, P., Simson, E., and Theriot, L. (1964). A locus that controls filament formation and sensitiviry to radiation in Escherichia coli K-12. Genetics *49*, 237–246.

Jenal, U., and Fuchs, T. (1998). An essential protease involved in bacterial cell-cycle control. EMBO Journal *17*, 5658–5669.

Jonas, K., Liu, J., Chien, P., and Laub, M.T. (2013). Proteotoxic stress induces a cell-cycle arrest by stimulating lon to degrade the replication initiator DnaA. Cell *154*, 623–636.

Joshi, K.K., Bergé, M., Radhakrishnan, S.K., Viollier, P.H., and Chien, P. (2015). An Adaptor Hierarchy Regulates Proteolysis during a Bacterial Cell Cycle. Cell *163*, 419–431.

Karzai, A.W., Roche, E.D. and Sauer, R.T. (2000) 'The SsrA–SmpB system for protein tagging, directed degradation and ribosome rescue', *Nature Structural Biology*, 7(6), pp. 449–455. doi:10.1038/75843.

Keiler, K.C. (2015). Mechanisms of ribosome rescue in bacteria. Nature Reviews Microbiology *13*, 285–297.

Keiler, K.C., Waller, P.R.H., and Sauer, R.T. (1996). Role of a Peptide Tagging System in Degradation of Proteins Synthesized from Damaged Messenger RNA. Science *271*, 990–993.

Kenniston, J.A., Baker, T.A., Fernandez, J.M., and Sauer, R.T. (2003). Linkage between ATP consumption and mechanical unfolding during the protein processing reactions of an AAA+ degradation machine. Cell *114*, 511–520.

Kim, D.Y., and Kim, K.K. (2003). Crystal Structure of ClpX Molecular Chaperone from Helicobacter pylori. Journal of Biological Chemistry *278*, 50664–50670.

Langklotz, S., Baumann, U., and Narberhaus, F. (2012). Structure and function of the bacterial AAA protease FtsH. Biochimica et Biophysica Acta - Molecular Cell Research *1823*, 40–48.

Lau, A.M., Claesen, J., Hansen, K., and Politis, A. (2021). Deuteros 2.0: Peptide-level significance testing of data from hydrogen deuterium exchange mass spectrometry. Bioinformatics *37*, 270–272.

Laub, M.T., Chen, S.L., Shapiro, L., and McAdams, H.H. (2002). Genes directly controlled by CtrA, a master regulator of the Caulobacter cell cycle. Proceedings of the National Academy of Sciences of the United States of America *99*, 4632–4637.

Lee, I., and Suzuki, C.K. (2008). Functional mechanics of the ATP-dependent Lon protease- lessons from endogenous protein and synthetic peptide substrates. Biochimica et Biophysica Acta - Proteins and Proteomics *1784*, 727–735.

Leslie, D.J. *et al.* (2015) 'Nutritional Control of DNA Replication Initiation through the Proteolysis and Regulated Translation of DnaA', *PLOS Genetics*. Edited by W.F. Burkholder, 11(7), p. e1005342. doi:10.1371/journal.pgen.1005342.

Levchenko, I., Seidel, M., Sauer, R.T., and Baker, T.A. (2000). A Specificity-Enhancing Factor for the ClpXP Degradation Machine. Science *289*, 2354–2356.

Liao, J.-H. *et al.* (2010) 'Binding and Cleavage of E. coli HUβ by the E. coli Lon Protease', *Biophysical Journal*, 98(1), pp. 129–137. doi:10.1016/j.bpj.2009.09.052.

Li, H., and Durbin, R. (2009). Fast and accurate short read alignment with Burrows-Wheeler transform. Bioinformatics *25*, 1754–1760.

Li, H., Handsaker, B., Wysoker, A., Fennell, T., Ruan, J., Homer, N., Marth, G., Abecasis, G., and Durbin, R. (2009). The Sequence Alignment/Map format and SAMtools. Bioinformatics *25*, 2078–2079.

Li, J. *et al.* (2021) 'Proteome-wide mapping of short-lived proteins in human cells', *Molecular Cell*, 81(22), pp. 4722-4735.e5. doi:10.1016/j.molcel.2021.09.015.

Liu, J., Francis, L.I., Jonas, K., Laub, M.T., and Chien, P. (2016). ClpAP is an auxiliary protease for DnaA degradation in Caulobacter crescentus. Molecular Microbiology *102*, 1075–1085.

Lopez, K.E., Rizo, A.N., Tse, E., Lin, J.B., Scull, N.W., Thwin, A.C., Lucius, A.L., Shorter, J., and Southworth, D.R. (2020). Conformational plasticity of the ClpAP AAA+ protease couples protein unfolding and proteolysis. Nature Structural and Molecular Biology *27*, 406–416.

Mahmoud, S.A., and Chien, P. (2018). Regulated Proteolysis in Bacteria. Annual Review of Biochemistry *87*, 677–696.

Mahmoud, S.A., Aldikacti, B. and Chien, P. (2021) *Plasticity in AAA+ proteases reveals ATP-dependent substrate specificity principles*. preprint. Molecular Biology. doi:10.1101/2021.08.18.456811.

Martin, A., Baker, T.A., and Sauer, R.T. (2008). Protein unfolding by a AAA+ protease is dependent on ATP-hydrolysis rates and substrate energy landscapes. Nature Structural and Molecular Biology *15*, 139–145.

Mizusawa, S., and Gottesman, S. (1983). Protein degradation in Escherichia coli: the lon gene controls the stability of sulA protein. Proceedings of the National Academy of Sciences of the United States of America *80*, 358–362.

Omnus, D.J. *et al.* (2021) 'The Lon protease temporally restricts polar cell differentiation events during the Caulobacter cell cycle', *eLife*, 10, p. e73875. doi:10.7554/eLife.73875.

Persat, A., Stone, H.A., and Gitai, Z. (2014). The curved shape of caulobacter crescentus enhances surface colonization in flow. Nature Communications *5*, 1–9.

Quinlan, A.R., and Hall, I.M. (2010). BEDTools: a flexible suite of utilities for comparing genomic features. Bioinformatics *26*, 841–842.

Quon, K.C., Marczynski, G.T., and Shapiro, L. (1996). Cell cycle control by an essential bacterial two-component signal transduction protein. Cell *84*, 83–93.

R Core Team (2019). R: A language and Environment for Statistical Computing (R Foundation for Statistical Computing).

Reisenauer, A. (2002) 'DNA methylation affects the cell cycle transcription of the CtrA global regulator in Caulobacter', *The EMBO Journal*, 21(18), pp. 4969–4977. doi:10.1093/emboj/cdf490.

Ripstein, Z.A., Vahidi, S., Houry, W.A., Rubinstein, J.L., and Kay, L.E. (2020). A processive rotary mechanism couples substrate unfolding and proteolysis in the ClpXP degradation machinery. ELife *9*.

Robinson, M.D., McCarthy, D.J., and Smyth, G.K. (2009). edgeR: A Bioconductor package for differential expression analysis of digital gene expression data. Bioinformatics *26*, 139–140.

Rogers, A. *et al.* (2016) 'The LonA Protease Regulates Biofilm Formation, Motility, Virulence, and the Type VI Secretion System in Vibrio cholerae', *Journal of Bacteriology*. Edited by V.J. DiRita, 198(6), pp. 973–985. doi:10.1128/JB.00741-15.

Sauer, R.T., and Baker, T.A. (2011). AAA+ Proteases: ATP-Fueled Machines of Protein Destruction. Annu. Rev. Biochem *80*, 587–612.

Schneider, C.A., Rasband, W.S., and Eliceiri, K.W. (2012). NIH Image to ImageJ: 25 years of image analysis. Nature Methods *9*, 671–675.

Shin, M., Puchades, C., Asmita, A., Puri, N., Adjei, E., Luke Wiseman, R., Wali Karzai, A., and Lander, G.C. (2020). Structural basis for distinct operational modes and protease activation in AAA+ protease Lon.

Skerker, J.M., Prasol, M.S., Perchuk, B.S., Biondi, E.G., and Laub, M.T. (2005). Two-component signal transduction pathways regulating growth and cell cycle progression in a bacterium: A system-level analysis. PLoS Biology *3*.

Smith, S.C., Joshi, K.K., Zik, J.J., Trinh, K., Kamajaya, A., Chien, P., and Ryan, K.R. (2014). Cell cycle-dependent adaptor complex for ClpXP-mediated proteolysis directly integrates phosphorylation and second messenger signals.

Proceedings of the National Academy of Sciences of the United States of America *111*, 14229–14234.

Stankeviciute, G. *et al.* (2019) 'Caulobacter crescentus Adapts to Phosphate Starvation by Synthesizing Anionic Glycoglycerolipids and a Novel Glycosphingolipid', *mBio*. Edited by H.A. Shuman, 10(2). doi:10.1128/mBio.00107-19.

Stein, B.J., Fiebig, A. and Crosson, S. (2020) 'Feedback Control of a Two-Component Signaling System by an Fe-S-Binding Receiver Domain', *mBio*. Edited by P.J. Kiley and D.K. Newman, 11(2). doi:10.1128/mBio.03383-19.

Suraweera, A. *et al.* (2012) 'Failure of Amino Acid Homeostasis Causes Cell Death following Proteasome Inhibition', *Molecular Cell*, 48(2), pp. 242–253. doi:10.1016/j.molcel.2012.08.003.

Tan, H.M., Kozdon, J.B., Shen, X., Shapiro, L., and McAdams, H.H. (2010). An essential transcription factor, SciP, enhances robustness of Caulobacter cell cycle regulation. Proceedings of the National Academy of Sciences of the United States of America *107*, 18985–18990.

Torres-Cabassa, A.S. and Gottesman, S. (1987) 'Capsule synthesis in Escherichia coli K-12 is regulated by proteolysis', *Journal of Bacteriology*, 169(3), pp. 981–989. doi:10.1128/jb.169.3.981-989.1987.

Wang, J.D., Herman, C., Tipton, K.A., Gross, C.A., and Weissman, J.S. (2002). Directed evolution of substrate-optimized GroEL/S chaperonins. Cell *111*, 1027–1039.

Wang, K.H., Sauer, R.T., and Baker, T.A. (2007). ClpS modulates but is not essential for bacterial N-end rule degradation. Genes and Development *21*, 403–408.

Williams, B. *et al.* (2014) 'CLPXP and CLPAP proteolytic activity on divisome substrates is differentially regulated following the *C aulobacter* asymmetric cell division', *Molecular Microbiology*, 93(5), pp. 853–866. doi:10.1111/mmi.12698.

Witkin, E.M. (1946). Inherited Differences in Sensitivity to Radiation in Escherichia Coli. Proceedings of the National Academy of Sciences of the United States of America *32*, 59–68.

Wortinger, M., Sackett, M.J., and Brun, Y. V. (2000). CtrA mediates a DNA replication checkpoint that prevents cell division in Caulobacter crescentus. The EMBO Journal *19*, 4503–4512.

Wright, R., Stephens, C., Zweiger, G., Shapiro, L., and Alley, M.R.K. (1996). Caulobacter Lon protease has a critical role in cell-cycle control of DNA methylation. Genes and Development *10*, 1532–1542.

Wu, D., Lim, E., Vaillant, F., Asselin-Labat, M.L., Visvader, J.E., and Smyth, G.K. (2010). ROAST: Rotation gene set tests for complex microarray experiments. Bioinformatics *26*, 2176–2182.

Yakhnin, A. V., Vinokurov, L.M., Surin, A.K., and Alakhov, Y.B. (1998). Green fluorescent protein purification by organic extraction. Protein Expression and Purification *14*, 382–386.

Ye, X., Lin, J., Mayne, L., Shorter, J., and Walter Englander, S. (2020). Structural and kinetic basis for the regulation and potentiation of Hsp104 function. Proceeding of the National Academy of Science.

Yokom, A.L., Gates, S.N., Jackrel, M.E., Mack, K.L., Su, M., Shorter, J., and Southworth, D.R. (2016). Spiral architecture of the Hsp104 disaggregase reveals the basis for polypeptide translocation. Nature Structural and Molecular Biology *23*, 830–837.

Zeinert, R.D. *et al.* (2020) 'The Lon Protease Links Nucleotide Metabolism with Proteotoxic Stress', *Molecular Cell*, 79(5), pp. 758-767.e6.

Zeinert, R.D., Liu, J., Yang, Q., Du, Y., Haynes, C.M., and Chien, P. (2018). A legacy role for DNA binding of Lon protects against genotoxic stress. BioRxiv.

Zhou, X., Eckart, M.R. and Shapiro, L. (2021) 'A Bacterial Toxin Perturbs Intracellular Amino Acid Balance To Induce Persistence', *mBio*. Edited by M.J. Blaser, 12(1), pp. e03020-20. doi:10.1128/mBio.03020-20.